PROCEEDING

INTERNATIONAL CONFERENCE AND WORKSHOP ON CHEMICAL ENGINEERING 2013

in conjuction with The 10th UNPAR National
Chemical Engineering Conference

"Chemical Engineering Role for Sustainable Development"

Kuta, Bali
December 4-5th, 2013

PREFACE

Dear all participants,
First of all, we would like to welcome all of you into the 1st UNPAR's International Conference of Chemical Engineering and Process Safety Workshop where this event is also in conjunction with the 10th National Conference of Chemical Engineering. This year, on April 2013, we are celebrating our 20th anniversary. Therefore in this special year, we are extending our conference scope from national to international event. It is also our intention to introduce our Chemical Engineering Department in theInternational level.

We are choosing Chemical Engineering Role for Sustainable Development as the conference theme. We realize that chemical engineering plays an important role to ensure the sustainability in every aspects starting from alternative renewable feedstocks for energy and chemicals, alternative green processes until waste minimization. Strongly related with the sustainable process development, chemical engineer also have to deeply involved in the process safety in order to bring this sustainable technology in the industrial level. It is our wish that the conference and the workshop will provide an excellent forum for academia, industry and Indonesia's government to share information, discuss recent knowledgeand technological advancement, as well as provide an up-to-date perspective on the sustainable development around the globe.

We are very pleased to have lectures given by our special keynote speakers. The topics are surely important and will stimulate a fruitful discussion about the chemical engineering role in many aspects for sustainable development. We would like to sincerely thanks our keynote speakers, Prof Djoko Said Damardjati from Indonesian Agency for Agricultural Research and Development (IAARD), Ministry of Agriculture, Indonesia, Prof Haryadi from Gadjah Mada University, Prof Yudi Samyudia from Curtin University,Prof. Leon Janssen, Prof H.J. Heeres, and Prof F. Picchioni from University of Groningen, Assoc. Prof. Kim Jaehoon from Sungkyunkwan University, and Prof. Xiao Dong Chen from Soochow University. We would like to give a special thanks to Bapak Ir Yos Triadmodjo, M.M., for his willingness to share and to bring his 30 years Industrial experiences in the Process Safety workshop.

We are also grateful to the Indonesian Center for Estate Crops Research and Development Indonesian Agency for Agricultural Research and Development (IAARD), Ministry of Agriculture, Indonesia and Research Centre for Chemistry, Indonesian Institute of Science (LIPI) for supporting our 1st International Conference and Workshop. Last but not least, I would like to express a very special gratitude to the scientific committee and the organizing committee for their time, efforts and contribution to this event.

And finally, I hope that you enjoy this event and wish you a pleasant stay in Kuta, Bali.

Sincerely,

Dr.Henky Muljana, ST.,M.Eng
Chairman of the Organizing Comitteee,
Head of Chemical Engineering Department
Parahyangan Catholic University

COMMITTEE

INTERNATIONAL SCIENTIFIC COMMITTEE

Prof. Dr. Ir. Ign. Suharto APU   (Unpar, Indonesia)
Assoc. Prof. Dr. Iir. Danu Ariono   (ITB, Indonesia)
Prof. Dr. Ir. Tjandra Setiadi   (ITB, Indonesia)
Prof. Dr. Moses O. Tadé   (Curtin, Australia)
Prof. Ir. Yudi Samyudia   (Curtin, Malaysia)
Prof. Dr. Ir. L. P. B. M Janssen   (RuG, Netherlands)
Prof. Dr. Ir. H. J. Heeres   (RuG, Netherlands)
Pof. Dr. Francesco Picchioni   (RuG, Netherlands)
Dr. Ir. CristiantoWibowo   (Waterbay, USA)
Assoc. Prof. Dr. Kim Jaehoon   (Sungkyunkwan, South Korea)
Dr. Joong Kee Lee   (KIST, South Korea)
Assoc. Prof. Dr. Yaya Rukayadi   (UPM, Malaysia)
Prof. Dr. Xiao Dong Chen   (Soochow, China)

ORGANIZING COMMITTEE

Chairperson   Dr. Henky Muljana, S.T., M.Eng.
Vice Chairperson Tony Handoko, S.T., M.T.
Finance   Ir. Y.I.P. Arry Miryanti, M.Si.

Logistic and Finance Committee
Chair   I Gede Pandega Wiratama, S.T., M.T.
Members   Mr. Putra Bagus Kusuma
             Mr. Ernest Arbita, S.T.
             Ms. Catherine
             Mr. Cahyadi Dwi Putra
             Mr. Kemal Kahfianto
             Mr. Michael Marcelinus Kosasi
             Mr. Robert Nathaniel Osmond

Program Committee
Chair   Ratna Frida Susanti, S.T. Ph.D
Members   Dr. Tedi Hudaya, S.T., M.Eng.Sc.
             Aditya Putranto, Ph.D.
             Mr. Stefen Kristanto
             Mr. Alfredo Nathanael
             Ms. Angela Rosali

Secretariat Committee

Chair	Anastasia Prima K., S.Si., M.T.
Members	Dr. Arenst Andreas Arie, S.T., S.Si., M.Sc.
	Dr. Asaf Kleopas Sugih, S.T., M.T., M.Eng.
	Ms. Susan Olivia Limarta, S.T.
	Ms. Theresia May Anggraini, S.T.
	Mr. Ken Hashigata

Technical Committee

Members	Dr. Ir. Budi Husodo, M.Eng.
	Dr. Ir. Judy Retti Witono, M.App.Sc.

Table of Contents

The International Conference on Chemical Engineering UNPAR 2013

Advanced biofunctional materials fabricated by plasma-based processes

Dave Mangindaan*

National University of Singapore, 4 Engineering Drive 4, Singapore 117576, Singapore

Abstract

This paper summarized some advances in creation of biofunctional materials by using plasma techniques. One of useful tools in the field of biomaterials science is surface chemical gradient, which find the application in biomedical devices and material or cell screenings. A wide-range wettability gradient with water contact angle spanned from 20° (hydrophilic) to 135° (hydrophobic) has been created on poly(propylene) (PP) membrane film, by treating it using O_2 plasma, and followed by controlled exposure of SF_6 plasma. A mask was employed as the key to discriminate the mass transfer of plasma species onto the polymeric substrate. The plasma mass transport phenomena have also been comprehensively elucidated in terms of numerical calculations and computational modeling to assist the fabrication of the gradient with different dimensions. Beside the gas-based plasma in the previously discussed section, another type of plasma is also exist as chemical vapor-based plasma, or more popular as plasma polymerization. In plasma polymerization, the organic precursors were vaporized and contacted with electricity, polymerized in highly crosslinked random structure, and followed by deposition of the thin polymer layer on the surface of various substrates. The kinetics, along with chemical and biological characterizations of plasma polymers from selected amine-containing precursors has been elaborated. From the aforementioned study, it was concluded that allylamine precursor is very promising for biofunctionalization. Hence, allylamine was further explored for the fabrication of amine-functionalized gradient, whether it is in form of one-dimensional or two-dimensional gradients. Beside the intensive investigation of the fabrication of gradients, plasma also found important role in modulation of biocompatibility of various polymer, namely poly(vinylidene fluoride) (PVDF) and polysulfone (PSf), with simple and fast treatment using O_2 plasma. Furthermore, integration of O_2 plasma and sol-gel technique on a porous biocompatible and biodegradable polycaprolactone membrane resulted in a new platform for wound dressing having topical drug release of ketoprofen (anti-inflammatory drug) and silver sulfadiazine (anti-bacterial component). The rigorous studies affirmed here demonstrated that plasma is a powerful tool for biomaterials science and biomedical applications.

Keywords: plasma; biofunctional materials; chemical gradients

1. Introduction

Polymers, generally inexpensive with excellent optical and mechanical properties and easy to process, have been applied extensively in fields such as protective coatings, friction and wear, composites, microelectronic devices, biomaterials and thin-film technology. For the success of the designated applications, special surface functionalities with regard to the chemical composition, hydrophilicity, roughness, crystallinity, conductivity, lubricity, and cross-linking density are usually required. For polymers that sometimes lack the required properties for the particular applications, surface functionalization or modification method provided an alternative solution to transform polymers into highly valuable finished products.

Essentially, different approaches (such as oxidation [1], amidation [2], glucosamination [3], coupling reaction [4], and platination/iodination [5]) were employed to incorporate amine functionalities onto surfaces. But unfortunately, these conventional methods to prepare amine-containing surfaces involved complex hierarchies of reaction procedures which required various solvents and the overall experiments were usually time-consuming. Therefore, there is a desire to utilize another alternative process to overcome these hindrances, which is plasma that will be comprehensively discussed in this paper.

Plasma is a gas mixture of electrons, positive ions, negative ions, neutral atoms, radicals, and molecules [6]. Commonly known as the fourth state of materials, plasma contains highly activated species and is able to initiate chemical and physical reactions at the surface of the sample [6]. Surface

modification by plasma is a uniform surface-specific modification with a wide variety of functional groups and is applicable for almost all polymers regardless of the structure and chemical reactivity. Problems such as residual solvent and substrate swelling can be avoided due to absence of solvent during plasma treatment. However, its complexity and highly system-dependent nature makes it difficult to obtain a detailed understanding about interactions between plasma components and the surface [7].

In general, reactions during plasma treatment can be classified as follows: plasma etching; plasma implantation; and plasma polymerization [6-8]. However, only plasma etching and plasma polymerization were employed in this study. When plasma etching occurs, the plasma exposure causes degradation and material removal from the surface. Argon, due to its low cost and high etching yield, is the most commonly used inert gas [7]. Oxygen- and fluorine-containing plasmas are also commonly used for the polymer etching.[8] During the course of plasma polymerization, vapor of organic monomer was introduced to high electric energy field to impart amine functionalities on the surface of substrate. Plasma polymerization differs from the conventional polymer synthesis with its highly complex structure, and with branched or crosslinked chains.[6] The course of plasma polymerization involves the generation and dissociation of complicated reactive species such as electrons, ions, radicals, atoms and molecules, rendering only few supporting literature detailed the relationships between the deposition kinetics with the physical-chemical properties of plasma polymers. [9-11]

2. Amine-containing surface functionality

Particularly, materials contain amine-functionalized surfaces attract great interests for their wide-range applications in membranes for wastewater treatments [12, 13], functionalization of carbon nanotubes [14], microspheres [15], biocompatibility improvement in biomedical materials [16, 17], and in sensor fabrications [14, 18, 19]. The precursors employed to integrate amine functionalization by plasma polymerization included ethylenediamine [14, 15, 18, 20-22], butylamine [12, 13, 23-25], heptylamine [16, 26, 27], aniline [28, 29], diaminocyclohexane [30, 31], acetonitrile [32, 33]m and allylamine [25, 34-42]. Among these molecules, allylamine, an amine conjugated with three carbons with double bond of $=CH_2$ group, was extensively studied.

Allylamine was widely applied as a coating layer on biomaterials such as polyethyleneterephthalate [43], polystyrene and polyethylene powder [44], stainless steel stents [45], or in fields of sensor technology [46]. The mechanism of allylamine plasma polymerization has been reported and reviewed by different research groups [34, 35]. However, the comparisons among plasma polymerizations with other C_3 amine molecules, i.e. propylamine [47, 48] and propargylamine [47]were less reported. Therefore we took initiative to study of plasma polymerization of amine-containing thin films from these three precursors, where the deposition kinetics was evaluated mathematically according to the model developed by Denaro and co-workers[49, 50]. Cell-surface interaction was studied by culturing L-929 fibroblast cells directly on Si wafer surfaces coated by the three amine plasma polymers from precursors of propylamine (PPP), allylamine (PPA), and propargylamine (PPG).

In the proposed mechanism of plasma polymerization, the radicals $R_n^\bullet$ produced via electron bombardment in plasma chamber can react in three ways: (i) react with monomer M_0 in the propagation step, (ii) recombine or disproportionate in a bimolecular process, and (iii) may become trapped in an unimolecular process. The corresponding reactions are expressed as following:

$$R_n^\bullet + M \longrightarrow R_{n+1}^\bullet$$
(1a)

$$R_n^\bullet + R_n^\bullet \longrightarrow P_{n+m} \ (\text{or Pn + Pm})$$
(1b)
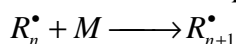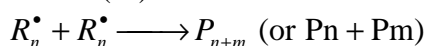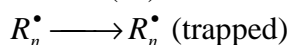
$$R_n^\bullet \longrightarrow R_n^\bullet \ (\text{trapped})$$
(1c)

The final form of deposition rate r_{dep} as function of power W is

$$r_{dep} = \frac{p}{p+2A} h \ W^n$$

(2)

where p is total pressure, A is trapping-propagation ratio, h and n are proportional constants to correlate the radical production rate with the applied power W. Complete elucidation of the mechanism has been derived in our previous work [51]. The improvement of biocompatibility (represented by L-929 mouse fibroblast cells) due to incorporation of amine-containing functionalities and also the plasma deposition kinetics from three different plasma polymers is shown in Fig.1.
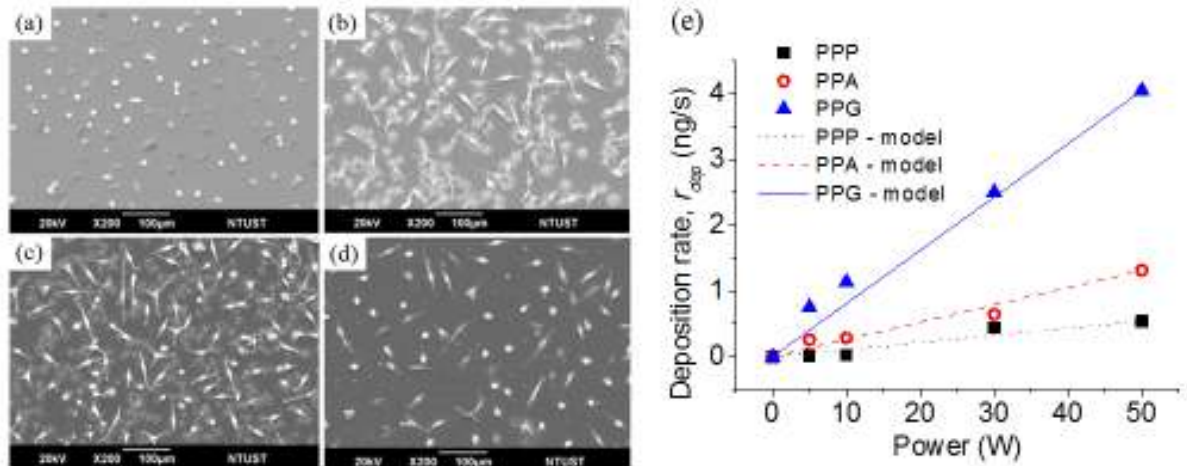
Fig 1. Cell responses of L-929 fibroblasts on surfaces of (a) bare Si wafer, (b) PPP, (c) PPA, and (d) PPG, with (e) kinetics modeling of the deposition rate of amine plasma polymers as function of applied power[51].

Although the PPA deposition rate is rather medium, but it exhibited the most cell growth more than that of PPP and PPG (the justification on both qualitative and quantitative aspects of this issue can be found in [51]). Therefore PPA will be further utilized for more advanced applications.

3. Surface chemical gradients
3.1. Gradients from plasma polymers

Surface gradients are surfaces with chemical or physical properties that gradually change over a given distance [52]. For the past few decades, various gradients have been created for the purposes of screening newly developed materials [53]. improving biochemical assays [54]. and investigating cellular interactions [55-57]. Surface gradients exhibit particular advantages for applications in nanotechnology and biomaterials such as high-throughput, efficient in time and consumables usages, and less operational error for samples prepared in different batches [52]. In general, surface-chemical gradients can be created in two ways, by surface coating or surface modification (by high energy application) methods. The preparation techniques of surface chemical gradients have been summarized in a very excellent review [52]. However, the application of plasma in creation of surface chemical gradients is quite limited [57-60]. Therefore, it motivated us to create ones by using plasma, with the aid of a mask as the key to discriminate the mass transfer of plasma species onto the polymeric substrate [61-64]. The design of the mask [61] and how it was placed [62] to create gradients is illustrated in Fig. 2.
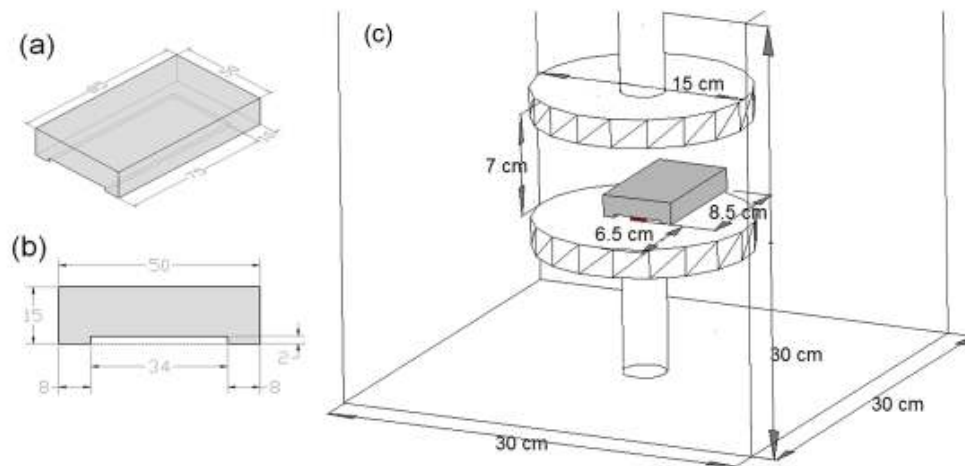
Fig 2. The design of the mask for creating the gradient: (a) top view of mask; (b) front view of the mask. The units presented are in mm. (c) Illustration of the position of the mask inside the plasma chamber[61, 62].

Based from the previous discussion in tethering amine surface functionality [51], allylamine is demonstrated to be very superior for improvement of bicompatibility. We therefore further investigated about the feasibility of creating PPA surface gradient [63]. A piece of Celgard poly(propylene) (PP) membrane was utilized in this study, and deposited by PPA, where the evolution of surface aspects (wettability (water contact angle, WCA), atomic content of nitrogen and C-N functional group (analyzed by using X-ray photoelectron spectroscopy XPS), and the cell density over gradients) is illustrated in Fig. 3a-d. It was shown that the position from open end is definitely exposed to the most allyamine, suggested by the drop of WCA (original surface: PP poly(propylene), WCA 110°) to less than 20° (hydrophilic), and confirmed by both the XPS analysis for contents of atomic nitrogen N1s and C-N chemical group, where it eventually amplified the growth of L-929 cells due to the rich amine concentrated in position 0 from open end. Based from this success, the PPA gradient was further advanced from 1-dimensional (1D) gradient to be a 2-dimensional (2D) gradient, where its creation is schematically drawn in Fig. 3e, where the sample was rotated +90° after the first exposure to PPA, continued for the second one. The profile of WCA and N1s content is shown in Fig. 3f and 3g, respectively, and the cell response on the 2D gradient in Fig. 3h, confirming that the various amine content prepared in gradual concentration is really governed the growth of the cells.
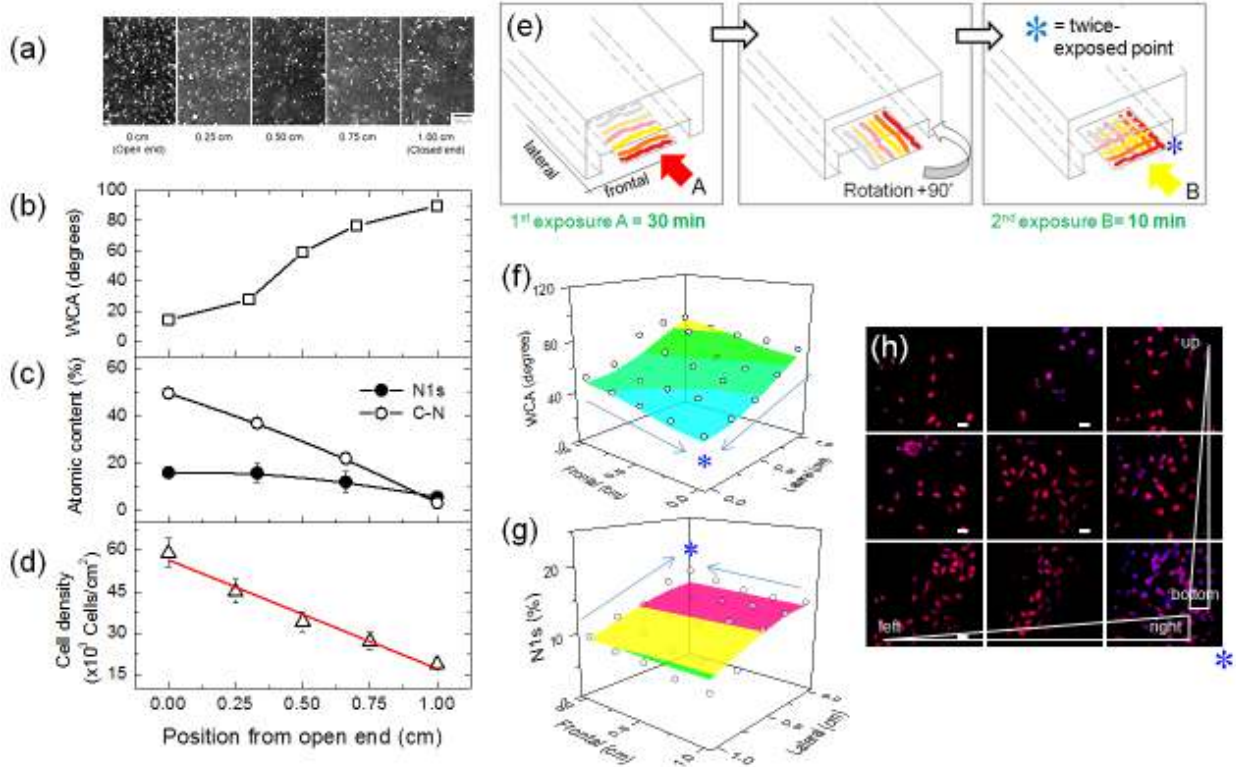
Fig 3. (a) Growth of L-929 cells on PPA gradient (1-dimension, 1D) [63] corresponds to the length of gradient as observed by SEM (scale bar: 100 µm). Evolution of (b) surface wettability (original surface: polypropylene, WCA 110°), (c) atomic nitrogen N1s content and C-N content from XPS, and (d) cell density, over the PPA gradient. (e) Schematic diagram on the creation of 2D (2-dimensional) PPA gradient [64], with the (f) wettability profile, (g) N1s profile, and (h) response of L-929 fibroblast cells as analyzed by using confocal laser microscopy.

3.2. Gradients from plasma treatment

As the surface gradients were successfully created by application of plasma polymerization, an intriguing question might be ask on whether plasma etching may or may not be able to create surface gradients. To do so, a PP membrane was employed as a substrate for creating wettability gradient (surface possessing both high hydrophobicity and high hydrophilicity on opposing ends) [61]. As the PP substrate is hydrophobic (WCA 110°), therefore it must be initially hydrophilized by employing O_2 plasma (no mask was applied), to impart some oxygen-containing moieties, thus get the WCA dropped to 20°Furthermore, the hydrophobization was conducted by using SF_6 plasma, where in this time a mask was applied to discriminate the mass transfer of plasma species, thus created a wettabilty gradient. This concept was successful where a surface (length 1 cm) exhibited WCA from 135 to 20° (Fig. 4a), where quantitave WCA profile is served in Fig. 4b, and atomic fluorine content in Fig. 4c, along with L-929 cell response on the wettability gradient in Fig. 4d. Furthermore, mathematical modelling was utilized to explore the possibility to comprehend the mechanism of the creation of wettability gradient, schematically drawn in Fig. 4e. The plasma mass transport phenomena have been comprehensively elucidated in terms of numerical calculations and computational modeling to assist the fabrication of the gradient with different dimensions [62]. The result for the modelling is demonstrated in Fig. 4, where the modelling matched the WCA profile (Fig. 4f) and also the atomic fluorine content (Fig. 4g), by a factor of 95%, under the condition of varied plasma treatment time of (i) 15, (ii) 60, (iii) 150, and (iv) 300 s.
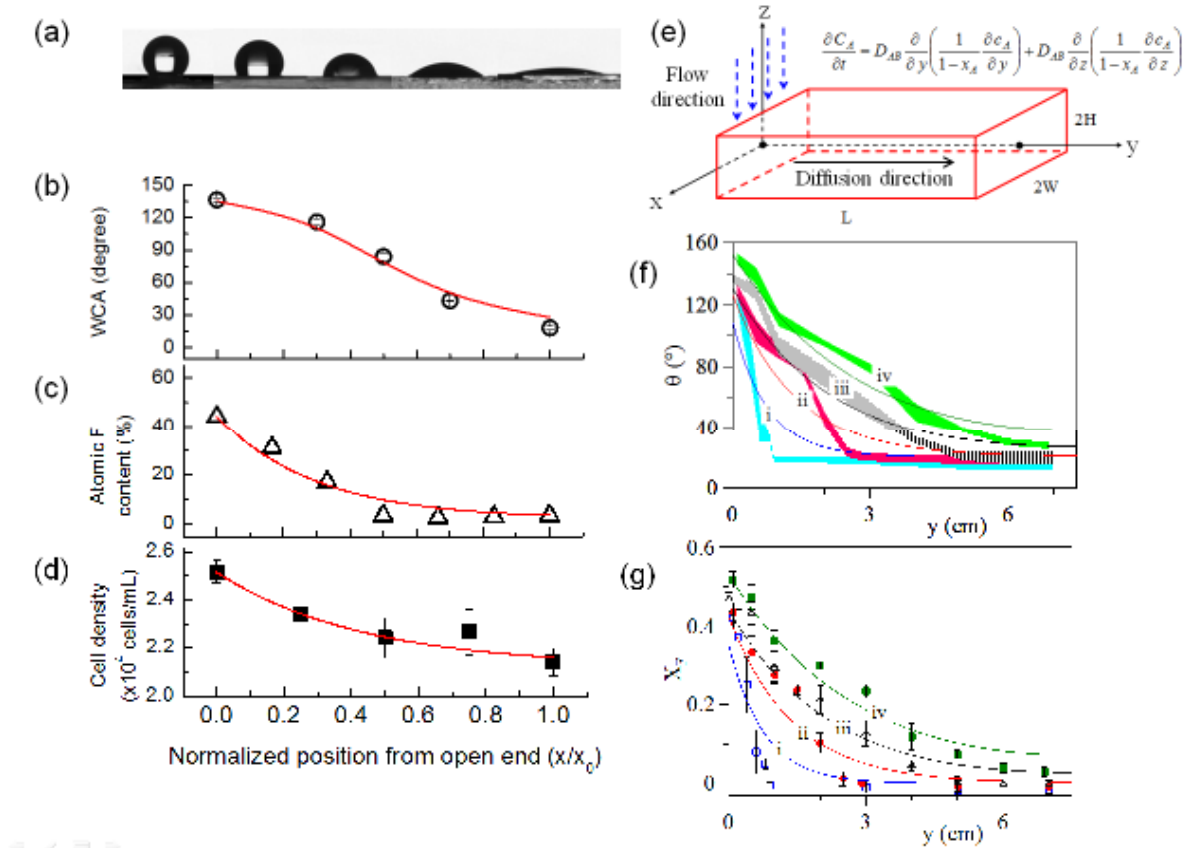
Fig 4. (a) Image of water droplet on the wettability gradient created by using SF₆ plasma [61]. The evolution of (b) surface wettability (original surface: polypropylene, WCA 110°), (c) atomic fluorine F1s content from XPS, and (d) cell density, over the wettability gradient. (e) Schematic diagram on mechanism of the creation of wettability gradient, along with the governing mass-transfer equation, solved and modeled in (f) WCA profile and (g) content of fluorine, where plasma treatment time was varied by (i) 15, (ii) 60, (iii) 150, and (iv) 300 s [62].

4. Plasma treatment for drug release and biocompatible materials

Besides creating various biofunctionalized chemical gradients, plasma is also versatile to be employed in different fields of biomaterials, such as for drug release and improvement of biocompatibility of several polymers. A synergistic combination of sol-gel and plasma-modified biodegradable porous poly(ε-caprolactone) (PCL)membrane was applied as a topical drug release platform [65].Firstly, the PCL surface was coated by using chitosan-SiO₂ sol-gel as drug binding system, subsequently continued with O₂ plasma that assisted the modulation of the release of ketoprofen (anti-inflammatory) and silver sulfadiazine (AgSD, antimicrobial agent) through the PCL barrier. When these drugs were administered onto the skin without a controlled topical drug release system, they may exhibits undesirable renal and gastric side effects and intoxication. The drug release profile for ketoprofen and AgSD is shown in Fig. 5. The O₂-plasma-modified PCL/sol-gel system delayed the drug release from about 10% (ketoprofen, 14 days release) up to 20% (silver sulfadiazine, 3 days), compared to that of pristine PCL. An alternative route to control the release of topical drug has been demonstrated, which provides further advancement in the fields of biomedicine.
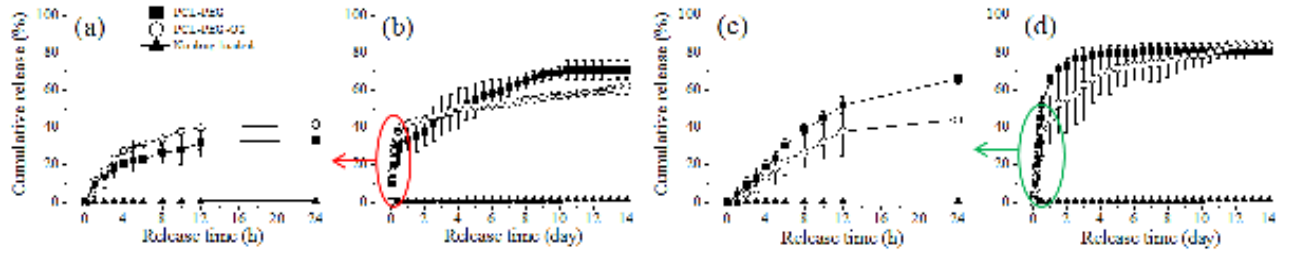
Fig 5. Cumulative release of (a and b) ketoprofen and (c and d) AgSD controlled release system over pristine and O$_2$ plasma treated PCL membranes for (a and c) short release time over 24 h, and (b and d) long release time over 14 days [65].

Poly(vinylidene fluoride) (PVDF) and polysulfone (PSf) are both polymers with excellent mechanical strength with promising potential for biomaterial applications. However, hydrophobic surface severely limited the applications as implant materials as cells scarcely adhere on both substrates naturally. In this study, the surface of PVDF and PSf were modified by O$_2$ plasma treatment to promote cell adhesion for applications in biocompatible materials [66], where the result in shown in Fig. 6. The plasma treatment demonstrated different results for PVDF and PSf. The cell density on pristine PVDF was about half of that on pristine PSf. However, O$_2$ plasma modified PVDF showed four folds increase of cell density, while the maximum two folds higher cell density was observed for plasma modified PSf. Significant cell spreading was observed on both plasma modified substrates. It is revealed by XPS that the O$_2$ plasma treatment oxidized the surface and reduced the F and S groups of PVDF, and PSf, respectively, where it is a possible mechanism behind the improvement of the biocompatibility.
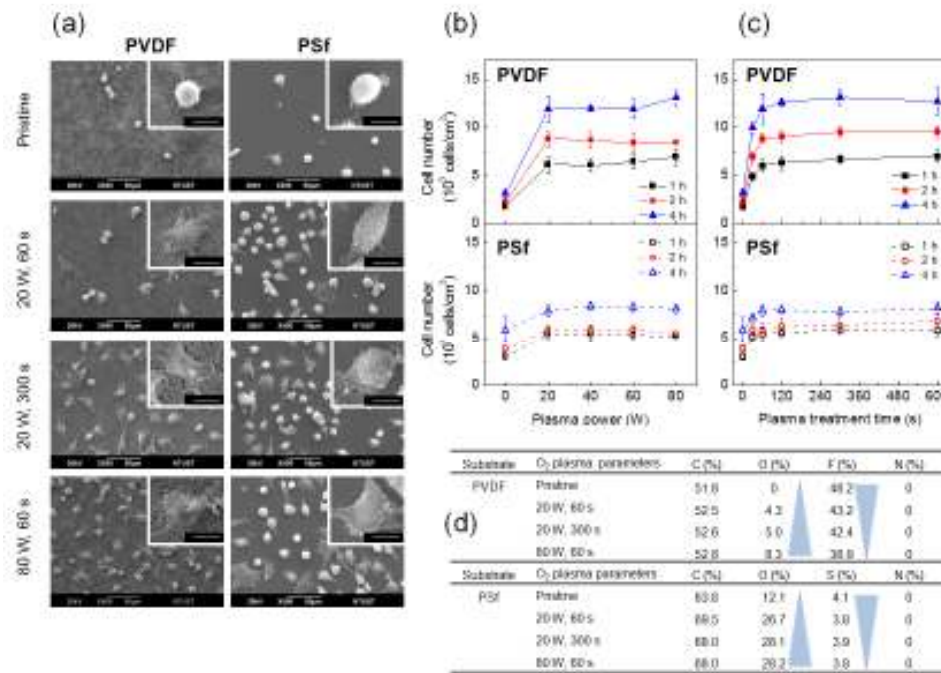
Fig 6. Responses of L-929 fibroblast cells cultured onto PVDF and PSf films modified by O$_2$ plasma treatment (taken at 500×, scale bar= 50μm). Inset: Corresponding cell morphology, taken at 2,000×, scale bar= 10μm). The responses as the effects of plasma parameters on the L-929 cell attachment were investigated as function of (b) applied power, and (b) plasma treatment time. (d) The surface chemistry as analyzed by XPS showed that oxygen functionalities were increased while F and S groups were reduced, for PVDF and PSF, respectively [66].

5. Conclusion

Some advanced biofunctional materials created by using plasma techniques were discussed in this paper. Various surface chemical gradients (1D and 2D gradients of amine functional groups, and wide-range hydrophobic-hydrophilic gradient), drug release platform, and transformation of less-biocompatible materials into promising biomaterials, are few examples as a demonstration of the versatility of plasma treatment and plasma polymerization in biomaterials field. Some kinetics and mass-transfer phenomena regarding the plasma reactions mechanisms have also been elucidated in this paper. Therefore, numerous exciting applications of plasma in biomaterials and other field, such as electronics, nanotechnology, or energy, are highly expected in the near future.

References

[1] Ramanathan, T., Fischer, F.T., Ruoff, R.S., 2005. Amino functionalized carbon nanotubes for binding to polymers and biological systems, Chem. Mater. 17, p. 1290.

[2] Huang, W., Taylor, S., Fu, K., Lin, Y., Zhang, D., Hanks, T.W., Rao, A.M., Sun, Y., 2002. Attaching proteins to carbon nanotubes via diimide-activated amidation, Nano Lett. 2, p. 311.

[3] Baher, J.L., Yang, J., Kosynkin, D.V., Bronikowski, M.J., Smalley, R.E., Tour, J.M., 2001. Functionalization of carbon nanotubes by electrochemical reduction of aryl diazonium salts: a bucky paper electrode, J. Am. Chem. Soc. 123, p. 6536.

[4] Jiang, K., Schadler, L.S., Siegel, R.W., Zhang, X., Zhang, H., Terrones, M., 2004. Protein immobilization on carbon nanotubes via a two-step process of diimide-activated amidation, J. Mater. Chem. 14, p. 37.

[5] Tsang, S.C., Guo, Z.G., Chen, Y.K., Green, M.L.H., Hill, H.A.O., Hambley, T.W., Saddler, P.J., 1997. Immobilization of platinated and iodinated oligonucleotides on carbon nanotubes, Angew. Chem. Int. Ed. 36, p. 2198.

[6] Inagaki, N., 1996. Plasma Surface Modification and Plasma Polymerization, Technomic Publishing Company, Inc., Basel, Switzerland, 1996.

[7] Chu, P.K., Chen, J.Y., Wang, L.P., Huang, N., 2002. Plasma-surface modification of biomaterials, Mater. Sci. Eng. R-Rep 36, p. 143.

[8] Chan, C.-M., Ko, T.-M., Hiraoka, H., 1996. Polymer surface modification by plasmas and photons, Surf. Sci. Rep. 24, p. 1.

[9] Collins, G.W., Letts, S.A., Fearon, E.M., McEachern, R.L., Bernat, T.P., 1994. Surface roughness scaling of plasma polymer films, Phys. Rev. Lett 73, p. 708.

[10] Oksuzoglu, R.M., Elmali, A., Weirich, T.E., Fuess, H., Hahn, H., 2000. Evolution of the surface roughness (dynamic scaling) and microstructure of sputter-deposited $Ag_{75}Co_{25}$ granular films, J. Phys.-Condes. Matter 12, p. 9237.

[11] Palasantzas, G., Tsamouras, D., De Hosson, J.T.M., 2002. Roughening aspects of room temperature vapor deposited oligomer thin films onto Si substrates, Surf. Sci. 507–510, p. 357.

[12] Gancarz, I., Pozniak, G., Bryjak, M., Tylus, W., 2002. Modification of polysulfone membranes 5. Effect of n-butylamine and allylamine plasma, Eur. Polym. J. 38, p. 1937.

[13] Pozniak, G., Gancarz, I., Bryjak, M., Tylus, W., 2002. N-butylamine plasma modifying ultrafiltration polysulfone membranes, Desalination 146, p. 293.

[14] Hiratsuka, A., Muguruma, H., Sasaki, S., Ikebukuro, K., Karube, I., 1999. A Glucose Sensor with a Plasma-Polymerized Thin Film Fabricated by Dry Processes, Electroanalysis 11, p. 1098

[15] Denizli, A., Salih, B., Piskin, E., 1997. New sorbents for removal of heavy metal ions: diamine-glow-discharge treated polyhydroxyethylmethacrylate microspheres, J. Chromatogr. A 773, p. 169.

[16] Dai, L., St.John, H.A.W., Jingjing Bi, P.Z., Chatelier, R.C., Griesser, H.J., 2000. Biomedical coatings by the covalent immobilization of polysaccharides onto gas-plasma-activated polymer surfaces, Surf. Interface Anal. 29, p. 46.

[17] Truica-Marasescu, F., Wertheimer, M.R., 2008. Nitrogen-Rich Plasma-Polymer Films for Biomedical Applications, Plasma Process. Polym. 5, p. 44.

[18] Nakamura, R., Muguruma, H., Ikebukuro, K., Sasaki, S., Nagata, R., Karube, I., Pedersen, H., 1997. A Plasma-Polymerized Film for Surface Plasmon Resonance Immunosensing, Anal. Chem. 69, p. 4649.

[19] Nakanishi, K., Muguruma, H., Karube, I., 1996. A Novel Method of Immobilizing Antibodies on a Quartz Crystal Microbalance Using Plasma-Polymerized Films for Immunosensors, Anal. Chem. 68, p. 1695.

[20] Biederman, H., Boyaci, I.H., Bilkova, P., Slavinska, D., Mutlu, S., Zemek, J., Trchova, M., Klimovic, J.,

Mutlu, M., 2001. Characterization of glow-discharge-treated cellulose acetate membrane surfaces for single-layer enzyme electrode studies, J. Appl. Polym. Sci. 81, p. 1341

[21] Cokeliler, D., Mutlu, M., 2002. Performance of amperometric alcohol electrodes prepared by plasma polymerization technique, Anal. Chim. Acta 469, p. 217.

[22] Kim, J., Park, H., Jung, D., Kim, S., 2003. Protein immobilization on plasma-polymerized ethylenediamine-coated glass slides, Anal. Biochem. 313, p. 41.

[23] Bryjak, M., Gancarz, I., Pozniak, G., 1999. Surface Evaluation of Plasma-Modified Polysulfone (Udel P-1700) Films, Langmuir 15, p. 6400.

[24] Xiang, J.-N., Cao, Z., Yin, X., Wang, K.-M., Lin, H.-G., Yu, R.-Q., 1999. Thickness-shear-mode acoustic-wave sensor based on n-butylamine plasma-deposition film for detection of carboxylic acid vapours, Anal. Chim. Acta 384, p. 37.

[25] Gancarz, I., Bryjak, J., Pozniak, G., Tylus, W., 2003. Plasma modified polymers as a support for enzyme immobilization II. Amines plasma, Eur. Polym. J. 39, p. 2217.

[26] Hartley, P.G., McArthur, S.L., McLean, K.M., Griesser, H.J., 2002. Physicochemical Properties of Polysaccharide Coatings Based on Grafted Multilayer Assemblies, Langmuir 18, p. 2483.

[27] Vasilev, K., Britcher, L., Casanal, A., Griesser, H.J., 2008. Solvent-Induced Porosity in Ultrathin Amine Plasma Polymer Coatings, J. Phys. Chem. B 112, p. 10915.

[28] Gong, X., Dai, L., Mau, A.W.H., Griesser, H.J., 1998. Plasma-polymerized polyaniline films: Synthesis and characterization, J. Polym. Sci. Pol. Chem. 36, p. 633.

[29] Wang, J., Neoh, K.G., Zhao, L., Kang, E.T., 2002. Plasma Polymerization of Aniline on Different Surface Functionalized Substrates, J. Colloid Interface Sci. 251, p. 214.

[30] Lassen, B., Malmsten, M., 1997. Competitive Protein Adsorption at Plasma Polymer Surfaces, J. Colloid Interface Sci. 186, p. 9.

[31] Burns, N.L., 1996. Surface Characterization through Measurement of Electroosmosis at Flat Plates, J. Colloid Interface Sci. 183, p. 249.

[32] Hiratsuka, A., Muguruma, H., Nagata, R., Nakamura, R., Sato, K., Uchiyama, S., Karube, I., 2000. Mass transport behavior of electrochemical species through plasma-polymerized thin film on platinum electrode, J. Membr. Sci. 175, p. 25.

[33] Lefohn, A.E., Mackie, N.M., Fisher, E.R., 1998. Comparison of Films Deposited from Pulsed and Continuous Wave Acetonitrile and Acrylonitrile Plasmas Plasmas Polym. 3, p. 197.

[34] Choukourov, A., Biederman, H., Slavinska, D., Hanley, L., Grinevich, A., Boldyryeva, H., Mackova, A., 2005. Mechanistic Studies of Plasma Polymerization of Allylamine, J. Phys. Chem. B 109, p. 23086

[35] Siow, K.S., Britcher, L., Kumar, S., Griesser, H.J., 2006. Plasma Methods for the Generation of Chemically Reactive Surfaces for Biomolecule Immobilization and Cell Colonization - A Review, Plasma Process. Polym. 3, p. 392.

[36] Hook, A.L., Thissen, H., Quinton, J., Voelcker, N.H., 2008. Comparison of the binding mode of plasmid DNA to allylamine plasma polymer and poly(ethylene glycol) surfaces, Surf. Sci. 602, p. 1883.

[37] Besch, W., Foest, R., Schröder, K., Ohl, A., 2008. Allylamine Plasma Polymer Coatings of Interior Surfaces in Small Trench Structures, Plasma Process. Polym. 5, p. 105.

[38] Tarasova, A., Hamilton-Brown, P., Gengenbach, T., Griesser, H.J., Meagher, L., 2008. Colloid Probe AFM and XPS Study of Time-Dependent Aging of Amine Plasma Polymer Coatings in Aqueous Media, Plasma Process. Polym. 5, p. 175.

[39] Zelzer, M., Alexander, M.R., 2010. Nanopores in Single- and Double-Layer Plasma Polymers Used for Cell Guidance in Water and Protein Containing Buffer Solutions, J. Phys. Chem. B 114, p. 569.

[40] Mishra, G., Easton, C.D., McArthur, S.L., 2010. Physical vs Photolithographic Patterning of Plasma Polymers: An Investigation by ToF–SSIMS and Multivariate Analysis, Langmuir 26, p. 3720.

[41] Fowler, G.J.S., Mishra, G., Easton, C.D., McArthur, S.L., 2009. A ToF-SSIMS study of plasma polymer-based patterned metal affinity surfaces, Polymer 50, p. 5076.

[42] Yang, Z., Wang, J., Luo, R., Maitz, M.F., Jing, F., Sun, H., Huang, N., 2010. The covalent immobilization of heparin to pulsed-plasma polymeric allylamine films on 316L stainless steel and the resulting effects on hemocompatibility, Biomaterials 31, p. 2072.

[43] Hamerli, P., Weigel, T., Groth, T., Paul, D., 2003. Surface properties of and cell adhesion onto allylamine-plasma coated polyethylenterephtalat membranes, Biomaterials 24, p. 3989.

[44] Tatoulian, M., Bretagnol, F., Arefi-Khonsari, F., Amouroux, J., Bouloussa, O., Rondelez, F., Paul, A.J., Mitchell, R., 2005. Plasma Deposition of Allylamine on Polymer Powders in a Fluidized Bed Reactor, Plasma Process. Polym. 2, p. 38.

[45] Yang, Z., Wang, X., Wang, J., Yao, Y., Sun, H., Huang, N., 2009. Pulsed-Plasma Polymeric Allylamine

Thin Films, Plasma Process. Polym. 6, p. 498.

[46] Yatsuda, H., Nara, M., Kogai, T., Aizawa, H., Kurosawa, S., 2007. STW gas sensors using plasma-polymerized allylamine, Thin Solid Films 515, p. 4105.

[47] Fally, F., Doneux, C., Riga, J., Verbist, J.J., 1995. Quantification of the functional groups present at the surface of plasma polymers deposited from propylamine, allylamine, and propargylamine, J. Appl. Polym. Sci. 56, p. 597

[48] Shard, A.G., Whittle, J.D., Beck, A.J., Brookes, P.N., Bullet, N.A., Talib, R.A., Mistry, A., Barton, D., McArthur, S.L., 2004. A NEXAFS Examination of Unsaturation in Plasma Polymers of Allylamine and Propylamine, J. Phys. Chem. B 108, p. 12472.

[49] Denaro, A.R., Owens, P.A., Crawshaw, A., 1968. Glow Discharge Polymerization - Styrene, Eur. Polym. J. 4, p. 93.

[50] Denaro, A.R., Owens, P.A., Crawshaw, A., 1969. Glow Discharge Polymerization II: α-methylstyrene, ω-methylstyrene and allybenzene, Eur. Polym. J. 5, p. 471.

[51] Mangindaan, D., Kuo, W.-H., Chang, C.-C., Wang, S.-L., Liu, H.-C., Wang, M.-J., 2011. Plasma polymerization of amine-containing thin films and the studies on the deposition kinetics, Surf. Coat. Technol. 206, p. 1299.

[52] Morgenthaler, S., Zink, C., Spencer, N.D., 2008. Surface-chemical and -morphological gradients, Soft Matter 4, p. 419.

[53] Genzer, J., Bhat, R.R., 2008. Surface-Bound Soft Matter Gradients, Langmuir 24, p. 2294.

[54] Kim, M.S., Khang, G., Lee, H.B., 2008. Gradient polymer surfaces for biomedical applications, Prog. Polym. Sci 33, p. 138.

[55] Carter, S.B., 1965. Principles of Cell Motility: The Direction of Cell Movement and Cancer Invasion, Nature 208, p. 1183

[56] Carter, S.B., 1967. Haptotaxis and the Mechanism of Cell Motility, Nature 213, p. 256

[57] Zelzer, M., Majani, R., Bradley, J.W., Rose, F.R.A.J., Davies, M.C., Alexander, M.R., 2008. Investigation of cell–surface interactions using chemical gradients formed from plasma polymers, Biomaterials 29, p. 172.

[58] Pitt, W.G., 1989. Fabrication of a Continuous Wettability Gradient by Radio Frequency Plasma Discharge, J. Colloid Interface Sci. 133, p. 223.

[59] Lee, J.H., Kim, H.G., Khang, G.S., Lee, H.B., Jhon, M.S., 1992. Characterization of Wettability Gradient Surfaces Prepared by Corona Discharge Treatment, J. Colloid Interface Sci. 151, p. 563.

[60] Zelzer, M., Scurr, D., Abdullah, B., Urquhart, A.J., Gadegaard, N., Bradley, J.W., Alexander, M.R., 2009. Influence of the Plasma Sheath on Plasma Polymer Deposition in Advance of a Mask and down Pores, J. Phys. Chem. B 113, p. 8487.

[61] Mangindaan, D., Kuo, W.-H., Wang, Y.-L., Wang, M.-J., 2010. Experimental and Numerical Modeling of the Controllable Wettability Gradient on Poly(propylene) Created by SF_6 Plasma, Plasma Process. Polym. 7, p. 754.

[62] Mangindaan, D., Kuo, C.-C., Lin, S.-Y., Wang, M.-J., 2012. The Diffusion-reaction Model on the Wettability Gradient Created by SF_6 Plasma, Plasma Process. Polym. 9, p. 808.

[63] Mangindaan, D., Kuo, W.-H., Kurniawan, H., Wang, M.-J., 2013. Creation of biofunctionalized plasma polymerized allylamine gradients, J. Polym. Sci. Part B: Polym. Phys. 78, p. 1361.

[64] Mangindaan, D., Kuo, W.-H., Wang, M.-J., 2013. Two-dimensional amine-functionality gradient by plasma polymerization, Biochem. Eng. J. 78, p. 198.

[65] Mangindaan, D., Chen, C.-T., Wang, M.-J., 2012. Integrating sol–gel with cold plasmas modified porous polycaprolactone membranes for the drug-release of silver-sulfadiazine and ketoprofen, Appl. Surf. Sci. 262, p. 114.

[66] Mangindaan, D., Yared, I., Kurniawan, H., Sheu, J.-R., Wang, M.-J., 2012. Modulation of biocompatibility on poly(vinylidene fluoride) and polysulfone by oxygen plasma treatment and dopamine coating, J. Biomed. Mater. Res. Part A 100A, p. 3177.

International Conference and Workshop on Chemical Engineering UNPAR 2013

Increased Electricity Generation in Single Chamber Microbial Fuel Cell (MFC) using Tempe Industrial Wastewater

Tania Surya Utami*, Rita Arbianti, Thika Herlani, Ester Kristin

Chemical Engineering Universitas Indonesia, UI Depok Campus 16424, Indonesia

Abstract

The increasing demand of electrical energy has led to researches toward innovative sustainable and environmental-friendly technology. Microbial fuel cell (MFC) is one of the alternatives that can be developed for producing electricity. The focus of this study was to increase the power density generated by MFC with Tempe synthetic wastewater and Tempe industrial wastewater using variations of waste volume and single reactor configuration for series, parallel and series-parallel connection. MFC reactor with a waste volume of 2000 mL has generated higher electricity than the MFC with 500 mL waste volume, which is 3.03 mW/m^2 with coulombic efficiency 0.14 %. The power density resulted in variation of reactor configuration are: 0.005 mW/m^2 in series configuration, 0.13 mW/m^2 in parallel configuration, and 0.006 mW/m^2 in series-parallel configuration. Efficiency of configuration is known by its power transfer. Power transfer that produced by series, parallel and series-parallel configuration are 51.6 %, 50.6 % and 52.6 %. Highest coulombic efficiency resulted in parallel configuration, which is 0.06 %. Single unit MFC reactor with the same total waste volume increased power density up to 3.03 mW/m^2 with coulombic efficiency 0.14 % and the power transfer reached 1000 %. The use of Tempe industrial wastewater can produce electricity in the MFC system. Further research in the MFC system and utilization of Tempe industrial wastewater as a substrate in MFC system, can reduce operating cost of MFC system, as well as making electricity-producing technology that is economical, environmentally friendly, and sustainable.

Keywords: coulombic efficiency; electricity; Microbial Fuel Cell; power density; single chamber

1. Introduction

Availability of petroleum that has been the main source of energy, in 2010 estimated only 25% of the total remaining oil available in the world. Efforts to procure renewable alternative energy and sustainable have been carried out in order to meet the energy needs now and in the future. One of alternative energy which uses bacterial activity in wastewater to produce electrical energy, known as Microbial Fuel Cell (MFC) technology.

MFC technology is a fuel cell that uses organic materials, such as organic wastewater, which is used by microbes as growth substrates and nutrients in metabolic activity [1]. Industrial wastewater, especially food wastewater contains a lot of nutrients that cause the development of microorganisms in the wastewater. Small industry wastewater, such as Tempe industrial wastewater, contains large amounts of carbohydrates (34.8%), protein (34.9%), fat (18.1%), salts, minerals and traces of chemicals.

MFC is an appropriate means to be used to process liquid wastewater. MFC systems could reduce the negative effects of wastewater on the environment, and also can generate electrical energy. MFC has several design that are single chamber MFC, double chamber MFC, MFC plate, and tubular MFC. Single chamber MFC has a simpler design and less cost than other designs [2]. Parallel series of ten single chambers MFC can generate voltages eight times greater than in the single-chamber MFC unit [3]. This study examined the power density generated by MFC with Tempe synthetic wastewater and Tempe industrial wastewater using variations of waste volume and single reactor configuration for series, parallel and series-parallel connection.

2. Methods

MFC experiments were performed by varying waste volume, electrode surface area, and single reactor configuration for series, parallel and series-parallel connection. Observations were made of the voltage generated by each circuit. Voltage circuits with the best will be used again to measure the

---

voltage on the original wastewater from the mill soybean. Voltage measuring instrument used in this MFC study is digital multimeter (APPA Electric Instrument N107/109).

2.1. Electrode Preparation

Graphite electrode used because it is not expensive, readily available and has a large surface [4]. Graphite electrode immersed in a solution of 1 M HCl for 1 hour and then rinsed using distilled water. Then the electrodes immersed in a solution of 1 M NaOH for 1 hour and rinsed again using distilled water. Then electrodes soaked with distilled water and ready for use. These aim to regenerate the electrode preparation and eliminate contamination of the metal electrode and the organic material [4].

2.2. Substrate Preparation

Substrate prepared in this study is the synthetic Tempe wastewater. Soybean (*Glycine max*) with a mass of 200 grams is boiled with 500 mL aquadest (ratio 1:2.5; w/v) for 15 minutes. This is done through the process of soaking soybeans in Tempe-making process, with the ratio of 3:5 (w/v). Boiled water and soybean is separated. Beans soaked with 500 mL of water, stored in a glass beaker and covered with aluminum foil and left overnight. After over 24 hours, the water from boiling water mixed with the immersion. Water that has been boiled and soaked mixed and neutralized using NaOH 1 M. Once neutral, the substrate was mixed with 0.15 gram NH_4Cl, 0.06 gram KCl, 2.48 gram KH_2PO_4dan 0.34 gram K_2HPO_4 using magnetic stirrer. Once done, the substrate is ready to put into the reactor. The above ingredients are used for experiments with a single reactor. Fill the reactor with a working volume of 500 mL to 500 mL mixture of substrate and reactor with working volume of 2000 mL with 2000 mL of mixed substrates.

2.3. MFC Configuration

The electrodes are connected by wires in the reactor and resistor, this is the anode part. Then, the other electrode mounted in front of the reactor and connected with cables, this is part of the cathode. Cables connected and then connected to the multimeter. For a variety of configurations, reactors connected in series, parallel and series-parallel.

2.4. MFC Experiments

Experiments performed with voltage measurement of MFC systems using a digital multimeter. Before measurements were made, digital multimeter calibrated. Data collection was performed every hour for 24 hours until the cycle is complete. Data in the form of voltage (V) will be processed to obtain the value of current (I) by using Ohm's law, V = IR, the resistance (R) of 100 Ohm. Then the existing data will be used to obtain current density (mA/m^2), which is the current per unit electrode surface area and power density (mW/m^2), the power per unit area of the electrode surface. Before and after the experiment, carbohydrates, fats and proteins content were measured quantitatively. Carbohydrate content calculated using Anthrone sulfate. Protein analysis performed by the Kjeldahl method. Fat analysis performed using Mojoinner method.

2.5. Calculations

Voltage data is extracted from this MFC experiments. Power density (mW/m^2) is the power per unit area of the electrode surface can be calculated by the following Eq. (1).

$$Power\ density\ (mW/m^2) = \frac{I \times V}{A} \tag{1}$$

I (mA) is current, V (mV) is voltage and A (m^2) is electrode surface area. Internal resistance or R_{INT} from electricity source can be calculated using Kirchhoff voltage law for connections voltage source connected to a known external resistance. This principle is used in all fields of physics, because it takes into account the principle of internal loss [3]. For all experiments the polarization, R_{INT} is determined by the first recorded voltage data, correlated with a current per unit area that is connected to the external resistance value that has been known.
R_{INT} is calculated using the Eq. (2) [3]:

$$R_{INT} = \left(\frac{V_{O-C}}{I_L}\right) - R_L \tag{2}$$

Where V_{O-C} is voltage resulted from highest power density in open circuit, I_L is current density and R_L is external resistance used. Maximum power transfer occurs when the load resistance value equal to the value of source resistance, both in series with a voltage source or current source in parallel (Jacobi law). Power transfer is actually comparable with 50% efficiency accepted when R_L (external resistance) = R_{INT} (impedance matching), which is happened when $V_L = \frac{1}{2} V_{O-C}$. In the other side, maximum efficiency will be achieved if $R_L \to \infty$, when power is weak or unstable, energy source external resistance and final efficiency $\eta \to 0\%$ as $R_L \to 0$ Ohm. Then, Coulombic efficiency calculations performed by the following equation [7].

$$\epsilon_{Cb} = \frac{M \int_0^{t_b} I \, dt}{F b v_{an} \Delta COD} \tag{3}$$

Where M is the molecular weight of oxygen, I is currents (A), F is Faraday's constant (9,64853 x 10^4 C/mol), b is the number of elecrons exchanged per mole of oxygen, v_{an} is wastewater volume (L), and ΔCOD is the change in COD over time t_b (g/L) [7]. I is the integration of currents with trapezoid method.

$$I = \int_a^b f(x)\, dx = \frac{h}{2}\left(f_0 + \left(2\sum_{i=1}^{N=1} f_i\right) + f_N\right) \tag{4}$$

3. Result and Discussion

Electron oxidized at the anode and oxygen in the reduced section around the cathode [5]. Eq. (5) explains the reaction that occurs at the anode:

$$nCH_2O + nH_2O \to nCO_2 + 4ne^- + 4nH^+ \tag{5}$$
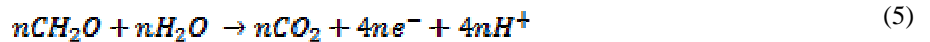
Electrons are transferred to the cathode through copper wires, because there is a potential difference between the anode and cathode. Proton is transferred to the cathode through the electrolyte in the anode and cathode. Proton is around the cathode oxygen reduction in contact directly on the other side of the cathode [5]. Reaction occurs at the cathode shown in Eq. (6):

$$nO_2 + 4ne^- + 4nH^+ \to 2nH_2O \tag{6}$$

Electrons cannot be in a free form, so every oxidation reaction is always accompanied by a reduction reaction. Biological oxidation reaction is catalyzed by the enzyme dehydrogenase. These enzymes transfer electrons and protons are released to the intermediate electron acceptors such as NAD^+ and $NADP^+$ to be formed into NADH and NADPH. Oxidative phosphorylation occurs when high-energy electrons are transferred to the electron transfer chain until eventually captured by oxygen or other oxidants that organic would be reduced to H_2O. High power density created by the migration of electrons and protons fast enough [6]. Rate that occurs not only created because of the reactions that occur at the electrode surface but also due to the presence of mass transfer on the surface of the solution and the electrode surface. Mass transfer can be caused by: 1) diffusion in a concentration gradient; 2) migration when electrical energy is generated; 3) resulting from convection stirring or vibration. Experiments with single chamber batch reactor without stirring, allowing the migration of protons from the anode to the cathode occurs because of diffusion. The existence of concentration gradients or differences in the concentration around the anode zone and the zone between the anode and cathode causes diffusion. In diffusion, protons will move from an area with a high concentration towards low concentrations, so that protons will move from the anode to the cathode. The higher the concentration differences in the substrate, the greater driving force is generated, so that the faster migration of protons to the cathode.

3.1. MFC Substrate

Quantitative test performed on these wastewaters to test the degradation of carbohydrate, protein and fat. These components are the largest component contained in Tempe. Quantitative test in synthetic wastewater for carbohydrate, protein, and fat, respectively are 4.45%; 0.49% and 0.05% while for industrial wastewater, respectively, are 5.96%, 0.49% and 0.06%.

3.2. Voltage Data Processing Results in Single Chamber MFC

The study was conducted by measuring the voltage and current for one batch cycle. Cycle time on MFC is the process of converting organic wastewater into electricity in the MFC system, starting from 24 hours after the preparation of the wastewater until there is stability in the voltage drop and current. On a single batch with a volume of 500 ml, it takes 159 hours for one cycle. Electrical power density in single chamber MFC curve in this experiment is shown in Fig.1.
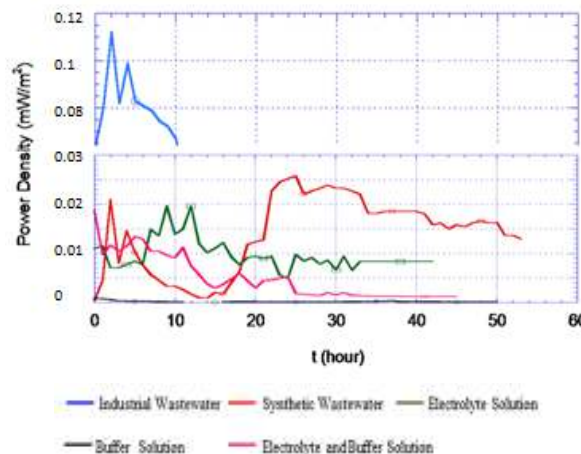
Fig 1. Electrical Power Density in Single Chamber MFC

Highest power density generated by Tempe industrial wastewater was 0.11 mW/m^2 while the power density produced by the synthetic wastewater was 0.02 mW/m^2, hence the power density generated by Tempe industrial wastewater is higher than the synthetic wastewater. This is because the Tempe industrial wastewater substrate is richer in nutrient than the synthetic wastewater.

Power density on the curve above also illustrates that the performance of the MFC is affected by many electrolytes and buffer usage. Electrolyte, buffer and electrolyte-buffer mix, produce a power density of $11x10^{-3}$mW/m^2; 10^{-4}mW/m^2 and 10^{-2}mW/m^2 respectively. In other words, without preparation wastewaters are also potential producers of electricity even when the power density wastewater not generated by the mixture.

The resulting power density is greater than the buffer electrolyte. This is evidence that the electrolyte is able to help improve the power density of the wastewater. While the buffer has a power density that tends to be stable, so it is evident that it serves in addition to stabilizing buffer pH too stabilize the voltage generated during the study.

3.3. Voltage Data Processing in MFC Reactor Configuration Variation

MFC reactor configuration variation study was conducted with four single chamber reactors. Four is the minimum amount of reactors to be able to form a series-parallel configuration. Power density circuits with the best results of the three variations of the circuit being tested on synthetic wastewater will be applied to Tempe industrial wastewater. This study was conducted to each of the configuration to complete one cycle.

Series configuration

Series configuration is an economical configuration if viewed in terms of the economy, because it does not require a lot of cable to connect the reactor to another reactor. Input from the reactor will come from the output of the other reactors, so each reactor could affect the others afterwards. In series circuit, if one component is removed or damaged, the other components will not function properly.

Power density curve of a series configuration is presented in Fig. 2a. MFC connected in series is the configuration with the longest cycle. The length of time it takes to complete one cycle is 125 hours. In the series circuit, the same current passes in each of the reactors. Highest power density in this connection is 5×10^{-3} mW/m^2. Power density and voltage vs. current density curve of a series configuration is presented in Fig. 2b. In the series configuration, the $\frac{1}{2} V_{o/c}$ value obtained is 2.2 mV, so through the calculation using Eq. (2), R_{INT} connection is about 93.8 Ohm, hence the maximum power transfer in series configurations 51.6 %.
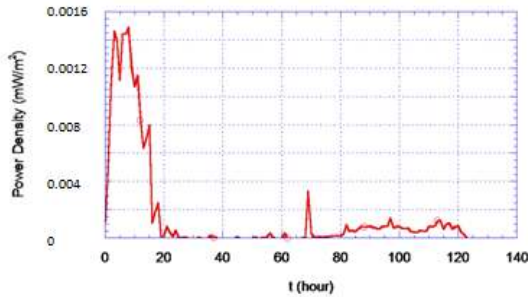
Fig 2a. Power Density Curve in MFC Series Configuration
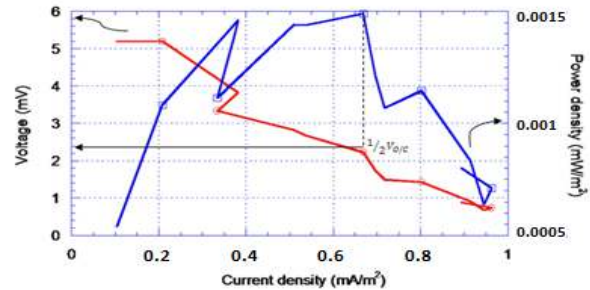
Fig 2b. Power Density and Voltage vs. Current Density in Series Configuration MFC

Parallel Configuration
Parallel electrical circuit is a circuit in which all the component input derived from the same source. This has led to a parallel arrangement of the electrical circuit to cost a lot more (more connecting cables is needed). However, a parallel circuit has advantages compared with the series system, if one of the reactors damaged or removed, then the other reactors still functioning properly. Power density curve of a series configuration is presented in Fig. 3a. Parallel configuration has a 51-hour cycle. In this study, a parallel configuration is a configuration with the shortest time. Highest power density in parallel configuration is 0.13 mW/m^2. In parallel configuration, the $\frac{1}{2} V_{o/c}$ value obtained is 14 mV, so through the calculation using Eq. (2), R_{INT} connection is about 97.45 Ohm, hence the maximum power transfer in parallel configuration is 50.6%. Power density and voltage vs. current density curve of a parallel configuration is presented in Fig. 3b.
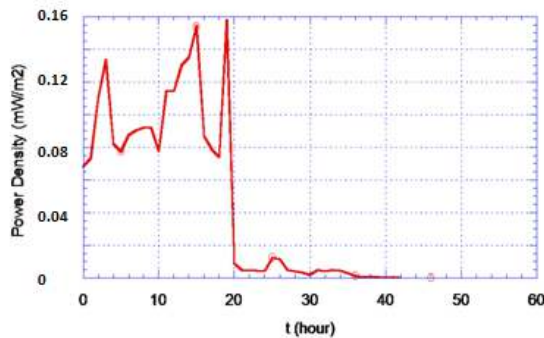
Fig 3a. Power Density Curve in Parallel Configuration MFC
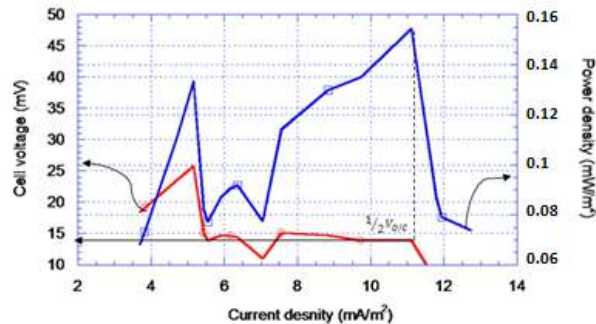
Fig 3b. Power Density and Voltage vs. Current Density in Parallel Configuration MFC

Series-parallel Configuration
Advantages and disadvantages of series-parallelconfiguration which are also contained in this series is a combination of series circuit and parallel circuit, there will be a disturbed system while others do not. Power density curve of a series-parallel configuration is presented in Fig. 4.
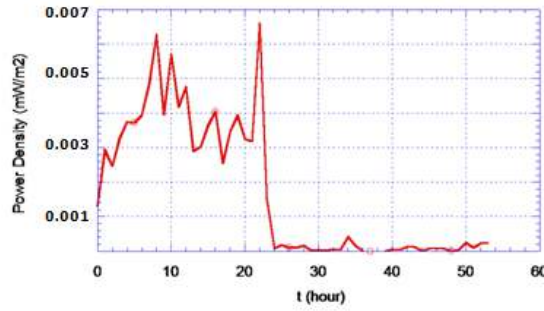
Fig 4. Power Density Curve in Series-Parallel Configuration MFC

Series-parallel configuration takes 53 hours to complete one cycle. In this configuration, highest power density obtained is $6x10^{-3}$ mW/m^2. Power density and voltage relationship in series-parallel connection MFC is shown in Fig. 5.
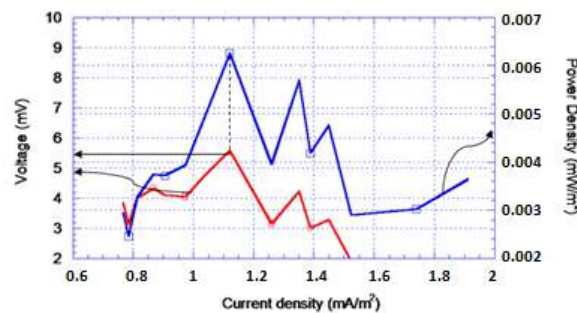
Fig 5. Power Density and Voltage Relationship in Series-parallel Connection MFC

In series-parallel connection, $\frac{1}{2} V_{o/c}$ value is 5.5 mV, so through the calculation using Eq. (2), R_{INT} connection is about 90 Ohm, hence the power transfer maximum in connection is 52.6%.COD removal and coulombic efficiency in MFC configuration shown in Table 1.

Table 1. COD Removal and Coulombic Efficiency in MFC Configuratio

Configuration	COD_{in} (mg/L)	COD_{out}(mg/L)	E_{COD} (%)	Coulombic Efficiency (%)
Series	18450	15681.90	15.00	9.79×10^{-3}
Parallel	19300	15517.90	19.59	0.06
Series-Parallel	18850	15754.40	16.42	0.01

In Table 1, it can be seen that the parallel configuration produced highest coulombic efficiency value and highest efficiency of COD removal value. E_{COD} parameter measures how much fuel is available that has been converted by the MFC, both in strong currents (in the coulombic efficiency) or biomass (in growth yield) or competitive reaction with alternative electron acceptors, such as oxygen, nitrate, and sulfate [7]. Based on calculations, it can be concluded that the parallel configuration of the MFC reactor is capable of converting the organic matter that is available in the substrate into electricity well, which is indicated by a straight comparison between E_{COD} and coulombic efficiency. This is likely due to fluid conductance in the parallel configuration is better than the series configuration or mix so that loss of current (shunt loss) is reduced [3] and make better electron transfer and conversion of organic matter to electricity is also increasing.

Sharp decline in coulombic efficiency on substrates with complex organic matter such as that contained in the wastewater, likely due to the competition of electrons by biomass, dissolved organic products, H_2, and CH_4, if oxygen as an electron acceptor is not desired into the anode. Moreover, H_2 is generally a result of fermentation products will be the electron donor for the methanogens to produce CH_4 [8]. Next in wastewater, fermentation is done by different microorganisms that have higher

growth yield than the anode-respiring bacteria (ARB) [8] and the growth of high yield can make biomass absorbs electrons resulting in lower coulombic efficiency. In some cases, microorganisms that attach to the anode, using the anode as a residence but did not carry out metabolism which electrons move toward the anode as methanogenesis or aerobic respiration. Then, when given the complex organic substrates as fuel, it is estimated that the microorganisms fermented elements into simpler substrates that reducing microorganisms in the microbial community of the anode to oxidize substrates [9]. Although tracking the path of the electrons in the MFC system is important, there have been no experimental studies that quantify the amount of income (loss) of electrons and make the balance of the electron [8].

3.4. Series, Parallel, and Series-parallel Configuration Comparison

Based on the comparison of the highest power density generated from each circuit, parallel circuit is a circuit with the best improvement, so that the circuit will be applied to Tempe industrial wastewater is a parallel circuit. Power density curves of the three series of configuration are presented in Fig. 6.
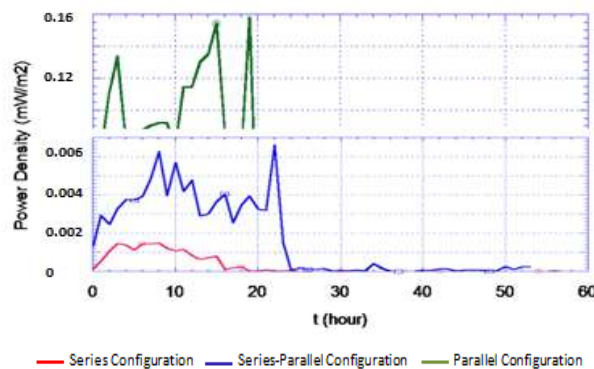
Fig 6. Power Density Curve in MFC Configuration

MFC research using Tempe industrial wastewater with a parallel circuit has a cycle for 64 hours. Highest power density resulting from this configuration was 0.23 mW/m^2. Configuration comparison curve using synthetic wastewater and industrial wastewater is presented in Fig. 7.
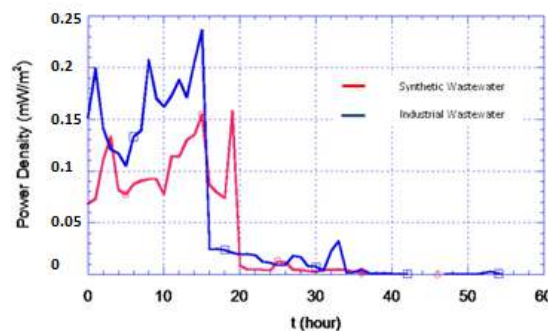
Fig 7. Power Density Curve in Synthetic Wastewater and Industrial Wastewater

In the picture above, it is seen that the power density results in industrial wastewater higher from synthetic wastewater, it is in line with research on single chamber MFC 500 mL, which is caused by the nutrients in the wastewater industry is higher than from the synthetic wastewater.

Value of existing power density is very likely to be improved or can be developed. Increase in power density in MFC can be done in various ways, for example, increase the volume of the reactor on the circuit, multiply the reactor in series, using a continuous circuit so as to ensure a steady flow of substrate to obtain a stable homogeneous condition or perform stirring periodically, changing the shape of the reactor into tubular and so on [6]. COD removal and coulombic efficiency of the parallel configuration shown in Table 2.

Table 2. COD Removal and Coulombic Efficiency in Parallel Configuration

Substrate	COD$_{in}$ (mg/L)	COD$_{out}$ (mg/L)	E$_{COD}$ (%)	Coulombic Efficiency (%)
Synthetic Wastewater	19300	15517.90	19.60	0.06
Industrial Wastewater	16555	11472.70	30.70	0.05

In Table 2, the parallel configuration of the MFC reactor is capable of converting the organic matter into electricity well. Even with industrial wastewater substrates, coulombic efficiency of the parallel configuration of the MFC system is not decreased much.

In domestic wastewater, most of the organic nitrogen is converted to ammonia in anaerobic decay and become nitrate or nitrite on aerobic decomposition [10]. Nitrate will act as an electron acceptor that electricity generation is not only captured by oxygen MFC for electricity production system but also will compete with nitrate. In addition, tempe industrial wastewater has suspended solid particles that more than tempe synthetic wastewater. More solid particles contained in the tempe wastewater because many used and other supplementary materials are added by manufacturers such as yeast. The tools used are also not cleaned on a regular basis so that the possibility of contamination by substances or bacteria from the process can occur [10]. Solids that remain in the original wastewater will reduce oxygen diffusion from the cathode to the MFC system and causes oxidation by other electron acceptors, biomass production, and fermentation [10]. The solid particles also increases the internal resistance of the MFC system that will reduce electricity production [11].

3.5. Comparison of Single Unit and Parallel Configuration with Total Constant Volume

Electricity generated by single unit MFC reactor with volume 2000 mL and four reactors in parallel connection with the same total volume, that is 2000 mL, is compared. Observations are shown in Fig. 8.
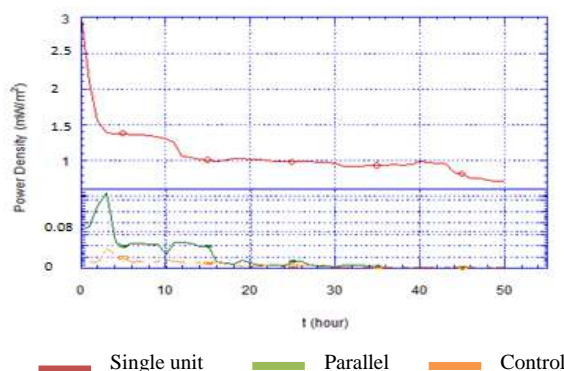
Fig 8. Power Density Curve in Parallel Configuration and Single Unit MFC

In Fig. 8 shown that maximum power density generate those produced by the reactor with a parallel configuration in the same volume, namely 3.03 mW/m^2. In a large volume of wastewater, the organic content that can be degraded by microbes are also many more so that more electrons can flow. Even so, it can be seen in Fig.8 that the value of the resulting power density reactor with a volume of 2000 mL decreased rapidly and stabilized at the 40th hour to the 44th hour. Many of the reactor with a large volume that has not been well designed in terms of total surface area of the electrode or the distance between the electrodes. In addition, when the substrate is completely consumed in the anode, there will be excessive biomass production in the cathode chamber and cause build-up that interferes with the diffusion of oxygen from the air through the cathode [7].

Although the reactor with a large volume generated higher electricity production, greater volumes require high operating costs and also impractical. Data and further research is needed to determine the performance of MFC reactors with a large volume [6]. Power density and voltage vs. current density in single unit and parallel configuration MFC using synthetic wastewater curve is depicted in Fig. 9.
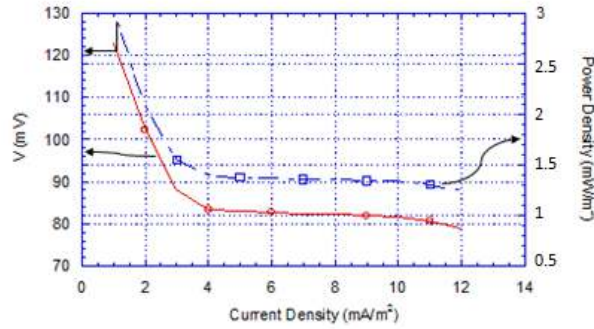
Fig 9. Power Density and Voltage vs. Current Density in Single Unit and Parallel Configuration MFC using Synthetic Wastewater

Using Eq. (2), the $\frac{1}{2}V_{o/c}$ value obtained is 121 mV so RINT connection gets lower, which is about 5.77 Ohm. Hence the maximum power transfer is higher, 106.1%. Power density and voltage vs. current density in single unit and parallel configuration MFC using industrial wastewater curve is depicted in Fig. 10.
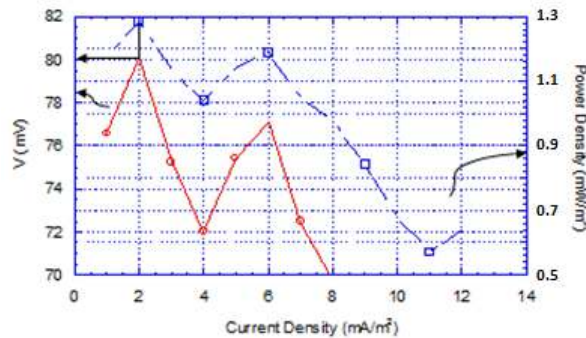
Fig 10. Power Density and Voltage vs. Current Density in Single Unit and Parallel Configuration MFC using Industrial Wastewater

Using Eq. (2), the $\frac{1}{2}V_{o/c}$ value obtained is 80 mV and the R_{INT} connection is about 3.64 Ohm. Hence the maximum power transfer is lower than using synthetic wastewater, 104%. COD removal and coulombic efficiency in this experiment shown in Table 3.

Table 3. COD Removal Efficiency and Coulombic Efficiency in Parallel and Single Unit

Configuration	COD_{in} (mg/L)	COD_{out}(mg/L)	E_{COD} (%)	Coulombic Efficiency (%)
Parallel (4 x 500 mL)	19300	15517.90	19.59	0.06
Single unit (2000 mL)	19450	15675	19.41	0.14

COD removal efficiency value in parallel configuration MFC is higher than the single unit parallel configuration, but the opposite occurs in the value of coulombic efficiency. In the MFC reactor configuration, one of the limiting factors in the production of electricity is the ohmic loss. Ohmic loss occurs because of resistance to the flow of ions in the electrolyte and the flow of electrons through the electrode [2]. Ohmic loss is dominated in series or parallel connection or stacked/stack MFC [3]. In addition, the ohmic loss is also affected internal resistance is affected by the microbes themselves (which is resistive in nature) and the rate of metabolic reactions that affect the conductivity of the solution around the anode [3].

3.6. Nutrition Amount and Voltage Relationship in MFC

In the reactor, the bacteria grow to form a suspension that can be seen the level of turbidity (turbidity). The more bacteria, the more nutrients in the substrate consumed. A large number of nutrition cause bacteria to grow more rapidly enabling a growing number of protons and electrons resulting from metabolic processes, so that the greater the voltage generated.

In this study, batch system is used so that no nutrients were added to the reactor, in other words, the amount of nutrients in the reactor is fixed. Only the metabolic processes of bacteria can cause changes in the amount of nutrients in the reactor. Proof of this is done with a quantitative assay substrate before and after the experiment took place. Wastewater is used for this test is synthetic wastewater. Quantitative test results carbohydrate, fat and protein on synthetic substrates wastewater before experimentation was 4.45%, 1.49%, and 0.05%, while for the synthetic wastewater after experimentation was 4.31%, 0.87% and 3×10^{-3}%.

Quantitative test of carbohydrates, fats and proteins after the experiment using the same method with the quantitative test before the experiment, the test with Anthrone carbohydrates, protein by Kjeldahl test and test with Mojoinner fat. Jutono (1981) stated that a bacterium has an enzyme that can hydrolyze polysaccharides, such as starch into simple sugars. Some bacteria are known to have biochemical properties include hydrolysis of fats, proteins and carbohydrates as well as the reduction of a variety of elements. The image below is a hydrolysis cycle that occurs in carbohydrate, protein and fat in the microbial fuel cell.

The result of the third test is the reduction of the nutrient content before and after the experiment. This is in accordance with the conditions of the voltage drop towards the close of the cycle. Here is a picture that presents the phenomenon of voltage drop across the parallel circuit experiments with industrial wastewater. Voltage drops curve in parallel configuration is shown in Fig. 11.
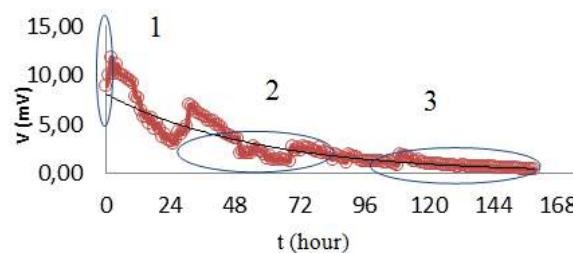
Fig 11. Voltage Drops in Parallel Configuration using Industrial Wastewater

In addition to showing the voltage drop across the system, the above picture also shows a pattern of bacterial growth curve with three phases is skipped. Bacteria need time to adapt to the new environment, because that's before the experiment started, first settling substrate overnight with conditions resembling the conditions maintained in the reactor. The bacterial phase consists of three phase. Phase 1, the adaptation phase, the bacteria will start to multiply after 24 hours. The number of bacteria is characterized by a high voltage results. Then with the displacement of the mixing container into a conditioned anaerobic reactor, indirectly eliminated aerobic bacteria, so the bacteria can survive is a facultative anaerobic and aerobic. Phase 2 is the exponential phase, the second phase of the process of bacterial growth. In this phase, the bacteria undergo binary fission. After the nutrients reduced the bacteria will undergo a phase where they lose viability or stop growing. In this phase the number of bacteria usually seen stationary on the charts, but the actual cells that are still dividing or die has not been determined. If the incubation of these systems continue to proceed without the replacement or addition of nutrients as the limit of the growth phase of the bacteria will experience the death of a nature contrary to current geometric or exponential growth phase. Phase 3 is the phase of polarization, where there are many internal obstacles so that electrons and protons are still difficult to perform the migration. This is due to a drastic decrease in nutrition followed by a decrease in the number of bacteria. This phase is also called the deaths of the phase [12]. From the above experiments, it can be concluded that the nutrients in the substrate was instrumental in MFC experiments. MFC experiments can also be run even if only using wastewater only. This is evidenced by the correlation between nutrition, the amount of bacteria and voltage.

4. Conclusion

On the variation of the reactor circuit configuration, the circuit with the greatest power density generated by the parallel circuit (13×10^{-2}mW/m^2) was followed by a series of mixtures (6×10^{-3}mW/m^2) and a series circuit (5×10^{-3}mW/m^2). Industrial wastewater produces more electricity than synthetic wastewaters with a power density of each wastewater were 0.23mW/m^2 and 0.13 mW/m^2. Industrial wastewater produces more electricity than synthetic wastewater as industrial wastewater contains more nutrients than synthetic wastewater; it is evidenced by a quantitative test of the wastewater. Carbohydrate, protein and fat contained in the wastewater industry is 5.96%, 1.49%, and 0.06%, while contained in synthetic wastewater was 4.45%, 1.49%, and 0.05%. MFC systems can reduce wastewater content as evidenced by a decrease in the concentration of nutrients in the wastewater before and after experimentation and also by the COD removal efficiency. Carbohydrate, protein and fat contained in the wastewater before the experiment was 4.45%, 1.49% and 0.05%, while the wastewater after the experimentation was 4.31%, 0.87% and 3×10^{-2}%. Highest COD removal efficiency resulted in parallel configuration, which is 19.59% and these data shows that MFC could be use as wastewater treatment technology.

Power transfer is produced higher in series-parallel (52.6%) followed by the series circuit (51.6%) and then parallel (50.6%). Parallel configuration produced highest coulombic efficiency compared to the other configurations, which is 0.06% However, the measurement of electricity production in the one MFC reactor (single unit) with the same total volume, power density up to 3.03 mW/m^2 with coulombic efficiency values are also higher at 0.14%.

Reference

1. Mohan, S. Venkata. Ragahavulu, S. Veer. Sarma, P.N. 2008. Biochemical evaluation of bioelectricity production process from anaerobic wastewater treatment in a single chambered microbial fuel cell (MFC) employing glass wool membrane. *Biosensors and Bioelectronics*.Vol. 23:1326–1332. India: Elsevier.
2. Du et al., 2007. A state of the art review on microbial fuel cells: A promising technology for wastewater treatment and bioenergy. ScienceDirect Biotechnology Advances 25: 464-482.
3. Ieropoulos, I., J. Greenman, et al. 2008. Microbial fuel cells based on carbon veil electrodes: Stack configuration and scalability. International Journal of Energy Research. Vol 32, No. 13: 1228-1240.
4. Novitasari, Deni. Optimasi Kinerja Microbial Fuel Cell (MFC) untuk Produksi Energi Listrik Menggunakan Bakteri *Lactobacillus bulgaricus*. Fakultas Teknik Universitas Indonesia. 2011.
5. Kim et al. 2008. Microbial Fuel Cells: Recent Advances, Bacterial Communities and Application beyond Electricity Generation. Korean Society of Environmental Engineers. Environ. Eng. Res. Vol. 1, No. 2: 52~65.
6. Rabaey, K., and Verstraete, W. 2005. Microbial fuel cell: Novel biotechnology for energy generation. Trends.Biotech. 23: 291-298.
7. Logan, B.E., P. Aelterman, B. Hamelers, R. Rozendal, U. Schröeder, J. Keller, S. Freguiac, W. Verstraete, K. Rabaey. 2006. Microbial fuel cells: methodology and technology. *Environ. Sci. Technol.* 40(17):5181-5192.
8. Lee, H.-S., et al., 2007. Evaluation of energy-conversion efficiencies in microbial fuel cells (MFCs) utilizing fermentable and non fermentable substrates. Water Res. (2007), doi:10.1016/j.watres.2007.10.036
9. Lovley, D.R. 2008.The microbe electric: conversion of organic matter to electricity. *Current Opinion in Biotechnology*2008, 19:1–8.
10. Drapcho, Caye M., Nuan, Ngiem Phu., dan Walker, Terry H.,2008. *Biofuels Engineering Process Techmology*. McGraw-Hill Companies:USA.
11. Liu, H, et al. 2008. Scale-up of membrane-free single-chamber microbial fuel cells. *Journal of Power Sources*179 : 274–279 Larminie, J. and Dicks, A. 2000. *Fuel cell systems explained* 2nd ed. John Wiley & Sons, Chichester. p. 308.

The International Conference on Chemical Engineering UNPAR 2013

Increased Lipase Activity with the Addition of Oil and Surface Tension-Lowering Ingredients

Dwina Moentamaria*, Achmad Chumaidi, Profiyanti H. Suharti

Chemical Engineering Department – State Polytechnic of Malang (POLINEMA), Malang – 65141, Indonesia
* Corresponding author. Tel.: +62-341-404424; fax: +62-341-404420. E-mail address*: dwina_mnt@yahoo.com*

Abstract

Diversity of the using of microbial lipases is more widely, especially in the food industries; pharmaceutical industries; paper industries; and tannery. Lipase is able to perform the hydrolysis reaction and transesterification on various specific substrates. In previous studies, lipase produced by *Mucor miehei* microbes has low activity and only reached 100 U/ml. Thus, this research was conducted to exploit the lipase to produce high activity. Method to increasing the lipase activity conducted through the modification of growing media from *Mucor miehei*. Modification of growing medium is done with the addition of oil and the surface tension-lowering ingredients. Temperature of incubation also used as variable in this research. The growing medium used are: 1) pepton, KH_2PO4, $FeSO4.7H2O$, Potato Dextrose, 2) pepton, KH_2PO_4, $FeSO_4.7H_2O$, olive oil, coconut oil, palm oil, 3) medium II plus surfactant (Tween 80) as surface tension lowering ingredients. *Mucor miehei* was inoculated on each medium and placed in an incubator shaker at 150 rpm for 6 days. The results are separated between cell biomass and crude supernatant. The supernatant was known as crude lipase. The relative lipase activity of crude lipase was obyained at temperatures 30, 35, 40, 45, and 50°C. The results showed an increase in lipase activity to 4-fold ie 400 U / ml with the addition of olive oil, coconut, palm oil and Tween 80. Best Relative lipase activity 100%, obtained at a temperature of 40°C incubation.
Keywords: lipases, surface tension, oil, *Mucor miehei*

1. Introduction

Lipases (triacylglycerol acyl hydrolases EC: 3.1.13) are ubiquitous enzymes, which are found in animal, plants, fungi and bacteria. Commercially useful lipases are usually obtained from microorganisms that produce a wide variety of extracellular lipases. Some important lipase-producing bacterial genera are *Bacillus, Pseudomonas and Burkholderia* and fungal genera include *Aspergillus, Penicillium, Rhizopus, and Candida*. Different species of yeasts belonging to seven different genera include *Zygosaccharomyces, Pichia, Lachancea, Kluyveromyces, Saccharomyces, Candida,* and *Torulaspora* [8, 23, 17, 26]. Most of industrial microbial lipase is derived from fungi and bacteria were listed in Table 1.

Lipases find promising applications in organic chemical processing, detergent formulations, synthesis of bio-surfactants, the oleo chemical industry, the dairy industry, the agrochemical industry, paper manufacture, nutrition, cosmetics, and pharmaceutical processing. Lipases had a wide range application, due to their ability towards extremes of temperature, pH and organic solvents. Some unique properties of lipase such as their specificity, pH dependency, activity in organic solvents and nontoxic nature leads to their major contribution in the food processing industries [21]. Many lipases are active in organic solvents where they catalyze a number of useful reactions including the hydrolysis and synthesis of esters formed from glycerol and long-chain fatty acid. Lipases can also catalyze reverse reactions, such as esterification and trans-esterification, in non-aqueous environments. Lipases are activated only when adsorbed to an oil-water interface and do not hydrolyze dissolved substrates in bulk fluid. Balashev, et. al. (2001) has studied the phenomenon how lipases and oil (lipid) interact at the interface. Lipase acts on the substrate in a specific or nonspecific manner. The hydrophobic patches on the surface of lipases are responsible for the strong interactions with the hydrophobic substrates at the interface

---

* Corresponding author. Tel.: +62-341-404424 ; Fax: +62-341-404420
E-mail address: dwina_mnt@yahoo.com

Moentamaria (2009) has produced lipases from *Bacillus subtilis* and *Mucor miehei* and have been using it to catalyze the biodiesel production from *kapok* oil. This study found that lipases produced from *Mucor miehei* more stable and has high activity than lipases from *Bacillus subtilis*. The best activity of lipases obtained from *Mucor miehei* only reached 100 U/ml.

Table 1. Microbial source of lipases and their applications

Microbial Type	Microorganism	Applications	References
Fungal	*Candida rugosa*	Hydrolysis triglyceride in the paper industry	[11]
	Colletrichum gloeosporioides	Hydrolysis triglyceride	[3]
	Rhizomucor miehei	Surfactants for baking industry	[9]
	Mucor miehei &Rhizopus arrhizus	Production of flavour ester	29
	Burkholderia cepacia	Organic synthesis	[11]
Bacterial	*P. alcaligenes*	Detergent additive	[11]
	P. mendocina	Detergent additive	[11]
	Ch. Viscosum	Organic synthesis	[11]
	Candida rugosa	Hydrolysis triglyceride in the paper industry	[11]

This study was conducted to obtain lipase with higher activity. Sharma et. al (2001) claim that the production of lipases is mostly inducer dependent, in many cases oils act as good inducers of the enzyme. Sharma et. al (2001) also stated that components such as olive oil, oleic acid, tween 80 seem to play an essential role in lipase synthesis. Thus, this research was conducted in order to exploit the lipases to produce higher activity. Methods to increase the lipase activity conducted through the modification of Mucor miehei growing media. Modification of the growing medium is done with the addition of oil and Tween 80 as a surface tension-lowering ingredient.

2. Materials and Methods

2.1. Micro-organisms

Mucor miehei was obtained and identified by Bioprocess Laboratory of State Polytechnic of Malang (POLINEMA) Indonesia. The fungus was deposited in the Bioprocess laboratory under the accession number MM072009.

2.2. Strain conservation

A *Mucor miehei* strain was obtained from Bioprocess Laboratory of POLINEMA and was maintained at 3.9% Potato Dextrose Agar (PDA). The tubes incubated at 40^0C for 4 days regenerated from the old strain. After dilution, spore suspension (about 10^6 per ml) was prepared and used as inoculum.

2.3. Culture conditions

Mucor miehei strain was cultured in Erlenmeyer containing 1000 ml of culture medium consisting of (1) 5% peptone, 1% KH_2PO_4, 0.001% $FeSO_4.7H_2O$ [base medium] plus 17% Potato Dextrose (called as Medium I), (2) Base medium + 1% olive oil, 1% coconut oil and 1% palm oil (called as Medium II), and (3) Base medium + 1% olive oil, 1% coconut oil, 1% palm oil, and 0.05% Tween 80 (called as Medium III).

The initial pH of culture medium was adjusted at 6.0. After inoculation with 1 ml spore suspension, growth temperature was held at 40^oC and shaken at 120 RPM. At 24 hour interval, the culture was filtered and the mycelium harvested was used for the necessary growth studies. To maximize the

separation, the filtrate was centrifuged at 4500 x g for 30 min. The filtrate was known as the source of the extracellular lipase or crude lipase.

2.4. Growth studies

After filtration, the residual substances, called as mycelium, were dried with Whatman paper at 105°C within 12 h and weighed until its weight constant. Before used, the Whatman paper was dried until its weight constant. Growth studies were held during 6 days with time interval 24 h. The dry cell weight was plotted with time to find the growth curve of *Mucor miehei*.

2.5. Determination of lipases activity

Crude lipases activity determination was carried out titrimetrically (using procedures adapted from Abbas, et. al, 2002). 2ml *kapok* oil and 1 ml buffer phosphate pH 7 was added to 1 ml enzyme. This mixture was incubated at 40°C and shaken at 120 rpm for 30 minutes. Phenolphthalein was used as indicator and 0.1 M NaOH was used as titrant. One unit of lipase activity was defined as the release of 1 μmol of fatty acid per minute under these conditions.

2.6. Determination of temperature and pH effects on the lipases activity

The optimal temperature for enzyme activity was determined by incubating the reaction mixture at 30, 35, 40, 45 and 50°C. Controls were performed with boiled enzyme. The mixture of 2 ml kapok oil, 1 ml buffer phosphate pH 7, and 1 ml enzyme was incubated at those various temperatures and shaken at 120 rpm for 1 hour. Activity determination was carried out titrimetrically with the same condition as 2.5.

3. Results and Discussion
3.1. Growth curve

The growth curve is used to determine the phase of growth of micro-organisms as the basis for production of cell and enzyme. The growth curve is also used as the basis for producing fermentation products that use these micro-organisms. Yuneta & Putra (2009/2010) and Ardiyansyah (2009) have obtained growth curve of *Bacillus subtilis*. The curve shows that B. subtilis has an exponential phase after 8 hours of incubation. This curve also used as reference for the production of lipases and the subsequent fermentation process. Other researchers have introduced the growth curve of *Streptomyces gulbargensis* that used to produce lipase in L-asparaginase production from fermentation of extract groundnut cake [12]. In this study, the growth curve of *Mucor miehei* strains was obtained from three different types of culture medium. The culture medium consisted of 5% peptone, 1% KH_2PO_4, and 0.001% $FeSO_4.7H_2O$ as base medium. The composition of each culture medium is shown in Table 2.

Table 2. Ingredients of Culture Medium

Type	Ingredients
Base medium	5% peptone, 1% KH_2PO_4, and 0.001% $FeSO_4.7H_2O$
Medium I	Base medium + 17% Potato Dextrose
Medium II	Base medium + 1% olive oil + 1% coconut oil + 1% palm oil
Medium III	Base medium + 1% olive oil + 1% coconut oil + 1% palm oil + 0.05% Tween 80

Figure 1 shows the growth curve of *Mucor miehei* in different culture medium. All curves show the same pattern in the lag phase, exponential phase, and stationary phase. Lag phase in all culture medium ended around 72-96 hours, but the dry cell mass obtained in each culture medium has different value. After 96 hours incubation period, the amount of dry cell mass in each culture medium respectively 0.3653, 0.454, and 0.5823 mg/ml. This difference was due to a number of carbon sources on each culture medium. Carbon was known as macro elements in the growth of the micro-organisms.

The ingredients of cultural medium that indicated as carbon sources in this study are coconut oil, palm oil, olive oil and Tween 80 (Polyoxyethylene (20) sorbitan monooleate). The largest component of coconut oil is lauric acid (C12) and myristic acid (C14), approximately 54% and 17.4%. The largest component of palm oil is oleic acid (C18.1) – 41.1% and palmitic acid (C16) – 35.5%, while olive oil has oleic acid (C18.1) – up to 83% and palmitic acid (C16) – up to 20%. Thus, it can be concluded that medium III has the most carbon sources than another culture medium. This causes the rate of growth of *Mucor miehei* in media III increased, as indicated by the highest number of dry cell mass at the end of exponential phase.
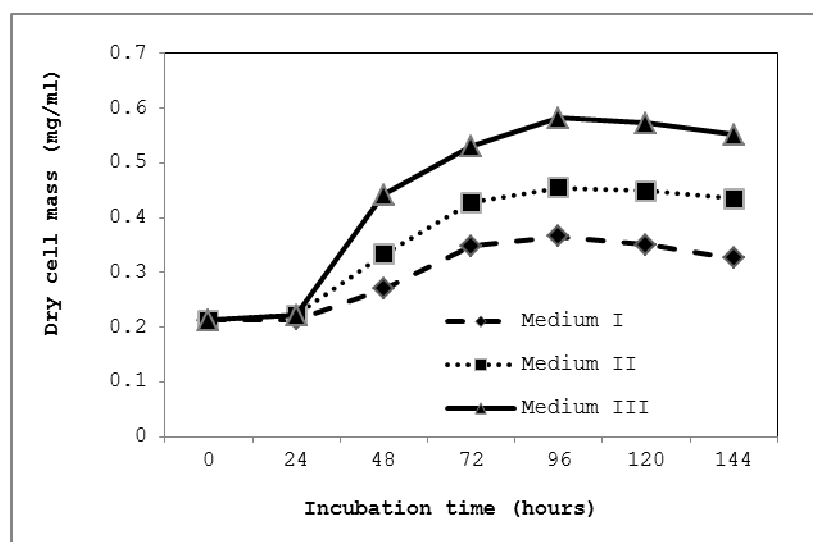
Fig 1. Growth curve of *Mucor miehei* in different culture medium

3.2. The effect of the addition oil and Tween 80 as surface tension lowering ingredients to lipases activity

Extracellular lipases are found in the culture broth when the fermentation is at the end of the exponential phase. Easily lipases can be induced since they are produced by the presence of oily materials or other sources as surfactants, fatty acids, some esters, glycerol and biliary salts [25]. This study uses *Mucor miehei* to produce crude lipases, at the end of the exponential phase or 96 hours as mentioned in point 3.1. Culture medium used in this study consisted of carbohydrates (potato), glucose (dextrose), oil (coconut, palm), and surfactant (Tween 80) as carbon sources. Figure 2 shows the lipase activity in standard culture medium and standard culture medium plus different oil and surfactant. Standard culture medium consisted of combination of carbohydrates and 17% glucose. Lipases in these standard medium had activity around 100 U/ml, while lipases in standard medium plus coconut oil was increased to 122 U/ml.

Uscategui have examined the use of glucose as a carbon source for lipase production. There was a cell growth inhibition at higher glucose concentration (above 5 g/l). The concentrations of glucose that favor the obtention of an acceptable growth of *P. aeruginosa* were 3 % and 5 %. This result agrees with Ito et. al (2001), who found that cell growth of *Pseudomonas aeruginosa* LST - 03 was affected by both glucose and ammonium concentration. In the same way, Takac & Marul (2008) stated that the high concentrations of glucose suppress the lipolytic activity. On the other hand, Beyenal et.al (2003) and Gupta, et. al (2004) pointed out that glucose in small amounts is necessary for the initial growth phase of microorganisms for the releasing of extracellular lipase.

The effect of oil and surfactant in the media can be seen also in Fig. 2. The addition of coconut oil on the standard culture medium has produced lipase with the lowest activity compared with palm oil or olive oil. Lipases activity in coconut oil which is added to the standard culture medium was 122 U/ml, whereas the additions of palm oil and olive oil respectively give 147 U/ml and 192 U/ml. This is due to differences in types of the largest component of each of these oils. Coconut oil mainly

contains of lauric acid (C12), while palm oil contains palmitic acid (C16) and olive oil contains oleic acid (C18.1). A large number of carbon sources will provide a significant increase in lipases activity. The addition of olive oil has shown the most significant effect of the increase in lipase activity. However, the effect was reduced when olive oil was added along with coconut oil and palm oil. This condition indicates that the micro-organisms taking nutrients derived from carbon sources that fit their
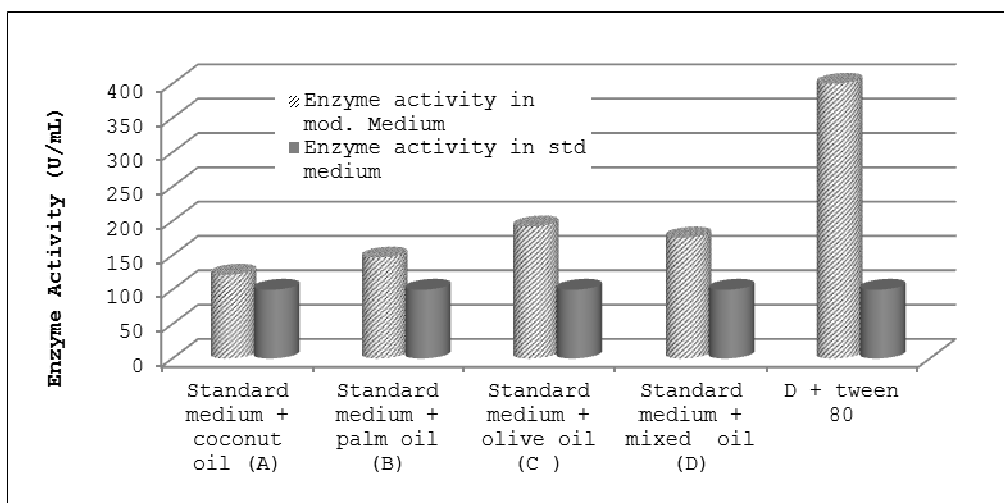
needs.
.

Fig 2. Comparison of lipases activity in standard medium and standard medium plus oil and surfactant

The use of coconut oil, palm oil, and olive oil, simultaneously or respectively, were able to improve lipases activity almost doubled compared to lipases activity without the addition of oil. This is because the oil has a role as an inducer. The production of lipases is mostly inducer dependent, and in many cases oils act as good inducers of the enzyme. Certain other inducers also have a profound effect on the stimulation of lipase production [21]. Previous studies have found the same conditions. Some of them are (1) Manikandan (2004) has conducted Lipase production by *B. sphaericushas* with sesame oil as an inducer and give maximum lipase activity, about 5.2 μmoles/mL.min, (2) Sharma, et. al (2001) has been shown to secrete extracellular lipase from the yeast *Candida rugosa*, upon induction by fatty acid, (3) Chang, et. al (1994) revealed that the presence of tween 80 and tween 20 in a culture medium not only promoted lipase production but also alter the production of various forms in cultured *C. rugosa*

The effect of the addition of Tween 80 was also seen in this study. The combined use of coconut oil, palm oil, olive oil, and 0.05% Tween 80 in medium III, has increased lipase activity 4-fold compared to the lipases activity in medium I. Tween 80 also giving rise lipase activity approximately 2-fold over the media II which is not used Tween 80. The maximum lipase activity of 400 U/ml was obtained when Tween 80 was added in the medium II. Tween 80 is a nonionic hydrophilic surfactant. Tween 80 has the ability to reduce the surface tension of the liquid. The surface tension of the liquid was formed by the attractive forces between molecules in a liquid with molecules of air above it. Tween 80 could break the force that holds the liquid molecules at the interface so that the surface tension will be reduced. This ability is due to the high value hydrophilic -lyophilic balance (HBL) of Tween 80. Tween 80 has a HBL value of about 15, which led Tween 80 is more soluble in water [13]. 0.05% of tween 80 was used in this study was able to attract the extracellular lipase enzymes from the surface and disperse into solution, so that the highest of lipase activity can be obtained. This result agrees with the studies of Nahas, 1987 and Dominiquez, et. al (2003), who used Tween 20, Tween 80 and Tween 100, and found the improvements on lipase production, although the results depend on the type of Tween used.

Kinetics of microbial product formation can be categorized into three classifications, namely (1) Growth Associated Product Formation, (2) Non-Growth Associated Product Formation, and (3) Mixed Mode Product Formation [22]. In this study, the kinetics of lipase formation from *Mucor miehei* can be classified as Growth-associated product formation. Product was formed simultaneously

with the growth of cells. The specific rate of product formation is proportional to the rate of cell growth. Fig. 3 was describes the production of lipase (shown by lipases activity) and microbial growth of *Mucor miehei* in three different types of medium. As mentioned before, coconut oil, palm oil, olive oil and Tween 80 were able to significantly increase the cell biomass and lipases activity. Growth pattern -associated product was also obtained by (Abbas, Hiol, Deyris, & Comeau, 2002) in produce extracellular lipase from *Mucor sp* strain. Abbas, et. al (2002) was obtained maximum lipase activity at 57 U/ml, with a medium consists of 4.5% peptone, 1.4 % KH_2PO_4, 0.24% K_2HPO_4, 0.04% $MgSO_4$. Compared with the results of this study, the use of coconut oil, palm oil, olive oil as inducer and Tween 80 as a surfactant can increase lipase activity approximately by 7-fold, to 400 U/ml. This activity was obtained at the maximum incubation time in 4 days (96 hours). The oil concentration for optimal biomass growth was 3 %, but the optimal production of lipase depends on the kind of oil was used. Inducer and surfactant were used to help in providing the requisite interface area.

3.3. Effect of temperature on stability of lipases

The research was carried out at pH 6 to see the stability of lipases at temperatures 30, 35, 40, 45 and 50°C. In accordance with point 2.7, the lipase activity was measured to obtain relative activity. Table 3 below has shown the influence of temperature on the activity of lipases, obtained after the end of the heating process. Growth of *Mucor miehei* on previous study has shown optimum temperature in 40°C [15]. As seen in Table 3, the optimum temperature conditions of the extracellular lipase enzyme was obtained at 40°C. At this temperature, lipases activity was remained relatively stable, after 1 hour incubation. Gulyamova & Davranov (1995) was stated that the temperature has a substantial influence on the activity of an enzyme – influencing, on the one hand, the rate of enzymatic reactions and, on the other hand, the stability of the enzyme. This study has shown that lipases from the fungus Mucor miehei is stable at 50°C for 5 hours.

(a)   (b)   (c)
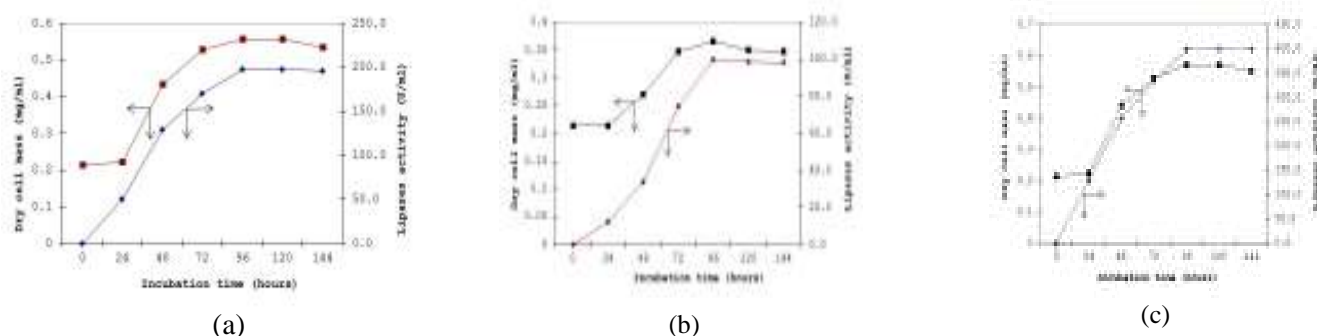
Fig 3. Microbial products (*Mucor miehei*) at Мedıum I (a), Medium II (b) and Medium III (c).

Table 3. Effect of temperature on stability of lipases

Temperature (°C)	Relative lipases activity (%)
30	58
35	81
40	100
45	73
50	47

4. Conclusion

Olive oil, coconut oil, palm oil has been able to increase lipase activity doubled when compared to using media-substrate Potato Dextrose. The oil acts as an inducer and derived from materials that contain a lot of carbon. If the surfactant was added to the oil, the lipase activity being 4-fold when compared to lipase activity produce with media-substrate Potato Dextrose. The growth of *Mucor miehei* can be categorized as growth associated product, whereas the lipase production remained stable at 40 ° C, same with an optimum growth temperature.

Acknowledgements

References

[1] Abbas, H., Hiol, A., Deyris, V., & Comeau, L. (2002). Isolation and Characterization of an Extracellular Lipase from Mucor sp strain Isolated from Palm Oil. *Enzyme and Microbial Technology 31*, 968-975.

[2] Ardiyansyah, Y. (2009). *Isolasi dan Karakterisasi Enzym Xilanase dari Bacillus Subtilis pada Media Nutrien Broth dengan Penambahan Xilan hasil Isolasi Jerami Padi.* Semarang: Jurusan Kimia, Fakultas MIPA, Universitas Diponegoro.

[3] Balaji, V., & Ebenezer, P. (2008). Optimization of extracellular lipase production in Colletotrichum gloeosporioides by solid state fermentation. *Indian Journal of Science and Technology, Vol. 1 No.7.*

[4] Balashev, k., Jensesn, t., Kjaer, K., & Bjornholm, T. (2001). Novel methods for studying lipids and lipases and their mutual interaction at the interface: Part 1. *Atomic Force microscopy. Biochimie*, 83:387-97.

[5] Beyenal, H., Chen, S., & Lewandiwski, Z. (2003). The double substrate growth kinetics of Pseudomonas aeruginosa. *Enzyme Microbiol Technol*, 92-98.

[6] Chang, R., Chow, S., & Shaw, J. (1994). Multiple Forms and Function of Candida Rugosa Lipase. *Biotechnol Appl Biochem, 19*, 93-97.

[7] Dominiquez, A., Costas, M., Longo, M., & Sanroman, A. (2003). A novel Application of solid state culture: production of lipases by Yarrrowia lipolytica. *Biotechnol lett.*, 25 (15): 1225-1229.

[8] Gupta, R., Gupta , N., & Rathi, P. (2004). Bacterial Lipases: An overview of production, purification and biochemical properties. *Appl. Microbiol. BioTechnol., 64*, 763-781.

[9] Herrgard, S., Gibas, C., & Subramaniam, S. (2000). role of electrostatic network of residues in the enzymatic action of Rhizomucor meihei lipase family. *biochemistry*, 2921-2930.

[10] Ito, T., Kikuta, H., Honda, H., & Ogino, H. I. (2001). Lipase production in two steps fed-batch culture of organic solvent-tolerant Pseudomonas aeruginosa LST=03. *J Biosci Bioeng*, 91 (3): 245-250.

[11] Jaeger, K.-E., & Reetz, T. (1998). Microbial lipases from versatile tools for biotechnology. *Trend Biotechnol. 16*, 396-403.

[12] Kattimani, L., Amena, S., Nandareddy, V., & Mujugond, P. (2009). Immobilization of Streptomyces gulbargensis in Polyurethane Foam : A Promising Technique for L-asparaginase Production. *Departement of Microbiology, Gulbarga university, Gulbarga-585106, karnataka, India, IRANIAN JOURNAL of BIOTECHNOLOGY Vol 7.*

[13] Kim, H. J., Kim, S. B., & Kim, C. J. (n.d.). The effect of ninionic surfactants on the pretreatment and enzymatic Hydrolysis of Recycled Newspaper.

[14] Manikandan, K. (2004). *optimixation of Media for Lipases Production by bacillus sphaericus.* Annamalai Nagar: M tech Thesis, Annamalai University.

[15] Moentamaria, D. (2009). Amobilisasi enzyme Lipase dari Bacillus Subtilis untuk produksi biodiesel dari Minyak Randu. Bandung.

[16] Nahas, E. (1987). Control of lipase production by Rhizopus oligosporus under various growth conditions. *J Gen Microbiol*, 134 (1): 227-233.

[17] Romo-Sanchez, S., Alves-Baffi, M., Arevalo-Villena , M., Ubeda_Iranzo, J., & Briones-Perez, A. (2010). Yeast biodiversity from oleic ecosystems: Study of their biotechological properties. *Food Microbiol., 27*, 487-492.

[18] Semeriva, M., & Dufour, C. (1972). further Study on The Extracellular Lipase of Rizopus Arrhizuz. *Biochimica et Biophysica acta 260*, 393-400.

[19] Sharma C., K., Sharma P., K., & Kanwar, S. (2012). Optimization of Production of Lipases from B. Licheniformis MTCC-10498. *res, J. Recent Sci*, 25-32.

[20] Sharma, C., & Kanwar, S. (2012). Purification of a Novel Thermophilic Lipase from B. licheniformis MTCC-10498. *ISCA J. Biological Sci., 1(3)*, 43-48.

[21] Sharma, R., Chisty, Y., & Banerjee, U. (2001). Production, Purification, Characterization, and Application of Lipases. *Biotecnol Adv, 19*, 627-662.

[22] shuler, M. L. (2002). *Bioprocess Engineering 2nd.* USA: Pretice Hall PRT.

[23] Singh, A., & Mukhopadhyay, M. (2012). Overview of fungal lipase: A review. *Appl. Biochem. Biotechnol., 166*, 486-520.

[24] Takac, S., & Marul, B. (2008). Effect of lipidic carbon sources on the extracellular lipolytic activity of a newly isolated strain of bacillus subtilis. *J Ind Microbiol Biotechnol*, 1019-1025.

[25] Uscategui, Y., Jimenez_Junca, C., Suarez, C., & Prieto_Correa, E. (2012). Evaluation of Induction of Lipolytic Enzymes from A Pseudomona aeruginosa Isolated from African Palm Fruit. *Vitae vol. 19 no.3.*

[26] Verma, N., Thakur, S., & Bhatt, A. (2012). Microbial Lipases: Industrial Applications and Properties (A Review). *Int. Research Journal Of Biological Sciences, Vol. 1(8)*, 88-92.

[27] Yuneta, R., & Putra, S. R. (2009/2010). *Pengaruh Suhu pada Lipase dari Bakteri Bacillus Subtilis.* Surabaya: Jurusan Kimia, Fakultas MIPA, Institut Teknologi Sepuluh Nopember.

International Conference and Workshop on Chemical Engineering UNPAR 2013

Preliminary study on bioethanol production from Coix lacryma-jobi L. using simultaneous saccharification and fermentation

H. M. Inggrid[a*] , I. Darmaji[a], T. Handoko[a], A. P. Kristijarti[a]

[a] *Chemical Engineering Department, Parahyangan Catholic University, Jl.Ciumbuleuit no.94, Bandung 40141, West Java, Indonesia*

Abstract

Bioethanol is one of the promising alternative biofuels. Bioethanol can be produced from sugar, starch, or lignocellulose material. One of the potential materials to produce bioethanol is Coix lacryma-jobi L. seeds that containing high starch and protein content. In this research, the flour of Coix lacryma-jobi L. seeds was made by dehulling seeds using disc mill. The flour was further added α-amylase enzyme (0.25%-v/w starch) and was heated at 90oC for 4 hours. Subsequently, glucoamylase enzyme (19.05%-w/w starch), yeast Saccharomyces cerevisiae (10%-v/v SSF, 108 cells/ml), and nutrient (22.5%-v/v SSF, containing yeast extract 1%-w/v suspension and peptone 2%-w/v suspension) were added to the starch suspension and simultaneous saccharification-fermentation process (SSF) was allowed to proceed anaerobically for 3 days in a laboratory shaker (30oC, 100 rpm). The number of yeast cells was determined using direct counting method with haemocytometer. The ethanol and glucose concentrations were analyzed using HPLC. To study the effect of different carbohydrate concentration on ethanol fermentation, two different carbohydrate concentrations, 10%-w/v suspension and 30%-w/v suspension, were successfully converted to ethanol. The result showed 5.06% (w/v) ethanol was converted from 10% (w/v) carbohydrate or 50.64% in yield, and 15.80% (w/v) ethanol was converted from 30% (w/v) carbohydrate or 52.66% in yield. According to the result, it can be concluded that 30% carbohydrate concentration gave higher ethanol yield.

Keywords: bioethanol ; Coix lacryma-jobi L. ; simultaneous saccharification-fermentation (SSF) ; Saccharomyces cerevisiae

1. Introduction

Fossil fuel is the most common energy source which is used widely in the world. Unfortunately, fossil fuels are not renewable and the carbon dioxide released from the burning fossil fuels is considered a major contributor to global warming. There are some alternative fuels to solve these problems and bioethanol is one of the promising biofuels from renewable sources[1,2]. Ethanol can be produced synthetically from ethylene, or by fermentation of sugar, starch, or lignocellulose materials. Common raw materials such as sugarcane, molasses, cassava, and corn were used to produce bioethanol[3].

Coix lacryma-jobi L. is a cerealia plant containing high starch content on its seeds. The protein content of Coix lacryma-jobi L. is higher than another common cerealia plant and it has more minerals[4]. The content of Coix lacryma-jobi L. shows it has potential to be used as starchy raw material to produce bioethanol. However, since Coix lacyma-jobi L. seeds is a starchy substrate, it must be first liquefied and saccharified.

Fermentation process involves microorganism activity in anaerobic condition[5]. Common fermentation can be performed by using microorganisms, such as Zymomonas mobilis and Saccharomyces cerevisiae from sugar raw material, as for other raw materials, starch and lignocellulose, need pretreatment process before fermentation stage.

Simultaneous saccharification and fermentation (SSF) is a process that performed saccharification together with fermentation, instead of as a separate step after hydrolysis[6]. It is useful for industrial applications because of its high ethanol yield, low energy consumption, and short processing time[6,7,8]. The inhibition of high glucose concentration can be avoided since the glucose produced from saccharification process is consumed by the microorganism immediately[7]. In this research, the SSF

---

process was performed using glucoamylase enzymes as a saccharification agent with help of yeast Saccharomyces cerevisiae as a fermentation agent.

Fuel alcohol manufactures normally ferment grain mashes containing 20-24 g of dissolved solids/100 g9,10. Lately, many commercial fuel ethanol production facilities employ very high gravity (VHG) fermentation. VHG was originally defined as the preparation and fermentation of mash containing 27 g or more of dissolved solids per 100 g of mash6,11. VHG technology can increase final ethanol concentration and productivity without facilities expansion, energy costs, and risk of bacterial contamination6. Low gravity fermentation (10%-w/v suspension) and VHG fermentation (30%-w/v suspension) were used as variation of this research.

2. Materials and methods
2.1. Materials

Coix lacryma-jobi L. seeds were obtained from local grain seller in Punclut, North Bandung, Indonesia. Bacteriological grade yeast extract, peptone, and maltose were obtained from Difco (Jakarta, Indonesia). Plate count agar was obtained from Merck (Jakarta, Indonesia) and bacteriological grade dextrose was obtained from Oxoid (Jakarta, Indonesia). The enzymes used to degrade starch were Liquozyme Supra (α-amylase enzyme) and Dextrozyme GA (glucoamylase enzyme). Both of the enzymes were technical grade and obtained from Novozyme (Kuala Lumpur, Malaysia). Yeast Saccharomyces cerevisiae, NRRL Y-132, was a gift from Agriculture Research Service (ARS,USDA) and was maintained on sterile yeast extract-maltose (YM) slant agar.

2.2. Pretreatment of starch

Coix lacryma-jobi L. seeds was dehulled and milled using laboratory scale disc mill until the flour size is -80 +100. The flour was analyzed to determine carbohydrate content (using HPLC) and protein content (using Kjedahl method). The fat content of the flour was determined using Soxhlet method, while the moisture content was measured gravimetrically. The starch suspension was made by mixing the flour with α-amylase enzyme (0.25%-v/w starch) dissolved in RO water, heated in a silicon oil at 90oC and stirrred for 4 hours.

2.3 Preparation of yeast inoculum

Saccharomyces cerevisiae NRRL Y-132 maintained in slant agar were transfered to yeast extract-peptone-dextrose (YPD) broth containing yeast extract 1%-w/v, peptone 2%-w/v, and dextrose 1%-w/v. The yeast was allowed to grow aerobically for 10 hours at 30oC in a laboratory shaker (100 rpm). Before it was used as an inoculum for the SSF process, the broth containing yeast was diluted until the number of cells was 108 cells/ml.

2.4. Simultaneous saccharification and fermentation process

The starch suspension was first sterilized in autoclave at 121oC for 15 minutes. Glucoamylase enzyme (19.05%-w/w starch) and nutrient (22.5% v/v SSF, containing yeast extract 1%-w/v suspension, peptone 2%-w/v suspension) were added to the suspension. Yeast inoculum (10%-v/v SSF) was added afterwards. The process was carried out anaerobically in a laboratory shaker at 30oC and 100 rpm. Samples were taken periodically for 3 days.

2.5. Yeast cells, glucose concentration, and ethanol concentration determination

The number of yeast cells was determined using haemocytometer under light microscope with 400x magnification. Glucose and ethanol concentration were analyzed using Hitachi High Performance Liquid Chromatography (HPLC) with a refractive index (RI) detector at 40oC and Bio-Rad Aminex Fermentation Monitoring column. Samples were first precipitated and the clear solution was diluted and centrifuged as well at 1300 rpm for 15 minutes. Sulphuric acid solution (0.005 M) was used as eluent with flow rate 0.6 ml/min. The oven temperature was 65oC and pump pressure was 2,5 MPa.

3. Results and discussion

In this research, bioethanol was produced from Coix lacryma-jobi L. seeds flour with help of glucoamylase enzyme and yeast Saccharomyces cerevisiae during the SSF process. The Coix lacryma-jobi L. seeds flour content is given in Table 1.

Table 1. Coix lacryma-jobi L. seeds flour content

Flour content	Percentage (%)
Carbohydrate	76.29
Protein	14.02
Fat	5.80
Moisture	12.28

The research was performed with two different carbohydrate concentrations, which were 10%-w/v suspension and 30%-w/v suspension. The nutrient made from yeast extract and peptone was added into the suspension. The saccharification and fermentation process was carried out in a laboratory shaker at 30oC and 100 rpm. The conversion of Coix lacryma-jobi L. starch to ethanol is shown in Scheme 1.
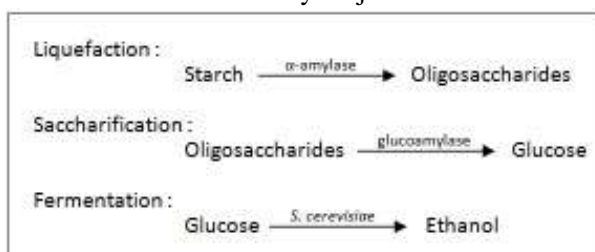
Scheme 1. Schematic representation of starch conversion to ethanol

In this research, the liquefaction process was performed using α-amylase enzyme to convert starch into oligosaccharides. Subsequently, the saccharification process was carried out using glucoamylase enzyme to reduce oligosaccharides. The fermentation process involved yeast Saccharomyces cerevisiae to convert glucose into ethanol. The result of the SSF process was shown in Figure 1 and Figure 2.
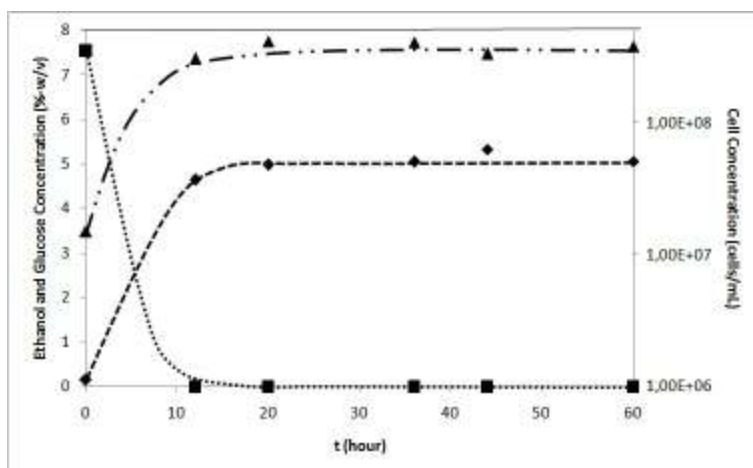
Figure 1. SSF result of 10%-w/v carbohydrate concentration

■, ... : glucose concentration

◆, -- : ethanol concentration

▲, -.. : cell concentration

Figure 1 shows the initial glucose concentration was about 7.5%-w/v, then decreased rapidly due to the production of ethanol. In some research, glucose concentration would increased during saccharification process. In Watanabe et.al. research, the glucose concentration was increasing within the first 8 hours and glucose was run out in 40 hours1. The glucose concentration in the research of Moon et.al. was increasing within the first 12 hours and glucose was run out in 42 hours7. Figure 1 shows the glucose concentration was not increasing and after 12 hours of SSF process, glucose concentration was already run out. It is hypothesized that the rate of ethanol production was higher than the rate of glucose production.

The yeast consumed glucose to produce ethanol, therefore the ethanol concentration increased while the glucose concentration decreased. After 12 hours of SSF process, glucose was fully converted to ethanol, however the starch was not fully converted to ethanol. The final ethanol concentration 5.06% (w/v) was produced from 10% (w/v) carbohydrate. The result yield was determined as the percentage of final ethanol concentration per carbohydrate concentration. The ethanol yield from 10%-w/v was 50.64%.

Figure 1 shows, the cell concentration was stable after 12 hours. The yeast activity for producing ethanol was good enough as it consumed glucose from the beginning of SSF process and needed only 12 hours to convert all glucose to ethanol. In this research, total cells and active cells were both counted. For 10% (w/v) carbohydrate experiment, the total cell concentration was almost represented by active cells, which meant 10% (w/v) carbohydrate concentration was adaptable for the yeast.
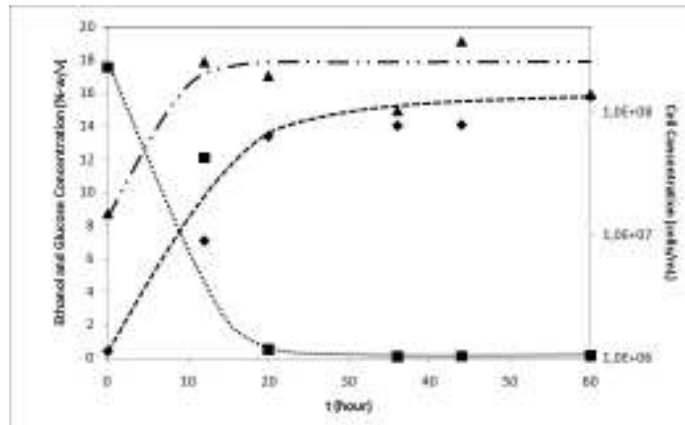
Figure 2. SSF result of 30%-w/v carbohydrate concentration
■, ... : glucose concentration
◆, -- : ethanol concentration
▲, -.. : cell concentration

The trend of Figure 2 is similar to Figure 1, however it took longer SSF time, 20 hours to fully converted glucose into ethanol. This phenomena was possibly caused by yeast adaptation to high glucose concentration. The initial glucose concentration from 30% (w/v) carbohydrate was about 17.5%-w/v and it was not increasing during the SSF process. After 20 hours, the glucose was almost fully converted and the final ethanol concentration was 15.80% (w/v), or 52.66% in yield. The result indicates that other components, such as maltosa and maltotriosa, were not perfectly hydrolyzed to give smaller reducing sugar. Further research is needed to increase ethanol yield.

The cell concentration increased 8 fold within the first 20 hours. However, the cell concentration around 40 hours was almost represented by dead cells. It was possibly caused by yeast adaptation to high ethanol concentration. The yeast was able to adapt the SSF condition after 60 hours. The research needs longer time to observe yeast activity during SSF process.

The obtained result was compare to Watanabe, et.al. research (using 40%-w/v potato as raw material), the final ethanol concentration from 30% (w/v) Coix lacryma-jobi L. starch was higher and it

took shorter time to produce ethanol1. The final ethanol concentration of 30% (w/v) Coix lacryma-jobi L. starch was also higher than Wang et.al. research (using rye and triticale, 28.5%-w/v) at 60 hours. However, Wang's final ethanol concentration (120 hours) was still higher than the obtained SSF result of 30% (w/v) Coix lacryma-jobi L. starch9. The comparison result shows it needs further research and development to observe detail aspects.

From the figures above, it can be concluded that the process of producing bioethanol was fast and the yeast Saccharomyces cerevisiae was able to adapt high carbohydrate concentration (30%-w/v). The ethanol yield from 30% (w/v) carbohydrate was higher than 10% (w/v) carbohydrate. The summary of the research is given in Table 2.

Table 2. Summary of the experiment

Carbohydrate concentration (%-w/v)	Final ethanol concentration (%-w/v)	Final glucose concentration (%-w/v)	Yeast cell concentration (cells/ml)	Ethanol yield (%)
10	5.06	0.00	3.80×10^8	50.64
30	15.80	0.13	1.41×10^8	52.66

4. Conclusions

From this study, the experiment result showed that ethanol with yield 50-53% were successfully produced from Coix lacryma-jobi L. using glucoamylase enzyme and yeast Saccharomyces cerevisiae during SSF process. The same SSF condition (temperature 30oC, shaking speed 100 rpm, and yeast extract-peptone as nutrient) was treated to 10% (w/v) carbohydrate and 30% (w/v) carbohydrate. 30% (w/v) carbohydrate concentration could produce higher ethanol yield (52.66%).

Acknowledgements

References

1. Watanabe T, Srichuwong S, Arakane M, Tamiya S, Yoshinaga M, Watanabe I, Yamamoto M, Ando A, Tokuyasu K, Nakamura T. Selection of stress-tolerant yeasts from simultaneous saccharification and fermentation (SSF) of very high gravity (VHG) potato mash to ethanol. Bioresource Technology 101 (2010):9710-9714.
2. Nag A. Biofuels refining and performance. McGraw-Hill;2008.
3. Gupta RB, Demirbas A. Gasoline, diesel, and ethanol biofuels from grasses and plants. Cambridge University Press;2010.
4. Wrigley C, Corke H, Walker CE. Encyclopedia of grain science. Elsevier Academic Press.
5. Bamforth CW. Food, fermentation and micro-organisms. Blackwell Science;2005.
6. Yingling B, Zongcheng Y, Honglin W. Optimization of bioethanol production during simultaneous saccharification and fermentation in very high-gravity cassava mash. Antonie van Leeuwenhoek 99 (2011):329-339.
7. Moon SK, Kim SW, Choi GW. Simultaneous saccharification and continuous fermentation of sludge-containing mass for bioethanol production by Saccharomyces cerevisiae CHY0321. Journal of Biotechnology;2011.
8. Nikolic S, Mojovic L, Rakin M, Pejin D. Bioethanol production from corn meal by simultaneous enzymatic saccharification and fermentation with immobilized cells of Saccharomyces cerevisiae var. ellipsoideus. Fuel 88 (2009):1602-1607.
9. Wang S, Thomas KC, Ingledew WM, Sosulski K, Sosulski FW. Production of fuel ethanol from rye and triticale by very-high-gravity (VHG) fermentation. Applied Biochemistry and Biotechnology Vol 69 (1998).
10. Thomas KC, Hynes SH, Ingledew WM. Proc Biochem 31 (1996):321-331.
11. Ingledew WM, Bayrock DP. Application of multistage continuous fermentation for production of fuel alcohol by very-high-gravity fermentation technology. J Ind Microbiol Bioetechnol 27 (2001):87-93.

International Conference and Workshop on Chemical Engineering UNPAR 2013

Preparation, Proximate Composition and Culinary Properties of Yellow Alkaline Noodles from Wheat and Raw/Pregelatinized Gadung (*Dioscorea Hispida Dennst*) Composite Flours

Andri Cahyo Kumoro*, Catarina Sri Budiyati, Diah Susetyo Retnowati and Ratnawati

Department of Chemical Engineering, Faculty of Engineering, Diponegoro University. Prof. H. Soedarto, SH Road-Tembalang, Semarang, 50275, Indonesia

Abstract

The steady increase of wheat flour price and noodle consumptions has driven researchers to find substitutes for wheat flour in the noodle making process. In this work, yellow alkaline noodles were prepared from composite flours comprising wheat and raw/pregelatinized gadung (*Dioscorea hispida* Dennst) flours. The purpose of this work was to investigate the effect of composite flour compositions on the cooking properties (cooking yield, cooking loss and swelling index) of yellow alkaline noodle. In addition, the sensory test and nutrition content of the yellow alkaline noodle were also evaluated for further recommendation. The experimental results showed that a good quality yellow alkaline noodle can be prepared from composite flour containing 20% w/w raw gadung flour. The cooking yield, cooking loss and swelling index of this noodle were 10.32 g, 1.20 and 2.30, respectively. Another good quality yellow alkaline noodle can be made from composite flour containing 40% w/w pregelatinized gadung flour. This noodle had cooking yield 8.93 g, cooking loss 1.20, and swelling index of 1.88. The sensory evaluation suggested that although the color, aroma and firmness of the noodles were significantly different ($p \leq 0.05$) from wheat flour noodle, but their flavor remained closely similar. The nutrition content of the noodles also satisfied the Indonesian National Standard for noodle. Therefore, it can be concluded that wheat and raw/pregelatinized gadung composite flours can be used to manufacture yellow alkaline noodle with good quality and suitable for functional food.

Keywords: yellow alkaline noodle; wheat; gadung; noodle quality; functional food

1. Introduction

Noodles are among the most important staple foods in many Asian countries and approximately 40% of total wheat flour consumption in this region is for the preparation of Asian noodles[1]. There are regional preferences for noodle color, size, shape, texture, flavor, shelf life, and ease of cooking. Therefore, based on their ingredients, noodles can be simply classified into Chinese types (Ramen), Japanese types (Soba), Korean types (Naengmyon), rice and starch noodles[2]. Among those types of noodle, white salted noodles and yellow alkaline noodles are the most commonly consumed in Southeast Asia, Korea, Japan, and China[3]. Usually, the appearance of regular salted noodles are bright, with clean color ranging from white to creamy white, and with a smooth, glossy surface after boiling[2]. Soft and elastic with a smooth surface are the preferred textural properties of boiled regular salted noodles by most Japanese and Koreans[4]. In contrast to that, most Chinese prefer regular salted noodles with firm, elastic, and chewy texture[5]. Although the original purpose of alkaline salts incorporation in noodle manufacturing was to extend noodle shelf life by inhibiting mould growth, it is now proven that alkaline salt also functions as a dough conditioner or texture quality improver. Alkaline noodles are originated from Southern China, but now they are widely adopted into the local cuisine of Malaysia, Singapore, Indonesia, Thailand, Taiwan and Hong Kong. The most popular types are fresh (Cantonese style), partially boiled (Hokkien style), and fresh or steamed with egg as an ingredient (Wonton noodles). In Japan, however, the most popular types of alkaline noodles are fresh and high moisture steamed noodles. The latter is often called Yakisoba (for stir-frying), or Kata-Yakisoba (for deep-frying) in Japanese[6].

Noodles are prepared by mixing of wheat flour, water, and salt and/or alkali, which contains protein and small amount of fatty acids to dough, sheeting the dough and cutting into noodle strands[7].

The qualities of noodles depend largely on flour characteristics and on conditions used during noodle preparation[8]. Starch (basically composed of amylose and amylopectin) is a predominant component of wheat flour, as it helps to improve the appearance and structure of wheat flour foods. Wheat used for noodle flour manufacture should have an appropriate balance of protein content, protein quality (as indicated by dough properties) and starch quality for the targeted noodle type[9]. The presence of excessive levels of α-amylase, either through preharvest sprouting or late maturity α-amylase, can have deleterious effects during processing and on the quality of the final product. These include increased boiling losses and reduced eating quality. High levels of protease, associated with rain damage, may lead to increased breakage of noodles during drying and poor color in both alkaline and nonalkaline noodles. Flour extraction levels and ash contents have a profound influence on noodle appearance[10]. Higher flour extraction levels generally lead to duller noodles with a higher tendency to darken during dough processing. Low flour extraction and ash levels are preferred for the manufacture of noodles that retain a clean, bright appearance after cooking. Therefore, the highest-quality noodle flours are associated with low extraction milling and low ash levels in the flour. The principal characteristics of flour that affect noodle texture are: protein content, reflecting the relative proportions of the two main components of the flour, protein and starch, and the compositions of these two components[11]. Other ingredients that may affect the appearance and texture of flour noodles are the presence of salt[12], alkali[13] and additives, such as gums, emulsifiers, enzymes and colorings[14].

Yellow alkaline noodles are manufactured with the addition of alkaline salts called kansui or 'lye water' (sodium and potassium carbonates), which affects starch gelatinization, strengthens the dough sheet of noodles and also gives it the distinctive yellow color[15]. Therefore, yellow alkaline noodles are firmer and more elastic than white salted noodles which are made of dough with NaCl. To obtain those properties, yellow alkaline noodles are made from relatively high protein content (10.5-12.0%) hard wheat. In contrast to that, low protein content (8.0-10.0%) soft wheats are used to prepare white salted noodles[16]. A number of previous researches have reported a negative relationship between protein content with noodle color and a positive relationship between protein content with hardness of cooked noodles[16]. Protein quality, such as sedimentation volume, mixograph mixing time, glutenin composition, glutenin polymer, and glutenin to gliadin ratio also influence dough properties and texture of yellow alkaline noodles[17]. Higher swelling power and peak viscosity of starch are negatively related to firmness and elasticity, and positively correlated with surface smoothness of cooked yellow alkaline noodles in sensory and instrumental tests[18]. The desired characteristics of yellow alkaline noodle are a bright, even, light yellow appearance, absence of any darkening and discoloration, a firm clean bite, a chewy and elastic texture with some degree of springiness and a satisfactory al dente reaction on biting.

High wheat flour price, especially in the developing countries has driven researchers to find substitutes for wheat flour in the noodle manufacturing process. Generally, researchers do intensive exploration to the potentials of the local resources as wheat flour substitute. A number of researches have been focused to incorporate other types of flour for wheat replacement, e.g., legume (pea, peanut, bean)[19,20], tuber (Jerusalem artichoke, sweet potato, tapioca)[21,22], and cereal grain (rye, rice)[23,24]. However, lower-quality noodles were usually obtained because of the inappropriate protein quality and content of the replacement flours.

Gadung (*Dioscorea hispida Dennst.*) is one of underutilized tubers, which is easily found in almost all parts of Indonesia's archipelago, Malay Peninsula, Thailand and India[25]. This tuber crop is rich in carbohydrates and therefore had been used as a staple food, especially by people in the tropical and sub-tropical regions during WW II[26]. The resistant starch contained in this tuber has been related with a slow digestion in the lower parts of the human digestion tract, resulting in slow release and absorption of glucose. Therefore, this tuber has been suggested to be utilized in the effort of reducing the risk of obesity, diabetes and other related diseases[27]. Similar to other tubers, gadung does not contain any gluten, which makes gadung tuber becomes an important substance in the reduction in the incidence of Celiac Disease (CD) or other allergic reactions[28]. In a rapidly changing world, with altered food habits and stressful lifestyles, it is more and more recognized that a healthy digestive

system is an essential factor in determining the overall quality of life[29]. Recently, gadung has received more attention from researchers in Indonesia for its potential as a food material[30]. The physico-chemical properties of raw and pregelatinised gadung flour have been investigated by Kumoro and his co-workers[31] who suggested gadung flour is highly potential substitute for wheat flour in noodle preparation. Noodles produced from the blends of wheat and raw/pregelatinized gadung flours with moderately high amylose and amylopectin might be explored as functional foods for normalizing the blood insulin levels and imparting other health benefits. Therefore, the objectives of this study were to evaluate the relationships between the composite flours (wheat-gadung) compositions and the culinary properties of yellow alkaline noodles, namely cooking yield (*CY*), cooking loss (*CL*), swelling index (*SI*), sensory and nutrition content by comparison with commercial wheat flour noodles.

2. Materials and Methods
2.1. Wheat flour and chemicals
Commercial wheat flour suitable for yellow alkaline noodles manufacturing was obtained from PT. Bogasari Flour Mills Tbk, Indonesia and was chosen as reference flour. All chemicals used in this work were of analytical grade and were purchased from Sigma-Aldrich Singapore Pte. Ltd.

2.2. Preparation of raw gadung flour
Raw gadung flour was prepared from gadung tuber of 9 months age using the method developed by Kumoro and his coworkers[30]. Gadung tubers were peeled, washed, sliced into chips before being leached using recycled flowing water for 3 hours. The chips were then dried in a hot air oven at 60°C for 8 hours. The dried gadung chips were milled and sieved through a 100-mesh sifter to obtain raw gadung flour sample.

2.3. Preparation of pregelatinized gadung flour
Pregelatinized gadung flour was prepared from matured gadung tuber of 9 months age by following the method previously described by Kumoro and his coworkers[31]. Gadung tubers were peeled, washed, sliced and leached using flowing fresh water for 3 hours. Then the sliced was cooked in boiling water at 100°C for 15 minutes. The chips were then dried in a hot air oven at 60°C for 8 hours. The dried chips were then milled and sieved through a 100-mesh sifter to obtain pregelatinized gadung flour sample.

2.4. Preparation of yellow alkaline noodles
Wheat-raw/pregelatinized gadung composite flour (100 g, 13% m.b, at various compositions) was mixed with a predetermined amount of warm (55°C) 2.7% Na_2CO_3 and 0.3% K_2CO_3 solution in a pin mixer (National Mfg.) for 20 min, with a head speed of 86 rpm. The mixture was then kneaded with water to dough consistency before being passed through the rollers of a noodle machine (Ohtake Noodle Machine Mfg., Tokyo, Japan) at 8 rpm and a 3 mm gap; dough was folded and put through the sheeting rollers. The folding and sheeting were repeated twice. The dough sheet was rested for 1 h and then put through the sheeting rollers 3 times at progressively decreasing gaps of 2.60, 2.33, 2.00, and 1.50 mm. The dough sheet was cut through No. 20 cutting rollers into noodle strands of about 30 cm in length, with a 0.3×0.2 cm cross section. The noodles were then transferred into hot water (95 - 98 ^{o}C), and heated for 50-70 seconds at this temperature before being introduced into cold water for cooling. When noodles were floated, they were withdrawn and dried. No additive was added during the whole procedure. The dried noodles were equilibrated at room temperature for 4 h, packed in clean pre-sterilized polyethylene bags and stored at room temperature before further analysis.

2.5. Determination of proximate composition of noodles
The following analyses were performed to all flours and selected noodles; moisture, fat, protein, ash and crude fiber content were determined according to American Association of Cereal Chemists (AACC) approved methods 44-15A, 30-10, 46-30, 08-01, and 32-05, respectively[32]. The starch and amylose content were measured using the methods suggested by Juliano[33].

2.6. Determination of culinary properties of noodles

The cooking yield (*CY*) and cooking loss (*CL*) of the noodles were determined as described in the AACC method[32]. While the swelling index (*SI*) was determined using the method developed by Akanbi *et al.*[34]. Ten grams (W_{BC}) of the noodles were introduced into a beaker glass containing 150 ml boiling water. The beaker glass was immediately covered with a watch glass and the noodles were let to cook for 10 min with slight agitation. The cooked noodles were allowed to drain for 5 min and then weighed thoroughly (W_{AC}). The cooking yield was then calculated. The gruel was poured into a 200 ml volumetric flask and adjusted to volume with distilled water. Ten milliliter sample was withdrawn from the solution and transferred to an aluminum dish. The weight of aluminum dish with the gruel sample inside was measured and recorded (W_{GD}). The sample was then dried in an electric oven at 105°C to a constant weight (W_{CGD}). The cooking loss during cooking was calculated as given below.

$$CY = (W_{AC} - W_{BC}) \qquad (1)$$

$$CL = (W_{GD} - W_{CGD}) \times 100 / W_{CGD} \qquad (2)$$

$$SI = W_{AC} / W_{BC} \qquad (3)$$

2.7. Sensory test evaluation

The noodle samples were cooked in boiling water for 4 min and then drained for 1 min. The cooked samples (50 g) were placed in covered, Styrofoam cups and were evaluated by 30 panelists using balanced in completed block design (t = 10, k = 3, r = 9, b = 30, λ = 2). A nine-point hedonic scale (1 = dislike extremely, 5 = neither like nor dislike, 9 = like extremely) was used to evaluate acceptability of sensory attributes (color, aroma, flavor, firmness and overall liking) of plain noodles. Evaluation was conducted mid-morning.

2.8. Statistical analysis

All data were subjected to statistical analysis, namely analysis of variance (ANOVA), Pearson correlation coefficient and F-test of multiple regressions[35]. Differences were considered significant at $p < 0.05$, unless otherwise specified[36]. All data were determined at least in duplicate and all were averaged.

3. Results and Discussion

3.1. The effect of raw gadung flour composition in the composite flours on the cooking properties of yellow alkaline noodles

The cooking properties of yellow alkaline noodles prepared from composite flours containing wheat and raw gadung flours are presented in Table 1. The cooking properties investigated consist of cooking yield, cooking loss and swelling index. It is clearly shown in Table 1 that the cooking yield and swelling index of the noodles increased as raw gadung flour composition in the composite flours increases from 0-20% w/w.

The increase in noodles quality with the addition of raw gadung flours is linked with the increase of amylose content in the composite flours to an optimum value, which is 24% [14]. On the other hand, the protein contents in the composite flours dropped to between 11.17-12.81%, but the values remained within the acceptable protein content of flour for noodle manufacturing. However, further addition of raw gadung flour caused reduction in cooking yield and swelling index of the noodles. Swelling index is closely related to the protein content and total starch in flour[37]. Highlevels of proteinin the flourcan causestarch granulestrapped betweenarigidmatrix of protein, and inhibitswater toenter the noodle structure and restrict the swelling power.Therefore, theflourwitha lowprotein contentandhighstarch contentwill havea highswellingindex. However, too high amylose content caused reduction in swelling index due to inhibition of water diffusion into the starch granules[38]. In addition, the flours

contained high fat content which may form a complex with amylose and the linear part of the amylopectin, and hence inhibit swelling[39,40].

Cooking loss values increased significantly following the increase in raw gadung flour composition in the composite flours. High cooking loss was likely to be affected by reduction of protein content[41] and improvement of amylose content which improves the fragility of the flour[38]. Hamaker and Griffin found that the lack of protein in flour improved the fragility of the starch granules and making it more accessible to water; thereby, causing an increased viscosity and gel strength because of larger swelling[42]. They also reported that proteins with disulfide bonds in rice flour hindered granule swelling and made the swollen granules easily breakable when shear was applied.

Table 1. Cooking properties of noodle prepared from composite flour containing raw gadung flour and wheat flour

Percentage of gadung flour (%)	Protein content (%)	Amylose content (g/100g)	*CY* (g)	*CL* (%)	*SI* (g/g)
0	12.81	21.30	5.30	0.00	1.53
5	12.54	21.97	7.23	0.00	1.72
10	12.26	22.64	7.96	1.20	1.80
15	11.99	23.31	9.33	1.20	1.93
20	11.72	23.98	10.32	1.20	2.30
25	11.45	24.65	7.30	2.40	1.73
30	11.17	25.32	8.08	2.40	1.81

Good yellow alkaline noodles were obtained from composite flours containing 20% w/w raw gadung flour with cooking yield, cooking loss and swelling index were 10.32 g, 1.20 %, and 2.30 g/g, respectively.

3.2. The effect of pregelatinized gadung flour composition in the composite flours on the cooking properties of yellow alkaline noodles

In general, the yellow alkaline noodles obtained from composite flours containing pregelatinized gadung flour has better appearance compared to those obtained from composite flour containing raw gadung flour. The cooking properties of them are tabulated in Table 2.

Table 2. Cooking properties of noodle prepared from composite flour containing pregelatinised gadung flour and wheat flour

Percentage of gadung flour (%)	Protein content (%)	Amylose content (g/100g)	*CY* (g)	*CL* (%)	*SI* (g/g)
0	12.81	21.30	5.30	0.00	1.53
20	11.31	23.98	5.69	1.20	1.56
25	10.93	24.65	5.90	1.20	1.59
30	10.56	25.32	7.15	1.20	1.71
35	10.18	25.99	8.80	1.20	1.88
40	9.81	26.66	8.93	1.20	1.88
45	9.43	27.33	9.28	3.60	1.93
50	9.06	28.00	5.80	7.20	1.58

It is clearly shown in Table 2 that increasing pregelatinized gadung flour composition from 0-45% w/w in the composite flours resulted improvement of cooking yield and swelling index of the noodles. Addition of pregelatinized gadung flour into wheat flour increased the amylose content of composite flours to some extent approaching the optimum amylose content in flour for noodle manufacturing, which is 24% w/w[14].

Besides, addition of pregelatinized gadung flour also reduced the protein content of the composite flour to between 9.43-12.81%, and still within the acceptable value. However, further addition of pregelatinized gadung flour caused reduction of cooking yield and swelling index. Table 2 shows that too high amylose content may lead to reduction of swelling index. Basically, the swelling behavior of starch is primarily the property of its amylopectin content, while the amylose act as both a diluent and an inhibitor of swelling, especially with the presence of lipid[38].

During boiling, the added water acted as a plasticizer and promoted the interaction between amylose and amylose or amylose and linear amylopectin branches[43]. This resulted in a denser granule structure and, finally lowered swelling power[40]. The evident is that the swelling indexes of yellow alkaline noodles manufactured from composite flours containing pregelatinized gadung flour were lower than those of noodles from composite flours containing raw gadung flour. In addition, the flours contained high fat content which may form a complex with amylose and the linear part of the amylopectin, and hence inhibit swelling[39,40].

The cooking loss values of noodles manufactured from composite flours containing up to 40% w/w pregelatinized gadung flour were constant at 1.20g. Unfortunately, further increase in pregelatinized gadung flour compositions in the composite flours was found to increase significantly the cooking loss of the noodles. The increase in cooking loss value was likely to be the effect of protein content reduction[41] and improvement of amylose content[38] of the composite flour, which improves the fragility of the flour. Low protein content in flour improved the fragility of the starch granules[42]. They also reported that proteins with disulfide bonds in rice flour hindered granule swelling and made the swollen granules easily breakable when shear was applied. Low protein content has been related in the literature with reduction of noodle hardness, while high amylose content causes inability of dough to absorb water to form strong noodle structure[44]. Good yellow alkaline noodles were obtained from composite flours containing 40% w/w raw gadung flour with cooking yield, cooking loss and swelling index were 8.93 g, 1.20 %, and 1.88 g/g, respectively.

3.3. The nutrition content the yellow alkaline noodle prepared from composite flour containing raw and pregelatinized gadung flours

The proximate compositions of yellow alkaline noodles made from wheat flour only and its composite flours containing 20% w/w raw gadung flour or 40% w/w pregelatinized gadung flour are shown in Table 3. The results showed that the addition of gadung flour caused reduction in carbohydrate, fat, protein and ash contents in the noodles, while the moisture and crude fiber content of the noodles increased. The protein, carbohydrate, crude fiber and moisture content of the noodles were significantly different ($p \leq 0.05$).

The results are not surprising because the carbohydrate, fat, protein and ash contents of wheat flour were higher than those of pregelatinized gadung flour. In the other hand, the swelling, water holding capacity and crude fiber content of gadung flour were higher than those of wheat flour[40,45]. Olaoye *et al*.[46] reported similar trend of crude fiber content of composites of wheat and breadfruit flours used for the preparation of some baked products. Previous researchers have also reported that crude fiber is best obtained from foods than supplement and can reduce symptoms of chronic constipation; heart problems associated with high cholesterol (hyperlipidemia) [47], diverticular disease[48], and reduce the risk of colon cancer[49]. Hence, gadung-wheat flour yellow alkaline noodles could be acceptable in places, especially by those require high fiber diets and lower fatty foods. An inference can therefore be taken that gadung-wheat flour noodles apart from being healthy, free of synthetic additives, also satisfies to the standards of SNI (Indonesia National Standard) and health regulatory agencies.

Table 3. Chemical composition of yellow alkaline noodle prepared from composite flour containing raw and pregelatinized gadung flours

No.	Flour Composition (wheat:gadung)	Moisture (%)	Fat (%)	Ash (%)	Protein (%)	Crude fiber (%)	Carbohydrate (%)
1.	100:0 (wheat flour only)	51.67	3.63	1.35	8.32	1.42	34.98
2.	80:20 (raw gadung flour)	52.79	3.54	1.06	5.93	2.81	33.87
3.	60:40 (pregelatinized gadung flour)	56.93	2.51	1.04	5.76	2.60	31.16
4.	SNI	35-60	1.0-2.5	-	4.5-6.0	-	30-60

3.4. The sensory test the yellow alkaline noodle prepared from composite flour containing raw and pregelatinized gadung flours

The mean values of the hedonic scores for sensory attributes of cooked yellow alkaline noodles samples prepared from pure wheat flour and composite flours containing 20% w/w raw gadung flour or 40% w/w pregelatinized gadung flour are shown in Table 4. The composition of raw and pregelatinized gadung flour in the composite flours in the preparation of yellow alkaline noodle was selected previously based on the cooking properties of the noodle, which were 20% w/w and 40% w/w, respectively. It is obvious that the addition of gadung flour affected ($p < 0.05$) the sensory acceptability of color, aroma, firmness and overall liking. The evidence is that the hedonic scale scores for color, aroma, firmness and overall liking of the products made with pure wheat flour were higher than those of products made with replacement by 20 % w/w raw gadung flour or 40% w/w of pregelatinized gadung flour. Fortunately, the addition of gadung flour did not significantly affect the flavor of the noodles.

Table 4. Sensory scores of yellow alkaline noodle prepared from composite flour containing raw or pregelatinized gadung flours

No.	Flour Composition (wheat:gadung)	Color	Aroma	Firmness	Flavor	Overall liking
1.	100:0	7.46	6.92	7.23	6.90	7.13
2.	80:20 (raw gadung flour)	5.84	6.17	6.93	6.65	6.40
3.	60:40 (pregelatinized gadung flour)	5.93	6.23	6.77	6.77	6.45

4. Conclusion

The results of this work revealed that beneficial noodles with health promoting factors can be manufactured from composite flour of wheat flour and raw/pregelatinized gadung flour containing 20% raw gadung flour or 40% pregelatinized gadung flour. The noodles showed acceptable proximate, culinary and sensory attributes. In addition, since gadung flour and wheat flours are rich in crude fiber which has been reported to reduce symptoms of chronic constipation, heart diseases associated with high cholesterol, diverticular disease and risk of colon cancer, therefore, an inference can be drawn that gadung-wheat flour composite noodles are more than just common noodles, but actually important functional foods.

References

1. Hatcher DW. Asian noodle processing. In: Owens G, editor. *Cereals Processing Technology*. Cambridge, UK: Woodhead Publishing; 2001. p. 131-157.

2. Nagao S. Noodles and pasta in Japan. In: Martin DJ, Wrigley CW, editors. *Cereals International*. Brisbane, Australia: The Royal Australian Chemical Institute Inc.; 1991. p. 22-25.

3. Ross AS, Quail KL, Crosbie GB. Physicochemical properties of Australian flours influencing the texture of yellow alkaline noodles. *Cereal Chem* 1997; **74(6):814**-820.

4. Crosbie GB, Ross AS. 2004. Asian wheat flour noodles. In: Wrigley C., editor. E*ncyclopedia of Grain Science*. Oxford, UK: Elsevier Ltd.; p. 304-312.

5. Huang S. China -the world's largest consumer of paste products. In: Kruger JE, Matsuo RB, Dick JW, editors. *Pasta And Noodle Technology* St. Paul, MN: American Association of Cereal Chemists; 1996. p. 301-329.

6. Fu BX. Asian noodles: history, classification, raw materials, and processing. *Food Res Int* 2008; **41:888**-902.

7. Heo H, Kang CS, Lee KS, Choo BK, Park CS. Characteristics of yellow alkaline noodles prepared from Korean wheat cultivar. *Food Sci Biotechnol* 2012; **21(1):69**-81.

8. Crosbie GB. The relationship between starch swelling properties, paste viscosity and boiled noodle quality in wheat flours. *J Cereal Sci* 1991; **13: 145**-50.

9. Crosbie GB, Ross AS, Moro T, Chiu PC. Starch and protein quality requirements of Japanese alkaline noodles (Ramen).*Cereal Chem* 1999; **76: 328**-34.

10. Miskelly DM. Flour components affecting paste and noodle colour. *J Sci Food Agric* 1984; **35: 463**-71.

11. Ross AS, Quail KJ, Crosbie GB. Physicochemical properties of Australian flours influencing the texture of yellow alkaline noodles. *Cereal Chem* 1997; **74:814**-820.

12. Huang S, Morrison WR. Aspects of proteins in chinese and british common (Hexaploid) wheats related to quality of white and yellow chinese noodles, *J Cereal Sci* 1988; **8: 177**-87.

13. Shiau SY, Yeh AI. Effects of alkali and acid on dough rheological properties and characteristics of extruded noodles. *J Cereal Sci* 2001; **33: 27**-37.

14. Hou G, Kruk M. Asian noodle technology. *Techn Bull* 1998; **20 (12): 1**-10.

15. Moss, H. J., Miskelly, D. M., Moss, R., 1986. The effect of alkaline conditions on the properties of wheat flour dough and Cantonese style noodles.*J Cereal Sci* 1986; **4: 261-**68.

16. Morris CF, Jeffers HC, Engle DA. Effect of processing, formulae, and measurement variables on alkaline noodle color-toward an optimized laboratory system.*Cereal Chem* 2000; **77:77**-85.

17. Zhang SB, Lu QY, Yang H, Meng DD. Effects of protein content, glutenin-to-gliadin ratio, amylose content, and starch damage on textural properties of chinese fresh white noodles. Cereal Chem 2011**;88: 296**-301.

18. Zhao LF, Seib PA Alkaline-carbonate noodles from hard winter wheat flours varying in protein, swelling power, and polyphenol oxidase. *Cereal Chem* 2005; **82, 504**-16.

19. Chompreeda P, Resurreccion AVA, Huang YC, Beuchat LR. Quality evaluation of peanut supplemented chinese type noodles. *J Food Sci* 1987; **52: 1740**-41.

20. Chompreeda P, Resurreccion AVA, Huang YC, Beuchat LR. Modeling the effect of peanut and cowpea flour supplementation on quality of chinese-type noodles. *Int J Food Sci Technol* 1988; **23: 556**-63.

21. Shin JY, Byun MW, Noh BS, Choi EH. Noodle characteristics of jerusalem artichoke added wheat flour and improving effect of texture modifying agents. *Korean J Food Sci Technol* 1991; **23: 538**-45.

22. Collado LS, Corke H. Use of wheat sweet potato composite flours in yellow alkaline and white salted noodles. Cereal Chem 1996; **73: 439**-44.

23. Kruger JE, Hatcher DW, Anderson MJ. The effect of incorporation of rye flour on the quality of oriental noodles.*Food Res Int* 1998; **31: 27**-35.

24. Batey IL, Curtin BM, Moore SA. 1997. Optimization of rapidvisco analyzer test conditions for predicting asian noodle quality. *Cereal Chem* 1997; **74: 497**-501.

25. Burkill IH. *Dioscorea hispida. A dictionary of the economic products of the malay peninsula*. London: The Crown Agents for the Colonies; 1935

26. Liu Q, Donner E, Yin Y, Huang RL, Fan MZ. 2006. The Physicochemical properties and in vitro digestibility of selected cereals, tubers and legumes grown in China. *Food Chem* 2006; **99:470**-77.

27. Aprianita A, Purwandari U, Watson B, Vasiljevic T. Physico-chemical properties of flours and starches from selected commercial tubers available in Australia. *Int Food Res J* 2009; **16: 507**-20.

28. Rekha MR, Padmaja G. Alpha-amylase inhibitor changes during processing of sweet during processing of sweet potato and taro tubers. *Plant Foods Hum Nutr* 2002; **52:285**-94.

29. Brouns F, Kettlitz B, Arrigoni E. Resistant starch and the butyrate revolution, *Trends Food Sci Technol* 2002; **13:251**-261.

30. Kumoro AC, Retnowati DS, Budiyati CS. Removal of cyanides from gadung (*Dioscorea hispida Dennst.*) tuber chips using leaching and steaming techniques.*J Appl Sci Res* 2011; **7(12):2140**-46.

31. Kumoro AC, Retnowati DS, Budiyati CS, Manurung T, Siswanto. Water solubility, swelling and gelatinization properties of raw and ginger oil modified gadung (*Dioscorea hispida Dennst*) flour. *Res J Appl Sci Eng Technol* 2012; **4(17): 2854**-60.

32. AACC. *Approved methods of the American association of cereal chemists*, St. Paul, MN: AACC Inc.; 2000

33. Juliano BO. A simplified assay for milled-rice amylose.*Cereal Sci Today* 1971; **16: 334**-40.

34. Akanbi TO, Nazamid S, Adebowale AA. Functional and pasting properties of a tropical breadfruit (Artocarpus altilis) starch from ile-ife, Osun state, Nigeria.*Int Food Res J* 2009; **16: 151**-57.

35. Steel RGD, Torrie JH. *Principles and procedures of statistic*. New York: McGrawHill; 1960.

36. Duncan DB. Multiple range and multiple F-test. *Biometric* 1955; **11:1**-42.

37. Woolfe JA. *Sweet Potato: An untapped food resource*. Cambridge: Cambridge University Press; 1992.

38. Tester RF, Morrison WR. Swelling and gelatinisation of cereal starches. I. Effect of amylopectin, amylose and lipids. *Cereal Chem* 1990; **67: 551**-9.

39. Hoover R. Composition, molecular structure, and physico-chemical properties of tuber and root starches: a review, *Carbohydr Polym* 2001;**45: 253**-67.

40. Tattiyakul J, Naksriarporn T, Pradipasena P, Miyawaki O. Effect of moisture on hydrothermal modification of yam Dioscorea hispida Dennst starch. *Starke* 2006; **58:170**-76.

41. Oh NH, Seib PA, Ward AB, Deyoe CW. Noodle. IV. Influence of flour protein, extraction rate, particle size and starch damage On the quality characteristics of dry noodles. *Cereal Chem* 1985; **62(6):441**-46.

42. Hamaker BR, Griffin VK. Effect of disulfide bond-containing protein on rice starch gelatinization and pasting.*Cereal Chem* 1993; **70(4):377**-80.

43. Gunaratne A., Hoover R. Effect of heat-moisture treatment on the structure and physicochemical properties of tuber and root starches. *Carbohydr Polym* 2002; **49:425**-37.

44. Toyokawa H, Rubenthaler GL, Powers JR, Schanus EG. Japanese noodle qualities. II. Starch components. *Cereal Chem* 1989; **66(4):387**-91.

45. Chung SY, Han SH, Lee SW, Rhee C. Physicochemical and bread-making properties of air flow pulverized wheat and corn flours. *Food Sci Biotechnol* 2000; **19(6):1529**-35.

46. Olaoye OA, Onilude AA. Microbiological, proximate analysis and sensory evaluation of baked products from blends of wheat-breadfruit flours. *Afr J Food Agric Nutr Dev* 2008;**8: 192**-203.

47. Odes HS, Lazovski H, Stern I, Madar Z. Double-blind trial of a high Dietary fiber, mixed grain cereal in patients with chronic constipation and hyperlipidemia. *Nutr Res* 1993; **13(9):979**-85.

48. Gear JSS, Fursdon P, Nolan DJ, Ware A, Mann JJ, Brodribb AJM, Vessey MP. Symptomless diverticular disease and intake of dietary fibre.*The Lancet* 1979; **313(8115): 511**-4.

49. Ready BS. Role of dietary fiber in colon cancer: an overview. *Am J Med* 1999; **106(1):16**-9.

International Conference and Workshop on Chemical Engineering UNPAR 2013

Microwave Sterilization of Oil Palm Fruits: Temperature Profile During Enzymatic Destruction Process

Maya Sarah[ab*] and Mohd. Rozainee Taib[a]

[a]*Universiti Teknologi Malaysia, Skudai, Johor 81310, Malaysia*
[b]*Universitas Sumatera Utara, Padang Bulan, Medan 20155, Indonesia*

Abstract
Microwave sterilization of oil palm fruits had significant advantage in quick process. It raised temperature of both mesocarp and kernel ina few minutes, which depended on decimal reduction time (*D*-values) of lipase inactivation. The *D*-value was recorded as less as 17 minutes and 90°C was reported as the highest temperature. The *D*-value wasa parameter of enzymatic destruction kinetic, which represented sterilization time in reduction of lipase activity by a factor of 10. Temperature and *D*-value relationship was studied during lipase inactivation. Mathematical modelof temperature distribution developed and evaluated at various *D*-values using Finite Difference Method. The results showedtemperature distribution of the model fitted with temperature distribution whichobtained from experimental data. Thus, indicated mathematical model from this study could be applied in estimating temperature distribution of oil palm fruits.

Keywords: Microwave; Sterilization; Oil Palm Fruits

1. Introduction

Microwave sterilization of oil palm fruits was purposed to protect palm oil quality, to soften the fruits, and to facilitate the bunch detachment [1]. Ithad significant advantages in term of quick sterilization process and low temperature application [2-10]. Palm oilobtained from this sterilization,reported having similar quality as compared to the palm oil from conventional sterilization [2-5]. Overall studies reported time of drying or heating in describing the time of exposure from microwave treatment, except from previous study, which had determined thermal death time for lipase inactivation by microwave irradiation [10].

Thermal death time defined by decimal reduction time (*D*-value), that represented time of exposure to inactivate half of microbe population or enzyme activity by a factor of 10 [10-14].The *D*-value of microwave sterilization reported as less than 17 minutes at frequency of 2450 MHz and power of 800 W. Temperature history during sterilization period only represented temperature at one location inside mesocarp [8], meanwhile microwave heating was non-uniformity heating, which created several hot spot on material. Several study on non oil palm fruits material reported several hot spot during microwave heating period, due to non-uniformity of temperature inside the material [15-17]. Temperature distribution inside mesocarp reported by Tan (1981) that observed temperature on center of fruit was higher as compared to others location and decreased along radial distances. Treatment with longer time of exposure observed elevated temperature. Tan (1981) only studied temperature distribution from heating process approach which concluded that temperature increased by elevated power and time of exposure [9].

Microwave sterilization showed different perspective ofheating process due to the *D*-value implementation. Lipase inactivation proceeded quickly (*D*-value was low or short time of exposure) at high microwave power or proceeded very slowly (longer time of exposure or *D*-value was high) at low microwave power. This paper discussed temperature profile of the mesocarp at various *D*-values and their relationship with power and power density. Finite Difference Methods used to estimate those distribution of temperature. The FFA concentration and water content of palm oil determined to evaluate effect of temperature to palm oil quality after those certain process.

---

* Corresponding author. Tel.: +62-812-606-1817; fax: +62-61-738-4628.
*E-mail address:*mayasharid@yahoo.com

2. Methodology
2.1. Materials and experimental setup

Materials of this study comprises of oil palm fresh fruits bunch (*Tenera* variety) that collected from UniversitiTeknologi Malaysia Plantation, microwave oven Sharp R-958A (2450 MHz, 800 W), data logger (Pico Temperature Data Logger PT 104), and screw presser (fabricated). The microwave oven was connected with data logger and computer, to monitortemperature of oil palm fruits during sterilization period.

a   **b**
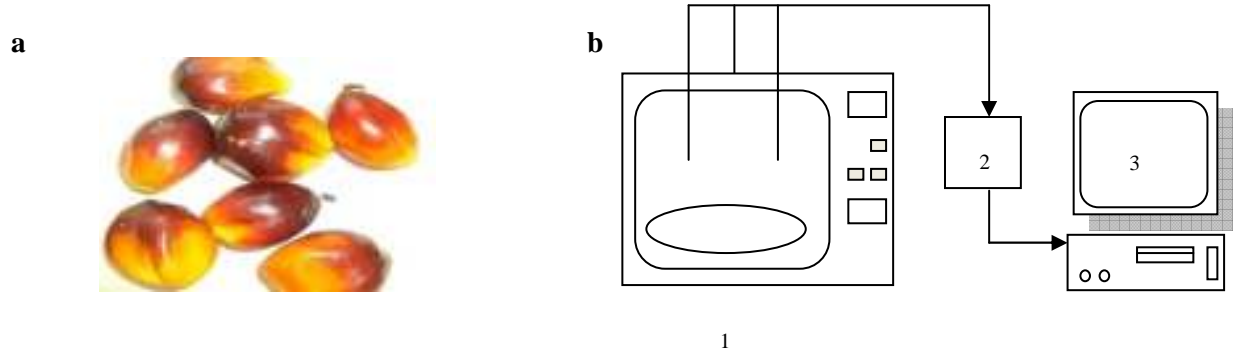
Fig 1. Material and experimental setup: (a) oil palm fruits, and (b) microwave oven (1) connected with data logger (2) and computer (3)

2.2. Sterilization Proces

Oil palm fruits bunch was cut by chain saw (Tokai 3600) into 0.5. 1.0 and 1.5 kg portion respectively. Thus, sample placed in the centre of the microwave and exposed to microwave irradiation at high, medium high and medium power level respectively. Temperature of mesocarp was monitored, measured and recorded at various *D*-valuesusing thermocouple type J, which was punched into the oil palm fruit at three points. The sterilization process carried out in triplicates.

2.3. FFA and Water Content Test

FFA concentration of palm oil was determined according to MPOB test method[18, 19] and water content was determined using Karl Fisher Titration (756 Metrohm KF Coulometer).

2.4. Dielectric Properties Measurement

Dielectric constant and dielectric loss factor measurement utilized a system, which consist of dielectric probe (8710-2038) and computer controlled (ENA Series Network Analyzer Agilent Technologies),at frequency range of 300 kHz to 20 GHz.

2.5. Modeling of Temperature Distribution

Heat transfer equation was applied to evaluatethe *D*-value and temperature distribution relationship during sterilizationperiod. Power absorbed by the fruit considered as a source term in heat transfer equation. The transient heat transfer equation with microwave source term [15-17, 20] could be written as Eq(1) and partial diffential equation of Eq.(1) for one dimensional body was given in Eq(2).

$$\rho c_p \frac{\partial T}{\partial t} = k \nabla^2 T + P(r,y,z,t) \qquad (1)$$

$$\frac{\partial T}{\partial t} = \left(\frac{k}{\rho c_p}\right)\left(\frac{\partial^2 T}{\partial r^2}\right) + \frac{P}{\rho c_p} \qquad (2)$$

Eq(2) was solved using Finite Difference Method (semi discretization, central different) and modeling was conducted by using Matlab R12a software. Temperature distribution inside mesocarp was modeled into radial direction at various *D*-values (inner mesocarp, r=0 to outer mesocarp, r=4.5 mm), as shown in Fig.2 to Fig.4, with boundary [15-17, 20]:

$$-k\frac{\partial T}{\partial r} = h_c(T - T_a) \tag{3}$$

Power from microwave that absorbed by dielectric of oil palm fruits per unit volume was given by Eq(4). [15-17, 20], while electric field could be estimated numericaly by using Eq(5).[21]:

$$P(r,t) = \frac{1}{2}\omega\epsilon_0\epsilon''|E|^2 \tag{4}$$

$$E_z = \frac{1}{2\pi}\frac{1}{\ln(b/a)}\int_a^b\int_0^\pi cos\square'\frac{\exp(-jkR')}{R'}\cdot\left[\frac{1}{\rho} - \left(jk' + \frac{1}{R}\right)\frac{(\rho-\rho'cos\square)}{R'}\right]d\square'd\rho' \tag{5}$$

Term R' and k' from Eq.(5)[21]are:
$$R' = [(z - z')^2 + \rho^2 + \rho'^2 - 2\rho\rho'cos']^{\frac{1}{2}} \tag{6}$$

$$k' = \frac{2\pi f}{c}\sqrt{(\epsilon_r' - \epsilon_r'')} \tag{7}$$

3. Results and Discussion
3.1. Effect of D-value and Power Density on Temperature
Fig.2 to Fig.4 show the *D*-value–temperature profile at various power level and oil palm fruits bunch mass portion. Temperatures historyhad observed below 100°C for overall treatments. Several studies that used microwave oven at frequency of 2450 MHz,either utilizing similar or different microwave power, had reported similar result elsewhere [3, 4, 6]. It was recorded that sterilization on a smaller portion of mass (0.5 kg) achieved maximum temperature at short heating duration (*D*-value were 8.333 and 9.708minutes, except for those at medium power level) as compared to sterilization of a bigger portion of mass (1.0 and 1.5 kg, except for those at medium high power level).
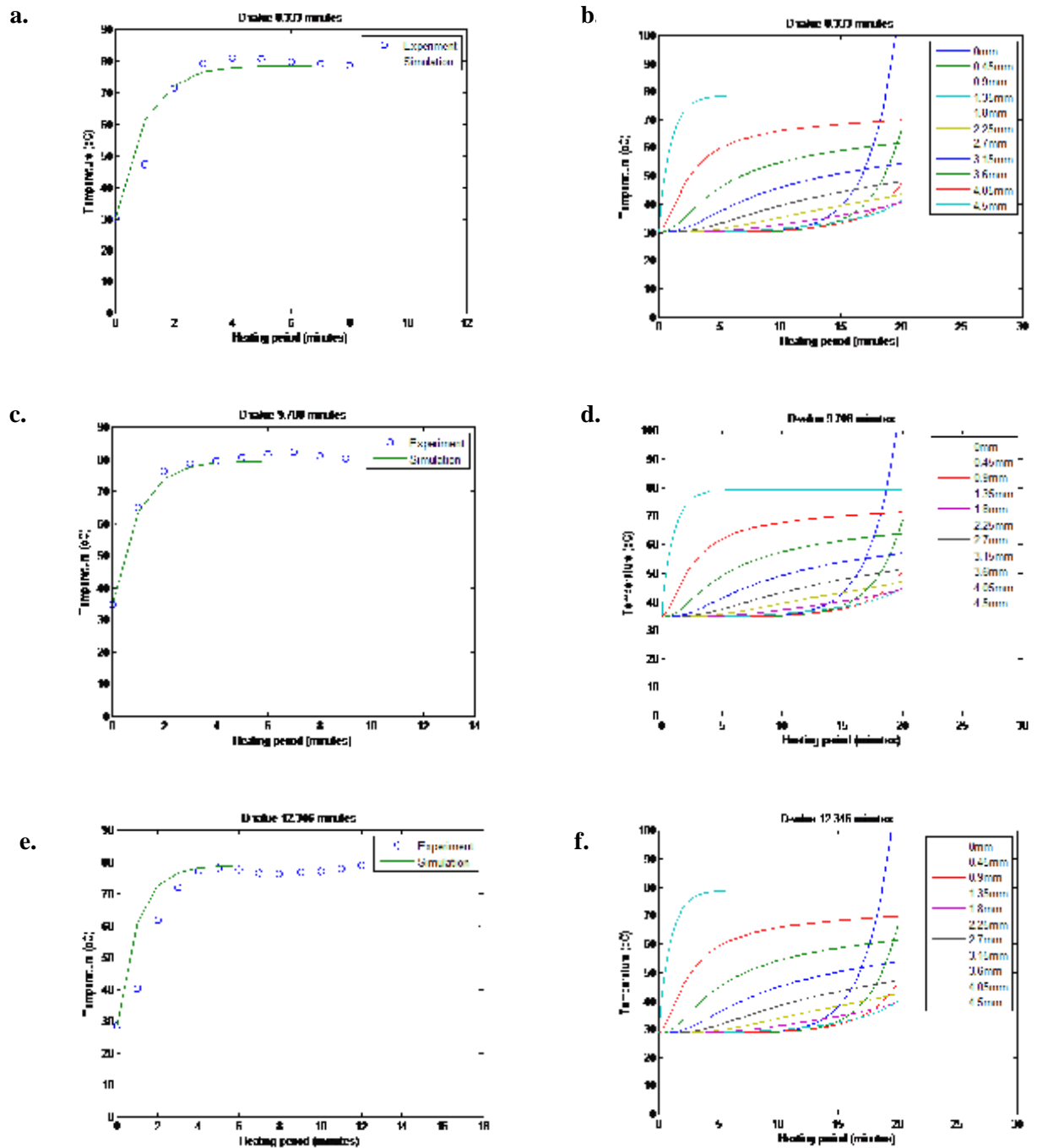
Fig 2. Model of *D*-value-temperature profile of 0.5 kg treatment at various *D*-value using high power
level (a&b), medium high power level (c&d), and medium power level (e&f)
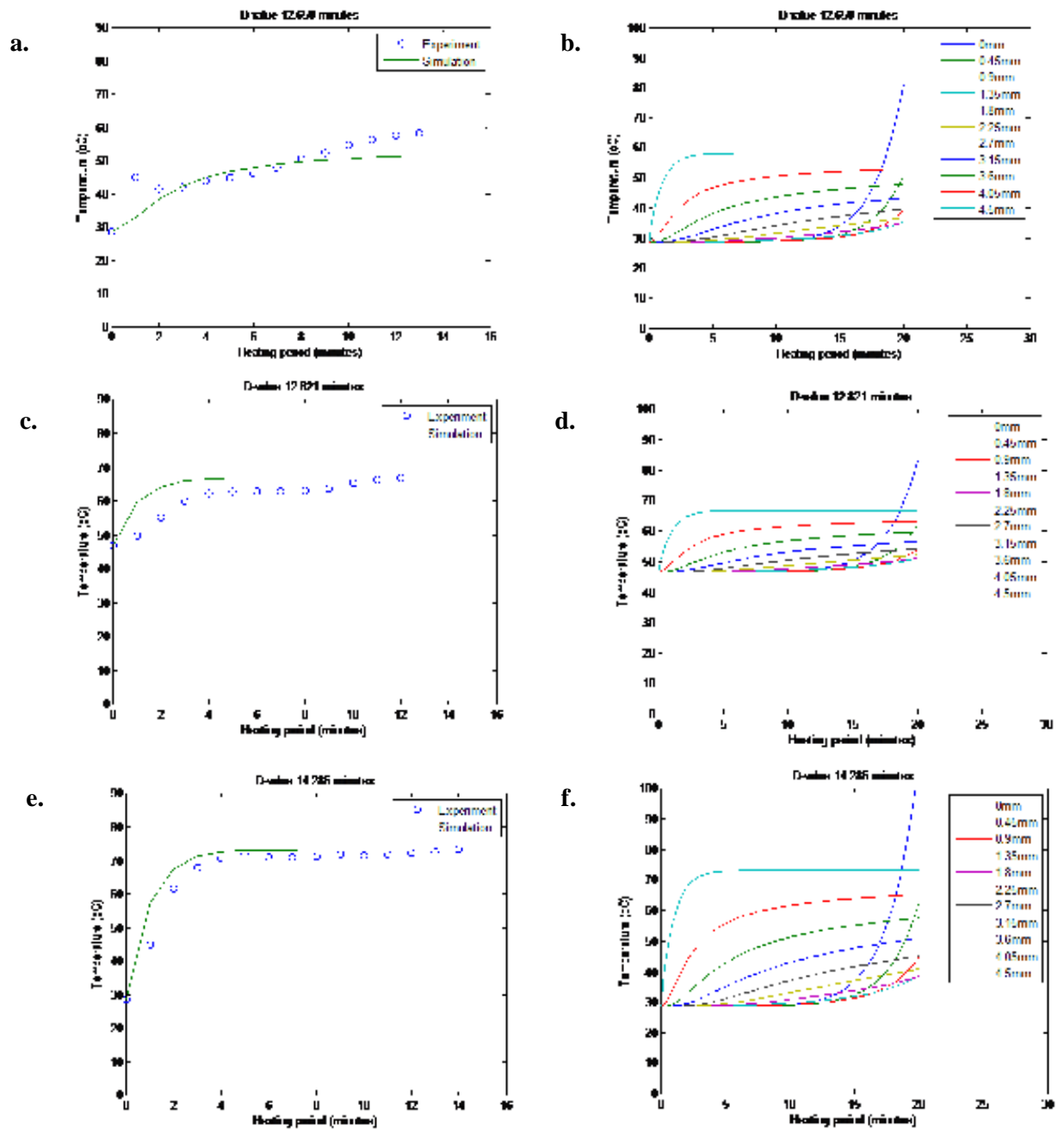
Fig 3. Model of *D*-value-temperature profile of 1 kg treatment at various *D*-value using high power
level (a&b), medium high power level (c&d), and medium power level (e&f)
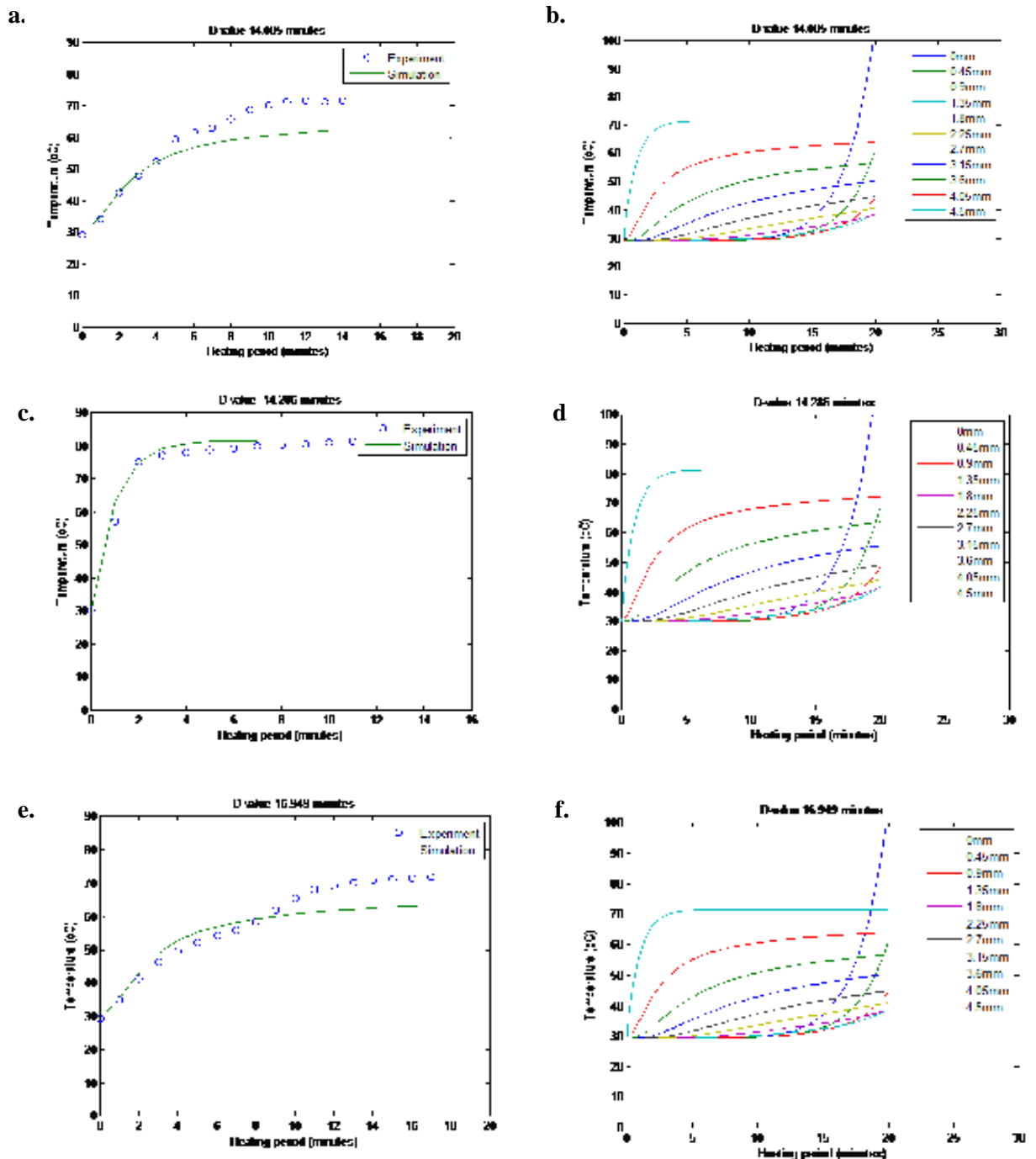
Fig 4. Model of *D*-value-temperature profile of 1.5 kg treatment at various *D*-value using high power level (a&b), medium high power level (c&d), and medium power level (e&f)

Microwave power provided higher power density for treatment at smaller portion of oil palm fruits. Power density expressed the number of power apply to the oil palm fruits sample per kg. High power density expressed effectiveness of microwave sterilization process due to maximum microwave energy absorbed by small sample. This state increased the temperature and activation energy (E_a), and lipase inactivation proceeded very quickly. Fig.2(a,c and e), Fig.3(a,c and e), and Fig.4(a,c and e) show that temperature of the model fitted with temperature which obtained from experimental data at a radial distance of 4.5mm, except for those with *D*-value of 12.658 minutes at radial distance of 4.05mm. Thus, indicated mathematical model from this study could be applied in estimating temperature distribution of oil palm fruit. Similar trend model of time-temperature distribution on

51

microwave heating of non oil palm fruits material using different methods reported byothers studies elsewhere [15-17, 22].

Treatments at *D*-value of 8.333 and 9.708 minutes showed rapid heating at initial 3 minutes, before recorded highest temperature at 82°C and 80.46^{o}C respectively, as shown in Fig.2(a) and (c). Increment of bunch portion from 0.5 kg to1 kg and 1.5 kg respectively, decreased maximum temperature to 80°C, and 78°C (for 1 kg) and 76.5^{o}C, and 75°C (for 1.5 kg) respectively. Treatments ofmedium power level, at any bunch portion, recorded maximum temperature that lower than those with medium high and high power level. The temperature observed for treatment of medium power level at 0.5 kg, 1 kg, and 1.5 kg, were 70.5^{o}C, 75°C and 70°C respectively. Those treatments at longer *D*-value (> 12 minutes) were mainly achieved maximum temperature after 4 minutes.

Fig.2(b,d and f), Fig.3(b,d and f), and Fig.4(b,d and f) show thermal runaway phenomena after 5 minutes heating duration, started from inner part (radial distance = 0 mm or/at outer surface of kernel) to outer skin of the mesocarp along with radial distance, except for those at skin surface that showed stationer temperature while heating at certain *D*-value. Clemens and Saltiel (1996) reported similar phenomena while heating non oil palm fruits material[23]. Runaway effect was uncontrolled rose in temperature in a material, which cause damage of material [24]. Others studies reported browning effect on kernel after heated up the oil palm fruit at 800 W for duration of 4 minutes [2] and 5 minutes [4], while this study observed hardening effect on fruit of 0.5 kg treatment, after heated up the fruits at high power density for more than 13 minutes.

3.2. Effect of D-value and Power to Palm Oil Quality

Evaluation of free fatty acid (FFA) concentration at any *D*-value show in Fig. 5(a). It was observed that FFA concentration as key parameter of palm oil quality measured below maximum standard of FFA requirement for commercial palm oil (maximum FFA concentration of commercial palm oil is 3.50%). The FFA level of concentration were observed between 0.30% to 1.39%(FFA average was about 0.70%). The FFA expressed lipase inactivation performance by microwave irradiation. High temperature and long heating time period usually obtained low level of FFA concentration.Similar results of FFA concentration from microwave sterilization of oil palm fruits were reported elsewhere [2-4].

a.

b.
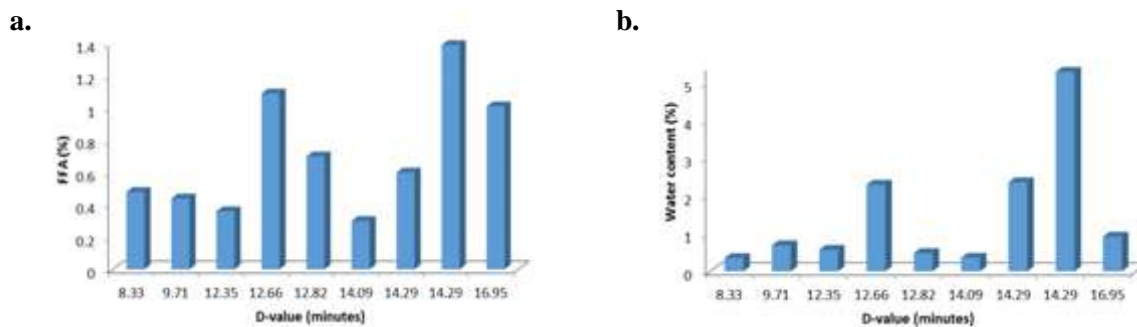
Fig 5. Palm oil quality at various *D*-value: (a) FFA concentration, and (b) water content

Fig 5(b) show water content of palm oil after microwave sterilization at various *D*-values. It was observed that water content of palm oil were between 0.3% (*D*-value was 12.658 minutes) to 5.3% (*D*-value was 14.286 minutes). Overall water content was recorded below 5% except for those treatments with *D*-value of 14.286 minutes and power density of 284.86 W/kg. Normally, water content for typical CPO is recorded at 2 to 5% maximum. Cheng et al.(2011) recorded water content of 0.05% after microwave irradiation for 1 to 4 minutes [2].

4. Conclusion

The microwave sterilization of a smaller portions of bunch fruits, proceeded very quick (*D*-value were 8.333 and 9.708 minutes). Treatments at *D*-value of 8.333 and 9.708 minutes recordedrapid heating during initial period of 3 minutes, before its achieved maximum temperature at 82°C and 80.46^{o}C respectively. The temperature of mesocarp obtained from experimental data fitted with model

at radial distance of 4.5mm, except for those with *D*-value of 12.658 minutes at radial distance 4.05 mm. Thus, indicated mathematical model from this study could be used to estimate temperature distribution of oil palm fruit.Palm oil quality that indicated by FFA concentration and water content were measured below maximum standard for commercial palm oil. FFA level of concentration were observed between the range of 0.30% to 1.39% (FFA average was about 0.70%),while water content of palm oil were recorded between the range of 0.3% to 5.3%. Overall water contents were recorded below 5% except for those treatments with *D*-value of 14.286 and power density of 284.86 W/kg.

References

[1]   K. Berger, "Production of Palm Oil from Fruit," *Journal of American Oil Chemists' Society,* vol. 60, pp. 206-210, 1983.

[2]   S. F. Cheng, M. Nor L, and C. H. Chuah, "Microwave pretreatment: A clean and dry method for palm oil production," *Industrial Crops and Products,* vol. 34, pp. 967-971, 2011.

[3]   M. C. Chow and A. N. Ma, "Microwave in the Processing of Fresh Palm Fruits," presented at the PIPOC International Palm Oil Congress (Chemistry and Technology), 2001.

[4]   M. C. Chow and A. N. Ma, "Processing of Fresh Palm Fruits Using Microwaves," *Journal of Microwave Power & Electromagnetic Energy,* vol. 40, p. 9, April 17, 2007 2007.

[5]   N. Sukaribin and K. Khalid, "Effectiveness of sterilisation of oil palm bunch using microwave technology," *Industrial Crops and Products,* vol. 30, pp. 179-183, 2009.

[6]   I. Umudee, M. Chongcheawchamnan, M. Kiatweerasakul, and C. Tongurai, "Sterilization of Oil Palm Fresh Fruit Using Microwave Technique," *International Journal of Chemical Engineering and Applications,* vol. 4, p. 3, June 2013 2013.

[7]   C. P. Tan, Y. B. Che Man, S. Jinap, and M. S. A. Yusoff, "Effects of Microwave Heating on Changes in Chemical and Thermal Properties of Vegetable Oils," *Journal of American Oil Chemists' Society,* vol. 78, pp. 1227-1232, 2001.

[8]   M. Sarah and M. R. Taib, "Key factors from sterilization of oil palm fruits by microwave irradiation," in *International Conference on Environmental Research and Technology*, Penang, 2012.

[9]   Tan, "Microwave heating of oil-palm fresh fruit samples," United Nations Educational, Scientific and Cultural Organization1981.

[10]   M. Sarah. and M. R. Taib., "Enzymatic Destruction Kinetics of Oil Palm Fruits by Microwave Sterilization," *International Journal of Chemical Engineering and Applications,* vol. 4, p. 5, June 2013 2013.

[11]   R. N. Smith, "Kinetics of Biocide Kill," *International Biodeterioration,* vol. 26, pp. 111-125, 1990.

[12]   P. J. Fellows, *Food Processing Technology. Principles and Practice*. Chichester, England: Ellis Horwood Limited, 1990.

[13]   M. Karel and D. B. Lund, *Physical Principles of Food Preservation*: Marcel Dekker, Inc., 2003.

[14]   C. Neef, S. A. van Gils, and W. L. IJzerman, "Analoqy between temperature-dependent and concentration-dependent bacterial killing," *Computers in Biology and Medicine,* vol. 32, pp. 529-549, 2002.

[15]   A. Navarrete, R. B. Mato, and M. J. Cocero, "A predictive approach in modeling and simulation of heat and mass transfer during microwave heating. Application to SFME of essential oil of Lavandin Super," *Chemical Engineering Science,* vol. 68, p. 10, 2012.

[16]   S. S. R. Geedipalli, V. Rakesh, and A. K. Datta, "Modeling the heating uniformity contributed by a rotating turntable in microwave ovens," *Journal of Food Engineering,* vol. 82, p. 10, 2007.

[17]   H. Zhang and A. K. Datta, "Electromagnetic, heat transfer, and thermokinetic in microwave sterilization," *AIChE Journal,* vol. 47, p. 12, 2001.

[18]   MPOB, *MPOB Test Method* 1ed. Kuala Lumpur: Malaysian Palm Oil Board, 2005.

[19]   B. Saad, W. L. Cheng, M. S. Jab, P. L. Boey, A. S. Mohamad Ali, W. T. Wai*, et al.*, "Determination of free fatty acids in palm oil samples using non-aqueous flow injection titrimetric method," *Food Chemistry,* vol. 102, pp. 1407-1414, 2007.

[20]   S. R. S. Dev, Y. Gariepy, V. Orsat, and G. S. V. Raghavan, "FDTD modeling and simulation of microwave heating of in-shell eggs," *Progress in Electromagnetics Research M,* vol. 13, p. 15, 2010.

[21]   L. L. Tsai, "A numerical solution for the near and far fields of an annular ring of magnetic current," *IEEE Transactions on Antennas and Propagation,* vol. AP-20, p. 8, September 1972 1972.

[22]   W. Klinbun and P. Rattanadecho, "Analysis of microwave induced natural convection in a single mode cavity (Influence of sample volume, placement, and microwave power level)," *Applied Mathematical Modelling,* vol. 36, p. 15, 2012.

[23]   J. Clemens and C. Saltiel, "Numerical modeling of materials processing in microwave furnaces," *International Journal Heat Mass Transfer,* vol. 39, p. 11, 1996.

[24]   A. C. Metaxas and R. J. Meredith, *Industrial Microwave Heating*. London: Peter Peregrinus Ltd, 1988.

The International Conference on Chemical Engineering UNPAR 2013

The Optimization Study on Material Condition to Reach Highest Quality of Virgin Coconut Oil

Arie Febrianto Mulyadi*

[ab]*Agroindustrial Technology Department, Faculty of Agricultural Technology, University of Brawijaya, , Veteran Street, Malang, 65141, Indonesia*

* Corresponding author. Tel.: +62 81 79642734 ;E-mail address: arie_febrianto@ub.ac.id.

Abstract

Virgin coconut oil (VCO) has been gaining popularity in recent times. The objectives of this research were to gain the best storage time prior to VCO processing for each plantation locations. The experimental design used in this study was a nested randomized design with two factors and the experiment was repeated three times. The first factor is the coconutplantation locations (L), which is composed of three regions,Lumajang, Malang, and the Blitar. The second factor is thecoconut storage time (W), which consists of three levels: 1 week, 2 weeks, and 3 weeks. The result showed that the storage time was significantly different on the yield of VCO, moisture content, free fatty acid, peroxide value, and relative density. It was found that the best treatment was obtained from combination between Blitar region with 3 weeks storage time. The results of chemical analysis from the best treatment were moisture content 0.0439%,free fatty acids0.0660%, peroxide value 0.0067 meq/k, relative density 0.9143 g/cm^3 and the yield 19,20%,

Keywords: free fatty acid, relative density, moisture content, peroxide value, relative density, yield, coconut storage time, plantation location

I. INTRODUCTION

Coconut (*Cocos nucifera*) is one of the important commodities in Indonesia, which has a total plantation area reached 3.712 million hectares. In terms of food, the chemical composition of coconut meat contains complete essential elements such as protein, fat, carbohydrates, calcium, phosphorus, and others. With this potential oil plants can produce various kinds of products to meet human needs. As a source of income, the role of the coconut plant is very large considering this plant has the ability to produce a continuous basis throughout the year and ready for sale to meet the needs of farm families. One of the utilization of coconut that has a high economic value is the processing of coconuts into virgin coconut oil.

The term VCO refers to an oil that is obtained from fresh, mature kernel of the coconut by mechanical or natural means, with or without the use of heat and without undergoing chemical refining (Villarino, Dy, & Lizada, 2007). Unlike RBD coconut oil which is tailor-made for cooking purposes, VCO is marketed lately as functional oil. Since its first introduction, virgin coconut oil has captured the attention of vast majority of publics. The beneficial properties of VCO are fast spreading. The availability of VCO is increasing in the market especially in South East Asia involving the Philippine, Thailand, Indonesia and Malaysia (A.M. Marina, Y.B. Che Man and I. Amin, 2009).

VCO and coconut oil have been traditionally used to enhance the beauty and promote the growth of our tresses, refine and moisturizes our skin conditions as well as being used as ailments for minor illnesses such as diarrhea and skin inflammations. Nevin and Rajamohan (2010) discovered that wound healing rate was increased in skin of rats treated with topical VCO. Lans (2007) reported that *Cocos nucifera* was also used as an "ethonomedicine" to treat gastrointestinal problems and minor cuts, injuries and swelling. The lauric acid, a medium chain fatty acid component in VCO showed potential use as anti-obesity treatment (St-Onge and Jones, 2002; Assunção *et al.*, 2009) as it

---

* Corresponding author. *Tel.: +62 81 79642734.*
E-mail address : arie_febrianto@ub.ac.id.

increases energy expenditure, directly absorbed and burnt as energy in the liver, resulted in early satiety and thus leading to weight loss.

Virgin coconut oil has received much attention recently. The demand for this oil continues to rise, which can be attributed not only to its superior flavor, but also to reports of its potential health benefits. Because no chemical or high heat treatment is imposed on the oil, the beneficial minor components in the oil are retained. Virgin coconut oil is reported to lower the lipid levels in serum and tissues, and possesses high potential in protecting low-density lipoprotein against oxidative stress induced by physiological oxidants (Nevin and Rajamohan 2004). Apart from that, coconut oil is also well known for its high content of medium-chain triacylglycerols, which are used in medical and cosmetic applications (A.M. Marina, et. Al, 2006)

Until now, the producers have not been paying much attention to the relationship between the condition of the raw material to the quality and yield of virgin coconut oil. Different planting site will produce different coconuts composition different anyway. Results of research conducted in Towaha, it showed that the composition of coconut meat Salak Genjah significantly different in any growing locations (Manoi and Tampake, 1999). Opinion was reinforced by statements of Setyamidjaja (1995) that each location contains coconut planting which has different nutrients and different in quality and yield of VCO. Result of taking raw materials of unknown origin causing the yield and quality of the VCO becomes unstable.

In addition, the storage time of the coconut fruit is also very influential. According Setyamidjaja (1995), the length of storage time will cause the overhaul of the ingredients of sustainable food reserves so it will damage compound that is converted into triglyceride fatty acids. During the storage, coconut oil is still doing the obvious result respiration changes the chemical composition of the fruit.

Currently VCO producers pay less attention to two facts above. Raw materials purchased from various planting locations and it is unknown how long in traders' storage. In an effort to develop the VCO industry, it needs to be studied more deeply about the relationship between storage time and planting site of coconut on yield and quality of the VCO. So, it is necessary to examine the relationship between the location and the storage time of coconut processing to obtain optimal of VCO quality.

II. MATERIAL AND METHODS
Materials and Tools

The main materials used are DALAM cultivar in three planting locations, namely Lumajang, Malang and Blitar Region. The other materials are water, filter paper, and cotton. The equipment used was a bucket, plastic jars, basins, funnels, milk strainer, filter cloth, scales, plastic tube, pipette, measuring cups and hand hydraulic press. Material analysis is benzene and methanol, neutral alcohol, 0.1 N NaOH, distilled water, ammonium thiocyanate, FeCl, and phenolphthalein (PP).

Equipment includes analysis and stative burette, measuring cup, funnel, pycnometer, glass breaker, spectrophotometer, decsicator, erlenmeyer, volumetric flask, OHAUS digital scales, pipette, pipette the volume of the oven, bath, stirrer, vortex, and centrifuge machine.

The Design of Experiments

The experimental design used in this study was a nested randomized design with two factors and the experiment was repeated three times. The first factor is the Coconut Planting Locations (L), which is composed of three regions, Lumajang, Malang, and the Blitar. The second factor is the Coconut Storage Time (W), which consists of three levels: one week, two weeks, and three weeks. Of the two factors combined treatments obtained nine treatment. (Table 1)

Table 1. Treatments Design

Storage time (W)	Planting Locations (L)		
	Lumajang (L1)	Malang (L2)	Blitar (L3)
1 week (W1)	L1W1	L2W1	L3W1
2 weeks (W2)	L1W2	L2W2	L3W2
3 weeks (W3)	L1W3	L2W3	L3W3

VCO Processing

Coconuts is collected from three locations, namely Lumajang, Blitar and Malang region. Coconuts were selected for the study was DALAM cultivar, the local varieties, in 12 months old and have been marked with brown coconut fibre. The size and weight of the fruit is used uniformly.

Coconuts after being picked and stored according to treatment (one week, two weeks, and three weeks). After reaching the specified time, it's ready to process as VCO. The first step is stripping the coconut husk and then separating the meat from the shells and taking its water. The clean coconut meat immediately shredded. Next step, weighed and added coconut water with a ratio of 1: 2. Mixture of coconut water and stir until evenly then squeezed by hand using a hydraulic press to form coconut milk. Coconut milk is collected subsequently settling for ± 60 minutes so that the water and coconut milk (kanil) splits. Kanil in the upper layers of the water is then taken and dumped in the bottom layer. Kanil centrifuged at a speed of 2,000 rpm for ± 30 minutes. After centrifuged, it will form three layers. The upper layer is a VCO, the middle layer is a protein (blondho) and the bottom layer is water. VCO is taken and made next filtering process.

The screening process is done by using a cotton filter paper and placed on top of the funnel. VCO flowed on top of the funnel and placed in the bottom of the funnel measuring cup to hold the droplet VCO.

Physicochemical analyses

Parameters measured were physical and chemical properties of the VCO. Physical properties include yield, moisture content (Apriyantono,et al., 1989), peroxide value (Sudarmadji, et al., 1997), and density (Ketaren, 1989). Chemical properties measured were the number of free fatty acids (FFA) (Mehlenbacher, 1960 in Sudarmadji, et al., 1997).

Data Analysis

All the physico-chemical analysis and functional property measurements were carried out in triplicate. Results are expressed as mean ± standard deviations. Significant differences between means were determined by one-way analysis of variance (ANOVA) using Microsoft Excel 2007. Significant differences among means were established at p<0.05 using Least Significant Difference (LSD). The best treatment is done by using the multiple attribute method.

III. RESULT AND DISCUSSION
Yield

The mean of VCO yield ranges from 12.90% to 21.84%. From the results of variance analysis yield is known that there is a significant influence (α = 0.01) between the length of storage time and coconut planting location on yield. The yield average in each treatment is shown in Table 2.

Table 2. The Mean Value of VCO Yield (%) Influenced by Coconut Storage Time in Each Coconut Planting Locations

	Lumajang	**Malang**	**Blitar**
1 week	12.90 a	13.49 A	13.37 a
2 weeks	16.71 b	17.78 B	21.84 c
3 weeks	15.96 b	17.12 b	19.20 b
LCD 5%	1.60		

Note: figures are accompanied by the same letter indicates no significant difference at LSD 5%

From Table 2 it is known that the highest yield in the treatment process on 2 weeks on Blitar planting location. While the lowest yield in the treatment process on 1 week on Lumajang planting location and significantly different from the others.

For the Blitar as planting location, The highest yield of VCO obtained at the storage time for 2 weeks is equal to 21.84% and the lowest yield obtained in the 1 week storage time that is equal to

13.37%. On Lumajang, the highest yield obtained at the storage time for 2 weeks is equal to 16.71 % and the lowest yield obtained in the storage time for 1 week process that is equal to 12.90% .On coconut planting locations in the Malang, the highest yield obtained at the storage time for 2 weeks is equal to 17.78% and the lowest yield obtained in the storage time for 1 week process that is equal to 13.49%.

According to Djatmiko (1983), oil composition is affected by soil type and fertility, climate and high places. This is according to research conducted by Torah, et al (1999) that there is a real effect of protein content, fat content, ash content, and crude fibre content, and the levels of free fatty acids in coconut planting location. A difference in climate and soil types at the three locations is shown in Table 3.

Table 3. Height Differences, Soil Type, Average Rainfall and Average Temperature At Three Locations Grow Coconuts

Location	Height	Soil Type	Rainfall Average/Year	Average Temperature
Lumajang	300-625 m dpl	alluvial, latosol	1.500-2.500 ml	24°C-32°C
Malang	250-500 m dpl	alluvial, latosol, andosol, mediteran, litosol, regosol, and brown sand	174 ml	23°C- 30°C
Blitar	± 167 m dpl	alluviums are: sand,clay, and volcanic.	172 ml	25°C– 27°C

Source: Anonymous (2005)

Table 3 shows that the height of the location of the Blitar is lower than the Malang and Lumajang. According to Warisno (2003) coconut crop in the lowlands (with a height of less than 200 m above sea level) can bear fruit more quickly and producing higher with a high oil content. Fertility of soil in the Malang relatively more fertile than other locations. Based on Warisno (2003), some types of soil are suitable for use as a coconut plantation is alluvial soil, soil grumosol, regosol soil, and volcanic soil.

Moisture Content

The mean of moisture content in VCO ranges from 0.0421% to 0.0992%. From the results of variance analysis of moisture content is known that there is a significant influence ($\alpha = 0.01$) between coconut storage time and coconut planting location on moisture content. The mean of moisture content of each treatment is shown in Table 4.

Table 4. Mean of moisture content in VCO (%) Influenced by Coconut StorageTime In Each Coconut Planting Location

	Lumajang	Malang	Blitar
1 week	0.0946 c	0.0940 C	0.0851 c
2 weeks	0.0721 b	0.0835 B	0.0644 b
3 weeks	0.0467 a	0.0526 A	0.0439 a
LCD 5%	0.0036		

Note: figures are accompanied by the same letter indicates no significant difference at LSD 5%

From Table 4 notes that the highest moisture content was obtained in the storage time for 1 week at the Lumajang planting site and significantly different from the others. While, the lowest of moisture content was obtained at 3 weeks on Blitar and significantly different from the others. Added by Fabian M. Dayrit, et.al (2007) moisture is an important factor that determines the product quality of VCO. High moisture increases hydrolysis, which leads to a higher free fatty acid content and hydrolytic rancidity. Table 4 shows that the moisture content of all treatments VCO is still below the allowed standard according to Asian and Pacific Coconut Community (APCC, 2003) (Table 1). Maximum moisture content standards approved by is at 0.

Table 5. Quality Factors of Virgin Coconut Oil

Parameter	Value
Moisture (%)	Max 0.1
Matters Volatile at 1200 C (%)	Max 0.2
Free Fatty Acid (%)	Max 0.2
Peroxide Value meq/kg	Max 3
Relative density	0.915 – 0.920
Refractive index at 40^0 C	1.4480 – 1.4492
Insoluble impurities per cent by mass	Max 0.05
Saponification Value	250 – 260 min
Iodine Value	4.1 -11
Unsaponifiable matter % by mass	max 0.2 - 0.5
Specific gravity at 30 deg./30 deg. C	0.915 – 0.920
Polenske Value, min	13
Total Plate Count	< 0.5
Color	Water clean
Odor and Taste	Natural fresh coconut scent, free of sediment, free from rancid odor and taste

Source: APCC, 2003

*Free Fatty Acid/***FFA**

Mean of free fatty acids in VCO ranges from 0.0660% -0.0963%. From the results of variance analysis of free fatty acids is known that there is a significant influence ($\alpha = 0.01$) between Storage Time process and coconut planting locations with mean of free fatty acids. Mean of free fatty acids in each treatment is shown in Table 6.

Table 6. Mean Free Fatty Acid (%) Influenced by Coconut Storage Time in Each Coconut Planting Locations

	Lumajang	Malang	Blitar
1 week	0.0940 C	0.0963 C	0.0850 C
2 weeks	0.0842 B	0.0837 B	0.0750 b
3 weeks	0.0780 A	0.0787 A	0.0660 A
LCD 5%	0.0007		

Note: figures are accompanied by the same letter indicates no significant difference at LSD 5%

Table 6 shows that the highest free fatty acids was obtained on the storage time for 1 week at Malang planting locations and significantly different from the others. While, the lowest free fatty acids was obtained in the coconut storage time for 3 weeks in Blitar planting locations and significantly different from the others.

The results showed that with increasing moisture content, the levels of free fatty acids in VCO also increase. Changes in free fatty acids during storage due to hydrolysis events enzymatic and non-enzymatic against fat contained. Table 6 also shows that the VCO free fatty acids resulting from all treatments were below the standard according to Asian and Pacific Coconut Community (APCC, 2003) (Table 5). Maximum free fatty acids standards approved by the is at 0.5 %.

Free fatty acids (FFAs) are naturally present at low amounts in all vegetable oils. During extraction and storage, additional FFAs may be formed by reaction with residual water in the oil. Hydrolysis can occur by chemical or enzymatic mechanisms. Enzymatic hydrolysis (e.g., with lipases) may occur through indigenous plant enzymes or microbial contaminants. High levels of FFA are undesirable because of their unpleasant taste (Fabian M. Dayrit, et.al, 2007). These FFA are contributes to the off taste and aroma in fats (Mansor, T.S.T, et. al, 2012).

Peroxide Value

The mean of peroxide value in the VCO ranges 0.0037 meq/kg - 0.0080 meq/kg. From the results of variance analysis. is known that there is a significant influence (α = 0.01) among treatments. The average value of peroxide in each treatment is shown in Table 7.

Table 7. Mean of Peroxide in VCO (meq/kg) Influenced by Coconut Storage Time in Each Coconut Planting Location

	Lumajang	Malang	Blitar
1 week	0.0047 a	0.0037 a	0.0043 a
2 weeks	0.0067 b	0.0067 B	0.0080 b
3 weeks	0.0063 b	0.0043 a	0.0067 c
LCD 5%	0.0006		

Note: figures are accompanied by the same letter indicates no significant difference at LSD 5%

In Table 7 note that the highest peroxide value was obtained at the storage time for 2 weeks in Blitar planting locations (0.0080) and significantly different from the others. Whereas, the lowest peroxide value was obtained in the storage time for 1 week at Malang planting locations (0.0037) and significantly different from the others. Table 7 also shows that the resulting of VCO peroxide mean of all treatments was below the allowable standards according to Asian and Pacific Coconut Community (APCC, 2003) (Table 5). Standard maximum peroxide value is equal to 3 meq/kg of oil. The low average peroxide value indicates that VCO samples do not undergo significant peroxidation during processing

Olefinic bonds in unsaturated fatty acids are oxidized over time or during high temperature processing resulting in the formation of hydroperoxides which leads to rancidity (Gunstone 1996). The peroxide value is based on the reaction of hydroperoxides with potassium iodide. This reaction yields molecular iodine (I_2), which is then titrated using standard solution of sodium thiosulfate. The peroxide value is expressed in meq active oxygen (peroxide) per kilogram of oil sample (Fabian M. Dayrit, et.al, 2007).

Relative Density

The mean of relative density in the VCO ranges 0.9157 g/cm^3 -0.9200 g/cm^3. From the results of variance analysis. is known that there is a significant influence (α = 0.01) among treatments. The average relative density in each treatment is shown in Table 8.

Table 8. The Mean of Relative Density in VCO (g/cm^3) Influenced by Coconut Storage Time in Each Coconut Planting Location

	Lumajang	Malang	Blitar
1 week	0.9193 c	0.9200 c	0.9183 C
2 weeks	0.9180 b	0.9183 b	0.9170 B
3 weeks	0.9157 a	0.9163 a	0.9143 A
LCD 5%	0.0007		

Note: figures are accompanied by the same letter indicates no significant difference at LSD 5%

From Table 8 it can be seen that the highest relative density obtained at the storage time for 1 week on location in Malang (0.9200) and significantly different from the others. While, the lowest relative density obtained at the storage time for 3 weeks at Blitar (0.9143). The results showed that the greater the water content of the VCO, the greater relative density. This is presumably because it is influenced by the density of water is higher than the density of the oil. Water density of 0.9998 g/cm3, while the relative density of oil ranged from 0.939 g/cm^3- 0.91 g/cm^3 at a temperature between 15^0-25^{0}C. Table 8 also shows that the relative density of VCO produced from all treatments was below the allowable standards according to Asian and Pacific Coconut Community (APCC, 2003) (Table 5). Standard maximum relative density allowed is equal to 0.920 g/cm^3.

CONCLUSION

Coconut planting locations and storage time significantly affect the moisture content, free fatty acid, peroxide value, relative density, and yield of VCO. Storage time of three weeks to process in the three locations can be tolerated because it produces moisture content, free fatty acid, peroxide value, and relative density of VCO in accordance with quality standards. Virgin coconut oil treatment derived from Blitar to coconut storage time as long as three weeks is best treated with a yield of 19.20%, moisture content 0.0439%, free fatty acid 0.0660%, peroxide value 0.0067 meq/kg, and the relative density 0.9143 g/cm^3.

REFERENCES

Anonymous[a], 2005. Keadaan Wilayah Kab. Lumajang. www.lumajang.go.id

Anonymous[b], 2005. Letak Geografis. www.kabmalang.go.id

Anonymous[c], 2005. Gambaran umum Kab. blitar. www.kabblitar.go.id.

A Apriyantono, D Fardiaz, NL Puspitasari, 1989. Analisis Pangan. IPB Press, Bogor

Asian and Pacific Coconut Community (APCC). (2003). Standard for virgin coconut oil. http://www.apccsec.org/standards.htm

Djatmiko, B. 1983. Pengolahan Kelapa. Fakultas Teknologi Pertanian IPB. Bogor.

Fabian M. Dayrit*, Olivia Erin M. Buenafe, Edward T. Chainani, Ian Mitchelle S. de Vera, Ian Ken D. Dimzon, Estrella G. Gonzales and Jaclyn Elizabeth R. Santos. Standards for Essential Composition and Quality Factors of Commercial Virgin Coconut Oil and its Differentiation from RBD Coconut Oil and Copra Oil. Philippine Journal of Science 136 (2): 119-129, December 2007 ISSN 0031 - 7683

Gunstone F. 1996. Fatty Acid and Lipid Chemistry. United Kingdom: Blackie Academic & Professional, Glasgow, Scotland. p. 103-4

Ketaren, S. 1986. Minyak dan Lemak Pangan. UI Press. Jakarta.

Lans, C. 2007. Comparison of plants used for skin and stomach problems in Trinidad and Tobago with Asian ethnomedicine. Journal of Ethnobiology and Ethnomedicine 3: 3-14

Marina, A.M., Che Man, Y.B. and Amin, I. 2009a. Virgin coconut oil: emerging functional food oil. Trends in Food Science and Technology 20: 481-487.

Marina, A.M., Che Man, Y.B., Nazimah, S.A.H. and Amin, I. 2009b. Chemical properties of Virgin Coconut Oil. Journal of the American Oil Chemists' Society 86: 301-307.

Mansor, T. S. T., Che Man, Y. B., Shuhaimi ,M, Abdul Afiq ,M. J. and Ku Nurul, F. K. M. Physicochemical properties of virgin coconut oil extracted from different processing methods. *International Food Research Journal 19 (3): 837-845 (2012)*

Mehlenbacher, V.C. 1960. "Analysis of fats and oils". Champaign. Ill.; The Garrand Press

Nevin, K.G. and Rajamohan, T. 2010. Effect of topical application of virgin coconut oil on skin components and antioxidant status during dermal wound healing in young rats. Skin Pharmacology and Physiology 23: 290-297

Setyamidjaja, D, 1995, Bertanam Kelapa Hibrida, Penerbit Kanisius, Yogyakarta.

St. Onge, M-P. and Jones, P.J.H. 2002. Physiological Effects of Medium-Chain Triglycerides: Potential Agents in the Prevention of Obesity. Journal of Nutrition 132: 329–332.

Sudarmadji, S., B. Haryono, dan Suhardi. 1989. Prosedur Analisa untuk Bahan Makanan dan Pertanian. Penerbit Liberty. Yogyakarta.

Towaha, J., F. Manoi, dan H. Tampake, 1999. Komposisi Kimia Daging Buah Kelapa Genjah Salak pada Tiga Lokasi Tumbuh, *Majalah Habitat*, Fakultas Pertanian, Universitas Brawijaya, Malang. 12 (2): 2.

Villarino, B.J., Dy, L.M. and Lizada, C.C. 2007. Descriptive sensory evaluation of virgin coconut oil and refined, bleached and deodorized coconut oil. LWT-Food Science and Technology 40: 193-199.

Warisno, 2003, Budi Daya Kelapa Genjah, Penerbit Kanisius, Yogyakarta.

Winarno, F.G. 1989. Kimia Pangan dan Gizi. PT Gramedia. Jakarta.

International Conference and Workshop on Chemical Engineering UNPAR 2013

Effectiveness of the addition of plant growth promoting bacteria (*Azospirillum sp*) in increasing *Chlorella sp* growth cultivated in tofu processing wastewater

Wahyunanto. A. Nugroho[a*], Angga D. S. Aji, Taif Maharsyah, Mustofa Luthfi

Faculty of Agricultural Technology, Brawijaya University, Malang, Indonesia. 65145
* Corresponding author. Tel.: +62 341 571708 *E-mail address*: wahyunanto@ub.ac.id.

Abstract

The objective of this research is to investigate the effect of the growth promoting bacteria (GPB) *Azospirillum sp* to the growth of microalgae *Chlorella sp* in the food industrial wastewater as a medium. The observe the influence, about 10^6 cells/ mL of *Chlorella sp* was cultivatd in 1 L of tofu industrial wastewater. The wastewater was an effluent of an aerobic treatment. Six different treatment was set regarding to the *Azospirillum sp* added to the medium. The glass was marked as A0 as no GPB inoculants added to the medium, and A2, A4, A6, A8 and A10 for 2 mL, 4mL, 6mL, 8 mL and 10 mL of GPB added to the medium respectively. The concentration of GPB was inoculant was 10^8 per mL. The result shows that the highest number of Chlorella was achieved by A6 in the day 10, while the highest maximum growth rate was achieved by A10.

Keywords: *Chlorella sp*., *Azospirillum sp*., tofu processing wastewater

1. Introduction

Food industrial wastewater containing high complex organic materials, carbohydrates, proteins, amino acids and fats in the form of suspended solids and dissolved. Several micro-elements also available in the food industrial wastewater, such as Fe, Mn, Si, Cu, Zn, Mo, N, P, K, Mg, and SO_4 (Jamil, 2001). The presence of organic compounds causes the wastewater contains high concentration of BOD, COD and TSS. Unwell removed of this component into the environment may lead to eutrophication in the water body. In another perspective, innovations to explore a wide range of renewable energy are being promoted in the world, including Indonesia. Bio-energy is a form of energy which is enough to get the attention in the world today. One form of energy that is being developed is biodiesel, which the raw materials can be extracted from microalgae.

Microalgae is organism that is potential to be used as bio-fuel feedstock production [1]. Lipid content in microalgae could reach to above 50% in the dry weight basis. Microalgae growth rapidly, and take about 10 days from the first cultivation until it is being harvested [2]. With mathematical estimation, the oil that can be produced by microalgae is about 120,000 kg biodiesel / ha year, or 20 times as much as the productivity of palm oil (5,800 kg biodiesel / ha year) and 80 times higher than that of castor oil, which was about 1,500 kg biodiesel / ha year [3].

In regard to the above description, it shows that the need for sustainable waste management and renewable energy can be met. The cultivation of this "energy crops" in the rich-nutrients wastewater is expected to suppress the use of fertilizers that commonly practiced in the microalgae cultivation.

To support the microalgae cultivation, de Bashan [4] reported that addition of *Azospirillum sp* could significantly increase the growth. It is because Azospirillum produce Indole Acetic Acid (IAA) that is widely recognized as growth hormone that is needed by a plant to grow. *Azospirillum sp* is a non symbiotic nitrogen-fixing soil bacterium. These bacteria live freely in the soil. Eckert et al [5] . reported

---

that *Azospirillum sp* can be used as biofertilizer, due its ability to tie up nitrogen (N_2). They also reported that about 40-80 % of the total nitrogen in rattan was tied up by *Azospirillum sp*, while in the corn cultivation; about 30 % nitrogen could be tied up by this bacterium. Akbari et al [6] stated that the bacteria also produce growth hormone up to 285.51 mg / liter of total culture medium, so as to improve the efficiency of fertilization. A few has been reported about the use of this bacterium in the aquatic ecosystem. It is expected that the addition of this bacterium could support the growth of the bacterium during its cultivation.

The objective of this research is to investigate the effect of the growth promoting bacteria *Azospirillum sp* to the growth of microalgae *Chlorella sp* in the food industrial wastewater as a medium.

2. Materials and Method

2.1. Materials

Materials used in this study were Chlorella sp seeds, and Azospirillum sp as growth promoting bacteria. The growth medium was effluent of anaerobic treatment process. The tools used in this study is a microscope to observe the total density of microalgae, beaker glass, aerator for air supplies, a thermometer to measure the temperature, 40-watt fluorescent lamps as source of light, haemocytometer, and lux meter.

2.2. Research Methods

Culturing *Chlorella sp*. Initial culture performed in a aquaculture laboratory, Brawijaya University with inoculants taken from BBAP Situbondo. lab workshop of the Faculty of Fisheries and Marine Sciences with inoculants results from Situbondo district. First, distilled water that has been given fertilizer (walne) 0.3 ml was put into another 50 ml of distilled water. This mixture was then sterilized. About 150 ml of Chlorella inoculants was put into it. Every 4 days, the number of the microalgae was counted until it reached around 10^6 cells/mL.

2.3. Media preparation.

The growth media was an effluent of anaerobic treatment of tofu industrial wastewater. The tofu processing industry is located in Batu City, East Java, Indonesia. Each glass jar (of all 6 jars) was filled with 1 litre of this wastewater. To avoid the dirt went into the jar, the wastewater was filtered out using a fabric. Each of the jars then was labeled (A0, A2, A4, A6, A8, and A10).

2.4. Mixing

In each liter of wastewater was added with *Chlorella sp*., and the microalgae concentration was set to be 10^6 of cell/mL. After that, *Azospirrilum sp* was added into the jar. The concentration of *Azospirillum sp* inoculants was 10^8 cfu/mL. The addition of the *Azospirillum sp* was regarding to the label, which were 0 mL, 2mL, 4mL, 6 mL, 8mL and 10 mL for A0, A2, A4, A6, A8, and A10 respectively.

2.5. *Observed Parameters*

The observed parameters were microalgae density, pH of the medium, the temperature of the media, dissolved oxygen, ammonium, nitrate and phosphate. The parameters measurement for microalgae density, temperature, pH, and DO was done 2 times a day, which were in the morning and afternoon.

2.6. The Growth Rrate

The microalgae growth rate was calculate using the following formulae:

$$(\mu_{maks}) = \frac{ln\,Nt\,max - ln\,No}{t\,max - t1} \tag{1}$$

3. Result and Discussion

Overall independent variables, which are temperature, pH and DO is summarized. The experiment show that the average temperature was fluctuative but still in the allowed temperature, which was between 25 ° C - 27 ° C. Slight temperature drops was shown at night, but remain above 20°C. The average pHof the experiment was between 8 and 9.1 in each treatment. Figure 1 shows that the pH of the medium tends to slightly increase with the increasing population of both *Azospirillum sp* and *Chlorella sp*. The increase in pH is predicted because along with the process of utilization of nitrogen fertilizer elements from the sewage out liquid by *Chlorella sp* cells and bacteria *Azospirillum sp* capable of producing nitrogen. This is probably agree with result of (Morel 1983), in the range of pH 7-9, there are two possibilities in the utilization of nitrogen from the nutrient medium by microalgae cells, the use of nitrogen in the form of nitrate and ammonium. It is predicted that that the pH increase was due to the nitrogen uptake by both microorganisms.
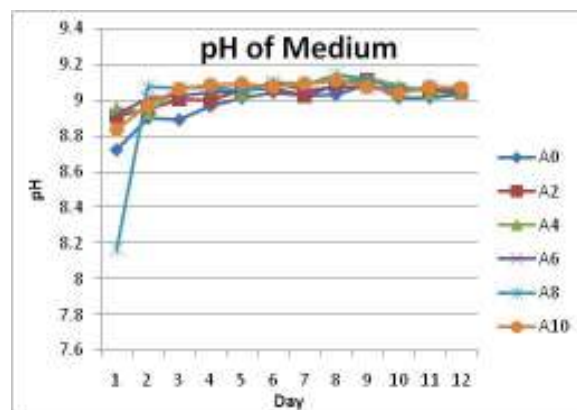
Figure 1. PH of the medium

The dissolved oxygen concentration was in the range of from 7.1-7.6 mg / L. The increase in DO occurred on day 3. It is predicted that this increase was because the addition of abundant photosynthetic O$_2$ form of *Chlorella sp*. At the end of the study population of *Chlorella sp* decreased, which was characterized by the number of dead biomass and settled in the bottom of the media. Since the decomposition process requires a number of O$_2$, this condition causes a deficiency of O$_2$ in the culture medium.
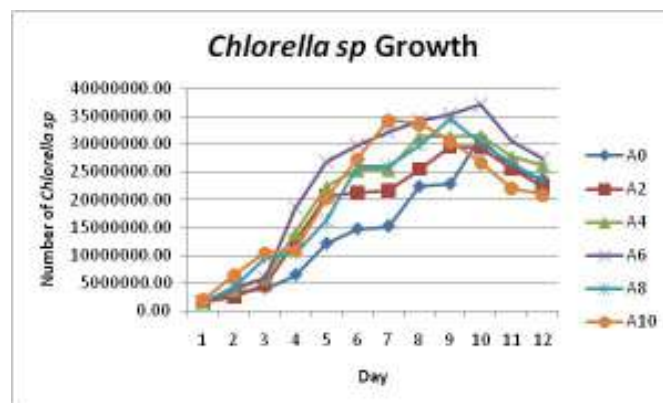
Figure 2. *Chlorella sp* population

Data shows from each dose of GBP added in the medium , treatment without GPB (A0) produced its *Chlorella sp* maximum growth rate (μ$_{max}$) of about 0.327 cells / day; while μ$_{max}$ of *Chlorella sp* for A2,

A4, A6, A8 and A10 was 0.364 cells / day, 0.332 cells / day, 0.373 cells / day, 0.38 cells / day and 0.463 cells / day respectively. This result shows that even though the highest number of microalgae was achieved by A6, the highest growth rate was achieved by A10. The highest μ_{max} of the microalgae of A10 was probably due to the highest IAA produced by the *Azospirillum sp.* By analyzing the variance, the result shows that the addition of different doses of GPB has given a significant influence on the μ_{max} *Chlorella sp.* This is evident F 5% < F count > F 1% dimana 3.34 < 21.654 > 5.56.

From the observation, it was found that population of Azospirillum had already existed in the wastewater, with the number around 23×10^6 cfu/mL, which was about one tenth of that of A2 initial population . Daily observations about population abundance *Azospirillum sp* throughout the study for each treatment is shown in figure3. Peak population abundance in each treatment occurred on day 8 where the A10 has the highest population abundance 2.1x1012 cells / ml and the lowest population abundance obtained in treatment A0 is 1.1×10^{10} cfu/mL.
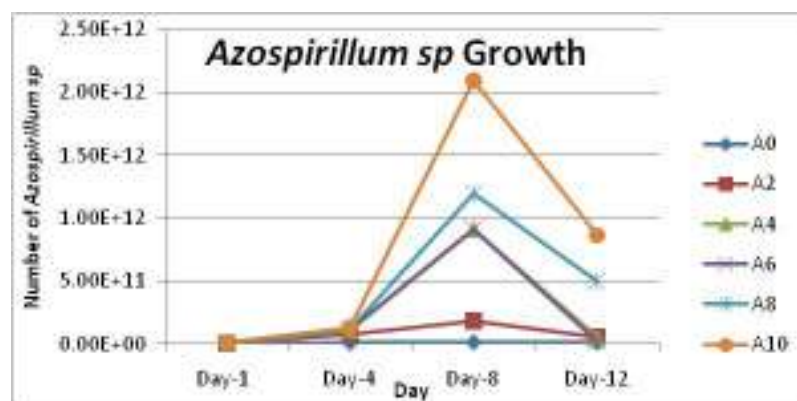
Figure 3. Population of *Azopirillum sp.*

References

[1} Li Y, Horsman M, Wu N, Lan C.Q, and Dubois-Calero N., 2008, Biofuels From Microalgae. Biotechnology Progress ; 24 (4) : 815–820.

[2] Hu, Q. 2004. Environmental effects on cell composition. In: Richmond, A., editor. Handbook of microalgal culture; biotechnology and applied psychology. Blackwell Publishing, Oxford OX4 2DQ, UK.

[3].Teresa M. M., Antonio A. M. dan Caetano, N.S. 2010, Microalgae for Biodiesel Production and Other Applications: A Review, Renewable and Sustainable Energy, 14 217-232.

[4] Luz E. de-Bashan et al. 2008. Involvement Of Indole-3-Acetic Acid Produced By The Growth-Promoting Bacterium Azospirillum Sp. In Promoting Growth Of Chlorella Vulgaris. Department of Soil, Water and Environmental Science, The University of Arizona, Tucson, Arizona, USA

[5] Eckert, B., Weber, O. B., Kirchhof, G., Halbritter, A., Stoffels, M., and Hartmann, A.(2001). Azospirillum doebereinerae sp. nov., a nitrogen-fixing bacterium associated with the C_4 –grass Miscanthus. Int. J. Syst. Evol. Microbiol. 51, 17–26.

[6] Akbari, Gh. Abbas, Arab, SM, Alikhani, HA, Allahdadi & Arzanesh MH. 2007. Isolation and selection of indigenous Azospirilum spp. and the IAA of superior strains effects on wheat roots', World J. Agric. Sci., vol. 3, no. 4, pp. 523-29.

The International Conference on Chemical Engineering UNPAR 2013

Comparison of Corrosion Product of Boiler Feed Water Treatment with Application of Oxidizing – All Volatile Treatment [AVT (O)] and Oxygenated Treatment [OT]

Profiyanti H. Suharti[a*], Yuliana Setyowati[a], Reni Kusumadewi[a], Erwan Yulianto[b]

[a]*Chemical Engineering Department – State Polytechnic of Malang, Malang – 65141, Indonesia*
[b]*Paiton Steam Power Plant, Probolinggo – 67291, Indonesia*

Abstract

The objective of this research was to determine the effect of the Oxidizing – All Volatile Treatment [AVT (O)] method and the Oxygenated Treatment [OT] method to corrosion products released in the boiler feed water treatment in the 3rd unit of Paitonsteam power plants (PLTU Paiton). OT method introduced by the Electric Power Research Institute (EPRI) in 2000 and recently applied tothe PLTU Paiton 3rd unit at the end of 2012. This method forms a protective layer which is considered more stable than the oxide layer formed using AVT (O) method. The effectiveness of the OT method in the 3rd unitof PLTU Paiton, in particular to reduce the amount of corrosion products released, were analyzed in this study and compared with the effectiveness of theAVT (O) method. The measurement of corrosion products released by both methods performed at two sampling points using Corrosion Product Sampler type CPS-11. Those sampling points are Economizer Inlet (EI) and High Pressure Heater Drain (HPHD). The variable used in this study was set point conductivity at economizer inlet. Set point used for AVT (O) method is 4.9 to 5.7 µS/cm and for OT method is 2 to 2.8 µS/cm. Corrosion product analysis performed using Atomic Absorption Spectrophotometer (AAS). The analysis showed that the lowest corrosion product for AVT (O) method is 0.376 ppb (at economizer inlet) and 0.290 ppb (at high pressure heater drain) on the conductivity of 5.1 µS/cm. While the OT method gives lower corrosion products' value, namely 0.224 ppb (at economizer inlet) and 0,249 ppb (at high pressure heater drain) on the conductivity of 2.6 µS/cm. This result showed that the OT method more effective to reduce the amount of corrosion productrelease in3[rd] unitPLTU Paiton.

Keywords: steam power plants, boiler feed water treatment, corrosion products.

1. Introduction

PT Paiton Energy is one of the companies that produce electrical energy in Indonesia. PT Paiton Energy is located in the Paiton industrial area, Probolinggo, East Java, Indonesia. The company has three steam power plants (PLTU) units i.e. 7/8th unit and 3[rd]unit, which rely on kinetic energy of steam to produce electricity. Thus, the steam generators become a major tool in steam power plants. Steam generator in the 3rd unitof PLTU Paitonis once through boilers with coal-fired capacity of 800 MW which operate at high pressure (supercritical pressure).

Feed-water for this supercritical boiler requires very high specification in order to eliminate problems in the operation of the boiler. Boiler feed-water in the PLTU Paiton derived from seawater and still contains a lot of minerals. Those mineral contents can reduce the efficiency of the boiler and piping systems in PLTU Paiton. Piping systems and boilers in PLTU Paiton, especially in 3rd unit, made of carbon steel which has several advantages, namely strong and cheap but susceptible to corrosion. Therefore, control of mineral contents that distributing in piping systems and boilers are becoming critical in order to eliminate corrosion and scaling.

Boiler feed-water treatment is required to remove those mineral contents so corrosion and scale deposits in the boiler and piping systems can be avoided. There are six basic water treatments used for utility units, including for the treatment boiler feed-water. There are (1) Congruent Phosphate, (2) Coordinated Phosphate, (3) Phosphate plus Hydroxide/Equilibrium Phosphate, (4) Sodium Hydroxide, (5) All Volatile Treatment – AVT and (6) Oxygenated Treatments – OT (Jonas, 2000).

---

* Corresponding author. Tel.: +62-341-404424; fax: +62-341-404420.
*E-mail address:*profiyantipolinema@yahoo.com.

All volatile treatment (AVT) is the main method of feed-water treatment for once-through boilers that is widely used in Japan (Mitsuhiro & Masamichi). AVT uses volatile alkalizing agents, commonly ammonia, to suppress corrosion. AVT can be done with the addition of reducing agents, called AVT (R), and with the presence of residual oxygen, called AVT (O). AVT restricts the conductivity of the boiler feed-water (BFW) to < 5 μS/cm for boiler with maximum heat transfer of 250 kW/m² and for heat transfer above to < 3 μS/cm (Hoehenberger)

The use and application of AVT method, especially AVT (R), have resulted in a wide range of problems. One of them was boiler deposits and increased in boiler pressure drop. AVT (O) and Oxygenated treatment (OT) was introduced to eliminate those problems. In 2005, Electric Power Research Institute, INC. (EPRI) had reported the increasing boiler pressure drop when operating with AVT (R) and the alleviation when converted to OT. When AVT method applied, boiler pressure drop reached 50 bars after 3500 operating hours. After converting to OT method, pressure drop decreased gradually to 40 bars and remained constant at this value after 5000 operating hours (Dooley & al, 2005).

Pressure drop decreases due to the formation of ferric oxide hydrate (FeOOH) or ferric oxide (Fe_2O_3) layer on the surface of the magnetite oxide (Fe_3O_4) layer and within the pores of the piping system. The FeOOH or Fe_2O_3 layer called as hematite layer and has a much lower solubility than Fe_3O_4 layer in feedwater. This Fe_3O_4 layer (magnetite layer) forms on all the ferrous surfaces throughout the feedwater system. Fe_3O_4 will be dissolved into the feedwater flow due the reducing environment. The amount of the protective layer that dissolve, either magnetite or hematite, calculated as corrosion product. If FeOOH layer more stable than Fe3O4, the corrosion product release will be reduced so the accumulation of corrosion product in the boiler will be reduced too. Thus, boiler pressure drop will be decreased (Dooley & al, 2005).

The major differences between AVT and OT are shown in Figure 1. The differences were (1) kind and amounts of chemical agents are used, (2) the location of the injection point, and (3) the concentration of dissolved oxygen in the entry point to the boiler called as economizer inlet. For the application of AVT, the condensate can be deaerated in two locations of the plant cycle. The first is the condenser and the second is the deaerator. Ammonia and hydrazine are used in AVT as the feedwater conditioning chemicals. OT uses oxygenated high purity water to minimize corrosion in the feedwater treatment. Oxygen, hydrogen peroxide, and air have been used as oxidants. In contrast with AVT, OT method can be applied only in plant cycles with all-ferrous metallurgy downstream of the condenser (Dooley & al, 2005).

Maintaining good feedwater is an important and fundamental aspect of any steam turbine power plant. A plant that maintains good feedwater achieves the following three benefits, (1) help to ensure maximum life out of its boilers, steam turbines, condensers, and pumps, (2) reduce maintenance expenses; (3) maintain optimal thermal performance. In order to gain these benefits and increase thermal performance of his steam generator system, PLTU Paiton applied OT method in 3rd unit steam generator system at the end of 2012. In this study, the effectiveness of OT method compared with the AVT method that applied before.
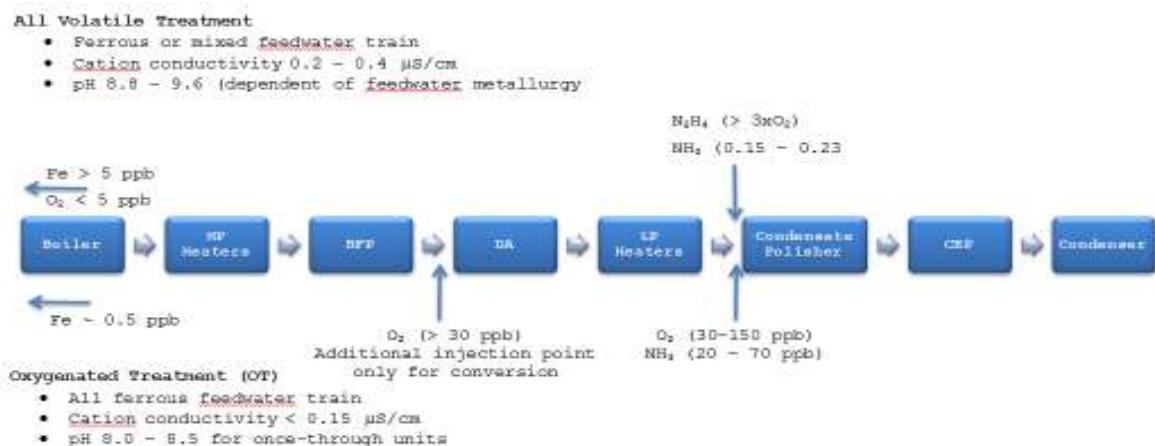

Figure 1. The major differences between AVT and OT

2. Methodological

The research was carried out experimentally in3rd units of PLTU Paiton. AVT (O) method and the OT method were applied alternatelyin3rd Unit of PLTU Paiton. The effectiveness of both methods was compared based on corrosion product release in the existing piping system. Corrosion products analyzed inline at several sampling points using Corrosion Product Sampler type CPS-11. Those sampling points are economizer inlet (EI) and high pressure heater drain (HPHD).The Economizer Inlet (EI) was chosen as sampling point because this point became the entry point for the boiler. Thus, the contaminants in this point should be kept at a low concentration to avoid the pressure drop in the boiler, as a result of scaling. HPHD was chosen in order to maintain the mineral contents in the recycled feedwater to the deaerator. The amount of contaminants in HPHD should always be kept at the lowest level in order to prevent the increase in pressure drop at the high pressure (HP) heaters as a result of these recycle streams.The two methods were appliedatvarious values ofconductivity. Conductivityvaluewillaffect thepH of the feedwater and theamount ofcorrosionproducts released.

The research was conducted by the following steps. (1) Set pointconductivityatthe economizer inletwas setaccording to thedesired value. (2) The feedwater parameters wereanalyzed in this condition. The feedwater parameters include the value of inline conductivity that can be achieved, pH, dissolved oxygen (DO), also sodium, silica and chloride contents. (3) Corrosion Product Sampler type CPS-11 was installed inthe piping systemof 3rd unit of PLTU Paiton. (4) The flowrate of the feedwater through CPS-11 was kept at aconstant value for 2 days. After 2 days, the filter paper in CPS-11 was taken and replaced by another filter paper to take another data experiment. (5) The filterpaperwas heatedanddissolvedin100mlof HCl solution until the corrosion products retained on the filter paper was dissolved perfectly. The number ofcorrosion products that dissolved in HCl solution was analyzed using an atomic absorption spectrophotometer(AAS).

3. Discussion

3.1. Adjustment of Conductivity and pH

The operating philosophy for once-through supercritical boilers recognizes that all soluble feedwater contaminants have to dissolve in the superheated existing steam. In figure 2, it was indicated by the red line. The contaminants must be within the allowable limits of turbine inlet steam purity. In other parts of the steam generator cycle (shown by Figure 2), the corrosion products transported to the steam have to maintain at a concentration level low enough to avoid excessive amount of contaminants in the steam turbine inlet. Therefore, the feedwater treatment has to be volatile, either AVT or OT must be used. The chemical used has to meet the requirement of being completely clean and not being thermally decomposed at existing superheated steam temperatures. so the contaminants in the superheat exixting steam can be minimized (Dooley & al, 2002).

Feedwater systems having carbon steel heaters and piping, like in the 3rd unit of PLTU Paiton, required to operate at pH of 9.2 – 9.6 to minimize flow accelerated corrosion (FAC). In AVT method, adjusting this pH required the addition of 500-2200 ppb of ammonium hydroxide as NH_3. This chemical was injected in the exit of Condensate Polisher. When OT method used, oxygenated high purity water used to minimize corrosion and FAC in the feedwater cycle. Oxygen as a corrosion inhibitor allows satisfactory operation over a wide pH range (Tsubakizaki, Takada, Suto, Kawashima, Ichihara, & Yoshida, 2012) so OT method operated at wider pH range of 8.8 – 9.2. pH adjustment in 3rd unit PLTU Paiton was done by setting the conductivity at economizer inlet. The relationship between set point of conductivity and the obtained pH value are shown in Figure 3.

3.2. Corrosion product release

Corrosion product release on both methods, either AVT and OT, was analyzed at two sampling point, i.e Economizer Inlet (EI) and High Pressure Heater Drain (HPHD). These sampling point marked with   in the Figure 2. The corrosion product release at EI was shown in Figure 4 (a), while Figure 4 (b) showed the corrosion product release at HPHD. The corrosion product release in AVT (O) and OT method has a differences value. OT method gives lower corrosion products release than AVT method. This causedby the formation of hematite layer (Fe_2O_3) in the presence of oxygen in OT method. The presence of oxygen,which is maintained at a level of 30-50 ppb for the once-through boiler, causes the formation of FeOOH and Fe_2O_3. The pore from the previous protective layer, which

is formed by reaction (1) – (3), will be filled by FeOOH and Fe_2O_3. In this way, the diffusion of Fe^{2+} ion from the steel surfacethrough the pores in the protective layer to the water phase boundary isstrongly inhibited.
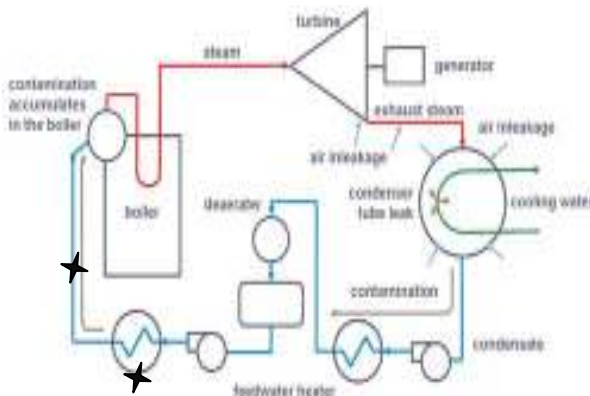
Fig 2. Water-steam cycle in high pressure – drum type boilers
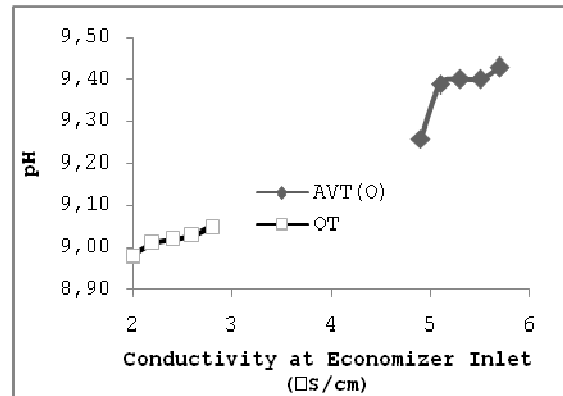
Fig 3. The relationship between set point of conductivity and the obtained pH value

In AVT (O) method, only reaction 1- 3was occured but the corrosion products release was remained at low value, <1 ppb.This condition was caused by the presence of Fe_3O_4, which is known as magnetite.The magnetite layer also serve as protective coating to prevent corrosion products dissolved, although the magnetite layer has lower solubility than hematite layer(Tsubakizaki, Achivement OT (oxygenated Feed-Water Treatment) Application ang Introducton of Countermeasure for Powdered Scale Deposit, 2012).The reaction of corrosion product formation are mentioned below.

$$Fe + 2H_2O \rightarrow Fe^{2+} + 2OH^- + H_2 \qquad (1)$$
$$2Fe^{2+} + 2H_2O \rightarrow 2Fe(OH)_2^+ + H_2 \qquad (2)$$
$$Fe(OH)^+ + 2Fe(OH)_2^+ + 3OH^- \rightarrow Fe_3O_4 + 4H_2O \qquad (3)$$
$$Fe_3O_4 + 2H_2O \rightarrow 3FeOOH + H^+ + e^- \qquad (4)$$
$$2\ Fe_3O_4 + H_2O \rightarrow 3Fe_2O_3 + 2H^+ + 2e^- \qquad (5)$$
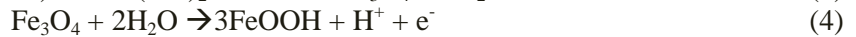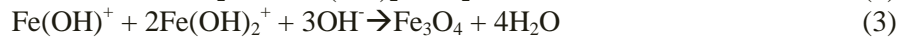
Figure 4 also shown the effect of pH to the amount of corrosion product release. (Khumar & Gupta, 2008) was stated that generally a higher pH will reduce the amount of corrosion products and flow accelerated corrosion. The result of this research slighly different with this statement. In this research, the increase in pH does not significantly affect the amount of corrosion products released. The minimum corrosion product released was gained at pH 9.39 for AVT (O) method and at pH 9.03 for OT method. This pH give the corrosion product as 0.376 ppb and 0.224 ppb. Based on the amount of corrosion products release, it can be concluded that the OT method was more effective than the AVT (O) method. This results agrees with (Tsubakizaki, Takada, Suto, Kawashima, Ichihara, & Yoshida, 2012)'s statement that OT is superior to AVT for once-through boiler.

(a)   (b)
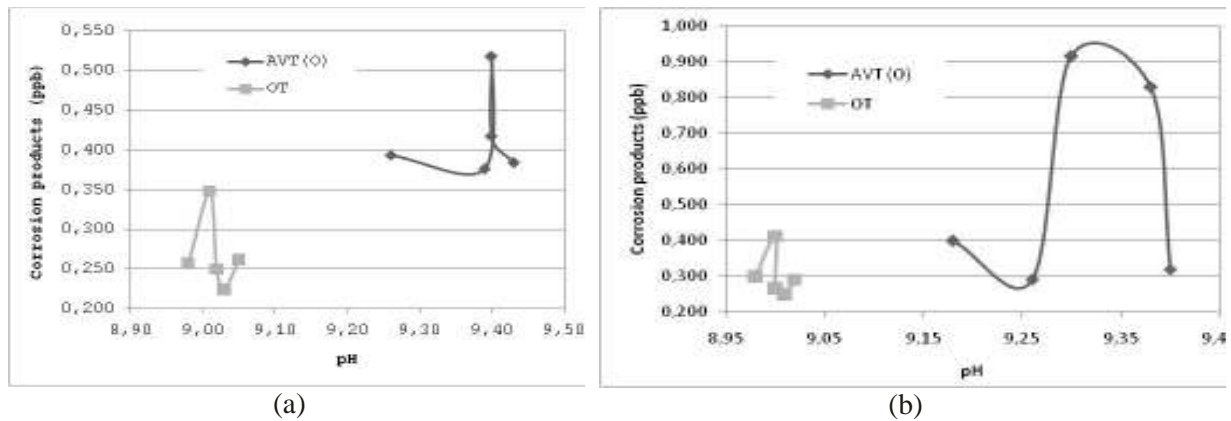
Fig 4. Corrosion product released at economizer inlet (a) and at high pressure heater drain (b)

The corrosion products in high pressure heater drain (HPHD) has a bigger value than corrosion products in economizer inlet (EI), as shown in Figure 4. For AVT (O) method, the maximum corrosion products in HPHD is 0.914 ppb. This value was obtained when the pH of feedwater reached 9.3. While at the economizer inlet, the maximum corrosion product release only 0.518 ppb for similar conditions.OT method also gives the same results. This results agrees with the statement of (Sawochka, Kassen, & Choi, 2000). They stated that corrosion product reaches the largest fraction of the total iron transport in high pressure heater drain.

3.3. Dissolved oxygen at feedwater cycles

Besides the corrosion products release, dissolved oxygen (DO) in feedwater cycles is also a parameter that must be considered. Reliable measurement of DObecame an essential requirementfor two main reasons. High concentrations of oxygen, when combined with ionic contaminants (particularly chlorides) can yield a risk of acidic corrosion, which can lead to sudden large scale tube failures in high-pressure boiler. Very low concentrations of oxygen can enable the development of enhanced iron transport and flow-accelerated corrosion in feedwater and in boiler water(IAPWS, Technical Guidance Document: Instrumentation for monitoring and control of cycle chemistry for the steam-water circuits of fossil-fired and combined-cycle power plants, 2009). (Tsubakizaki, Takada, Suto, Kawashima, Ichihara, & Yoshida, 2012) and (IAPWS, Technical Guidance Document : Volatile treatment for steam water circuits of fossil and combined cycle/HRSG power Plants, 2010) said that the allowable range of DO for AVT (O) and OT method are respectively ≤ 10 ppb and 20-200 ppb. The results of DO measurement for this research are presented in Figure5 below.

(a)   (b)
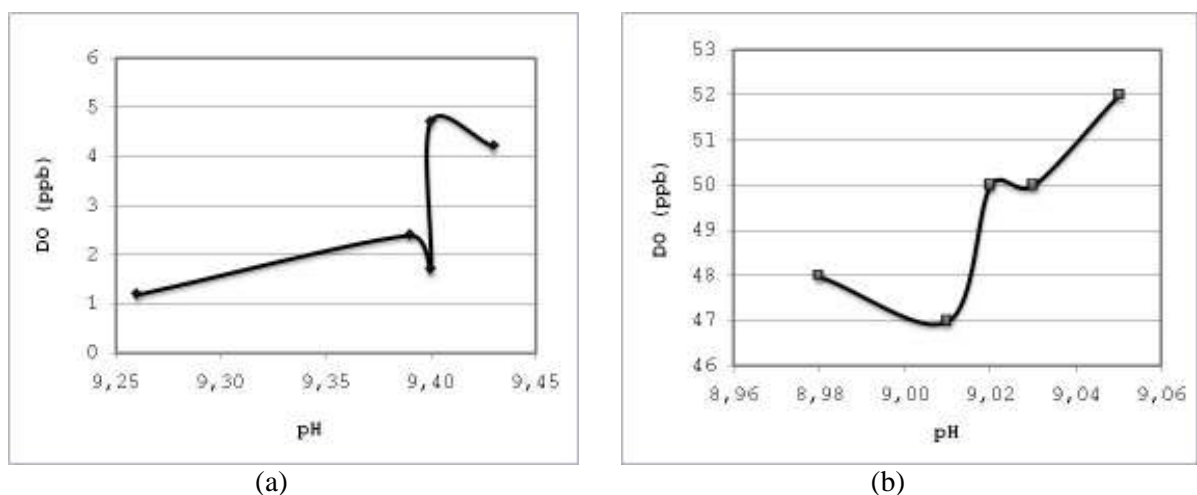
Fig5. Dissolved oxygen at economizer inlet for AVT (O) method (a) and OT method (b)

4. Conclusion and Suggestion

When applied in 3rd unit of PLTU Paiton, the OT method gives lower corrosion products value, namely 0.224 ppb (at economizer inlet) and 0,249 ppb (at high pressure heater drain) on the conductivity of 2.6 µS/cm. For AVT (O) method, optimum pH that give the minimum corrosion products at economizer inlet was 9.39 and reach at the set point of conductivity 5.1 µS/cm. So, it can be concluded that OT method more effective than AVT (O) method.

Sampling point for corrosion product measurement need to be propagated, such as in Condensate Pump Discharge (CPD) and Condensate Polisher Outlet (CPO), in order to make the comprehensive comparison of both methode.

5. Reference

[1] Dooley, R. B., et. al (2005). *Cycle Chemistry Guidelines for Fossil Plants: Oxygenated Treatment.* California: Electric Power Research Institute, Inc.

[2] Dooley, R., et. al. (2002). *Cycle Chemistry Guidekines for Fossil Plants: All Volatile Treatment (Revision 1).* California: Electric Power Research Institute, Inc.

[3] Hoehenberger, L. *Water Treatment, Cycle Chemistry, Boiler Operation and Related Problems/Failures on Steam Generator System >30 bar.* Munchen, Germany: TUV SUD.

[4] IAPWS. (2010). *Technical Guidance Document : Volatile treatment for steam water circuits of fossil and combined cycle/HRSG power Plants.* Canada: Niagara Falls.

[5] IAPWS. (2009). *Technical Guidance Document: Instrumentation for monitoring and control of cycle chemistry for the steam-water circuits of fossil-fired and combined-cycle power plants.* International Association for the Properties of Water and Steam.

[6] Jonas, O. (2000). Effective Cycle Chemistry Control. *ESAA Power Station Chemistry Conference.* Queensland, Australia.

[7] jones, D. A. (2000). *Principle and Preventetion of corrosion.* New York: Macmillan Publishing Company.

[8] Khumar, S., & Gupta, S. (2008). Feed Water Treatment Optimization for Controlling Flow Accelerated Corrosion (FAC). *Symposium on Operational and Environmental Issues Concerning Use of Water as Coolant in Power Plants and Industries - OPENWAC 2008*, (hal. 108-115). Kalpakkam.

[9] Mitsuhiro, Y., & Masamichi, M. Evaluation of Oxygenated Water Treatment. *14th International Conference on the Properties of Water and Steam*, (hal. 461-466). Kyoto.

[10] Sawochka, S., Kassen, W., & Choi, S. (2000). *Effect of Oxygen Concentration on Corrosion Product Transport at South Texas Project Unit 1.* California: EPRI.

[11] Tsubakizaki, S., Takada, M., Suto, T., Kawashima, H., Ichihara, T., & Yoshida, A. (2012). *Achivement OT (oxygenated Feed-Water Treatment) Application ang Introducton of Countermeasure for Powdered Scale Deposit.* Mitsubishi Heavy Industries Technical Review Vol. 49 No.1.

The International Conference on Chemical Engineering UNPAR 2013, ICCE UNPAR 2013

MODIFICATION ON MACERATION EXTRACTION METHOD TO THE YIELD AND COMPONENTS OF RED GINGER OLEORESIN

Jayanudin*[a], Dhena R Barleany[a], Rochmadi[b], Wiratni[b], Ari Sugiartati[a], Yoga D Kusuma[a]

[a]Chemical Engineering, Faculty of Engineering, Sultan AgengTirtayasa University, Jl. JendralSudirman km.3 Cilegon42435, Indonesia[b]Chemical engineering, Faculty of Engineering, GadjahMada University, Jl.Grafika No. 2 Yogyakarta 55281, Indonesia
* Corresponding author. Tel.: +62-254-395502; fax: +62-254-395440.e-mail address:jaya_hisyam@yahoo.com.

Abstract

Oleoresin is a mixture of essential oils and resins or gums resulted from the extraction of spices using organic solvents, and it has many uses. Red ginger oleoresin contains useful components in pharmaceutical and food industries, such as shogaol and zingerone. The purpose of this research is to determine the effect of stirring speed and temperature as the modification of maceration extraction to the % yield of red ginger oleoresin and components contained in the red ginger oleoresin using *Gas chromatography–mass spectrometry (GC-MS)*. This research was divided into two stages; the first stage was the extraction of 20 grams dried red ginger -50+60 mesh in a three neck flask equipped with a condenser and contained ethanol as the solvent. Weight ratios between the red ginger and ethanol were 1:4, 1:5 and 1:6, and the extraction temperature variations were 40°C, 50°C, 60°C with stirring speeds of 600, 700 and 800 rpm for 6 hours. The second stage was separation using distillation method at 80°C. The highest yield of liquid that was resulted from the extraction process was then analyzed using GCMS to identify the components contained in the red ginger oleoresin.Result of this research showed that the highest yield 13% of oleoresin was obtained when the weight ratio of red ginger with ethanol was 1:4, at 50°C temperature and 600 rpm stirring speed. The GCMS showed that the components contained in red ginger oleoresin were zingerone, zingiberenol and shogaol.

Keywords: Maceration extraction; Oleoresin; Red ginger; Shogaol; Zingerone

1. Main text
Background

Red ginger (*ZingiberofficinaleRoxb*) is one of the medicinal plants that have many properties which are very useful as beverage of body warmers, lozenges, raw material of cosmestics, even as anticancers. Those properties are related with the active components which are contained in ginger: shogaol, gingerol and zingiberene. Gingers are widely used for medicines, especially red ginger because it tastes more spicy than the other types of ginger such as white ginger and yellow ginger [1].

Dry Ginger contains essential oil and fixed oil. The main components of essential oil are zinginberene and zingiberol, and the main components of fixed oil are gingerol, shogaol and resin. These components lead to the spicy flavor of ginger [1]. Oleoresin is one of the products of extraction using organic solvent that contains essential oils and resins, so the components in the oleoresin is the combination of the components contained in essential oil and fixed oil.

Red ginger oleoresin contains the active components which are useful as raw material for medicines, cosmetics, foods and beverages. Advantages of the oleoresin application compared with the original material are (a) the quality of foods mixed with oleoresin are more easy to control, it is because of the chemical contents in oleoresin are less than the original material, (b) the use of oleoresin is more efficient, due to oleoresin is the extract of the herb - spice so it will require less oleoresin compared with original spice powder to get the desired taste, (c) oleoresin is more hygienic, because it has to be kept in a sterile condition from bacteria and (d) oleoresin extract is more easily dispers when mixed into foods and beverages compared with the original material (spice

---

* Corresponding author. Tel.: +62-254-395502; fax: +62-254-395440
E-mail address: jaya_hisyam@yahoo.com

powder).

Red ginger oleoresin is produced from red ginger extraction process by using an organic solvent such as methanol, ethanol, ether, hexane and other organic solvents. Organic solvent is selective, so the use of different type of solvent will produce different component. The use of solvent should be considered to be able to produce the desired active component. Another factor need to be considered in the use of solvent is the amount of yield of production this is related to the value of organic solvent polarity.

Another factor that determines the quantity and quality of the oleoresin is the extraction methods that are used. There are three types of extraction methods that can be used; they are maceration, socletation and percolation. Maceration is a simple extraction method. Maceration is done by soaking the powdered crude drugs in the extraction solvent. The solvent will penetrate the cell wall that contains the active substance, then the active substance will dissolve due to the concentration difference, finally the concentrated solution is pushed out. That event is repeated, so it will reach the balance between the solution concentration outside and inside the cell. The advantage of filter method with maceration is the workmanships and the equipments used are simple and easy to commercialize. The disadvantage is that the process is so long and less than perfect [2].

Socletation is the extraction technique which is performed using volatile organic solvent and the compounds is dissolved under hot condition, so that mass transfer process takes place very easy. The advantage of the Socletation method is that the organic solvent can be used repeatedly and no need a lot of solvent [3] .

In that principle, percolation using a solvent in which the solvent is passed slowly (drop by drop) to the material contains organic compounds. This technique is also used on non-volatile solvents, it results large quantities of dissolve organic compounds contained in these materials. Percolation is used when the chemical constituents contained in the material is a bit. When filtrate was obtained, the solvent was then evaporated with rotary evaporator tool.

The most simple extraction method is maceration, but the drawback takes a long time, so this study was modified from the maceration extraction by using temperature changes and changes in stirring speed. These parameters will accelerate the extraction process. The magnitude of the temperature will increase solubility of the solvent and enlarge pores of ginger granules, so that the product yield will increase. Stirring speed relates to the magnitude of the Reynolds number indicates greater turbulence in the extraction process. The amount of turbulence will reduce the thickness of the film so as to increase the speed of extraction. With the depletion layer of film grain surrounds the nutmeg then transfer to the surface of a solid solute will be larger [4]. The purpose of this study was to determine the effects of temperature and stirring speedto the maceration extraction yield and active components contained in oleoresin.

Experimental

This research was divided into two stages. The first stage was the extraction by incorporating 20 grams of dried red ginger that had been pulverized by the size of -50 +60 mesh and then extracted in a three-neck flask equipped with a condenser and containing ethanol as a solvent. Weight ratios of red ginger with ethanol were 1:4,1 : 5 and 1 : 6 , the extraction temperatures were $40^{o}C$, $50^{o}C$, $60^{o}C$ with a stirring speeds of 600, 700 and 800 rpm for 6 hours. The second stage was separation process by distillation at $80^{o}C$ temperature. Products obtained were weighed to determine the amount of yield produced. Greatest yield was analyzed using Shimadzu GCMS QP2010. Type column: phase type capillary RTX - 5MS (60m; 0:25 mmID) , temperature : $50^{o}C$, carrier gas: Helium and Column Flow rate : 0.85 ml / min.

Result and Discussion
1. Effect of Weight Ratios With Solvent Against Red Ginger Oleoresin Yield

This research was using 96 % ethanol to extract 20 grams of dried red ginger for 6 hours. Effect of ratios between red ginger and ethanol used in this research was showed in Figure 1.
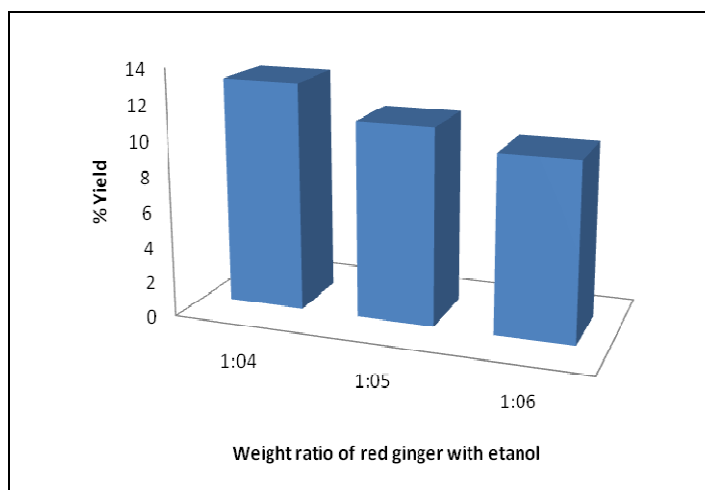
Fig. 1. Effect of the weight ratios of red ginger with solvent to yield

This research resulted the highest yield was obtained with a 1:4 ratio and the yield was 13 % as shown in Figure 1. This result is higher than the study that have been done by Jayanudin et al (2011), which generated the yield of 11.65 % when using the weight ratio of solvent and red ginger 1 : 6. This comparison illustrates that highermass of ginger extracted causes less yield of oleoresin obtained.

Amount of solvent will affect the amount of yield produced, this is related to the distribution of solvent to get into the pores and dissolve solid components contained in the solids. Solute diffuses out of solid particles, then the surface moves around the solid and finally get into the solution.

Another factor that affects the magnitude of the yield obtained by the distillation process is the process of purification of the oleoresin product. Product analysis showed that the are amounts of solvent contained due to distillation process which is not perfect affected the low purity of oleoresin product.

2. Effect of Temperature Extraction Against Oleoresin Yield
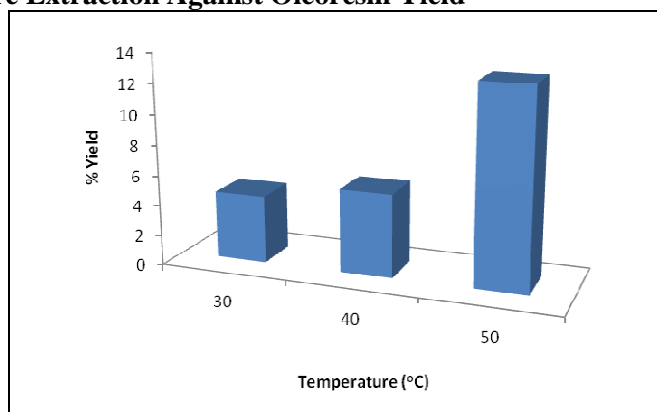
Fig. 2. Effect of Temperature Extraction against Oleoresin Yield

This research obtained the highest yield 13% at 50°C temperature. This research were limited the variations of extraction temperature from 30 to 50°C, because the main components in the red ginger oleoresin are shogaol and gingerol which are sensitive at a high temperature.

The increasing in temperature will cause the ethanol dissolves easily and diffuses into oleoresin better than at room temperature. Therefore, oleoresin which interacts and leads to mass transfer of solutes from solid samples towards the larger solvent will be greater [6].

The higher temperature causes greater amount of oleoresin produced. The use of temperature depends on the solvent used, but the use of too high temperatures will damage the oleorein [7]. Effect

of temperature on the extraction process is very important due to the rising of temperature will cause more random movement of the ethanol molecules as a solvent when diffuses into the pores to dissolve ginger oleoresin.

3. Effect of Stirring Speed Against The Oleoresin Yield
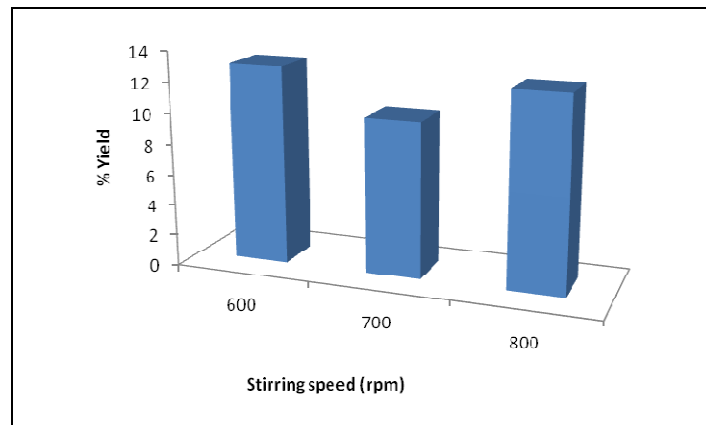
Fig. 3. Effect of Stirring Speed against the Oleoresin Yield

Figure 3 shows the highest yield 13%, and it was resulted at a speed of 600 rpm.The yield is higher than 12,5% yield which was resulted at the speed of 800 rpm. This is related to the effectiveness of stirring speed on the extraction process. Fast stirring encouraged the red ginger grains to follow current round of solvent, so that the extraction process became ineffective and obtained a small yield.

Solid - liquid extraction speed depends on the mass transfer from the liquid to the solid surface and diffusion from inside solids to the solid surface. If the differences were almost the same, then the extraction rate is determined by two processes. In the other hand, if the speeds of the two phases are different enough, so the slowest one controls the rate [8]. Mass transfer rate from the surface of the solid to the fluid following equation (1):

$$N_A = k_c(C_A^i - C_A) \tag{1}$$

C_A* is the equilibrium concentration of oleoresin in solution with the solid surface of oleoresin content. Equilibrium relationship between the concentration of oleoresin in solids and solutions follows the Henry's law.

$$C_A^i = H.X_A \tag{2}$$

Extraction speed is the solute mass transfer from the solid surface to the gas film across the body of fluids. Stirring speed affects the gas film to coat the solids. Faster stirring causes decreasing in thickness of liquid film on the solid surface. Greater rotational speed of stirring causes increasing of turbulence value in the system, thus will result thin liquid film and lead to further increasing in the magnitude of the extraction rate or value of kc.

4. Results of Oleoresin Analysis Using Gas Chromatography Mass Spectrometry (GCMS)

GCMS of red ginger oleoresin conducted on 2 pieces of sample. The samples were first extracted at 50^oC and the stirring condition at 600 rpm.
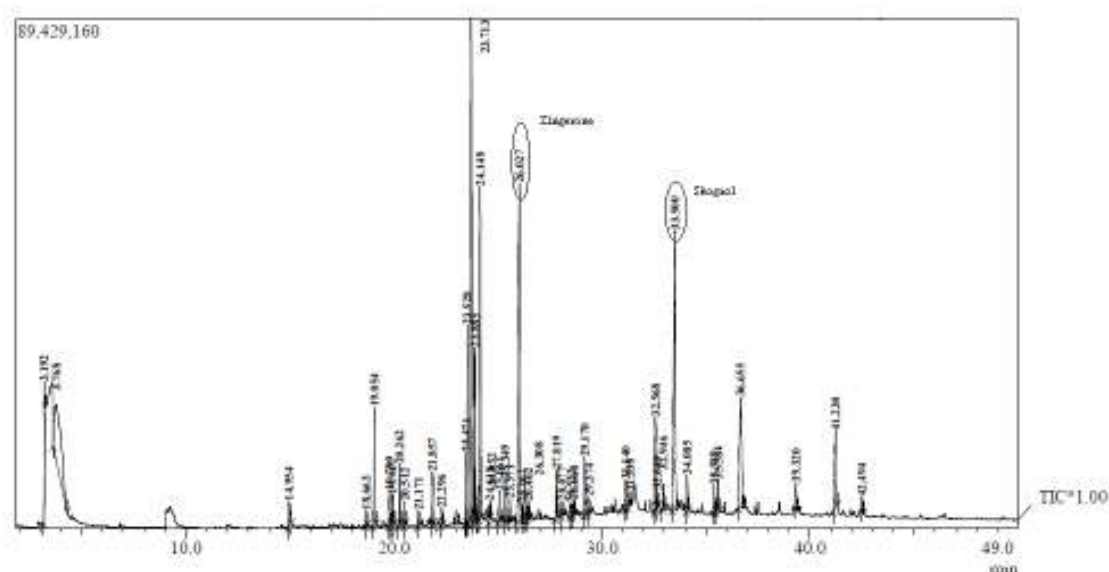
Fig 4. Results of Red Ginger Oleoresin GCMS Analysis

GCMS analysis was done to identify the main components which are contained in the oleoresin. Figure 4 shows the number of components found in oleoresin samples through GCMS analysis by heating and stirring process. Table 1 shows some components detected by GCMS analysis

Table 1. Analysis Result of Gas Chromatography Mass Spectrometry

Peak	R. Time	Conc (%)	Name
7	19.947	0.71	trans-Geraniol
10	21.171	0.35	Phenol, 4-ethenyl-2-methoxy-
14	23.528	3.44	Benzene, 1-(1,5-dimethyl-4-hexenyl)-4-methyl- (CAS) ar-Curcumene
23	26.027	14.13	Zingerone
25	26.308	1.01	Zingiberenol
26	26.462	0.32	FARNESOL 1
30	28.668	0.33	Hexadecanoic acid, methyl ester (CAS) Methyl palmitate
31	29.170	1.61	Hexadecanoic acid (CAS) Palmitic acid
32	29.374	0.37	Hexadecanoic acid, ethyl ester (CAS) Ethyl palmitate
33	31.140	1.21	Urs-12-en-28-ol
34	31.338	0.40	9-Octadecenoic acid (Z)-, ethyl ester (CAS) Ethyl oleate
36	32.649	0.34	2-Butanone, 4-(4-hydroxy-3-methoxyphenyl)- (CAS) Zingerone
37	32.946	0.49	Hexadecanoic acid (CAS) Palmitic acid
38	33.500	11.22	trans-6-shogaol
39	34.085	0.99	(E)-4-(2',6',6'-Trimethyl-1',2'-epoxycyclohexyl)-3-penten-2-one
40	35.389	0.90	Furan, 2,5-dibutyl- (CAS) 2,5-Dibutylfuran
41	35.584	0.91	Pentalene, octahydro-1-(2-octyldecyl)-
42	36.655	5.67	Benzenamine, N-(cyclopropylmethyl)-2,6-dinitro-N-propyl-4-(trifluoromethyl
43	39.320	0.98	Furan, 2,5-dibutyl- (CAS) 2,5-Dibutylfuran
44	41.230	3.25	trans-10-shogaol
45	42.494	0.48	(E)-4-(2',6',6'-Trimethyl-1',2'-epoxycyclohexyl)-3-penten-2-one

Conclusion

Based on the result of this research, the greatest yield of 13% oleoresin could be reached from the extraction process using 1:4 weight ratio of red ginger with ethanol, at temperature of $50^{o}C$ and stirring speed 600 rpm. The main components of the red ginger oleoresin detected by GCMS are shogaol amounted to 11.22% and zingerone amounted to 14.13% .

Acknowledgements

References

[1] Faleh, S.B., 2009. Pengambilan Oleoresin Dari Ampas Jahe (Hasil Samping Penyulingan Minyak Jahe) dengan Proses Ekstraksi, Teknik. Vol.30 No.3

[2] Hertik. 2010. "Pengaruh Pelarut yang Digunakan terhadap Optimasi Ekstraksi Kurkumin Pada Kunyit (Curcuma domestica, Val.). Laporan Skripsi Universitas Muhammadiyah Surakarta : Surakarta

[3] Azis, Yelmida dan Drastinawati. 2005. Ekstraksi Senyawa Metabolit Sekunder dari DaunTanamanTutup Bumi. Jurnal Sains dan Teknologi Universitas Riau :Pekanbaru

[4] Faleh, S.B dan Sasongko S.B., 2009. Koefisien Transfer Massa Pada Proses Ekstraksi Kayu Manis (Cinnamomum Burmanni). Reaktor.Vol. 12 No. 4.Hal. 232-238

[5] Jayanudin, Nofa Purwaningtyas dan Yunita Adining Tiyas, 2011. Pengambilan Oleoresin Jahe Merah Menggunakan Ekstraksi Maserasi Dengan Pelarut Metanol. Prosiding Seminar Nasional Integrasi Proses. Jurusan Teknik Kimia. Universitas Sultan AgengTirtayasa.

[6] Treybal, R.E., 1981.MassTransfer Operations.3rd ed.McGraw-Hill, New York.

[7] Gaedcke, F. and Feistel, B., 2005. Ginger Extract Preparation, U.S. Patent No. 10/496885.

[8] Sediawan, W . B., dan Prasetya, A., 1997. Pemodelan Matematis dan Penyelesaian Numeris dalamTeknik Kimia dengan Pemrograman Bahasa Basic dan Fortran. Edisi I. Penerbit Andi Offset,Yogyakarta.

International Conference and Workshop on Chemical Engineering UNPAR 2013

Effect of Polymerization Reaction Time on Synthesis Polyester From Methyl Ester Palm Fatty Acid Distillate (PFAD)

Renita Manurung, Ida Ayuningrum*, Ahmad Rozi Tanjung

Chemical Engineering Department, Faculty of Engineering, University of Sumatera Utara
St. Almamater Kampus USU Medan 20155, Indonesia

Abstract

Palm Fatty Acid Distillate (PFAD) can be used as raw material for synthesis polyester. Objective of this research is to synthesize polyester and todeterminethe effect of reaction time on polymerization methyl ester PFAD. The esterification stage wasdone at temperature 70^oC, reaction time120minute, reactant ratio 1:8 (PFAD: methanol), concentration of catalyst (H_2SO_4) 1% (w/w) PFAD; polymerization stagewasdone at temperature 126-132°C, concentration of catalyst (BF_3-diethyl etherate) 9.2 % (w/w) methyl ester, variation of polymerization reaction time 3, 4, and 5 hours; and polyesterification stage wasdone at temperature 175-200 ^oC, reactant ratios (w/w) 1:1 (polymerized ME : ethylene glycol), reaction time 4 hours and all of stage was stirred at 150 rpm. The results showed, in the esterification stage was obtained methyl ester with iodine value 77.29 g I_2/100 g, viscosity 6.90 cP, density 859.91 kg/m^3 and analysis by using GC-MS showed that the purity of methyl ester was 82.23% and molecular weight 267.97 g/mol. Decreasingin iodine value from 77.294 I_2g/100 g to 63.45-61.14 g I_2/100 g indicated that the polymerization process had taken place. Inpolyesterification stage was obtained gel polyester, viscous, darkbrown colored solid at room temperature with acid value from 13.13 to 21.65 mg KOH/g, viscosity from 14.3 to 19.1 P, and molecular weight 995.03 to 1,522.07 g/mol which is more suitable for application ofmodified polyester. Analysis by using GC showedthat the purity of polyester is equal to 65.49%.

Keywords: polyester; palm fatty acid distillate; polymerization reaction time; biodegradable polymer

1. Introduction

Indonesia is one of the largest palm oil producer in the world [1]. In the processing of palm oil, some derivatives such as PFAD are usually obtained [2].PFAD has a potential use as a raw material in the synthesis of polyester.

Polyester has many uses such as for making bottles, films, tarpaulin, canoes, liquid crystal displays, holograms, filters, fiber and etc [3]. Polymer is the most important chemical industrial products that are used in many applications. Almost the most current polymer is produced from petrochemical substance that cannot be renewed. Therefore, the alternative material needs to be known.Currently, vegetable oils are excellent source of renewable materials as an alternative material for oil-based polymers because of ecological and economical concern.

Polyesterification is a process of condensation or step-growth polymerization where in the process will be produced polyester and water or alcohol as by product. Direct reaction of diacids or anhydrides with diols are often avoided because of the high temperatures required to completely eliminate water. However, this reaction is used to produce low molecular weight. Using dimethyl ester has been used to advantage instead of direct esterification with diacid or dianhydride because reaction is fast and dimethyl ester is often more easily purified and has better solubility characteristics [4]. Therefore, initial step in this research, PFAD was reacted with methanol to form methyl ester PFAD.

The polyesterification becomes a much more economically feasible reaction when it is catalyzed by an external acid [4]. Polymerization on methyl ester PFAD will be catalyzed by boron trifluoride diethyl etherate as strong acid. Polymerization is done to form di- or trimethyl ester that is for the next step is reacted with ethylene glycol to form polyester. In the processing of polymer, polymerization reaction time has important rule in rate determing step for entire process. Therefore, it is important to determinethe effect of reaction timeon polymerization methyl ester PFAD. Objective of this research is to produce polyester and to

---

* Corresponding author
E-mail address: ida.ayuningrum@y7mail.com

determine the effect of reaction time on polymerization methyl ester PFAD.

2. Materials and Methods

Main materials that are used in this research such as PFAD (Indonesian Oil Palm Research Institute), BF$_3$-diethyl etherate (Aldrich), methanol (Merck), sulfuric acid (Merck) and ethylene glycol (Bratachem). The main equipments are a glass batch reactor, a hotplate with magnetic stirrer, reflux condensor and thermometer.

2.1. Procedure

Esterification stage [5], that is reaction between PFAD and methanol was held in a glass batch reactor on the top of a stirring hotplate for 120 minutes with mole ratio 1:8 at 70°C by using 1% sulfuric acid (w/w) PFAD and 150 rpm stirring. Density (by using picnometer), viscosity (by using viscosimeter Ostwald), iodine value (by using AOAC 920.158 method) and composition (by using GC-MS with coloumn oven temp. 70°C, injection temp. 280 ^{o}C, split injection mode) of product methyl ester was analyzed.

Polymerization stage [6], that is reaction methyl ester by using catalyst BF$_3$-diethyl etherate with ratio to methyl ester was 9.2% (w/w) at 126-132°C for varied time 3, 4, and 5 hours and 150 rpm stirring. Iodine value of polymerized methyl ester was analyzed(by using AOAC 920.158 method).

Polyesterification stage [6], that is reaction between polymerized methyl ester and ethylene glycol in the same reactor for 4 hours with mass ratio 1:1 at 175-200°C, 150 rpm stirring and sampling was performed every 1 hours for analysis of acid value (by using ASTM D4662-03 method). Viscosity (by using viscotester VT-04F), molecular weight (by using the end group method), structure (FT-IR Simadzu) and composition (GC) of polyester was analyzed.

3. Result and Discussion

The initial material that was used for the synthesis of polyester was methyl ester by esterification of methanol and PFAD by using sulfuric acid as catalyst. The result of analysis composition PFAD by using GC-MS was shown in Figure 1.
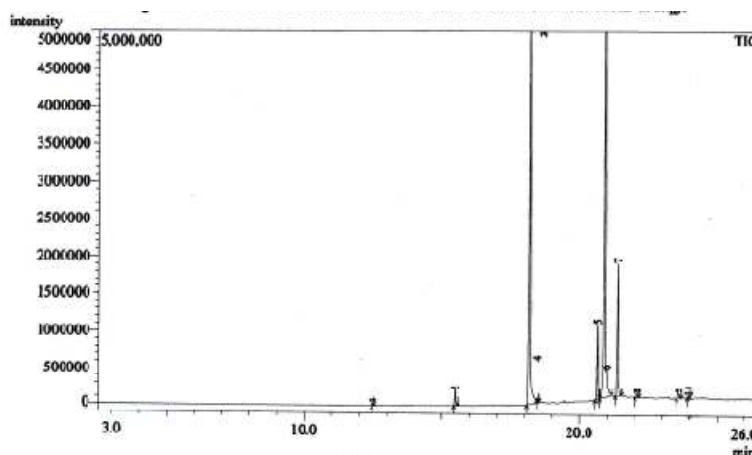
Fig 1. GC-MS of PFAD

GC-MS showed that the average molecular weight of PFAD was 270,84 g/mole with 53,27% unsaturated fatty acids (see App. A.1.). PFAD would be reacted to produce methyl ester by the following reaction [7] :
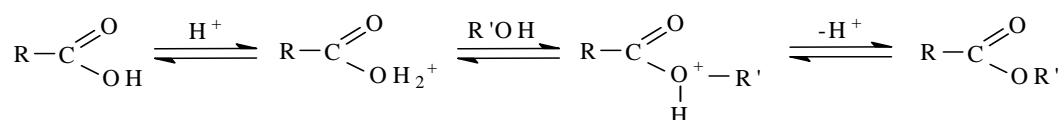
Fig 2. Esterification by using acid catalyzed

The result of analysis composition methyl ester by using GC-MS was shown in Figure 3.
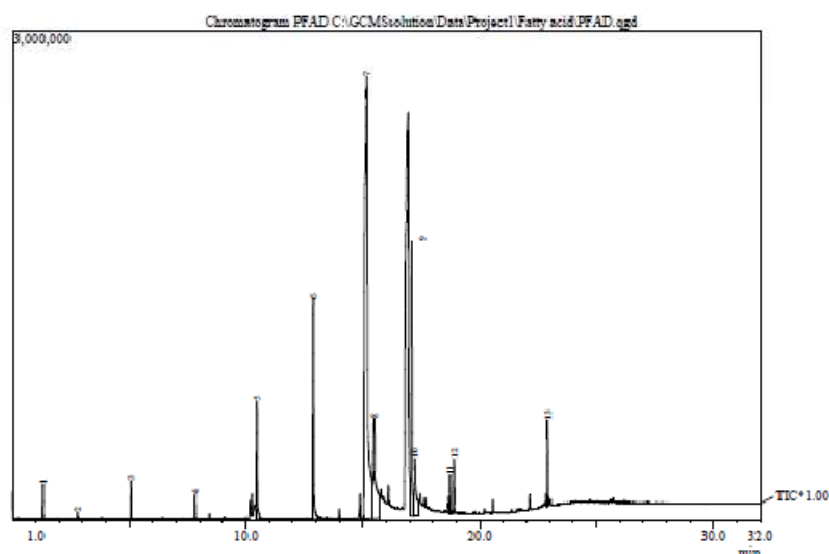
Fig 3. GC-MS of Methyl Ester PFAD

GC-MS showed that the average molecular weight of PFAD was 267,97 g/mole with the purity 82,23% (see App. A.2). Methyl ester would be used as a raw material for polyester. Analysis of the characteristics of methyl ester PFAD were shown in table 1.

Table 1. Characteristics of Methyl Ester PFAD

Parameter	Value
Iodine value	77.29 g I_2/100 g
Viscosity (30 ^{o}C)	6.90 cP
Density (30 ^{o}C)	859.91 kg/m^3

Polymerization reaction stage of methyl ester PFAD was performed by using catalyst boron trifluoride diethyl-etherate and then polyesterification stage of polymerized methyl ester and ethylene glycol to produce polyester following the reaction [6]:
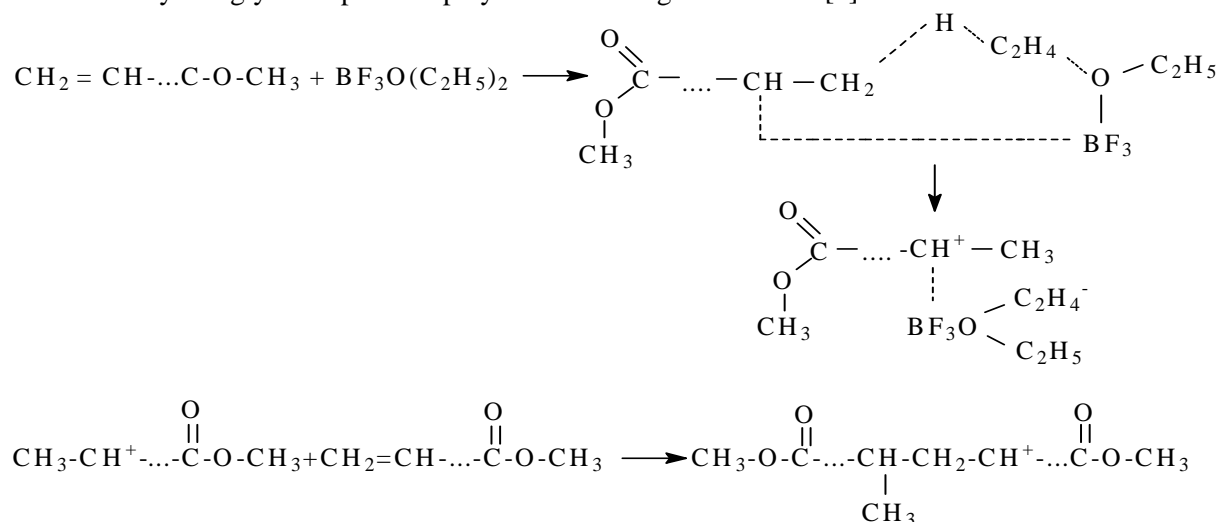
Fig 4. Polymerization Reaction of Methyl Ester PFAD

$$nCH_3-O-\overset{\overset{\displaystyle O}{\|}}{C}-....-CH_3-\overset{\underset{\displaystyle CH_3}{|}}{C}=CH-....-\overset{\overset{\displaystyle O}{\|}}{C}-CH_3 + \underset{\underset{\displaystyle OH}{|}}{CH_2}-\underset{\underset{\displaystyle OH}{|}}{CH_2} \rightleftharpoons$$

$$nCH_3-O\left[-\overset{\overset{\displaystyle O}{\|}}{C}-....-CH=CH_2-....-\overset{\overset{\displaystyle O}{\|}}{C}-O-CH_2-CH_2-O-\right]nH + (2n-1)CH_3OH$$
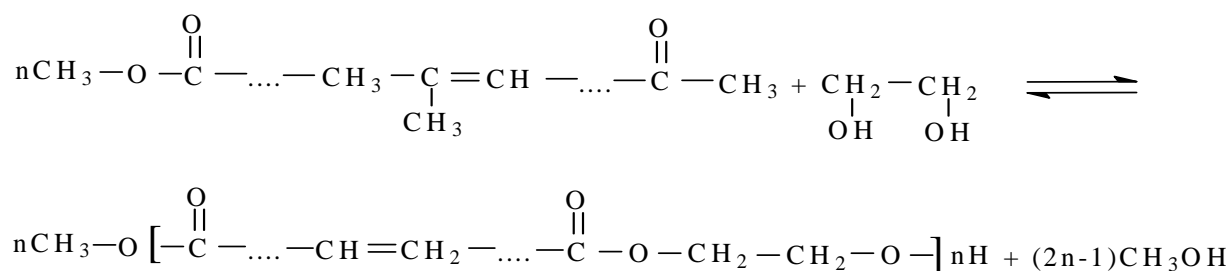
Fig 5. Polyesterification Reaction of Polymerized Methyl Ester PFAD and Ethylene Glycol

For all variation of reaction time was obtained gel polyester, viscous, darkbrown colored solid at room temperature. Polyester that has synthezed has a group of molecules that can be identified by using FT-IR. The result of analysis spectrum of polyester was shown in Figure 6.
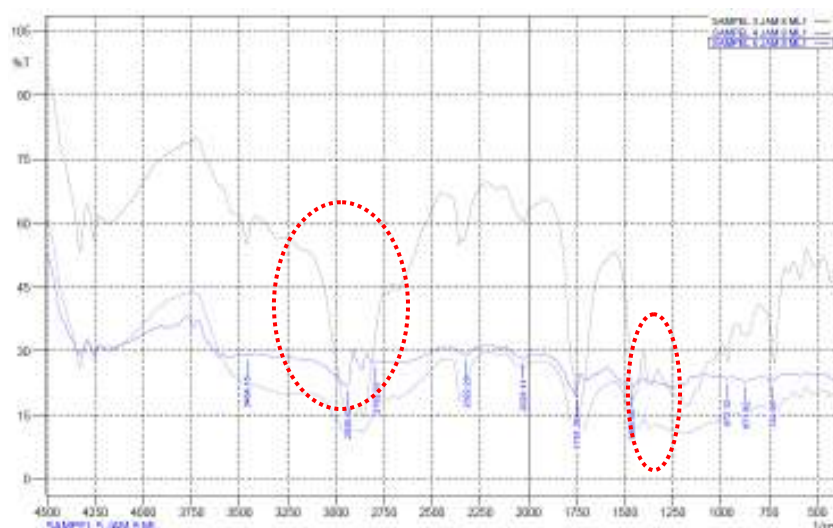
Fig 6. FT-IR of Polyester

An ester compound was characterized by the presence of stretching band C=O, C-O and O-H [8]. The formation of polyester was shown by vibration peak at wave number 1751,36cm^{-1}(area in dot line) that indicated a stretching band C=O ester for all run. The difference between the C=O group of acid and ester wasat wave number 1730-1700 cm^{-1}for acid whereas at wave number 1760-1793 cm^{-1}for ester [21]. On the other hand, the weakening of the stretching band O-H hydrogen bond at wave number 3500 cm^{-1} - 3400 cm^{-1}(area in dot line) supported the formation of polyester.

Polymerization was characterized by the absence of vinyl group (-C = CH$_2$-) at wave number 990 cm^{-1} - 910 cm^{-1} that indicated decreasing of unsaturated bond. The result of analysis qualitative for composition polyester by using GC was shown in Figure 7.
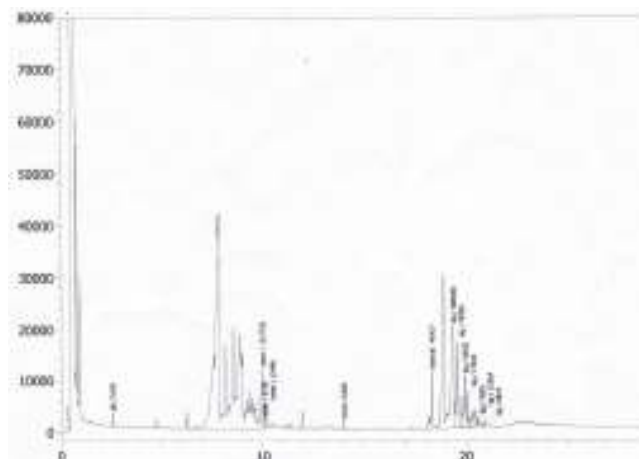
Fig 7. GC of Polyester

Analysis of polyester by using GC shown the purity of polyester was 65.49% (see App. A.3).

3.1. Effect of Polymerization Reaction Time on Iodine Value of Polymerized Methyl Ester

Effect of polymerization reaction time on iodine value of polymerized methyl ester was shown in Figure 8.
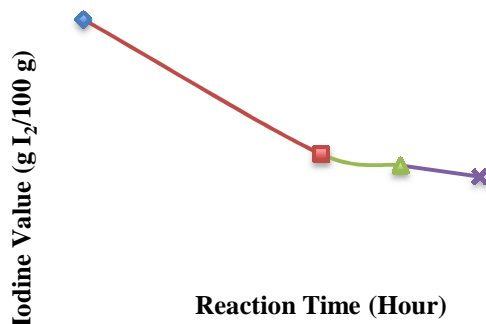
Fig 8. Effect of Polymerization Reaction Time on Iodine Value of Polymerized Methyl Ester

Figure 8showed that iodine value tends to decrease with increasing in polymerization reaction time. The most important parameter in the synthesis of a polymer was the number of double bonds that exist in a sample which can be shown by iodine value.

With the increasingin reaction timewould decrease iodine value and tend to a constant value [10]. This is suitable with the results that wasobtained in this research. In addition, the reduction in iodine value could be observed visually by the occurrence of a change of color along the process of polymerization. Iodine value will affect the appearance of the oil, the higher iodine value will be clear appearance of such oils [11]. Decreasing in iodine value would influence to be darker color of sample.

3.2. Effect of Polyesterification Reaction Time on Acid Value of Polyester

Effect of polyesterification reaction time on acid value of polyester was shown in Figure 9.
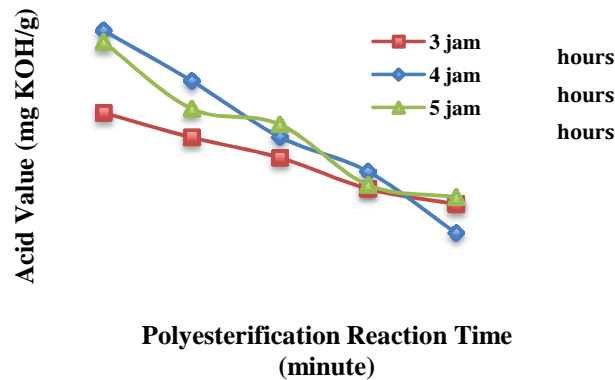
Fig 9. Effect of Polyesterification Reaction Time on Acid Value of Polyester

Figure 9showed that acid value decreased with increasing polyesterification reaction time. Analysis of acid valuewas done to find out the progress of the polyesterification.

The reaction was assumed to take place if acid value decreased. Decreasing in acid value happened because of extension of the chain of reactive carboxyl to form polymers. Acid value could be used as a parameter of quality polyester. The higher acid value indicated quality of polyester would get worse. This is due to the high acid value showed high ability of material to absorb water [4]. Commercial polyester in the market had a standard acid numbers ≤32 mg KOH/g [12]. Polyesterthat was obtained in this study hadacid value ≤32 mg KOH/g, therefore it was polyester with a good quality of acid value.

3.3. Effect of Polymerization Reaction Timeon Viscosity of Polyester
    Effect of polymerization reaction time on viscosity of polyester was shown in Figure 10.
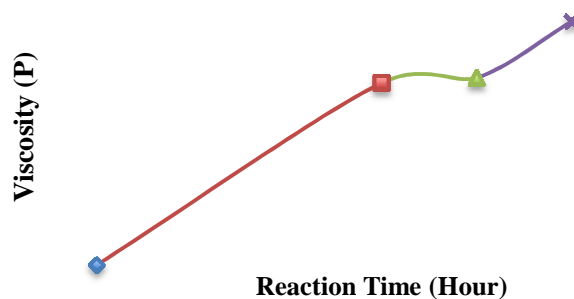
Fig 10. Effect of Polymerization Reaction Time on Viscosity of Polyester

Figure 10 showed that viscosity increase with increasing in polymerization reaction time. The viscosity increase during polymerization reaction. This condition occured because of reduction of carbon bond in polyesterification and increasing viscosity in the media reaction at high concentrations. This double bonds cause a reduction of barriers on fluid flow in viscotester which led to the appointment of the larger viscotester value [13]. This result was suitable for this research.
3.4. Effect of Polymerization Reaction Time on Molecular Weight of Polyester
    Effect of polymerization reaction time on molecular weight of polyester was shown in Figure 11. Figure 11showed that molecular weight fluctuated with increasing in polymerization reaction time. Increasing in polymerization reaction timewould increase polymer molecular weight very slowly except in the early of the reaction [4].

Molecular weight of polymer was the main attention in practice of synthesis polymer. Polyester had the carboxyl end group and hydroxyl group at the other end [14]. Zhang, et. al. (1994) usedend group methods to determine molecular weight in the synthesis of polycaprolactone [15]. Molecular weight of polyester in this research was also determined by end group methods.
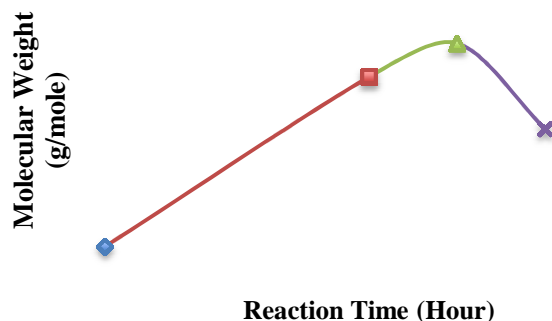
Fig 11. Effect of Polymerization Reaction Time on Molecular Weight of Polyester

Polyester with linear high molecular weightpolymer,was generally thermoplastic with a molecular weight about10,000 – 30,000 g/mole. High molecular weight of polyester could be used for the application of powder coating and drying binder. Polyester with low molecular weight that is between 500-7,000 g/mole. Polyester with low molecular weight may be linear or branched with carboxyl and hydroxyl end group. For special purposes, polyester with low molecular weight 1,000-5,000 g/molewas modified due to functional group being more reactive than polyester with high molecular weight [16].

Polyesterification was reversible polycondensation reaction. Increasing in reaction time will provide conversion as mush as possible. However, if equilibrium has been reached, it will not give the best result. The results showed that increasing in polymerization reaction time would increase molecular weight. But atpolymerization reaction time 5 hours, decreasing in molecular weight had occured. This condition happened because viscosity increase during polymerization reaction. This large viscosity decreases efficiency of alcohol removal and may lead to the observed decrease in the reaction rate with increasing conversion. High viscosity in the high conversion region may also lead to failure of the assumption of equal reactivity of functional group-specifically to a decrease in functional group reactivity at very large molecular size if there is too large a decrease in molecular mobility [4].

On the other hand, it may be expected that reaction between polymer and monomer have occured to form shorter cain polymer as following reaction [15].
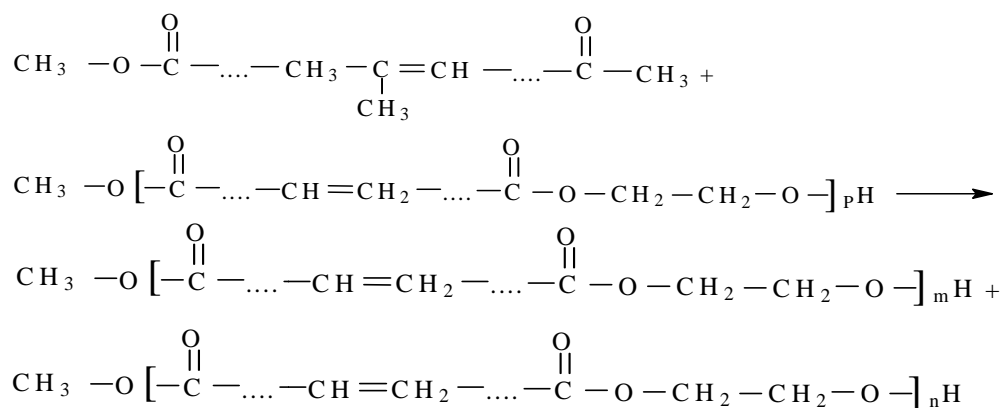
Fig 12. ReactionMonomer and Polymer

The results showed thatproduct of polyester had a range of 995.03-1522.07 g/mole. Therefore, this polyester could be counted polyester with relatively low molecular weight that was more suitable for the application of the modified polyester. The low molecular weight polyester was formed due to the raw material which was used was a methyl ester of PFAD which had alittle double bonds.

4. Conclusions

The conclusion that can be drawn from this research is the product of polyester from PFAD has physical properties that close to the commercial polyester has a good quality of acid value and can be classified in low molecular weight of polyester which is more suitable for the application of modified polyester. The polyesterification is reversible reaction in which the acquisition of the product depends on the reaction time.

Appendix A.

A.1 GCMS of PFAD
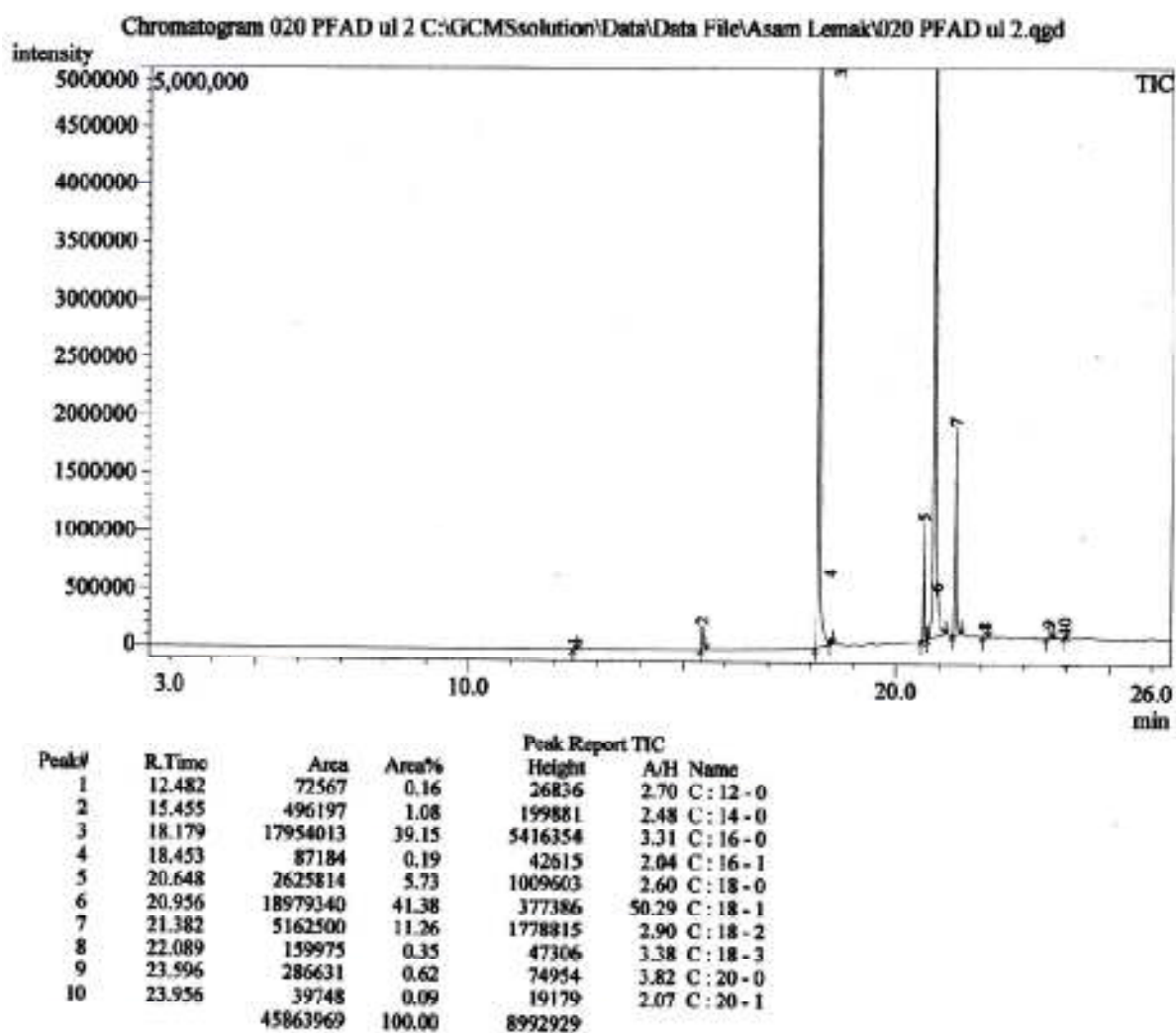
Fig 13. GCMS of PFAD

A.2 GCMS of Methyl Ester PFAD

Chromatogram PFAD C:\GCMSsolution\Data\Project1\Fatty acid\PFAD.qgd

Peak Report TIC

Peak#	R.Time	Area	Area%	Height	Name
1	1.305	331425	0.75	216372	Hexane
2	2.770	70014	0.16	46276	Hexanoic acid, methyl ester
3	5.070	397580	0.90	240735	Octanoic acid, methyl ester
4	7.814	270932	0.61	152923	Decanoic acid, methyl ester
5	10.460	1749009	3.95	720102	Dodecanoic acid, methyl ester
6	12.881	3332589	7.52	1350169	Methyl tetradecanoate $$ Tetradecanoic acid,
7	15.181	24591627	55.48	2717246	Hexadecanoic acid, methyl ester $$ Palmitic
8	15.482	4308755	9.72	611286	n-Hexadecanoic acid
9	17.094	4904778	11.07	1680513	Octadecanoic acid, methyl ester
10	17.229	2175919	4.91	353217	Oleic Acid $$ 9-Octadecenoic acid (Z)- $$ .d
11	18.738	467131	1.05	232345	Octadecanoic acid, 10-oxo-, methyl ester
12	18.892	662263	1.49	333254	Eicosanoic acid, methyl ester
13	22.918	1059893	2.39	527329	Squalene
		44321915	100.00	9181767	

Fig 14. GCMS of Methyl Ester PFAD

A.3 GC of Polyester

Peak#	Ret.Time	Area	Height	Area%	Name
1	2.546	6146	2650	0.3011	ali
2	4.733	6934	1781	0.3397	
3	9.962	1317735	11556	64.5516	ester
4	10.050	6738	1898	0.3301	ester
5	10.125	12496	4632	0.6121	ester
6	11.236	6784	1081	0.3323	
7	11.926	14810	3527	0.7255	
8	14.002	6285	1476	0.3079	mono
9	18.303	45417	10957	2.2248	internal
10	19.362	365648	20080	17.9119	da
11	19.547	72955	16675	3.5738	da
12	19.761	51800	6107	2.5375	da
13	19.958	59535	10135	2.9164	da
14	20.091	17923	6766	0.8780	da
15	20.164	7695	1751	0.3770	da
16	20.308	20330	3022	0.9959	da
17	20.478	15264	3483	0.7477	da
18	20.849	6872	1353	0.3366	da
Total		2041367			

Peak Table - Channel 1

Fig 15. GC of Polyester

References

[1] Kurniasih. 2008 .Pemanfaatan Asam Lemak Sawit Distilat Sebagai Bahan Baku DietanolamidaMenggunakan Lipase (*Rhizomucor meihei*). *Tesis*. Sekolah Pascasarjana, UniversitasSumatera Utara. (Indonesian)

[2] Silviana, N. A. 2008.Analisis Kadar Asam Lemak Bebas dari Palm Fatty AcidDistillate (PFAD) dan Coconut Fatty Acid Distillate (CFAD).*Karya Ilmiah*,Departemen Kimia, FMIPA, USU. (Indonesian)

[3] Giwangkara, E.G. 2012. *Citing Internet Sources* URL http://kimia-aplikasi.wordpress.com. (Indonesian)

[4] Odian, G. 2004.*Principles of Polymerization*. Fourth Edition. Reading, New York: John Wiley & Sons, Inc.

[5] Alfitra. 2012. *Pembuatan Biodiesel dari Palm Fatty Acid Distillate (PFAD) dengan Katalis Asam. Citing Internet sources* URL http://repository.usu.ac.id. (Indonesian)

[6] Nurmian, et. al. 2000. Sintesis Poliester Dari Minyak Goreng Yang Berasal Dari Crude Palm Oil (CPO). *Laporan Penelitian* Jurusan Teknik Kimia, UniversitasSumatera Utara. (Indonesian)

[7] William W. Christie. 1993. *Preparation Of Ester Derivatives Of Fatty Acids For Chromatographic Analysis.*The Scottish Crop Research Institute, Invergowrie, Scotland DD2 5DA.

[8] Nugraha, A. 2006. Sintesis Ester Glukosa Oleat antara Glukosa Pentaasetat dan MetilOleat. *Skripsi*, Departemen Kimia, FMIPA, IPB. (Indonesian)

[9] Pavia L. D, et. al. 1996. *Introduction to Spectroscopy*. Second Edition. Reading. Washington: W.B. Saunders.

[10] Handayani A. S.; Sidik M.; M. Nasikin dan M. Sudibandriyo. Reaksi Esterifikasi Asam Oleat dan Gliserol Menggunakan Katalis Asam.*Jurnal Sains Materi Indonesia*, Edisi Khusus Oktober, 2006 : hal. 102-105. (Indonesian)

[11] Dwitri, S. 2003. Pembuatan Minyak Goreng dari RBD-Minyak Sawit Tanpa Pemisahan Olein dan Stearin dengan Cara Reaksi Interesterifikasi dengan Minyak Nabati Cair. *Tesis* Program Pascasarjana, USU. (Indonesian)

[12] National Petrochemical Campany/Shahid Tondguyan Petrochemical Complex (5 Mei 2013).*Citing Internet sources* URL http://nipc.ir.

[13] Perdana, A. R. 2013.Produksi Biosolar Dari Minyak Goreng Bekas. FakultasTeknik Kimia, Sultan Ageng Tirtayasa, Banten,*Citing Internet sources* URL*http://www.scribd.com*.(Indonesian)

[14] Handayani, P. A. 2010. Polimerisasi Akrilamid Dengan Metode Mixed-Solvent Precipitation Dalam Pelarut Etanol-Air. Volume 8, No.1, 2010.(Indonesian)

[15] Zhang, Q., et. al. 2010. Synthesis of Polycaprolactone WithTwo Carboxyl End Group.*Journal Matter Sci. Technol*, Vol 10, 2010.

[16] H.F. Huber and D. Stoye. 2006. *Polyesters- Coating Technology Handbook*. Third Edition. Taylor& Francis Group, LLC.

International Conference and Workshop on Chemical Engineering UNPAR 2013

Semibatch Bubble Column Reactor Design for Biodiesel Production

Wahyudin[a*] , Joelianingsih[a], Armansyah H. Tambunan[b]

[a]*Chemical Engineering Study Program, Institut Teknologi Indonesia, Jl. Raya Puspiptek Serpong Tangerang Selatan 15320 , Indonesia*
[b]*Graduate School, Agricultural Engineering Science, Bogor Agricultural University, Darmaga Campus, Bogor 16002, Indonesia*

Abstract

The application of bubble column reactors are widely spread out due to a number of advantages both in design and operations compared to other reactors. The first one is they have excellent heat and mass transfer characteristic. The second is low cost of operation and maintenance, and the last is high durability of the catalyst. Owing to the wide application area of bubble column reactors, the design and scale up of the reactors, the complexity of hydrodynamic and operational conditions have put on the attention of engineers. The performance of bubble column reactor is proven for transesterification process reported by Joelianingsih et. al.; nevertheless, the conversion and the yield of the product are still low. The reaction operated at atmospheric condition in the absence of catalyst will lead to more economic process for industrial application. Thus, the improvement of reactor design is necessary especially in order to increase the yield and conversion of the product. The bubble column reactor is designed with height to diameter ratio of 5 equipped with vaporizer, superheater and condenser. The material for all the equipments is made of stainless steel (316 SS) except for vaporizer is made of 304 SS. The performance of bubble column reactor for methyl esterification is increased both on the quality and the quantity of the biodiesel product. The analysis on quality of biodiesel showed that the free glycerol contents, monoglycerides, diglycerides, and triglycerides has satisfied both EN 14214 standard and SNI 718:2012. The quantity of the product is improved as showed by higher yield obtained. The future work shall be focused on utilizing various spargers to gain optimum results and also attaining continuous methanol separation setup from end product for recycling.

Keywords: bubble column; design ratio; yield; conversion; biodiesel.

1. Introduction

The general types of multiphase reactor comprise of three main categories namely the fluidized bed reactor, the trickle bed reactor (fixed or packed bed), and the bubble column reactor. In principle, a bubble column reactor is a cylindrically vessel equipped with gas sparger at the base of reactors to dispense gas in the form of bubbles into either liquid phase or solid-liquid phase. The bubble column reactors are intensively used as multiphase reactor and contactor in chemical, petrochemical, biochemical and metallurgical industries [1]. These typical reactors are especially utilized in chemical processing such as oxidation, chlorination, polymerization, alkylation, and hydrogenation, in producing synthetic fuel, in biochemical process, and waste water treatment [2,3].

The application of bubble column reactors are widely spread out due to a number of advantages both in design and operations compared to other reactors. The first one is they have excellent heat and mass transfer characteristic. The second is low cost of operation and maintenance, and the last is high durability of the catalyst [1]. Furthermore, continuous catalyst supply and withdrawal ability and plug-free operation are their superiority among other reactors [3]. Owing to the wide application area of bubble column reactors, the design and scale up of the reactors, the complexity of hydrodynamic and operational conditions have put on the attention of engineers.

Joelianingsih, et al. [4] reported the performance of bubble column reactor for uncatalyzed methyl esterification of free fatty acids. The performance of bubble column reactor is proven for esterification process; nevertheless, the conversion and the yield of the product are still low. The reaction operated at atmospheric condition in the absence of catalyst will lead to more economic process for industrial

---

* Corresponding author *Tel.: +62-21-7561092; fax: +62-21-7561092*

E-mail address: wahyudin@iti.ac.id, whyd23@yahoo.com

application. Thus, the improvement of reactor design is necessary especially in order to increase the yield and quality of the product.

2. The bubble column reactors concept and technology

The main interest of bubble column reactor studies are focused on design and scale-up, hydrodynamics and regime analysis and characteristics parameters. This study mainly focused on design and scale-up of bubble column reactor for biodiesel productions in order to increase conversion rate of methyl esterification/transesterification.

In general, the design and scale-up of bubble column reactors rely on at least three characteristic: (i) heat and mass transfer (ii) mixing (iii) chemical kinetics. Although the construction of bubble column is straightforward, precise and successful design and scale-up require an improved understanding of multiphase fluid dynamics and its influences. Industrial bubble column usually operate with a length to diameter ratio of at least 5 [1].

Shah et al. [2] reported that the effect of column diameter is insignificant on gas holdup when larger than 10-15 cm. On the other hand, Luo et al. [5] reported that the column height effect is negligible when the height is higher than 1-3 m and the the aspect ratio is larger than 5. Vandu and Krishna [6] reported that $k_la/_g$ demonstrated a slight increase with column diameter. The volumetric mass transfer coefficient, k_la increases with gas velocity, gas density and pressure while it decreases with increasing solid concentration and liquid viscosity. The presence of large bubbles should be avoided in industrial columns for effective mass transfer [7].

Table 1. Mass transfer coefficient correlations for gas-liquid bubble columns

Researcher	Correlation	Reference
Akita and Yoshida	$\frac{k_l a D_T^2}{D_{AB}} = 0.6 \left(\frac{\upsilon_l}{D_{AB}}\right)^{0.5} \left(\frac{g D_T^2 \rho_l}{\sigma}\right)^{0.62} \left(\frac{g D_T^3}{\upsilon_l^2}\right)^{0.31} \varepsilon_g^{1.1}$	[8]
Shah et al.	$k_l a = 0.467 V_g^{0.82}$	[2]
Kang et al.	$k_l a = K \times 10^{-3.08} \left(\frac{D_T V_g \rho_g}{\mu_l}\right)^{0.254}$ where K is the correlation dimension	[9]

Heat transfer in bubble column reactor is important since many chemical reactions are usually involved with energy supply (endothermic) or energy removal (exothermic) process. Hence, the heat transfer from the reactor wall and inserted coils became interesting discussion in many literatures [10]. Many hydrodynamic studies examined the heat transfer between the heating objectives and the system flow to understand the effect of hydrodynamic on the heat transfer for improving the design and operation of bubble column reactors [11]. It can be stated that the heat transfer coefficient increases with increasing temperature, but decreases as a function of liquid viscosity and particle density [7].

Bubbles size and distribution also important in bubble column operations. Their holdup contribution and rise velocities have significant impact on altering the hydrodynamics, as well as heat and mass transfer coefficient in bubble column reactors. The distribution of bubbles firstly influence by the bubbles formulation by the sparger.

For any given gas sparger size with pre-determined number of openings or holes size, the gas initial force at the sparger orifice is related to the surface tension forces. This relationship is best described by Weber number (We), which is often used to design the gas sparger. The Weber number for gas is given as follow:

$$We = \frac{\rho_G U_{G,o}^2 d_o}{\sigma} = \frac{\rho_G U_G^2 D_C^4}{N_o^2 d_o^3 \sigma}$$

(1)
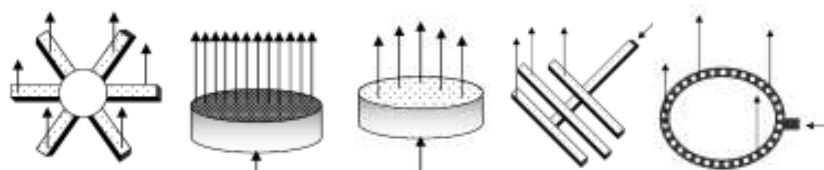
Fig 1. Sparger types utilized in bubble column reactor (a) spider shape (b) porous plate (c) perforated plate (d) multiple orifice nozzle (e) perforated ring [12]

3. Design and scale-up

In this project, the design of bubble column reactor is straight forward with height to diameter ratio is 3 to 5 (more preferably 5). The bubble column reactor setup equipped with a methanol vaporizer, a superheater, and a condenser. All main materials are made of stainless steel 316 SS except for vaporizer made of 304 SS. The flow rate of methanol controlled by Chengfeng Flowmeter LZB-DK800-4 and the temperature system is controlled by automatic PID temperature controller YFYB (Type XMTG) equipped with thermocouple type-K. Overview of the setup are shown in Fig 2 to Fig. 4
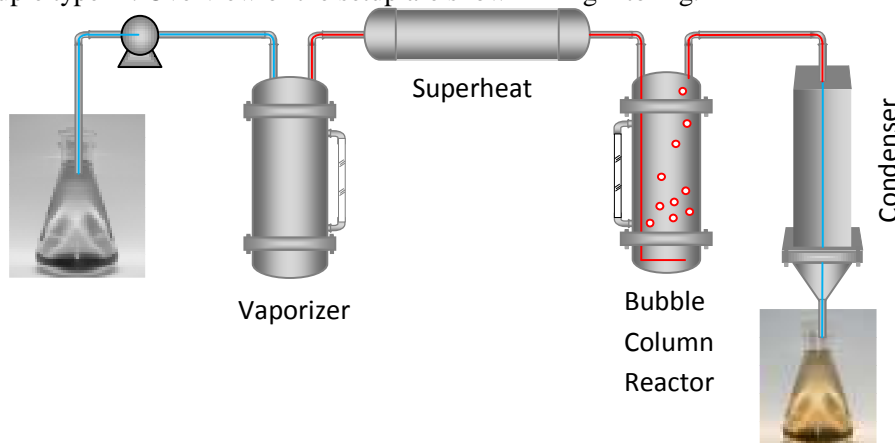
Fig 2. Schematic diagram of the bubble column reactor setup equipped with vaporizer, superheater, and condenser
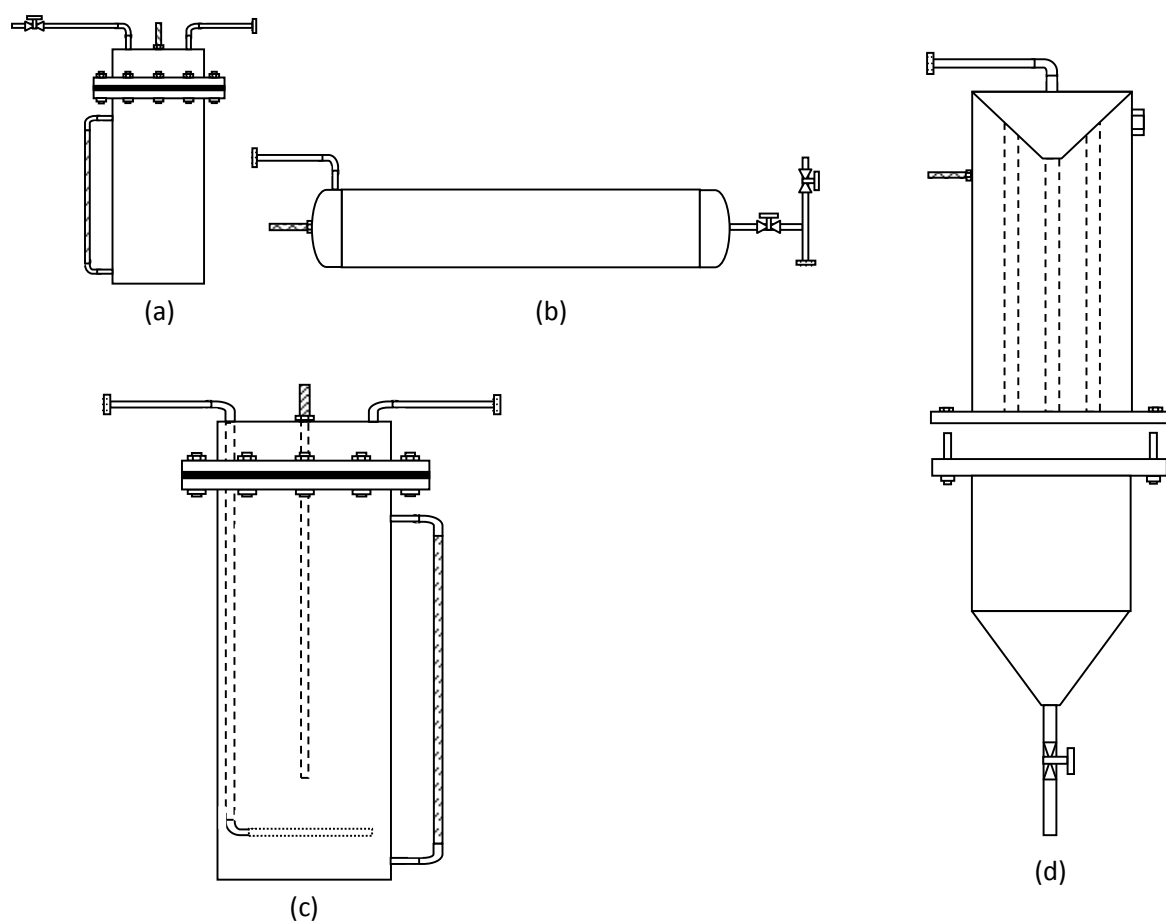
Fig 3. The bubble column reactor designed (a) vaporizer (b) superheater (c) reactor (d) condenser

Fig 4. The bubble column reactor setup and rotary evaporator for final product separation from methanol

All the heating elements are using band heater built on design with power supply 500 to 750 watt capable to generate heat up to 500 ^{o}C. The methanol vaporizer is designed to convert methanol in liquid phase directly to vapor phase with the temperature range between 75 to 250 ^{o}C. The superheater is designed to give additional heat energy to methanol vapor at 250 – 500 ^{o}C depend on reaction temperature in the reactor. The superheater is horizontally positioned in order to have more efficient heat transfer and flow of superheated vapor into the reactor. Should we place superheater vertically; the pressure drop is higher than previous position. The sparger used in the reactor is simply a perforated tube sparger and a perforated ring sparger with holes diameter each 1 mm. The condenser is equipped with temperature control in order to maintain operating condensation operation at 10 – 20 ^{o}C.

4. Performance test

The prototype of bubble column reactor designed is tested initially for producing biodiesel non-catalytically from frying palm oil with methanol feed rate of 5 and 10 mL/minute. The temperature condition carried out at 250, 270, and 290 ^{o}C at atmospheric pressure. The results of bubble column performance test are shown in Table 2.

Table 2. Bubble column reactor prototype performance test results

Methanol feed rate mL/minute	Temperature ^{o}C	Yield %
5	250	0.71
5	270	4.16
5	290	12.07
10	250	0.96
10	270	2.32
10	290	9.25

From Table 1 it showed that the highest yield should performed at high temperature 290 ^{o}C with suitable methanol feed rate i.e. 5 mL/minute. At the same temperature 290 ^{o}C with methanol feed rate 10 mL/minute, the yield of product is lower due to short contact time between methanol vapor and the oil. It is found that the number of bubbles formed at low methanol feed rate i.e. 5 mL/minute are much more uniform and even. Therefore, the contact between the reactants particles are more frequent and in results more reactants converted into the product. The formation of bubbles at high feed rate of methanol i.e. 10 mL/minute, resulting an excessive interfacial contact between reactants particles. The bubbles size are larger and more turbulence. For high methanol feed rate, an additional roof perforated plate should be placed to increase gas hold up and accordingly increase contact time between the reactants.

The biodiesel product were analyzed by gas chromatography (GC 2010 Shimadzu) with modified EN 14105 standard methods [13] and presented in Fig 5 to Fig 8.

Fig 5. Chromatogram of free glycerol from biodiesel product
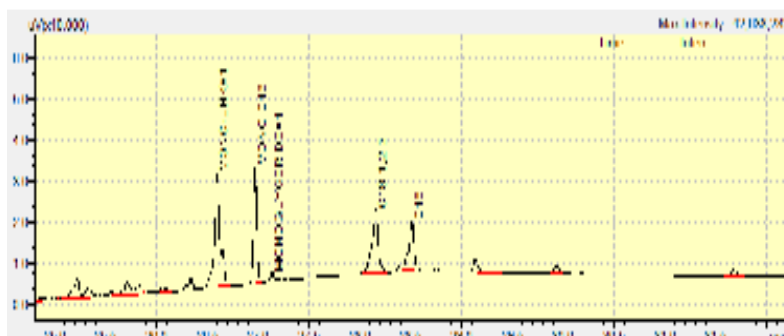
Fig 6. Chromatogram of monoglycerides from biodiesel product
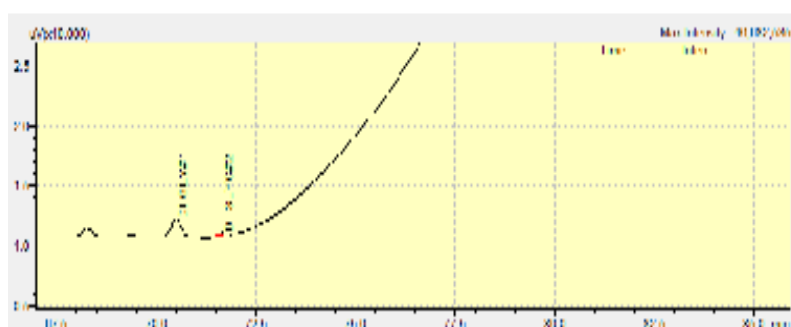
Fig 7. Chromatogram of diglycerides from biodiesel product
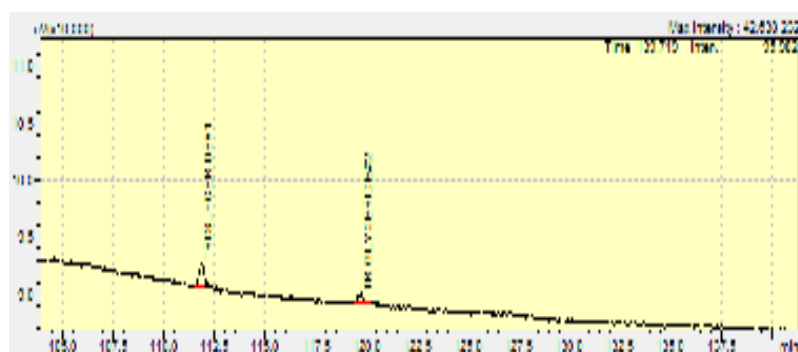
Fig 8. Chromatogram of triglycerides from biodiesel product

Table 3. Biodiesel product analysis

Parameter	EN 14214	SNI 718:2012	Biodiesel sample (%w/w)
Free glycerol	Max 0.02	Max 0.02	0.018
Monoglycerides	Max 0.80	NA	0.005
Diglycerides	Max 0.20	NA	0.001
Triglycerides	Max 0.20	NA	0.017
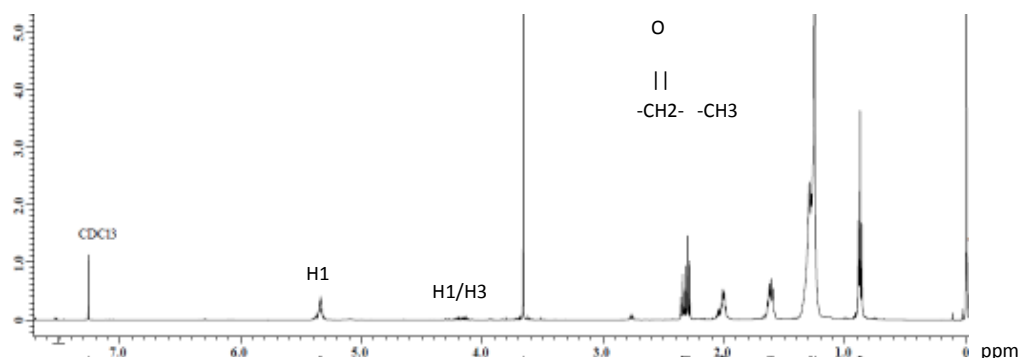
Fig 9. ^{1}H-NMR spectrum of reactant in the bubble column reactor after 3 hr reaction at 250 ^{o}C reaction condition

From the ^{1}H-NMR analysis showed that after 3 hour reaction, most of the triglycerides are already breaking out into monoglycerides. The double bonds originally from TG also reduced into straight chain (alkanes) resulting product that easily be frozen at room temperature.

Transesterification reaction of oil/triglyceride (TG) with methanol (MeOH) takes place in 3 stages as in equation (1), (2) and (3). One mole of TG react with 1 mole of MeOH produces 1 mole of FAME and 1 mole of diglycerides (DG). Furthermore, 1 mole of DG reacts with 1 mole of MeOH produces 1 mole of FAME and 1 mole of monoglycerides (MG). Finally, 1 mole of MG reacts with 1 mole of MeOH produces 1 mol of FAME and 1 mole of glycerol (GL) [14].

$$TG + MeOH \leftrightarrow DG + FAME \qquad (1)$$
$$DG + MeOH \leftrightarrow MG + FAME \qquad (2)$$
$$MG + MeOH \leftrightarrow GL + FAME \qquad (3)$$

The third phase reaction is the slowest reaction as MG is the most stable compound compared to DG and TG [15]. Based on the literature sources [16] monoglycerides compound has a freezing point above room temperature so that at room condition it will easily be frozen. Fig 10 (a) showed the liquid condition in the bubble column reactor after 3 hour reaction at 250 ^{o}C. The bottom layer is monoglycerides compound that has not reacted yet with methanol to form FAME and glycerol. No formation of two layers in the reaction products showed that the GL product produced is still very small as a result of the slow reaction stage 3 as shown in Fig 10 (b).

(a) (b)
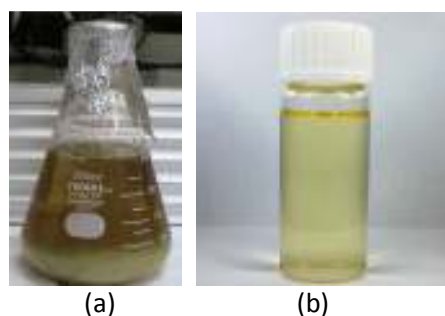
Fig 10. (a) The liquid condition in the bubble column reactor, and (b) biodiesel product after 3 hr reaction at 250 ^{o}C reaction condition

5. Conclusion

The bubble column reactor designed performance for methyl esterification is increased both on the quality and the quantity of the biodiesel product compared to previous work done by Joelianingsih et al.. The analysis on quality of biodiesel showed that the free glycerol contents, monoglycerides, diglycerides, and triglycerides has satisfied both EN 14214 standard and SNI 718:2012.

To obtain good results in quality and quantity, sparger in the reactor system must be redesigned in order to produce more methanol bubbles and smaller so that the reaction between two phases (oil and methanol vapor) can take place evenly throughout the liquid in the reactor, accordingly the yield of oil products will increase.

The future work shall be focused on utilizing various spargers to gain optimum results and also attaining continuous methanol separation setup from end product for recycling.

Acknowledgements

References

[1] Badan Pusat Statistik: Katalog Badan Pusat Statistik, Kalimantan Barat, 2010.

[1] Degaleesan S, Dudukovic M, Pan Y. 2001. Experimental Study of Gas-induced Liquid-flow Structures in Bubble Columns. AIChE J 47:1913-31.

[2] Shah YT, Godbole SP, Deckwer WD. 1982. Design Parameters Estimations for Bubble Column Reactors. AIChE J 28:353-79.

[3] Prakash A, Margaritis A, Li H. 2001. Hydrodynamics and Local Heat Transfer Measurements in a Bubble Column with Suspension of Yeast. Biochem Eng J 9:155-63.

[4] Joelianingsih, Nabetani H, Hagiwara S, Sagara Y, Soerawidjaya TH, Tambunan AH, Abdullah K. 2007. Performance of a Bubble Column Reactor for The Non-Catalytic Methyl Esterification of Free Fatty Acids at Atmospheric Pressure. J. Chem. Eng. Jpn. Vol. 40, No. 9, p. 780-785.

[5] Luo X, Lee DJ, Lau R, Yang G, Fan L. 1999. Maximum Stable Bubble Size and Gas Holdup in High-pressure Slurry Bubble Columns. AIChE J 45:665-85.

[6] Vandu CO, Krishna R. 2004. Volumetric Mass Transfer Coefficients in Slurry Bubble Columns Operating in Churn-turbulent Flow Regime. Chem Eng Process 43:987-95.

[7] Kantarci N, Borak F, Ulgen KO. 2004. Review Bubble Column Reactors. Process Biochem 40:2263-2283.

[8] Akita K, Yoshida F. 1973. Gas Hold-up and Volumetric Mass Transfer Coefficients in Bubble Columns. Ind Eng Chem Process Des Dev 12:76-80.

[9] Kang Y, Cho YJ, Woo KJ, Kim SD. 1999. Diagnosis of Bubble Distribution and Mass Transfer in Pressurized Bubble Columns With Viscous Liquid Medium. Chem Eng Sci 54:4887.

[10] Kawase Y, Moo-Young M. 1987. Heat Transfer in Bubble Column Reactors with Newtonian and Non-Newtonian Fluids. Chem Eng Res Des 73:697.

[11] Lin TJ, Wang SP. 2001. Effect of Macroscopic Hydrodynamics on Heat Transfer in Bubble Columns. Chem Eng Sci 56:1143-9.

[12] Behkish, A. 2004. Hydrodynamic and Mass Transfer Parameters in Large-Scale Slurry Bubble Column Reactors, Disertation at University of Pittsburgh, p. 22-28.

[13] Joelianingsih, Indra, I., and Purwaningsih, I.S. 2013. Modification Method of EN14105 for Determination of Free Glycerol and Mono-Di-Triglycerides Contents in Biodiesel. International Seminar on Bio-renewable Resources Utilization for Energy and Chemicals 2013, ITB Bandung, 10-11 Oktober 2013.

[14] Diasakou, M., Louloudi, A., and Papayannakos, N. 1998. Kinetis of The Non-Catalytic Transesterification of Soybean Oil. Fuel, Vol.**77**, No.12. p. 1297-1302.

[15] Warabi, Y., Kusdiana, D., and Saka, S. 2004. Reactivity of Triglycerides and Fatty Acids of Rapeseed Oil in Supercritical Alcohols. Bioresource Technology, Vol. 91, p. 283-287.

[16] Gunstone, F.D., Harwood, J.L., and Padley, F.B. 1994. The Lipid Handbook, 2nd edition, Chapman & Hall, University Press, Cambrigde, p. 443-446.

International Conference and Workshop on Chemical Engineering UNPAR 2013

Evaluation of Butanol-Water Distillation Column with Heat Integration to Obtain Minimum Total Annual Cost (TAC)

Renanto Handogo[a*], Musfil Achmad Sukur[a], Satrio Pamungkas[a], Tri Hartanto[a],

[a]Chemical Engineering Department, Institut Teknologi Sepuluh Nopember, Surabaya 60111, Indonesia

Abstract

Butanol-water azeotropeis a heterogeneous mixture that is difficult to separate using only ordinary distillation columns. In this case the separation of butanol-water using a decanter and two distillation column with pressure variation, where the equilibrium of Vapor Liquid Liquid Equilibrium (VLLE) was predicted using UNIQUAC equation. The research is conducted by computer simulation using Aspen Plus to find the best operating conditions in decanter to obtain the minimum heat needs of the reboiler distillation column I and II. Optimization is considered by comparing the profit and aims to obtain maximum profit. From the difference of column pressure, it can be determined the heat integration between the fluid that comes out from the bottom of the distillation column I (on the reboiler) and fluid coming out from the top of the distillation column II (the condenser). It is necessary to change the operating conditions by changing pressure in the distillation column II to meet the requirements of ΔT between T overhead distillation column II with T Bottom distillation column I (ΔT ≥ 20K). Total Annual Cost (TAC) was calculated to determine the cost savings for the system with the best operating conditions. The result for the best conditions on the butanol-water separation system where ΔT ≥ 20 K is decanter at temperature of 343 K, with the first distillation column pressure of 51 kPa and the second distillation column pressure of 172kPa. In terms of economics, when compared to the base case, it can be concluded that heat integration for this system is not profitable. The Total Annual Cost (TAC) for the base case is IDR 7.026.122.520, while for heat integrated system is IDR7.275.696.840.

Keywords: Aspen Plus, Heat Integration, Butanol-Water Distillation, Total Annual Cost (TAC).

1. Introduction

In chemical industry, analyzing and optimizing a plant unit is one of important parts for process efficiency. Optimization is the base of engineering, because one of engineer responsibles is to design better system, cheaper and more efficient as well as to think of a procedure to improve current system.Lately, changes in technology and information currents quickly happened. These changes require chemical engineer to follow it. Chemical engineering tools and softwares are also greatly improved. These things can be utilized to advance industries and to do optimization and efficiency of existing process. Most of processes in industry have undergone change at least once in lifetime to get benefit from the latest technology, which can be an improvement in energy efficiency and production capacity. This makes design with heat integration problem become important.To apply the result of an optimization theory mathematically and numerically on a concrete problem, it is very important to set the boundary of the system which is going to be optimized, to determine quantitative criterion which will become base candidate which will be ranked to determine the best one, to choose system variable which will be used to identify candidate and to define model which can express changes in another interacting variables [1].

With the increasing of the fuel price, it is important for a industry to reevaluate its processes so fuel wastage can be minimalized. In Butanol plant, there is a distillation column which will be used as case study in this research. Butanol usually used in many industries, for example plastiziser, resin and coating and the latest it is used as additive for gasoline. Distillation process is a process that use intensive energy so that evaluation on this plant will give quite big saving.Thesis by Nanda and Candra evaluated ethanol-water distillation column by utilizing heat integration [2]. This study applied heat integration in butanol-water system which the result can be used to minimize the need of hot and cold stream, especially steam required in reboiler which the price is more expensive than cooling water.

---

* Corresponding author : *Tel.: +6231-594-6240, fax: +6231-599-9282*
E-mail address: renanto@chem-eng.its.ac.id

Heterogeneous distillation means that during the distillation the liquid phase of the mixture is immiscible. In this case on the plates can be two liquid phases and the top vapour condensate splits in two liquid phases, which can be separated in a decanter. The simplest case of continuous heteroazeotropic distillation is the separation of a binary heterogeneous azeotropic mixture. In this case the system contains two columns and a decanter. The fresh feed is added into the decanter directly. From the decanter the butanol is withdrawn as reflux into the first column while the water is withdrawn as reflux into the second column. This mean the first column produces "butanol" and the second column produces "water" as a bottoms product. In the industry the butanol-water mixture is separated with this technique.
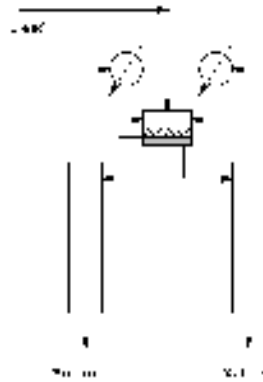
Fig 1. Design of Butanol-Water Separation

2. Research Methodology

Data needed for this research consist of operation condition data based on literature by Luyben and distillation column pressure variation data based on thesis by Santi [3-4]. The simulation feed flow rate is 1000 kmol/h with feed composition 60% water and 40% butanol. The output observed are reboiler and condenser duty in distillation column I and II, difference between distillation column II overhead temperature and distillation column I bottom temperature for heat integration, also mole fraction of butanol and water in the product to keep product purity. Some data like stream condition and component need to be inputed into Aspen Plus [5]. Proses optimization is done to get reboiler duty in maximal operation condition. Butanol-water separation system can be seen in Figure 2.
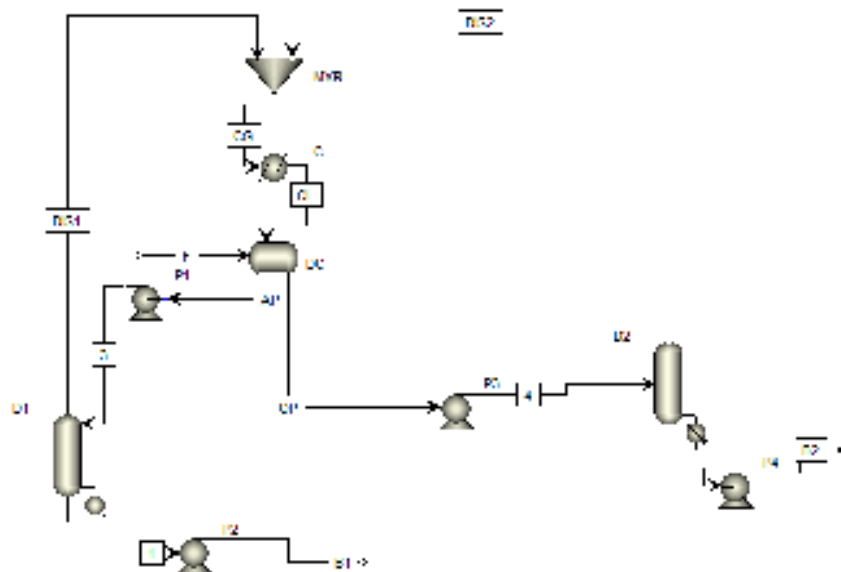
Fig. 2. Butanol-Water Separation System in Aspen Plus Software

Heat integration can be conducted by changing pressure. The requirements of heat integration can be conducted are [6]:

- ΔT minimum of 20 K (Luyben, 2006)
- The amount ofheatthatwill beexchanged smallerorequal to theheatthatwould receive.

System of butanol-water separation with heat integration is illustrated in Figure 2.

3. Result and Discussion

In this research,the validation of simulation results is needed. This validation is a baseline which show that the simulation can approach the real condition. Validation was conducted by step for butanol-water separation system by using two distillation columns and a decanter. It is important given the tight connection of the complex component involvement in feed. If a step in validation do not give minimal output, the next step in validation will be affected. Data which are taken from literature by Luyben [3]. After the literature data are obtained, butanol-water separation process diagram can be made by using Aspen Plus, which will be used in this research.

This research was done by using Aspen Plus. Steady state simulation for base case is the first step to do the simulation to get the optimum operation condition. In the steady state simulation, the selection of tray type and distillation column type to get simulation model that corresponds to the actual condition of the literature was done. This simulation use UNIQUAC as thermodynamic model because the feed which is used in this system is organic mixture between butanol and water, beside that, butanol-water system exhibit a liquid-liquid equilibrium (LLE).

In this simulation the feed of 1000 kmol /h with the composition of butanol is 0.4 and the water is 0.6 with butanol target product in the distillation column II has a fraction of 0.99936. Base case condition are made based on data in the literature [3]. The steady state base case simulation resultsare shown in Table 1.

Table 1. Steady state simulation results

Variable	Luyben	Simulation with AspenPlus
Distillation column I pressure	51 kPa	51 kPa
Distillation column II pressure	51 kPa	51 kPa
Decanter temperature	343 K	343 K
Distillation column I overhead temperature	348 K	348,00926 K
Distillation column I bottom temperature	357 K	354,4658 K
Distillation column II overhead temperature	348 K	348,503 K
Distillation column II bottom temperature	376 K	375,4277 K
Decanter feed	1000 kmol/h	1000 kmol/h
Butanol mole fraction	0,4	0,42013577
Water mole fraction	0,6	0,57986423
Distillation column I product mole flow	600,1 kmol/h	599,99393 kmol/h
Butanol mole fraction	0,001	0,00063999
Water mole fraction	0,999	0,99936
Distillation column II product mole flow	399,9 kmol/h	400,002777 kmol/h
Butanol mole fraction	0,999	0,999

Water mole fraction	0,001	0,001
Distillation column I reboiler heat duty	1,21 MW	1,21342629 MW
Distillation column II reboiler heat duty	6,70 MW	6,67595483 MW
Condenser duty	6,83 MW	7,0353724 MW

Having obtained the simulation stage of steady state, then the next step is to re-simulate using Aspen Plus and input the research variable to obtain optimum condition of distillation column butanol-water separation system. The first variable to be inputed in the simulation of butanol-water separation is the temperature at the decanter of 339 K, 341 K, 343 K with pressure on the distillation column I and II equal to 51 kPa.

Table 2. Steady state simulation results with decanter temperature variable

| T (K) | Mole Fraction (Product) | | | | Q (MW) | | |
| | Distillation column I | | Distillation column II | | Q condensor | Q reboiler (D II) | Q reboiler (D I) |
	Butanol	Water	Butanol	Water			
343 (base case)	**0.00064**	**0.99936**	**0.999**	**0.001**	**7.0353724**	**6.67595483**	**1.21342629**
341	0.00064	0.99936	0.999	0.001	7.0911335	6.88452743	1.44096256
339	0.00064	0.99936	0.999	0.001	7.0905410	7.28576838	2.01740899

Table 2 shows that temperature changes at the decanter affect the size of the duty of the reboiler and condenser in the distillation column I and II. In this study the duty of the reboiler and condenser are all concerned because   later   on this   research beside   observing   the purity of the butanol produced on distillation column, the economic side is also observed. In the table can be seen that the best condition is obtained at a temperature of 343 K. The simulation can not be done at   temperature   over   343   K,   because   at   this   temperature   most   of   butanol   and water have changed phase from liquid to vapor, as shown in Figure 3. Decanter temperature increase also cause the increase in reboiler duty in distillation column I and II as shown in Figures 4 and 5, but there is a decrease in the condenser duty as shown in Figure 6.
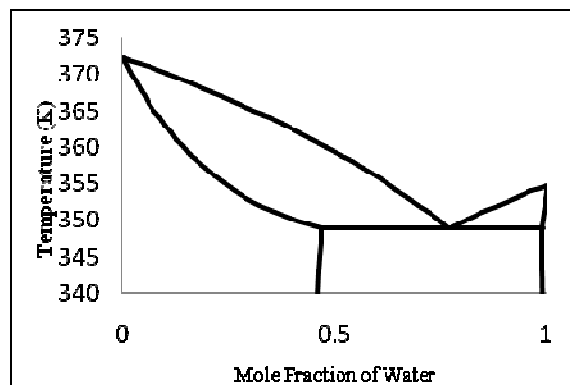
Fig 3. VLLE of butanol-water system at 51 kPa
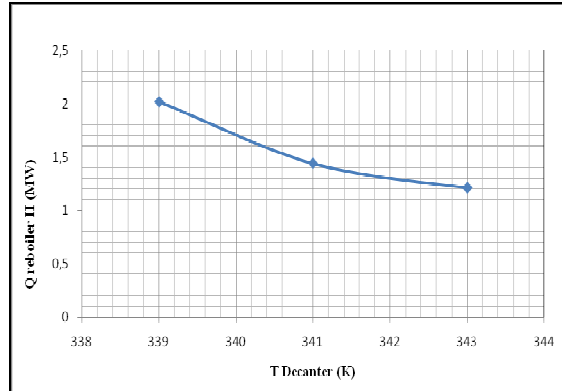
Fig 4. Decanter temperature increase effect on distillation column I reboiler duty
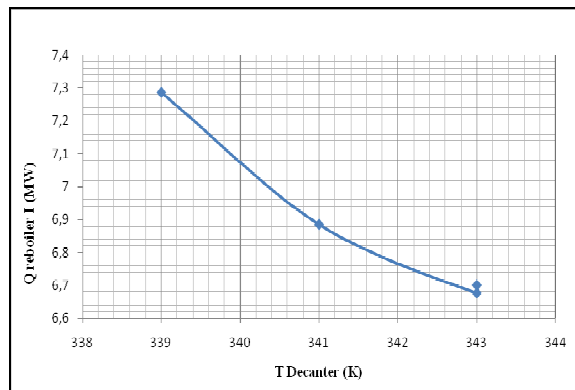
Fig 5. Decanter temperature increase effect on distillation column II reboiler duty
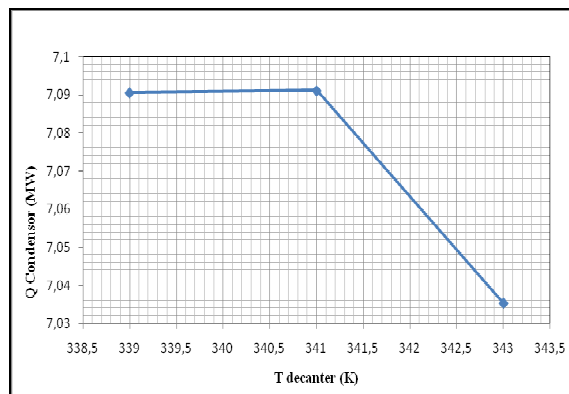
Fig 6. Decanter temperature increase effect on the condenser duty

After getting the optimum conditions with decanter temperature variable, the next step is to locate and determine the heat integration for the heat integration system I by using Aspen Plus and input the pressure variable on the distillation column I.

The variables to be inputted are 110.325 kPa, 111. 5 kPa, 122 kPa, 132kPa, 141.8 kPa, 152 kPa with the pressure in the distillation column II fixed at 51 kPa and decanter temperature of 343 K. The savings between before and after integration therefore are known. The heat integration system I can be seen in Figure 7, as follows:
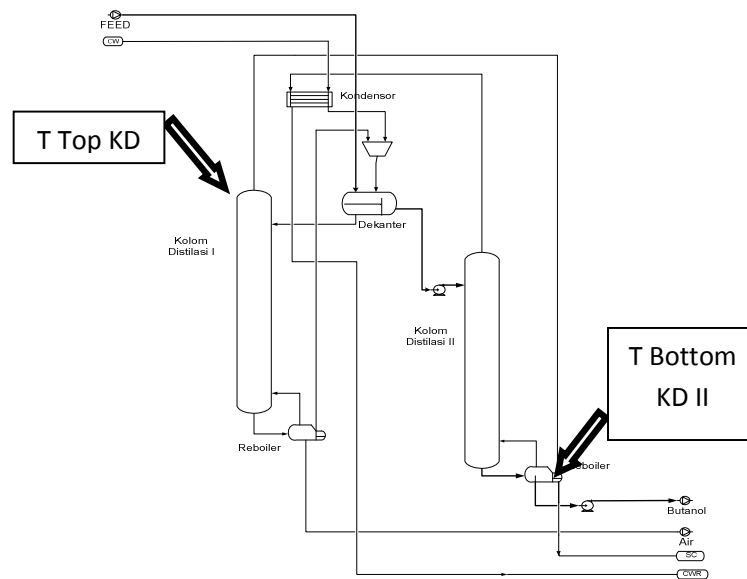
Fig 7. Heat integration system I in Butanol-water separation

Table 3. Steady state simulation with pressure variable in distillation column I

P (kPa)		Q (MW)			T top D I	T bottom D II	ΔT (K)
D I	D II	Q condenser	Q reboiler		(K)	(K)	
			D I	D II			
152	51	7.0712433	0.6370029	6.6750261	376.59532	375.294076	1.301246
141.8	51	7.068736	0.6506458	6.6774726	374.6393	375.294076	-0.654772
132	51	7.0660841	0.6678739	6.6751686	372.56488	375.294076	-2.729196
122	51	7.0632675	0.6889384	6.6774631	370.35472	375.294076	-4.939353
111.5	51	7.0602596	0.715438	6.6755141	367.98724	375.294076	-7.306837
110.325	51	7.057029	0.7484083	6.6779385	365.43504	375.294076	-9.859036
51	51	7.0353724	1.2134263	6.6759548	348.00926	375.4277	-27.41844

Table 3 shoes that to get heat integration, if distillation column I pressure is increased, unqualified temperature difference will be gotten, where temperature difference needed is 20 K, as seen in table, until pressure of 152 kPa, the temperature difference is around 1.3013 K. Therefore in this study, distillation column I pressure for heat integration system I is assumed constant at 51 kPa and heat integration system I can not be done. The next step is to input pressure data in distillation column II to get heat integration system II. This system can be seen in Figure 8.

Fig 8. Heat integration system II in butanol water separation

Table 4. Steady state simulation results with pressure variable on distillation column II

P (kPa)		Q (MW)			T top D II (K)	T bottom D I (K)	ΔT (K)
		Q condenser	Q reboiler				
D I	D II		D I	D II			
51	172.2	7.274775	1.2141617	9.79481483	379.896997	354.490419	25.406578
51	162.12	7.261032	1.2148789	9.59320698	378.131647	354490419	23.641228
51	152	7.2466555	1.2137955	9.38412561	376.279727	354.490419	21.789308
51	141,8	7.2315552	1.2130815	9.1705709	374.330796	354.490419	19.840377
51	132	7.2156541	1.2141712	8.94391163	372.271476	354.490419	17.781057
51	122	7.1988148	1.2149188	8.70663038	370.086509	354.490419	15.59609
51	111,15	7.1809238	1.2137727	8.45930684	367.755315	354.490419	13.264896
51	110,325	7.1617629	1.2130605	8.19855878	365.253971	354.490419	10.763552
51	91,2	7.1411456	1.2141756	7.92693739	362.548542	354.490419	8.058123
51	88,2	7.1186992	1.2142603	7.6378206	359.597699	354.490419	5.10728
51	51	7.0353724	1.2134263	6.67595483	348.503	354.4658	5.9628

Table 4 shows that to get heat integration, if distillation column II pressure is increased, the temperature difference needed will be obtained. The required distillation column II pressure for heat integration is between 152 to 172 kPa or more. If the pressure of 172 kPa and 51 kPa is compared, the duty needed is not far different, which is 7.275 MW for condenser duty, 1.214 MW for reboiler I duty, and 9.795 MW for reboiler II duty for the pressure of 172 kPa and 7.83 MW for condenser duty, 1.21 MW for reboiler I duty, dan 6.7 MW for reboiler II duty for the pressure of 51 kPa. From this difference, it is expected that by using heat integration, the duty of the system with pressure of 51 kPa can be substituted by that of the 172 kPa. Increase in distillation column cause an increase in the top product temperature of the distillation column II. After the optimum condition is gotten, the next step is to seek and determine heat integration in Aspen Plus and to input the variable, which is decanter temperature of 343 K, distillation column I pressure of 151 kPa and distillation column II presssure of 132 kPa to get heat integration system as can be seen in Figure 7. The savings between before and after integration will be known.

Table 5. Heat integration simulation result with pressure variation on distillation column II

P (kPa)		T DECANTER (K)	ΔT (K)	QR1 (MW)	QC2 (MW)
D I	D II				
51	152	343	21.789308	1.21379552	-1.2137687
51	162.12	343	23.641228	1.21379552	-1.2137756
51	172.2	343	25.406578	1.21379552	-1.2137838

From Table 5, it can be seen that the higher the temperature, the higher the duty, therefore the pressure of 172.2 kPa will be used in distillation column II. Beside has the smallest duty difference between before and after integration, this pressure meet the requirement for heat integration, which is the temperature difference more than 20 K. In heat integration, it is suggested that the temperature difference is more than 20 K because if temperature difference is too small, the heat transfer area will be too big. This affects the equipment used. From Table 6 can be seen the heat transfer area (A), where the greater the column pressure, the greater the heat transfer area.

Table 6. Simulation result of heat transfer area (A) with distillation column II pressure variation

Note	P (kPa)		Heat Transfer Area (A)			ΔT (K)
	KD I	KD II	Condenser (m^2)	Reboiler I (m^2)	Reboiler II (m^2)	
Base Case	51	51	176.501	13.289	198.353	-
Before	51	152	176.5018	13.293	365.925	21.79
After	51	152	165.18	2.829	314.529	
Before	51	162.1	176.5021	13.299	383.574	23.64
After	51	162.1	152.17	2.829	353.222	
Before	51	172	176.5037	13.306	401.369	25.41
After	51	172	147.36	2.829	361.926	

After obtaining the result from heat integration in the optimum condition, the tray sizing data is inputted before Total Annual Cost (TAC) calculation. The data inputted is type and amount of tray, feed tray and product tray. The type of tray that is used is sieve tray, with total 10 trays as in Luyben [3]. Feed tray is in tray 2. Next is Total Annual Cost calculation for every distillation column II variation. Calculation done by using Aspen Plus. The calculation results is shown in Table 7.

Table 7. Total Annual Cost before and after heat integration wih variation in distillation column II pressure

Note	P (kPa)		Total Operating Cost ($/Year)	Total Capital Cost ($/Year)	Total Annual Cost ($/Year)	Total Annual Cost ($/Year)
	D I	D II				
Base Case	51	51	351.790	425.780	777.570	7.026.122.520
After heat integration	51	152	376.530	428.660	805.190	7.275.696.840
	51	162.1	399.329	433.321	832.650	7.523.825.400
	51	172	419.467	433.321	852.788	7.705.792.368

From Table 7, it can be seen that increase in distillation column II pressure cause economically ineffectiveness, where TAC for distillation column II with base case pressure (51 kPa) smaller than that of with pressure after heat integration (172 kPa). Based on calculation from Aspen Plus, heat integration system do not give profit, so in this research heat integration system with pressure of 172 kPa is not satisfactory. In this system, the compressor is added to increase distillation column I top product pressure, so that the buatnol water separation system can run well because of the difference in pressure in distillation column I and II. In fact, without the adding of the compressor, this system still can be run in Aspen Plus without changing the results. TAC for the system with the addition of compressor are as follow:

Table 8. Total Annual Cost with addition of compressor

Note	P (kPa)		Total Annual Cost (IDR/Year)	Total Annual Cost + Compressor (IDR/Year)
	D I	**D II**		
Base Case	51	51	7.026.122.520	-
After	51	172	7.275.696.840	8.389.835.640

In Table 8, there is addition to TAC when the compressor is added, and if it is compared with the base case, TAC with compressor added is bigger, so that although the presence or absence of heat integration, the system is still not profitable from economic standpoint. The next step is comparing TAC from Aspen Plus calculation result and from Peters and Timmerhauss (2003) literature. The results is as follows:

Table 9. Total Annual Cost comparison between Aspen Plus and literature

Note	P (kPa)		*Total Annual Cost (IDR/Year) (Peters dan Timmerhauss)*	*Total Annual Cost (IDR/Year) (AspenPlus)*
	D I	**D II**		
Base Case	51	51	6.249.343.788	7.026.122.520
After integration	51	172	6.861.944.838	7.275.696.840

From Table 9, there is difference between Total Annual Cost from Aspen Plus calculation and from literature. In base case system, there is a quite significant difference. This may be caused by because in literature calculation, the equipment cost index data in 2002 is used, which then converted to 2010 by least square method [7]. While in the calculation using Aspen Plus, cost index used in newer or closer to cost index in 2010. Equipment cost index always increases every year, this makes a quite significant difference in Annual Capital Cost. The tendency of cost index that getting higher can be seen in the Total Annual Cost in Aspen Plus.

4. Conclusion

Simulation in Aspen Plus give best condition for heat integration for butanol-water separation system with decanter temperature is 343 K, distillation column I pressure is 51 kPa and distillation column II pressure is 172 kPa.The best heat integration is at temperature difference 25.41 K, with distillation column II reboiler duty 9.79 MW.From economic aspect, if compared to the base case, it can be concluded that Total Annual Cost for system with heat integration is less profitable, the Total Annual

Cost is IDR 7.026.122.520 for base case system and IDR 7.275.696.840 for heat integrated system with distillation column II pressure 172 kPa.

References

[1] [1] Ravindran, A., Ragsdell, K. M. dan Reklaitis, G. V. 2006,*Engineering Optimization.*John Wiley & Sons, Inc,USA.

[2] Nanda, F.dan Candra K. 2005,*Kolom Distilasi Pabrik Etanol Dengan Integrasi Panas*, Skripsi Teknik Kimia FTI-ITS,Indonesia.

[3] Luyben,W.L. dan Chien, I.L. 2008,*Design and Control of Distillation Systems for Separating Azeotropes.*John Wiley & Sons, Inc., Hoboken, New Jersey.

[4] Santi, S.S.2000,*Simulasi Pemisahan Campuran Heterogen Azeotrop Butanol-Air.*Thesis Teknik Kimia FTI-ITS,Indonesia.

[5] Aspen Plus.2006,*Getting Started Modeling Petroleum Processes*. Cambridge ,Aspen Technology, Inc.USA.

[6] Luyben,W.L.2006,*Distillation Design and Control Using Aspen^{tm} Simulation*. A John Wiley & Sons, Inc,USA.

[7] Peters,Max S. dan Timmerhaus,K D.2003,*Plant Design and Economics for Chemical Engineers,Fifth Edition.*The McGraw-Hill Companies, Inc,USA.

The International Conference on Chemical Engineering UNPAR 2013

Optimization of Nicotine Extraction In Tobacco Leaf (Nicotianatabacum L.) :(Study : Comparison of Ether and Petroleum Ether)

Arie Febrianto Mulyadi[a] , Susinggih Wijana[b], Arif Setyo Wahyudi

[ab]*Agroindustrial Technology Department*, *Faculty of Agricultural Technology, University of Brawijaya, , Veteran Street, Malang, 65141, Indonesia*

* Corresponding author. Tel.: +62 81 79642734 ;E-mail address: arie_febrianto@ub.ac.id.

Abstract

Tobacco (Nicotianatabacum L.) belonging to the genus Nicotiana. The main products of the tobacco crop is cigarettes. Tobacco as its main raw materials containing hazardous substances. One of the hazardous substance is nicotine. Nicotine has the alternative to be used, in the form of other products. Extract nicotine from tobacco leaves, then extract the nicotine may be a better product in order to have value, such as pesticides or insecticides in agriculture.The properties of nicotine is soluble to some types of solvents. This is the reason for the extraction of nicotine by using a solvent extraction method. Later in the extraction of nicotine as an alkaloid in tobacco, ether and petroleum ether solvent is advantageous because it is selective in dissolving the alkaloid substances. Using the right combination of ether and petroleum ether will optimize time of extraction and the yield of nicotine on nicotine extraction process. The method used is the response surface method with central composite designconsisting of two factors: the addition of ether and petroleum ether. While the dependent variables or response time of extraction and nicotine yield. The result of the research revealed that the addition of ether and petroleum ether solvent significantly affect the response time of extraction and yield. Predicted results obtained optimal solution is the addition of 59.46 ml of ether and 30.12 ml of petroleum ether. The lowest possible values for the extraction time is 477.343 seconds and the highest is 887.623 seconds. Then the standard to yield the lowest possible value is 4.18025% and the highest is 5.4321%. While the results obtained on the model prediction of the response time of the addition of ether extraction on the treatment of 59.46 ml and 30.12 ml of petroleum ether reaches 682,483 seconds, then to achieve the yield response of 4.80617%.

*Keywords:*optimization, solvent extraction, nicotine, tobacco, RSM

I. INTRODUCTION

Tobacco (*Nicotiana tabacum L*) belong to the genus Nicotiana, and is native to America. These plants spread all over Indonesia and have utility primarily for raw material for making cigarettes. In 2005 the land area is 198 367 ha of tobacco, consists of various types of tobacco, with production of 149 263 tonnes of tobacco leaf (Ditjenbun, 2006). As a raw material cigarettes, the health aspects are considered to have adverse effects. This is because cigarettes with tobacco leaves as its main raw materials containing substances which are harmful to the human body. One of a hazardous substance is nicotine.

Nicotine is a specific organic compounds contained in tobacco leaves. Nicotine in cigarettes when smoked will cause psychological stimulus for smokers and makes it addictive. It also has pharmacological properties that can increase blood pressure and heart rate (Wolf, 1994).

Nicotine has another alternative in the form of more useful products. With the extract of tobacco leaf extract can be used nicotine products has greater value to, for example as an insecticide in agriculture. Thus, the extract nicotine from tobacco leaves will be much more useful than in the form of cigarettes smoked. Besides nicotine after undergoing further processing can be utilized for both industries to mix the drug, supplement drink mix, sleep medicine, and cosmetic products, the price is more expensive and the market is wide open, 100 mg price reaches 900,000 rupiahs.

Nicotine is soluble to some types of solvents such as alcohol, chloroform, ether, petroleum ether, kerosene, and water. This is the basis for the extraction of nicotine from tobacco by using a solvent extraction method. Choice of solvent is important because each solvent has its own advantages and disadvantages, by using a combination / mixing two types of solvents and extraction

* Corresponding author. *Tel.: +62 81 79642734*
E-mail address : arie_febrianto@ub.ac.id.

time allegedly generated more nicotine yield optimal. According to Wolf (1994) which has been extracted nicotine is hygroscopic, oily liquid which is miscible (can be mixed) with water in its basic form. As a basic nitrogen, nicotine salt form with an acid which is usually solid and water soluble.

In this study the solvent used is ether and petroleum ether. It is based on previous journal and preliminary research that has been done, where ether and petroleum ether is very beneficial because it is selective in dissolving the alkaloid substances (Karbalai, 2009). According to Ronald (2008), two solvents with different polarities can be mixed or combined to obtain optimum solvent that can work in the extraction process. So to get the optimal proportion of solvent will produce nicotine extract yield and extraction time are more optimal than using a single solvent.

II. MATERIAL AND METHODS
Materials and Tools

Materials used is tobacco Temanggung. Tobacco has been obtained in the form of dried tobacco that has been milled to 60 mesh size. Tobacco Temanggung selected in this study because tobacco contains more nicotine than other types. Material for analysis include: solvent p.a (ether, petroleum ether were purchased from a local chemical store in Malang, East Java), 5% NaOH, methanol, picric acid, distilled water, potassium carbonate.

The tools used were 250 ml beaker, pipettes, filter paper, stirrer, heater, spoon, glass wool Buchner, basin, digital scales and extraction tools.

Experimental design methods

The method used is the response surface method with centralized composite design consisting of two factors, namely the addition of ether and petroleum ether. Then take the midpoint 50 ml ether ($X_1 = 0$) and 50 ml petroleum ether ($X_2 = 0$). According to the response surface method 2 factors, loop made at the midpoint ($X = 0$) as much as 5 times. Value of α chosen k = 2 is 2k / 4 = 22/4 = 1.414. The next step to determine the level of each factor in the experiment is described as follows:
1. Determine the 22 factorial design (effect of 2 factors) as a trial order first and set levels to be studied as follows:
   a. Factors ether (E) with the level of factor:
   • Ether 25 ml (code $X_1 = -1$)
   • Ether 75 ml (code $X_1 = 1$)
   b. Factors petroleum ether (P) with the level of factor:
   • Petroleum ether 25 ml (code $X_2 = -1$)
   • Petroleum ether 75 ml (code $X_2 = 1$)
2. Having established the factor levels corresponding to the 22 factorial design, the factors set levels corresponding to the center point $X_1 = 0$ and $X_2 = 0$. Ether soluble factors known to successive levels ie 25 ml ($X_1 = -1$), 75 ml ($X_1 = 1$), 50 ml ($X_1 = 0$) as the center point with the distance between the level factor is 25 ml, so that the relationship between variable X_1 with the original variables can be expressed as follows:
$$X_1 = \frac{E - 50}{25} \quad , E = 25\, X_1 + 50 .... \quad (1)$$

On factors petroleum ether relationships between variables X2 with the original variables can be determined in the same way that stated as follows:
$$X_2 = \frac{P - 50}{25} \quad , P = 25\, X_2 + 50 .... \quad (2)$$

3. Determining factor levels corresponding to values $\alpha = -1.414$, and $\alpha = 1.414$ by calculation through relationship variables X_1 and X_2 with the original variables in equation (1) and (2).
Of equation (1) note that:
For $X_1 = -1.414$. Then E = 25 (-1.414) + 50 = 14.65 For X1 = 1.414. Then E = 25 (1.414) + 50 = 85.35 from equation (2) note that:
For $X_2 = -1.414$. Then P = 25 (-1.414) + 50 = 14.65
For $X_2 = 1.414$. Then P = 25 (1.414) + 50 = 85.35
Experimental design using a centralized composite experimental design, with variables such as the level above calculations. By entering the desired response, it can be arranged an experimental design

that can be seen in Table 1.

Implementation Research

Dried tobacco leaves that have been milled to 60 mesh size powder weighed as much as 10 g and placed in 250 ml beaker. After that add as much as 5% NaOH in 10 ml beaker and then stirred using a stirrer for 15 minutes. Then filtered using Buncher glass wool.

The above explanation is how to get one sample filtrate for 1 treatment. While it takes 13 samples of filtrate for all treatments as shown in Table 1. Filtrate to obtain the same treatment for all the filtrate will be collected together in one process at a time. Then collected in the same bottle for further sampled for all treatments.

The next process is to move the filtrate obtained on filter paper and extract using solvents. Performed using solvent extraction comparison ether and petroleum ether according to the experimental design shown in Table 1. Extraction process by passing a solvent in the filtrate. The extraction process is assisted by vacuum extraction tool to speed up the extraction process. Upon subsequent solvent extraction using potassium carbonate as adding 1 teaspoon and then filter.

After that is done using the evaporation basin of heated water with a temperature of 60 ° C to 10 ml of liquid remaining. Then add 4 ml of methanol extraction on the results that have been evaporated. Methanol is used to bind the remaining oil in the previous process. Then added 10 ml of picric acid solution and put it in the fridge. Once out of the fridge and then filter the nicotine that has been crystallized and silence to dryness and aged in a desiccator to avoid direct contact with air. Last is the weighing and counting nicotine produced nicotine yield.

Table 1. Centralized Composite design of experiments

No	Code Variable		Original Variable	
	X_1	X_2	E : Ether (ml)	P : PE (ml)
1	-1	-1	25	25
2	1	-1	75	25
3	-1	1	25	75
4	1	1	75	75
5	-1,414	0	14,64	50
6	1,414	0	85,36	50
7	0	-1,414	50	14,64
8	0	1,414	50	85,36
9	0	0	50	50
10	0	0	50	50
11	0	0	50	50
12	0	0	50	50
13	0	0	50	50

Response Model Analysis and Optimization of Response
Response Surface Method

The data were then carried out observations of the results of the final product and the duration of extraction, by using the Design Expert 8.0.4 Trial Version DX7 obtained from www.statease.com site. The data was then entered in the central composite design with 2 factors and 5 repetitions at a midpoint with 2 responses.

Prediction results of the Optimal Solution

Optimal solution with the computational results using DX7 program Design Expert 8.0.4 Trial Version which has been selected by a high desirability value or close to 1 to verify that the solution is applied to the actual conditions. Then analyzed the factors that result in deviations from the optimal point

Validation of Prediction Results Optimal Solutions

Validation is done by comparing the results of the optimal solution and computational results

predicted by experiments on the best treatment that has been carried out laboratory analysis.

III. RESULT AND DISCUSSION

Response Time Extraction

In the extraction studies used nicotine alkaloid isolation means in general that is extracted with an organic solvent, the formation of alkaloid salts with bases, then extraction with certain solvents. First of nicotine in the tobacco used to form alkaline by adding NaOH 5%, then it will form insoluble salts with certain solvents. Nicotine in the form of salts and then re-extracted with a solvent mixture of ether and petroleum ether. So nicotine dissolved and entrained with solvent ketahapan then enter the next process. Based on data obtained from laboratory studies of nicotine extraction of tobacco leaves (*Nicotiana tabacum*) analysis results obtained by using response surface method. Data of extraction time response are presented in Table 2.

Table 2. Extraction Time Response

No	Code Variable		Original Variable		Response
	X_1	X_2	E : Ether (ml)	P : PE (ml)	Extraction Time (second)
1	-1	-1	25	25	503,61
2	1	-1	75	25	756,11
3	-1	1	25	75	941,72
4	1	1	75	75	1122,41
5	-1,414	0	14,64	50	518,34
6	1,414	0	85,36	50	806,66
7	0	-1,414	50	14,64	458,17
8	0	1,414	50	85,36	1028,27
9	0	0	50	50	872,96
10	0	0	50	50	819,55
11	0	0	50	50	831,62
12	0	0	50	50	819,55
13	0	0	50	50	831,57

Table 2 shows that the response time is 458.17 seconds the fastest extraction obtained from the comparison treatment 50 ml ether and petroleum ether 14.64 ml. While the longest extraction time is 1122.41 seconds obtained from the comparison treatment 75 ml ether and 75 ml PE. Then the response time value extraction contained in Table 7 will be used as input data to be processed and analyzed using Design-Expert 8.0.4 software. The data processing results can be seen in Figure 1 and Figure 2
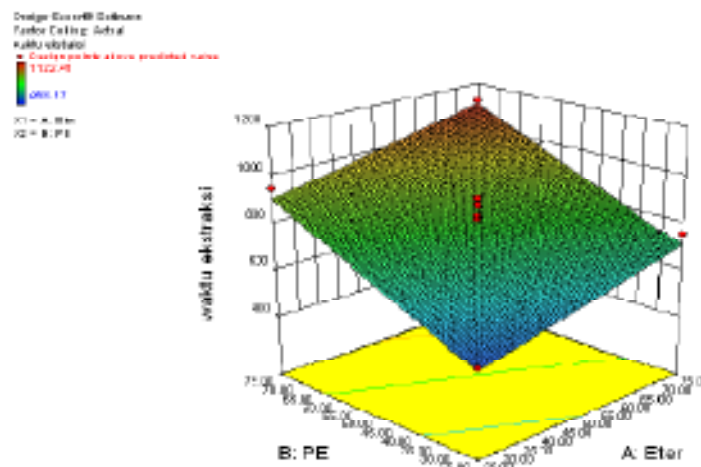

Figure 1. Relationship between the type of solvent (Ether and Petroleum Ether) Against Extraction Time

Based on the response surface curves and contour plots contained in Figure 1 and Figure 2 it can be seen that the addition of ether and petroleum ether have a significant effect on the extraction time. Known F-value of 22.58 implies that the model is significant. There are only a 0.01% chance that this model is wrong. Value of F> Prob less than 0.05 indicate the model terms are significant, while values greater than 0.1000 indicate the model terms are not significant.
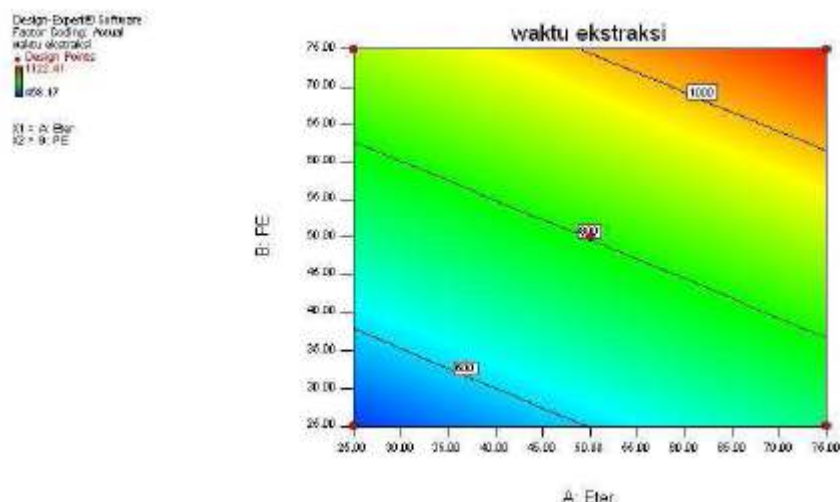

Figure 2. Contour Plot Relationship Type Solvent (Ether and Petroleum Ether) Against Extraction Time

In the treatment of the fastest extraction time on the addition of 50 ml of ether and petroleum ether 14.64 ml ($X_1 = 0$, $X_2 = -1.414$), it is known that the amount of ether used is greater than petroleum ether, in addition to the total volume of solvent also includes small compared other treatments. The results obtained in the treatment of extraction time 458.17 sec. Whereas the opposite treatment is the addition of 14.64 ml ether and 50 ml petroleum ether ($X_1 = -1.414$, $X_2 = 0$), the total volume of the same solvent but the amount of petroleum ether more. The results obtained in the treatment of a longer extraction time is 518.34 seconds.

Seen that the addition of ether over time effect on the efficiency of extraction of nicotine . So it can be said ether solvent in dissolving nicotine better than petroleum ether . According to Darwis (2000) percolation extraction is the process of organic solvent in the sample skipped so the solvent will bring together organic compound solvent . Effectiveness of this process depends on the organic compound soluble in the solvent used . In the extraction process by using the pressure difference the right choice of solvent will have a positive influence on the extraction time (Astu, 2004) . According to Jones (2001) in the extraction of alkaloids by using various methods such as percolation extraction , maceration , liquid - liquid extraction , steam distillation , soxhlet can be concluded that the ether solvent is better than petroleum ether . Whereas the longest extraction time seen in the addition of 75 ml ether and 75 ml petroleum ether ($X_1 = 1$, $X_2 = 1$) , in the treatment of the amount of ether and petroleum ether as large and the total volume of the solvent is high compared to most other treatments . The results obtained in the treatment of extraction time 1122.41 sec . Whereas the opposite treatment with low total solvent volume but the ratio of petroleum ether and ether ether at which the addition of 25 ml and 25 ml petroleum ether ($X_1 = -1$, $X_2 = -1$) . The results obtained in the treatment of a shorter extraction time is 503.61 seconds .

It seems clear that the volume is very influential on the extraction time Based on the above it can be seen increasingly large volumes of solvent then the time required to complete the extraction process is also getting old. According to Susanto (2001) in percolation extraction, solvent volume will affect the extraction process and the amount of organic compounds carried away.

Linear model was selected for the response time of extraction nicotine tobacco leaves (*Nicotiana tabacum*) results in the following equation:

$$Y_1 = 189{,}95885 + 4{,}20468\,X_1 + 8{,}05327\,X_2$$

Description:
Extraction Y_1 = time (sec)
X_1 = Ether (ml)
X_2 = Petroleum ether (ml)

Based on the linear model suggests that each additional ether and petroleum ether solvent will influence the addition of extraction time. The more solvent is used it will be the longer time required for extraction. Coefficient of X_1 (Ether) is smaller than the value of the coefficient of X_2 (petroleum ether), so if that is the expected time efficiency then the value X_1 (ether) will be more influential in the model. This means that in ether solvent extraction nicotine use will be an effect on the efficiency of the extraction time compared to petroleum ether. The model significantly affect the response because the probability value 0.0001 (0.01%) of the response variable extraction time.

Nicotine yield response
Nicotine yield research results can be seen in Table 3. Greatest yield is 5.36% obtained from the use of comparative treatment factors Ether 75 ml and 75 ml petroleum ether factors. While the smallest yield was obtained from treatment comparisons using factor Ether 25 ml and 25 ml petroleum ether factor is 3.14%.

Table 3. Yield Response

No	Code Variable		Original Variable		Response
	X_1	X_2	E : Ether (ml)	P : PE (ml)	Yield (%)
1	-1	-1	25	25	3,14
2	1	-1	75	25	4,84
3	-1	1	25	75	3,34
4	1	1	75	75	5,36
5	-1,414	0	14,64	50	3,31
6	1,414	0	85,36	50	5,17
7	0	-1,414	50	14,64	3,99
8	0	1,414	50	85,36	5,13
9	0	0	50	50	5,11
10	0	0	50	50	5,09
11	0	0	50	50	4,87
12	0	0	50	50	5,02
13	0	0	50	50	4,91

Yield values contained in Table 2 will be used as input data to be processed and analyzed using the software Design-Expert 8. Data processing results can be seen in Figure 3 and 4.
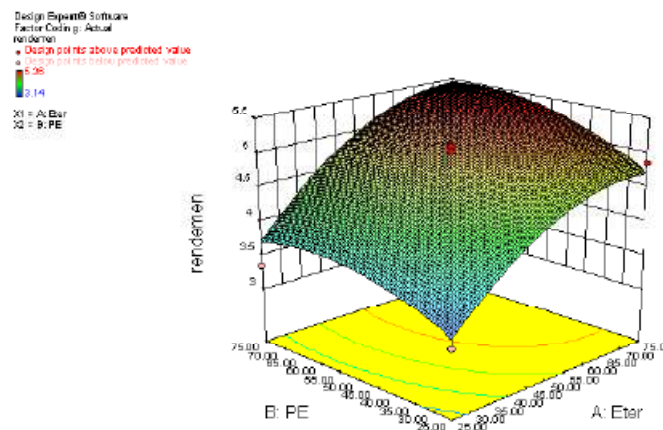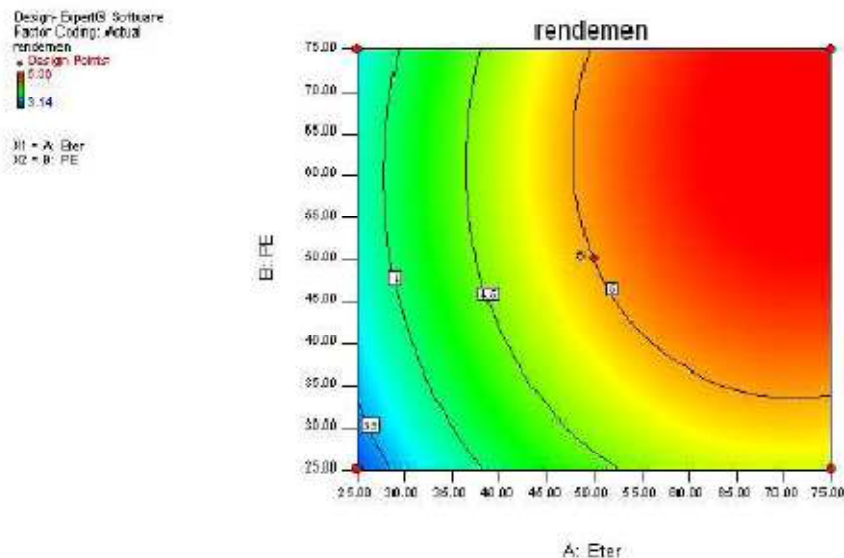

Figure 3. Relationship of solvent (Ether and Petroleum Ether) To Yield

Based on the response surface curves and contour plots contained in Figure 3 and 4 it can be seen that the factor of ether and petroleum ether have a significant effect on the results of nicotine yield of tobacco leaves (*Nicotiana tabacum*). Known F-value of 24.18 implies that the model is significant. There are only a 0.09% chance that this model is wrong. Value of F> Prob less than 0.05 indicate the model terms are significant, while values greater than 0.1000 indicate the model terms are ot significant.

Figure 4. Contour Plot Relationship Type Solvent (Ether and Petroleum Ether) To Yield

The treatment and the addition of 75 ml ether 25 ml petroleum ether ($X_1 = 1$, $X_2 = -1$) , it is known that the amount of ether used is greater than petroleum ether . The results obtained in the treatment of nicotine yield of 4.84 % . Whereas the opposite treatment is the addition of 25 ml ether and 75 ml petroleum ether ($X_1 = -1$, $X_2 = 1$) , the amount of petroleum ether more. The results obtained in the treatment of nicotine yield is 3.34 % less . Seen that the addition of more ether effect on nicotine yield results . So it can be said ether solvent in dissolving nicotine better than petroleum ether .

According to Guenther (1987), the solvent is one of the determining factors in the extraction process . Solubility of the solvent so as to produce the extract as much as possible . According to Ronald (2008), the effectiveness of organic solvents can be achieved by mixing different polarity solvents , such as hexane and chloroform . Whereas in this study it is to be achieved by mixing ether and petroleum ether . According to Jones (2001) in the extraction of alkaloids by using various methods such as percolation extraction , maceration , liquid - liquid extraction , steam distillation , soxhlet can be concluded that the ether solvent is better than petroleum ether .

The treatment with the greatest yield on addition of 75 ml ether and 75 ml petroleum ether ($X_1 = 1$, $X_2 = 1$) , it can be seen that the amount of ether and petroleum ether as large and the total volume of the solvent is high compared to most other treatments . The results obtained in the treatment of nicotine yield of 5.36 % which is the largest yield results . Whereas the opposite treatment is the addition of 25 ml ether and 25 ml of petroleum ether ($X_1 = -1$, $X_2 = -1$) , with the smallest total volume of solvent and the ratio of petroleum ether and ether are the same . The results obtained in the treatment of nicotine yield is 3.14 %, the smallest yield .

Seen that the addition of ether over time effect on the efficiency of extraction of nicotine . So it can be said the volume of solvent effect on nicotine yield results . According to Darwis (2000) in the extraction of organic solvent percolation who missed the amount of solvent in the sample will affect the amount of organic compounds with solvent –borne.

So in general for the same solvent the amount of solvent that more will get more extractable compounds . Meanwhile, according to Susanto (2001) volume of solvent will affect the amount of the resulting extracts . The greater the volume of solvent to be used , the larger the extract to be obtained . Quadratic model was selected for nicotine yield response of leaf tobacco (*Nicotiana tabacum*) results

in the following equation :

$$Y_2 = 0,28934 + 0,095352\ X_1 + 0,049661\ X_2 + 0,000128\ X_1\ X_2 - 0,0007\ X_1{}^2 - 0,000444\ X_2{}^2$$

Description:
Exrtraction Y_2 = Yield (%)
X1   = Ether (ml)
X2   = Petroleum ether (ml)

Quadratic model for yield shows that there is a condition in which not happen again additional yield generated at a certain point. This is because there is no more nicotine that can be dissolved by the solvent at the time the rest of the extraction process. Based on the quadratic model equation for yield response can be seen that the coefficient of X_1 (0.095352) Bigger than the X_2 coefficient (0.049661). So it can be said that more ether factors influence the results of nicotine yield of tobacco leaves (*Nicotiana tabacum*). This value indicates that the model significantly affect the response because the probability value 0.0002 (0.002%) of the response variable yield.

Extraction time optimization and yield of the Central Composite Design
Optimization calculations performed with the limits established in accordance expected goals . The goal of this optimization is to optimize the effect of the limit and petroleum ether to ether extraction and extraction time on the extraction of nicotine tobacco leaves (*Nicotiana tabacum*) .

Determination of the lower limit and upper extraction time based on research results obtained , for the lowest value of the extraction time is defined as the lower limit , while for the highest value of extraction time is defined as the upper limit . Lower limit value for the extraction time was 458.17 seconds on the addition of 25 ml ether and 25 ml of petroleum ether , while the upper limit of the extraction time is 1122.41 seconds on the addition of 75 ml ether and 25 ml of petroleum ether to function minimization .

Determination of lower and upper bounds yield based on research results obtained , for the lowest yield value determined as the lower limit , while for the highest yield value is determined as the upper limit . Lower limit value for the yield was 3.14 % on the addition of 25 ml ether and 25 ml of petroleum ether , while the upper limit is 5.36 % on the addition of 75 ml ether and 25 ml of petroleum ether with maximizing function .

Value interest rate for the extraction time is 3 and the value of interest rate yield is 3 . Optimization in accordance with the limitations specified then the optimal solution obtained computational results as shown in Table 4.

Table 4. Computing Solution Results

No	Ether (ml)	PE (ml)	Extraction Time (second)	Yield (%)	Desirability	
1	59,46	30,12	682,483	4,80617	0,705	Selected

From Table 4 obtained an optimal solution which has a precision value (desirability) high. According to Montgomery (1991) desirability function is to determine the degree of accuracy of the optimal solution. The closer to one, the higher accuracy values. So it can be said to be the optimal solution value of desirability of this study by using Design-Expert 8.0.4 is equal to 0.705, in other words the level of optimal solution of 70.5% accuracy. Solution chosen computational results with most of the response condition in order to get value value addition of 59.46 ml of ether and petroleum ether 30.12 ml.

Desirability value can be more clearly seen in Figure 9 for the contour plot of the optimal solution. Optimal point obtained and seen the value of deviations that may occur. Results predicted optimal solution on the addition of ether and 59.46 ml 30.12 ml PE can be seen in Table 5.

Table 5. The Result Prediction Optimal Solutions (59.46 ml Ether Addition and Petroleum Ether 30.12 ml)

Response	Prediction	SE Pred	95% PI low	95% PI high
Extraction Time (second)	682,483	92,0677	477,343	887,623
Yield (%)	4,80617	0,2647	4,18025	5,4321

From Table 5 it can be seen that the lowest value possible standards for the extraction time was 477 343 seconds and the highest is 887 623 seconds. Then the lowest value possible standards for nicotine yield was 4.18025% and the highest is 5.4321%. The results obtained on the model of the extraction time on the treatment response of the addition of ether and petroleum ether 59.46 ml 30.12 ml reached a value of 682.48 seconds. As for the response to reach yield 4.80617 shown in Table 5
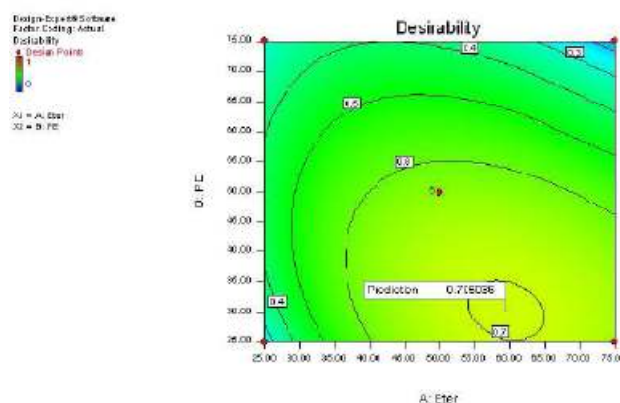
Figure 5. Plot Contour Relationship Type Solvent (Ether and Petroleum Ether) Against Prediction of Optimal Solutions

Validation results

Optimal solution using Design-Expert 8.0.4 software necessary to test the validation of the results of the extraction time and extraction nicotine tobacco leaves (*Nicotiana tabacum*). Results of the validation should be done to compare the results of computing solutions in Table 10 with the results of experiments on the best treatment. In Table 6 there is a comparison between the computational results with experimental results on the optimal treatment.

Table 6. Validation Test

Response	Computational Result			Validation Results
	Low Prediction	Prediction	High Prediction	
Extraction time (second)	477.343	682.483	887.623	702.96
Yield (%)	4.18025	4.80617	5.4321	4.83

Validation results in Table 6 indicate that the extraction time and yield results of experiments on the best treatment showed no significant differences in mathematical calculations. Time value extraction and validation yield results respectively 702.96 and 4.83. This value is not appreciably affect the computational results. Due to the predicted value for the extraction time between 477343-887623 and to yield between 4.18025 to 5.4321. So the validation results on the extraction of nicotine tobacco leaves (*Nicotiana tabacum*) with optimal treatment as feasible.

CONCLUSION

The addition of ether and petroleum ether solvent significantly affect the extraction and recovery time. Prediction results obtained optimal solution is the addition of 59.46 ml of ether and petroleum ether amounted to 30.12 ml. Lowest possible values for the extraction time was 477.343 seconds and the highest is 887.623 seconds. Then the lowest value possible standards for nicotine yield was 4.18025% and the highest is 5.4321%. While the results obtained on the model predictions of the response time of the addition of ether extract in the treatment of 59.46 ml and 30.12 ml petroleum ether reaches the value 682.483 sec, then to achieve the yield response of 4.80617%.

REFERENCES

Darwis, D. 2000. **Basic Laboratory Techniques In The Study Of Natural Material Compounds, Human Resource Development Workshop In The Field Of Organic Chemistry Biological Natural Ingredients**. State University of Andalas. Padang.

Guenther, E. , 1990. **Essential Oils**. Volume III. Jakarta: University of Indonesia

Jones, Nadia. M. 2001. **Comparison of Methods for Extraction of Tobacco Alkaloids**. Journal of AOAC International, Vol.84, No. 2 : 309-317. Lisbon. Portugal.

Karbalai, N.S., Ghotbi, and Yadollah, Y. 2009. **Experimental study and modeling of supercritical ekstraction of nikotin from tobacco leaves**. Iran Journal Chem Eng, Vol. 28, No. 4, 2009. I.R. Iran.

Ronald, E.M. , 2008. **Practical Aspects of Solvent Extraction**. http://chromatographyonline.findanalytichem.com/lcgc. accessed on December 26, 2010 at 7:50 pm.

Susanto, E. , 2001. **Effect Of Extraction Methods On Yield**. Warta IHP / J. Of Agro-based Industry. 18 (1-2): 32-36.

Wolff, Manfread. , 1994. **Principle - Principle of Medicinal Chemistry**. The fourth edition. Gajah Mada Press. Yogyakarta.

International Conference and Workshop on Chemical Engineering UNPAR 2013

Hydrolysis of Coconut Pulp Using *Aspergillus niger* and *Trichoderma reesei* to Produce Reducing Sugar and Bioethanol

Lucy Arianie [a*] , Riysan Octy Shalindry[a], Winda Rahmalia [a]

[a]*Department of Chemistry, Faculty of Mathematics and Natural Sciences, Universitas Tanjungpura,*
Jl. A. Yani 73 Pontianak 78124, Indonesia.
Email : lucy.arianie@gmail.com

Abstract
Reducing sugar production through hydrolysis of coconut pulp was carried out. This research aims to convert coconut pulp into bioethanol through enzimatic hydrolysis using combination of *Aspergillus niger* and *Trichoderma reesei*. Organosolv delignification method was firstly processed using methanol:aquadest = 1:1 (v/v), 25 g of coconut pulp and 6% natrium hydroxide as catalyst which produced 89 % of cellulose fiber. Ratio of *Aspergillus niger* and *Trichoderma reesei* is 2:1 (v/v) respectively. Research investigation showed that the best volume ratio was 80:40 (v/v) which produced 2075.5 ppm of reducing sugar. Fermentation by using *Saccharomyces cerevisiae* for 5 day created 1.03% ethanol.

Keywords: Aspergillus niger; Bioethanol; Coconut Pulp; Trichoderma reesei.

1. Introduction
Cellulose sources are commonly derived from forestry, agriculture and industrial wastes. West Kalimantan, Indonesia has coconut production almost 78 ton/Ha in 2010 [1]. Coconut pulp is waste of coconut which its coconut milk was taken and most people assumed it has no nutritional value. In fact, coconut pulp contains 46.68; 17.5 and 20.5% of cellulose, lignin and hemicelluloses respectively [2]. The high content of cellulose in coconut pulp is potentially converted into bioethanol. On the other hand, enzymatic hydrolysis of cellulose can be done using cellulase from *Aspergillus niger and Trichoderma reesei*. *Trichoderma reesei* is a mold that produce endoglucanase and exoglucanase highly except β-glucosidase. Furthermore, *Aspergillus niger* could produce lots of β-glucosidase [3]. The aim of this research is combine *Aspergillus niger* and *Trichoderma reesei* to produce reducing sugar and convert it into bioethanol by using coconut pulp as raw material.

2. Methods
2.1. Materials
This research was done in laboratory scale. The materials in this research were oven, dessicator, incubator, reflux equipment, fermentation equipment, *bulb*, pH-meter, coconut pulp from traditional market (Dahlia and Teratai market) in Pontianak West Kalimantan - Indonesia, aquadest, *Saccharomyces cerevisiae*, *Aspergillus niger, Trichoderma reesei*, HNO_3, HCl, H_2SO_4, NaOH, reagen for Somogyi – Nelson and PDA. All the procedures below was done triplo. Coconut pulp was dried under sunlight, milled and screened having particle size 40 mesh. Oven dried at 105 ^{0}C for 4 hours was done as preparation step.

2.2. Organosolv Delignification
Pulp organosolv was made by 50 g of coconut pulp in methanol:aquadest (1:1 v/v) and NaOH 6% as catalyst and heated in a reflux system at 100 ^{0}C for one hour. Ratio of coconut pulp and solvent is 1:10. The product obtained was filtered. Delignification process was determined gravimetrically by adding H_2SO_4 72% on the filtrate (which resulted from reflux process) until pH 2. Presipitated of lignin was then

---

washed by methanol and aquadest until neutral (pH 7) and oven dried on 60 ^{0}C for 24 hours [4-5]. Lignin was determined its functional group using Fourir Transform Infra Red. Coconut pulp delignificated was stored for next procedure.

2.3. Reproduction of Aspergillus niger and Trichoderma reesei

Aspergillus niger and *Trichoderma reesei* were reproduced using Potato Dextrose Agar and incubated at room temperature for one week.

2.4. Nutrient solution

Nutrient solution was made by adding $(NH_4)_2SO_4$ 0,35 g; KH_2PO_4 0,5 g; $MgSO_4.7H_2O$ 0,075g; $CaCl_2.H_2O$ 0,1 g; $FeSO_4.7H_2O$ 0,00125 g; $MnSO_4.H_2O$ 0,004 g; $ZnSO4.7H_2O$ 0,00035 g in 1 L aquadest and arranged in pH 3.

2.5. Production of Cellulase

Substrate that consist of 5 g of coconut pulp and 25 mL of sterilized nutrient solution pH 3 were added by one block of *Trichoderma reesei* dan *Aspergillus niger* (approximately size is 2 cm^2, aged 7 days. This compound was incubated for 7 days at 50 ^{0}C for *Aspergillus niger* and 60 ^{0}C for *Trichoderma reesei* [6].

2.6. Extraction and Activity Assay of Cellulase

Aquadest which conceive 0.1% of Tween 80 was added to incubated coconut pulp, shaked on 175 rpm for 2 hours at room temperature. The mixture obtain was then centrifugated on 3.000 rpm for 15 minutes. Supernatant was stored at 4 ^{0}C and will be used as crude enzyme extract [6-7]. Enzyme activity was determined using spectroscopy at maximum wavelength in equation as follows [8]:

$$Enzime\ Activity\left(\frac{U}{mL}\right) = \frac{G\ x\ Fp}{\tau} \tag{1}$$

G = Glucose concentration (µg/mL)
Fp = Dilution factor
T = Incubation time (minute).

2.7. Hydrolysis of Coconut Pulp

Delignificated of coconut pulp was added by cellulase's *Aspergillus niger* and *Trichoderma reesei*. Ratio of cellulase from *Aspergillus niger* and *Trichoderma reesei* were 2:1 consecutively [7]. Variation of each enzyme volume as follows: 10:5, 20:10, 30:15, 40:20, 50:25, 60:30, 70:35, 80:40, 90:45, and 100:50 (mL). Aquadest was added to this mixture until 150 mL accurately then heated slowly until reach 40 ^{0}C. This mixture was arranged at pH 5, 160 rpm for 7 hours. Glucose concentrations were evaluated by Somogyi-Nelson method.

2.8. Fermentation, Determination of Glucose and Ethanol Concentration

Sterilized hydrolysate pH 5 was added by incubated inoculum in ratio 90: 10 mL and one ose of *Saccharomyces cerevisiae*. Incubation was done on 125 rpm for 7 days [9]. Glucose concentration was observed each 24 hours using Somogyi-Nelson method at wavelength 695 nm. Fermentation product was separated by using destilation process on 76-80 ^{0}C and ethanol which resulted was analyzed using gas chromatography .

3. Result and Discussion

3.1. Delignification Process and Infra Red Spectrum

Preparation of coconut pulp purposes to hinder of decay, reduce moisture content and extends sample surface. Minimizing of sample size is similar to extend coconut pulp surfaces therefore open up probability of intern contact and causing disconnection of polymer chain [10].

Organosolv pulping aims to separate the soluble lignin and cellulose residue pulp. Organosolv pulping is a well-known environmently process, free-sulphur and solvent recovery is can be done. Acid delignification using H_2SO_4 72% caused ether protonation in Cα of benzyl. Lignin solubility was affected by pH of mixture. At low pH, hydroxyl phenolic will be protonated, condensed and finally precipitated in polar solvent [11-12].
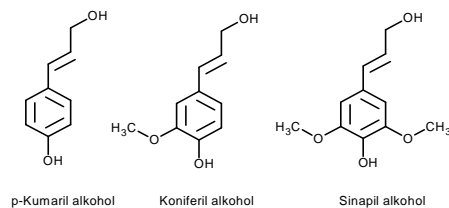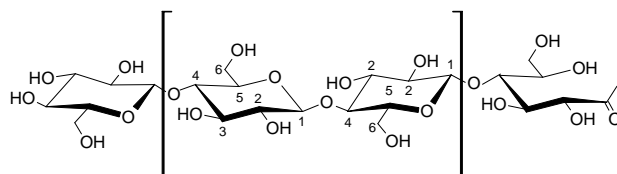

p-Kumaril alkohol   Koniferil alkohol   Sinapil alkohol

Fig 1. Lignin monomer

Fig 2. Cellulose chain

R = H, aril atau alkil   Ion benzilium   Ion oksonium
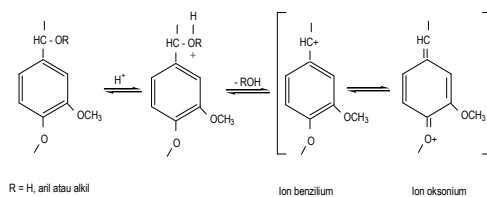
Fig 3. Benzylium and oxonium ions which resulted by adding of sulfuric acid to lignin filtrate that contains ether phenolic

R = H, aril atau alkil   Ion benzilium   Ion oksonium
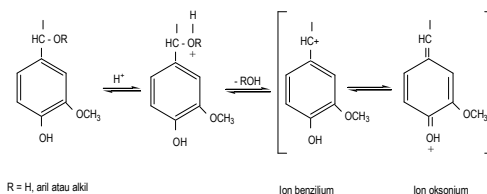
Fig 4. Benzylium dan oxonium ions which resulted by adding sulfuric acid that contains phenol ic groups.

In isolation process, condensation of benzylium ions could be done. This nucleophile reacted with lignin at C1 and C6 (or C5) from phenylpropanoid units and finally produced lignin sediment. The illustration was described as follows [11-12].
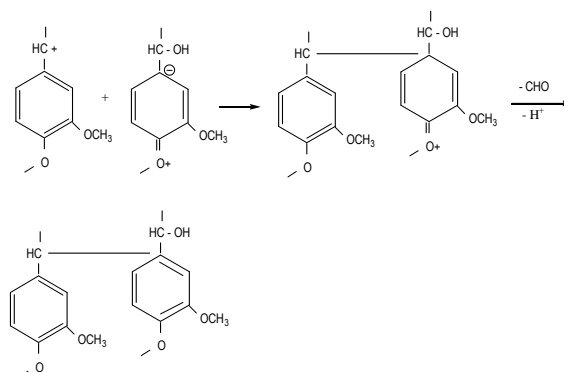
Fig 5. Condensation of benzylium ion with weak nucleophile at C1
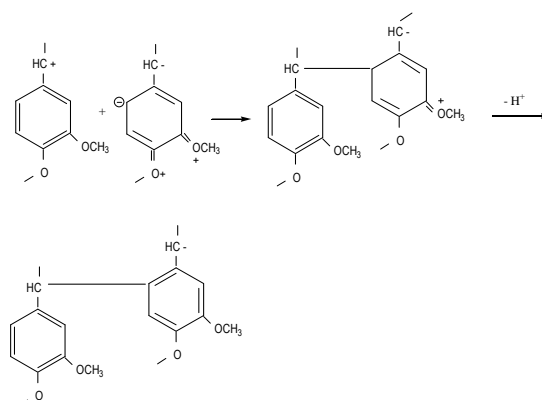
Fig 6. Condensation of benzylium ion with weak nucleophile at C6

Soluble lignin is clearly indicated in filtrate signed with forms of black liquor. Delignification process also signified by mass sample reducing from 25.0035 g to 22.2033 g. Spectrum of lignin isolate was displayed on Fig. 7.
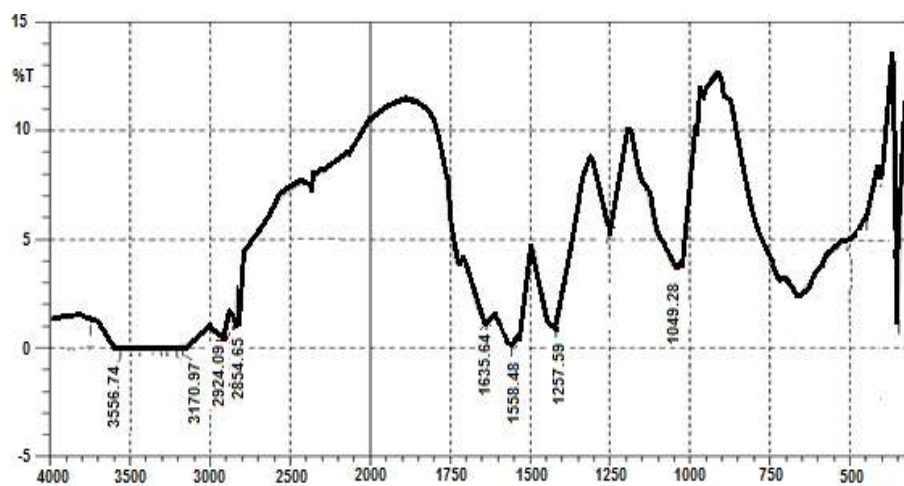
Fig 7. Infra Red Spectrum of Lignin

Table 1. Comparison of lignin isolate and lignin standard

Interpretation of functional group	Wavenumber of lignin (cm⁻¹)	
	Isolate	Standard [13]
Str. OH	3556.74 - 3170.97	-
Str Asym –CH_3	2924.09	-
Str. Asym –CH_2	2854.65	-
C=O in aryl keton conjugated	1635.64	1675 – 1655
Aromatic vibration	1635.64	1593 - 1605
Str. Sym C=O that showed G ring	1558.48	1266 – 1270
C-H aromatic in deformation G>S and showed C-O form	1257.59	1030 – 1035

Catalyst which used for organosolv delignification is comprise of acid organosolv that usually used H_2SO_4 and base organosolv such as NaOH. Base organosolv process frequently used for increasing lignin hydrophilicity and to ease lignin solubility [14].
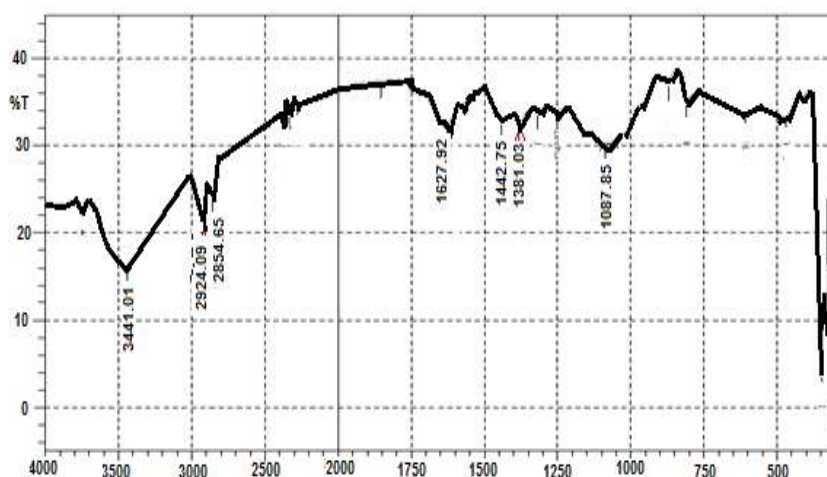
Fig 8. Infra Red Spectrum of Cellulose

Table 2. Comparison of cellulose isolate and cellulose standard

Interpretation of functional group	Wavenumber of cellulose (cm⁻¹)	
	Isolate	Standard [15]
OH	3441.01	3400
Str Asym –CH_2	2854.65	2900
H-O-H	1627.92	1640
C-O-H	1442.75	1420
C-O-C	1381.03	1370
C-O from β-1,4 glycosidic	1087.85	1087.60

Infra red spectrum of cellulose illustrate OH absorbance on wavenumber 3441.01 cm⁻¹, CH_2 atom on 2854.65 cm⁻¹, and H-O-H bond on 1627.92 cm⁻¹, C-O-H bond on 1442.75 cm⁻¹ and C-O-C bond on 1381.03 cm⁻¹. Specific character appears on 1087.85 cm⁻¹ shows C-O bond of β-1,4 glycosidic of cellulose.

3.2. Enzymatic Hydrolysis

Cellulase derived from *Aspergillus niger* has activity 0.345 UI and cellulase of Trichoderma reesei 0.388 UI. Cellulase is combination of endoglucanase, exoglucanase and β-glucosidase. Endoglucanase function is break cellulose randomly and forms the end chain free. Exoglucanase is continuing endoglucanase process that attack end chain free and release cellubiose from cellulose chain[16-17]. Moreover, β-glucosidase will hydrolyse cellubiose into glucose. Ilustration of this breaking chain is displayed on Fig 9. Glucose was then analyzed using Somogyi-Nelson method at wavelength 695 nm [18].
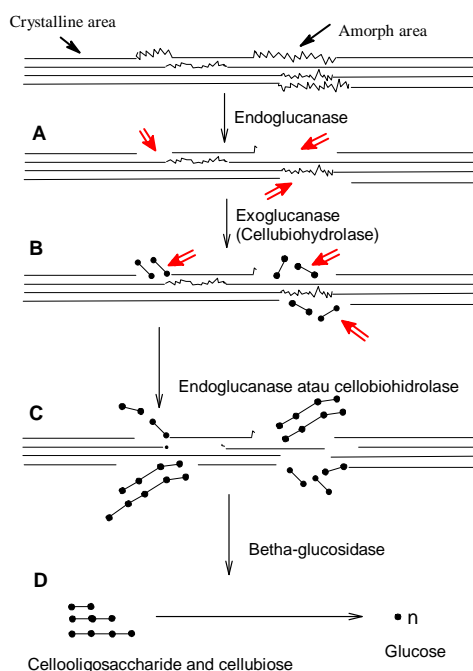
Fig 9. Scheme of enzymatic hydrolysis (modified from Enari) [19]

Glucose was analyzed by using Somogyi-Nelson method at wavelength 695 nm [18]. The highest glucose concentration was reached on cellulase of *Aspergillus niger's* volume is 80 mL and *Trichoderma reesei's* volume is 40 mL. Figure 10 showed that higher volume added, higher glucose concentration until optimum condition. After optimum state, there is no increasing of glucose concentration. It could be done because all of the substrate has been bounded with active site enzyme that causing substrate was saturated. Variation of each enzyme volume as follows: 10:5, 20:10, 30:15, 40:20, 50:25, 60:30, 70:35, 80:40, 90:45, and 100:50 (mL).
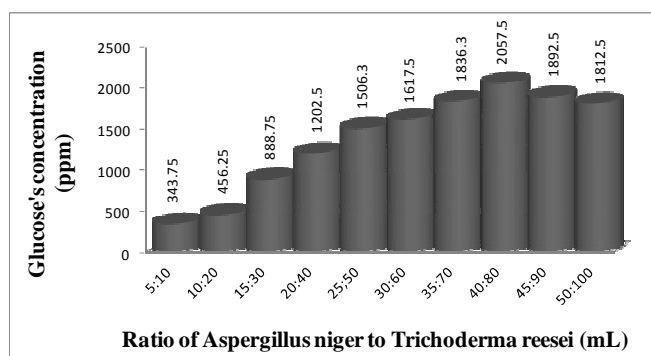
Fig 10. Glucose consentration in variation of enzyme volume composition

3.3. Fermentation

Fermentation was done at optimum hydrolysis condition which glucose was reached i.e. *Aspergillus niger* 80 mL dan *Trichoderma reesei* 40 mL. Hydrolysis was repeated on this optimum condition. Afterward, hydrolisate pH 5 added by *Saccharomyces cerevisiae* and anaerob incubation was done for 7 days, glucose concentration investigated every 24 hours. Analyzing of residual glucose aims to investigated glucose usage by *Saccharomyces cerevisiae*. In general, reducing of glucose concentration directly proportional with time of fermentation. Figure 11 shows glucose concentration on first until seventh day respectively are 1996.25 ppm; 1827.5 ppm; 1645 ppm; 1396.25 ppm; 982.5 ppm; 861.25 ppm and 813.75 ppm. Decreasing of glucose is comparable with fermentation time. It is evidence of glucose usage by *Saccharomyces cerevisiae.*
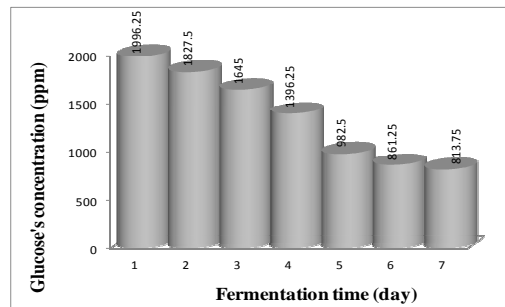
Fig 11. Decreasing of glucose concentration toward fermentation time

Figure 12 displays the lag phase or adaptation phase occurred on first day. In this phase, *Saccharomyces cerevisiae* is still in acclimatization phase for environment that cause its activity is not optimum yet. In this stage cell mass increase slowly. On the fourth until fifth day, exponential phase occurred, cell multiplication happens. Variation of microorganism growth is depend on genetic factor [20]. In exponential phase occurs maximum growth which can be seen on fifth day, there is maximum reduction of glucose. On sixth and seventh day occurs stationer phase i.e *Saccharomyces cerevisiae* was not optimally worked, amount of dead and live cell is relatively same. Furthermore, mortality phase was happened.
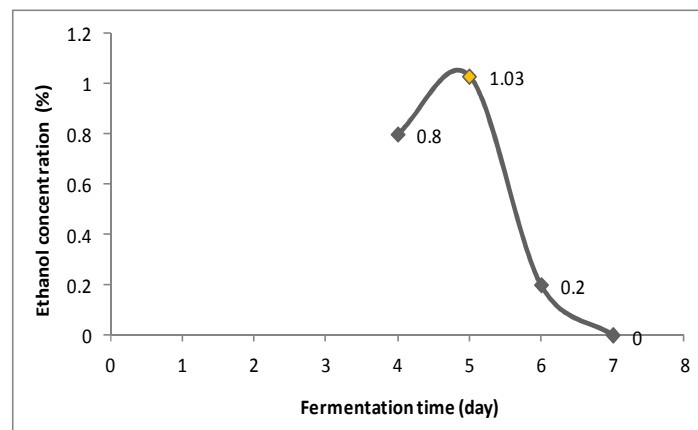
Fig 12. Influences of ethanol concentration toward fermentation time

Etanol concentration which fermented at fourth to seventh days were evaluated by Gas Chromatography. Its all because glucose decreasing was occured at fifth day fermentation and the point of view will focused on these day observation. Ethanol concentration at fourth, fifth, sixth and seventh day fermentation consecutively are 0.8 %; 1.03%; 0.2 % dan 0%. Optimum ethanol concentration gained on fifth day fermentation which destilate volume was 5 mL and 5 g of coconut pulp as raw material.

The small of ethanol concentration caused by imperfect hydrolysis, all cellulose didn't convert to glucose and ethanol. Declining of ethanol concentration after fifth day fermentation is caused by decreasing of glucose and nutrient concentration. Its impact for invertase which convert glucose into ethanol, then *Saccharomyces cerevisiae* enter to mortality phase.

Chromatogram of gas chromatography displays three component such as ethyl acetate, ethanol and propanol. Ethyl acetate was resulted from side reaction of ethanol and acetic acid which has boiling temperature 77 ^{0}C near ethanol boiling point (78 ^{0}C). Anaerob fermentation commonly produce small energy, carbondioxide, water and other organic metabolite namely acetic acids and ethanol [21]. The reaction shown on Fig 13 and all the chromatograms demonstrated on Fig 14 until Fig 17.
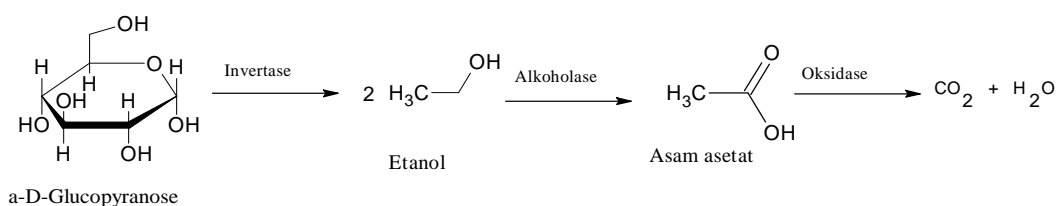
Fig 13. Reaction in fermentation process (Modified from Hasanah [22])
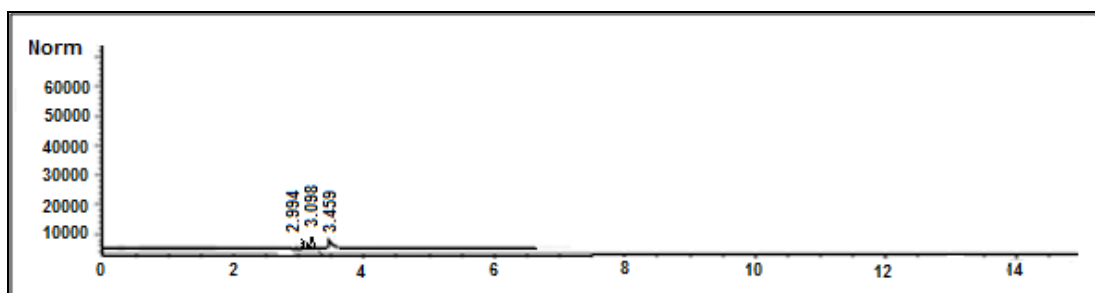
Fig 14. Chromatogram of gas chromatography at fourth day
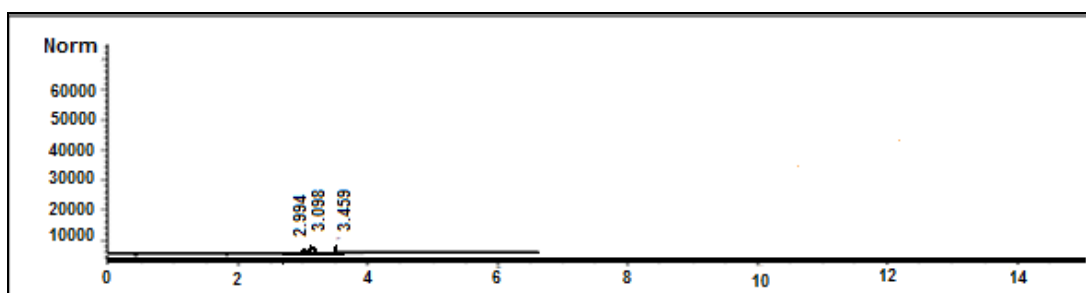
Fig 15. Chromatogram of gas chromatography at fifth day
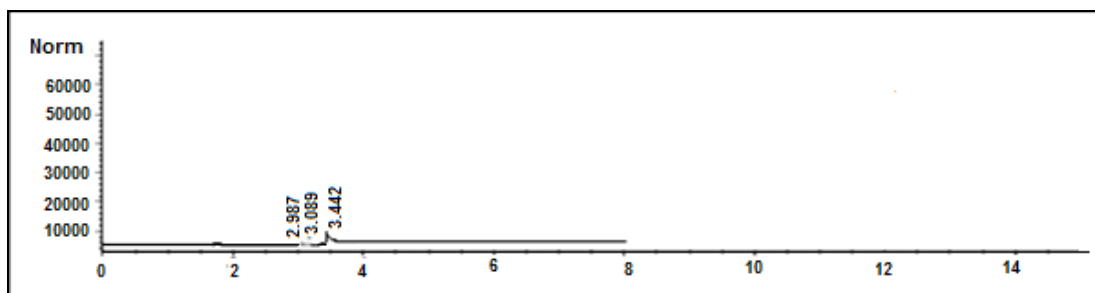
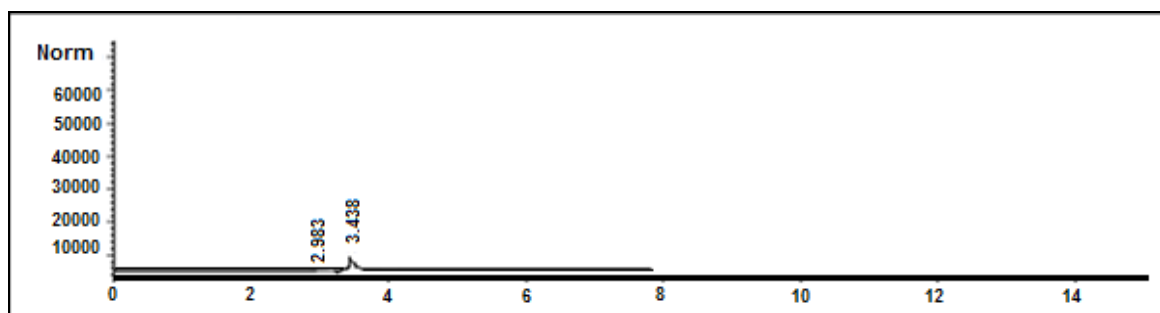**Fig 16.** Chromatogram of gas chromatography at sixth day

Fig 17. Chromatogram of gas chromatography at seventh day

4. Conclusion

- Glucose concentration resulted from enzymatic hydrolysis of coconut pulp is 2057.5 ppm and optimum ratio of cellulase from *Aspergillus niger* and *Trichoderma reesei* is 80:40 mL.
- Maximum ethanol concentration was 1.03% which obtained in fermentation at five day.

Acknowledgements

References

[1] Badan Pusat Statistik: Katalog Badan Pusat Statistik, Kalimantan Barat, 2010.

[2] Datta, R., 1981. Acidogenic Fermentation of Lignocellulose-acid Yield and Conversion of Components. Biotechnology and Bioengineering   23 (9), p. 2167-2170.

[3] Martins, L.F., Kolling D., Camassola, M., Dillon A.J.P. and Ramos L.P., 2008. Comparison of *Penicillium echinulatum* and *Trichoderma reesei* Cellulase in Relation of Their Activity Againts Various Cellulosic Substrates, Bioresource Technology 99, p. 1417-1424.

[4] Heradewi, 2007. Isolasi Lignin dari Lindi Hitam Proses Pemasakan *Organosolv* Serat Tandan Kosong Kelapa Sawit, Skripsi, Institut Pertanian Bogor, Fakultas Teknologi Pertanian, Bogor.

[5] Herfiyanti, 2012. Pembuatan Bioetanol dari Tandan Kosong Sawit melalui Delignifikasi Organosolv, *Skripsi,* Universitas Tanjungpura, Fakultas Matematika dan Ilmu Pengetahuan Alam, Pontianak.

[6] Sanjaya, W. Dan Adrianti, S., 2010, Optimasi Hidrolisis Jerami Padi Menjadi Glukosa untuk Bahan Baku Biofuel Menggunakan Selulase dari *Trichoderma reesei* dan *Aspergillus niger*, Skripsi, Institut Teknologi Sepuluh Nopember, Surabaya.

[7] Anwar, N., Widjaja, A., Winardi, S., 2010. Peningkatan Unjuk Kerja Hidrolisis Enzimatik Jerami padi Menggunakan Campuran Selulase   Kasar dari *Trichoderma reesei* dan *Aspergillus niger*, Makara Sains, 14(2), p 113-116.

[8] Kamila, L., 2003. Pencirian Selulolitik Isolat Khamir Rhodotorula sp. dari Tanah Hutan Taman Nasional Gunung Halimun, Skripsi, Institut Pertanian Bogor, Fakultas Matematika dan Ilmu Pengetahuan Alam, Bogor.

[9] Samsuri, M., Gozan, M., Hermansyah, H., Mardias, R. M., Nasikin, M., Presetya, B., dan Wijanarki, A., 2007. Pemanfaatan Selulosa Bagas untuk Produksi Bioetanol Melalui Sakarifikasi dan Fermentasi Serentak dengan Enzim Xylanase, Makara Teknologi, 11(1), p.17-24.

[10] Sun, R. J., Fang, J., and Bolton, J., 1999. Physicochemical and Structural Characterization Of Alkali Soluble Lignins From Oil Palm Trunk and Empty Fruit bunch fiber, J. Arg food chem. 47 p. 2930-2936

[11] Arianie, L., 2002. *Studi Pemanfaatan Lignin dan Lignosulfonat Sebagai Aditif pada Perekat Fenol Formaldehid,* Tesis Magister, ITB Bandung.

[12] Syahmani, 2001. Isolasi, Sulfonasi dan Asetilasi Lignin dari TKS dan Studi Pengaruhnya Terhadap Proses Pelarutan Urea, Tesis Magister, ITB Bandung.

[13] Pan, X-J. and Sano, Y., 1999. Atmospheric Acetic Acid Pulping of Rice Straw IV : Physico-Chemichal Characterization of Acetic Acid Lignins from Rice Straw and Woods, *Holzforschung*, 53.

[14] Achmadi, S.S.,1990, Kimia Kayu, Departemen Pendidikan dan Kebudayaan, Direktorat Pendidikan Tinggi Pusat Antar Universitas Bioteknologi, Institut Pertanian Bogor, Bogor.

[15] Wisastra, R. and Santoso, M., 2009. "Abedo Markisa Konyal Sebagai Bahan Baku Pembuatan Kertas dengan Metoda *Organosolv,*" Prosiding Seminar Kimia Bersama UKM-ITB VIII.

[16] Hermiati, E., Mangunwidjaja, D., Sunarti, T.L., Suparno, O., and Prasetya, B., 2010. Pemanfaatan Biomassa Lignoselulosa Ampas Tebu untuk Produksi Bioetanol, J. Litbang Pertanian, 24(2), p. 121-130.

[17] Resita, E.T., 2006. Produksi Selo-Oligosakarida dari Fraksi Selulosa Tongkol Jagung Oleh Selulase *Trichoderma viride*, Skripsi, Institut Pertanian Bogor, Fakultas Teknologi Pertanian, Bogor.

[18] AOAC, 1990. Official Methods of Analisis, Association of Official Analitycal, Penerbit UGM, Yogyakarta.

[19] Enari, T.M., 1983. Microbial Cellulase, Microbial Enzyme and Biotechnology. Applied Science Publisher. New York.

[20] Ruso S., Ahmad A., and Nafie N.L., 2010. Pembuatan Bioetanol dari Batang Rumput Gajah (*Pennisetum purpureum Schumach*) dengan Sistem Fermentasi Simultan Menggunakan Bakteri *Clostridium acetobutylicum,* J. Teknologi, 13(2).

[21] Buckle, K. A., Edwards, R.A., Fleet, G.H., and Wooton, M., 1985. Ilmu Pangan, UI-Press, Jakarta.

[22] Hasanah, H., 2008. Pengaruh Lama Fermentasi Terhadap Kadar Alkohol Tape Ketan Hitam (*Oryza sativa L var forma glutinosa*) dan Tape Singkong (*Manihot utilissima Pohl*), Skripsi, Universitas Islam Negeri malang, Fakultas Sains dan Teknologi, Malang.

International Conference and Workshop on Chemical Engineering UNPAR 2013

Synthesis of Biodiesel from Crude Palm Oil and Rubber Seed Oil-Crude Palm Oil Blend

Siti Shafriena Mohd Afandi[a], Yoshimitsu Uemura[a, *], Suzana Yusup[b], Noridah Osman[a]

[a]*Centre of Biofuel and Biochemical Research, Universiti Teknologi Petronas, Tronoh Perak, Malaysia*
[b]*Department of Chemical Engineering, Universiti Teknologi Petronas, Tronoh Perak, Malaysia*

Abstract

Crude palm oil (CPO) is the main feedstock for biodiesel production in Malaysia due to high production of palm oil. However, the poor cold flow characteristics of crude palm oil have been the drawback of CPO to use in the lower temperature region. The blend with non-edible rubber seed oil (RSO) was found to improve the cold flow characteristics by reducing the concentration of saturated fatty acids in the feedstock, thus increase the fatty acid methyl ester (FAME) yield. The aim of this paper is to study the transesterification of crude palm oil and the effect of the varying ratio of CPO and RSO pre-blend mixture to the fatty acid methyl ester (FAME) yield. Transesterification of crude palm with methanol and potassium hydroxide (KOH) catalyst was conducted in batch reactor with the highest FAME yield achieved was 98%. The effect of varying ratio RSO and CPO blend was conducted from the optimum condition of previous experiment. Pre-blend is to blend the oil at the beginning of the process with varying ratio of 10 and 30 vol % of RSO to CPO. The mixture was first undergoing fixed operating condition of esterification and transesterification. Esterification is a pretreatment process to reduce free fatty acid (FFA) by reacting with methanol and sulfuric acid as a catalyst. The FAME yield was studied in this paper to find its optimum condition. The FAME yield and FAME content were measured using the high performance liquid chromatography and gas chromatography according to the European standard.

Keywords: Crude palm oil, biodiesel, cold flow characteristics, rubber seed oil, fatty acid methyl ester, free fatty acid, potassium hydroxide.

1. Introduction

Throughout the world, 95% of biodiesel is produced from edible vegetable oils, such as soybean, rapeseed, sunflower oils and palm oil. Those edible oils are easily available on a large scale from the agricultural industry [1]. Palm oil is forecast to be the suitable feedstock for biodiesel production in Malaysia due to its abundance.

Malaysia is the world's second largest producer of palm oil after Indonesia which is 5 million hectares of plantations in 2011, accounting for 87 % of the global net exports of oils and fats. Palm oil is the main agricultural crop in Malaysia, however occupies only 15% of Malaysia's land. Palm oil is the only oil that is certified as sustainably produced by the Food and Agriculture Authority (FAO) and cheaper compared to any other vegetable oils used in biodiesel production. A perennial crop with an economic cycle of 25 years, oil palm is less susceptible to changes in weather patterns [2].

Malaysian government had shown interest in biodiesel commercialization. Since 2010, the industry has been identified as one of the 12 National Key Economic Areas (NKEA) under the Economic Transformation Program. One focus under NKEA is to increase crude palm oil production to 6 MT/ha/yr. Another focus is on value added downstream activities like processed foods, oleo derivatives and biodiesel [3]. This situation had encouraged researchers to optimize the main process of converting crude palm oil to biodiesel which is transesterification.

A chemically reversible reaction called transesterification or alcoholysishas been widely used to reduce the high viscosity of triglycerides in the oil [4]. In this reaction, vegetable oil reacts with an alcohol such as ethanol or methanol in the presence of a catalyst, such as sodium or potassium hydroxide [5]. The products of this reaction are fatty acid methyl esters (biodiesel) and glycerol.

---

* Corresponding author.
*E-mail address:*yoshimitsu_uemura@petronas.com.my

Glycerol has commercial value as it can be used to form soap. The properties of resulting biodiesel are quite similar to those of conventional diesel fuel.

However, too much dependent on edible oil may cause a negative impact on the world, such as depletion of food supply and finally leading to economic imbalance. This is because the competition between biodiesel production and food supply will occur. The solution to this is that finding non-edible oil as an alternative. The example of non edible oil for producing biodiesel are jatropha, rubber seed, castor (Ricinuscommunis L.), sea mango (Cerberaodollam or Cerberamanghas), and Pongamiapinnata (abbreviated hereafter as P. pinnata) [6]. In addition to that, using non-edible oil which is much cheaper than edible oil would reduce the production cost as feedstock is the main contribution [7].

The non-edible vegetable oil such as rubber seed oil is preferable as a new biodiesel feedstock because of its high content of unsaturated fatty acid. According to the Association of Natural Rubber Producing Countries, Kuala Lumpur, Malaysia has an estimated acreage of 1.2 million hectares of rubber plantation in 2007 (Malaysian Rubber Board, 2009) which yield 1.2 million metric tons of rubber seeds annually. Rubber seed from rubber tree can produce 35% to 40% of oil yield. Rubber seed oil contains high unsaturated fatty acid which indicates good cold flow properties of biodiesel during cold weather. Instead of being thrown as waste, rubber seed can be extracted and converted into biodiesel. Rubber seed oil contains high FFA which may distract the transesterification process. This problem can be solved by an acid esterification process which reduced the FFA content in oil.

The objective of this study is to optimize the operating conditions of crude palm oil transesterification process by looking at the individual effect of methanol to oil ratio and catalyst concentration. The second aim is to synthesize biodiesel from 10% and 30% rubber seed oil blend in crude palm oil (by volume).

2. Methodology

2.1. Material

The crude palm oil used in this study was purchased at FELCRANasaruddin, Bota, Perak, Malaysia. The rubber seed oil used in this study was purchased from Kinetic Chemical SdnBhd which had been imported from Vietnam. Certified methanol of 99.8% purity was obtained from Merck Chemical, German. The potassium hydroxide (KOH) as a catalyst was supplied from R&M Chemicals.

2.2. Equipment

The experiment was conducted in a round bottom flask with three necks. The flask was immersed in a stainless steel water bath placed on the plate of magnetic stirrer. The reactor was connected with a reflux condenser. A thermocouple which was connected to the magnetic stirrer was used to detect and control the temperature in the round bottom flask with the set temperature.

2.3. Esterification Procedures

The esterification reaction was conducted in a laboratory-scale experimental setup. Esterification was only conducted for blended oil due to high FFA in the rubber seed oil. The experiment was started by weighing the oil in a three neck round bottom flask. The flask was immersed in a water bath with temperature $60^{o}C$. Meanwhile, 15:1 methanol to oil molar ratio and 3 wt% sulphuric acid as catalyst were prepared.

The mixture was heated to a temperature of $60^{o}C$ for 1 hour with mixing speeds of 400rpm. Later, 25g of $50^{o}C$ distilled water and 25g n-hexane were prepared. After 1 hour reaction time, distilled water and n-hexane were poured into the flask alternately until finish. Finally, the mixture was poured into separating funnels and leave for 24 hours.After 24 hours, the bottom layer (glycerol) was removed and the upper layer left were collected for transesterification step.

2.4. Transesterification Procedures

The experiment was started by weighing the oil in a three neck round bottom flask. The flask was immersed in a water bath with temperature 60°C. Meanwhile, methanol and potassium hydroxide as catalyst were prepared and stirred together to form a potassium methoxide solution. As soon as the potassium methoxide solution was poured, the reaction time started. The mixture was heated to a temperature of 60°C for 1 hour with mixing speeds of 400rpm. Later, 25g of 50°C distilled water and 25g n-hexane were prepared. After 1 hour reaction time, distilled water and n-hexane were poured into the flask alternately until finish to enhance clear separation between glycerol and FAME. Finally, the mixture was poured into separating funnels and leave for 24 hours. After 24 hours, the bottom layer (glycerol) was removed and the upper layer left were taken for analysis.
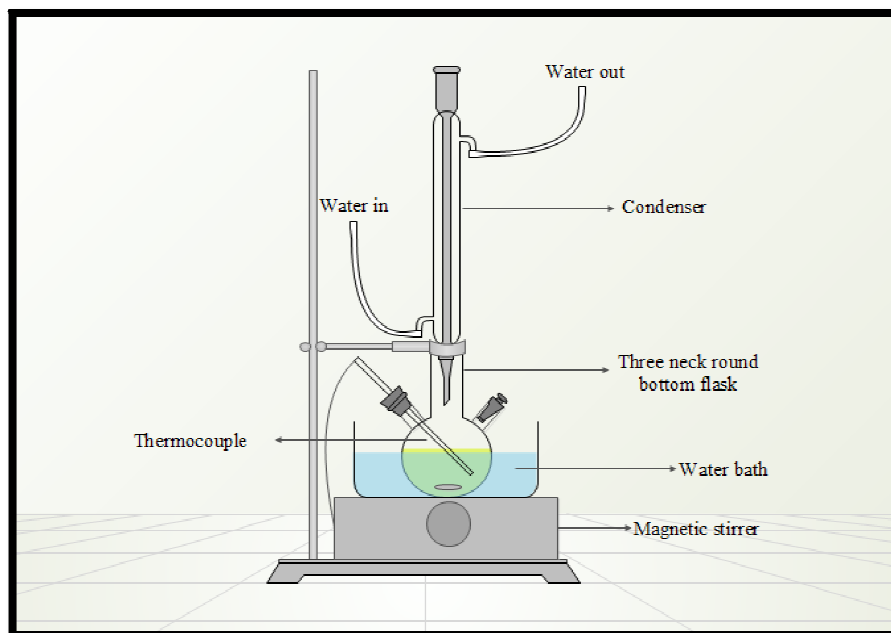
Fig. 1. Experimental setup for esterification and transesterification

3. Analytical Method

3.1. FAME yield

The FAME yield of the product was measured using high performance liquid chromatography (HPLC) from Shimadzu Japan, equipped with a silica gel column (Shim-pack CLC-SIL). 100 μL of biodiesel was diluted in 3mL of hexane and wasinjected into the HPLC column. The mobile phase was n-haxane/2-propanol = 99.5/0.5 (v/v). The FAMEyield was calculated as follows;

FAME yield = ...(Equation 1)

Where,

       , is the density of methyl oleate,

       , is the density of CPO,

        is the molecular weight of CPO,

        , is the molecular weight of methyl oleate,

     , is the area of FAME

   Y, is the area of methyl oleate

3.2. FAME content

The FAME content or purity of the product was measured using gas chromatograph (GC) model GC-2010 from Shimadzu, Japan. The GC was equipped with aflame ionization detector (FID) with capillary column BPX 70. According to EN 14103, 10 mg/ml methyl heptadecanoante solution was prepared by diluting with heptane. Approximately 250mg of theproduct was weighed and put in a 10 ml vial. 5ml of methyl heptadecanoate solution was added using apipette. The FAME content, C was

calculated using thefollowing formula;

$$C = \frac{(\Sigma A) - AEI}{AEI} \times \frac{CEI \times VEI}{m} \times 100\%$$ ....(Equation 2)

where:

ΣA = total peak area from the FAME $C_{14:0}$ to $C_{24:1}$

AEI = peak area of methylheptadecanoate

CEI = concentration, in mg/mL, of the methylheptadecanoate solution

VEI = volume, in mL, of the methylheptadecanoate solution

m = mass, in mg, of the sample

4. Result and discussion

4.1. Characterization of crude palm oil

i. Physical Observation

The crude palm oil was observed to solidify at temperatures lower than room temperature due to the high melting point of saturated fatty acid found in the oil. It was heated to 60°C before experimental works begin.
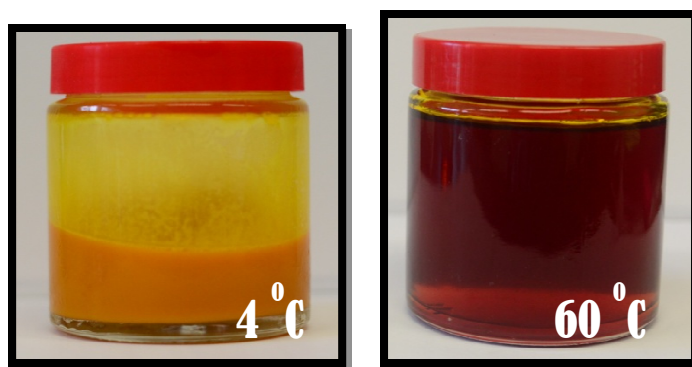
Fig. 2. Crude palm oil at 4°C and 60°C

ii. Physical properties

Table 1 shows the physical properties of crude palm used in this experiment with comparison from previous literature.

Table 1: Physical properties of crude palm oil

Feedstock	Crude palm oil	Literatures (24)
Source	Bought from palm oil mill,FELCRANasaruddin, Bota, Perak	-
Acid value (mgKOH/g)	10.02	-
FFA (wt%)	3.91	5.6
Water content (mg/L)	577.8	2200
Density @ 20°C (g/cm^{3})	0.9165	0.928
Viscosity [mPa.s]	24.4	-
Molecular weight (g/mol)	831.66	-

iii. Fatty acid composition

The fatty acid composition has been measured using GC-FID. Table 2 summarized the fatty acid composition of crude palm oil. Crude palm oil is composed of 50% of saturated fatty acids which imply several properties such as good oxidation stability and higher flash point. However due to lower concentration of unsaturated fatty acids or double bond in the triglycerides, crude palm oil gives poor cold flow properties, or higher cloud point and pour point.

Table 2: Fatty acid composition of crude palm oil

Type	Fatty acid	C:D	wt%	Literature (wt%) (24)
Saturated fatty acid (50.41%)	Lauric acid	12:0	0.25	0.16
	Myristic acid	14:0	0.98	0.99
	Palmitic acid	16:0	43.93	43.03
	Stearic acid	18:0	4.03	4.31
	Arachidic acid	20:0	0.34	-
	Behenic acid	22:0	0.06	-
	Lignoceric acid	24:0	0.82	-
Unsaturated fatty acid (49.59%)	Palmitoleic acid	16:1	0.15	0.19
	Oleic acid	18:1	40.07	39.47
	Linoleic acid	18:2	9.03	10.82
	Linolenic acid	18:3	0.26	0.29
	Erucic acid	22:1	0.08	-

4.2. Transesterification of crude palm oil

i. Methanol to oil ratio

Methanol to oil ratio is considered one of the most affecting factors in transesterification. Stoichiometrically, 3 moles of methanol are required for 1 mole of triglycerides to form 3 moles of fatty acid methyl ester (FAME). However, extra amount of methanol is required in order to shift the equilibrium to the FAME.

The effect of methanol to oil ratio to FAME yield was studied by varying from 4:1 to 8:1 mol ratio. The KOH concentration was fixed at 1.0 wt %, with a temperature of 60°C and reaction time 1 hour. The result in Fig. 3 shows that, the highest yield achieved is reported at 7:1 molar ratio which is 92 %. The decrease of FAME yield at 8:1 molar ratio could be attributed to the fact that excess methanol interferes with the separation of glycerol because of the increase in solubility. The excess methanol tended to blur the separation border between glycerin and biodiesel, making it difficult to extract the biodiesel.

It is reported that the transesterification is insufficient at the ratios of methanol/oil below 5:1 [8]. Bradshaw (9,10) stated that a 4.8:1 molar ratio of methanol to vegetable oil led to a 98% conversion. He noted that ratios greater than 5.25:1 interfered with gravity separation of the glycerol and added useless expense to the separation. In contrast, other investigators (11-13) obtained high ester conversions with a 6:1 molar ratio.
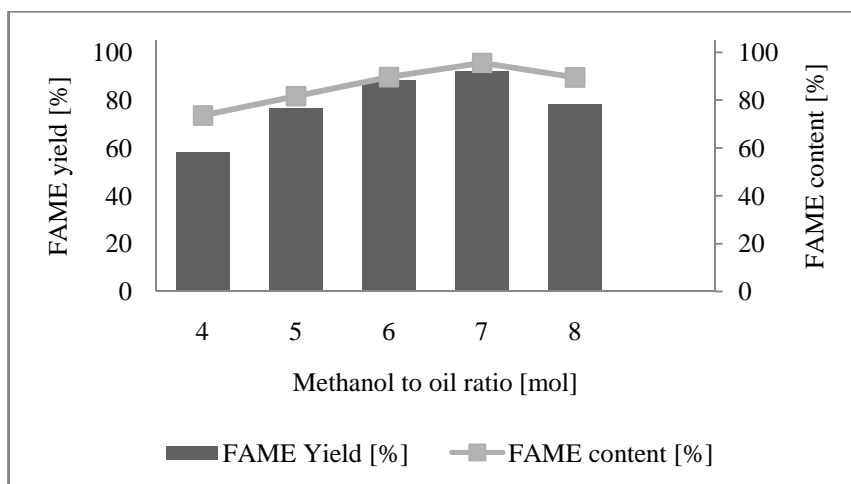
Fig. 3. Effect of methanol to oil ratio

As soon as methanol is added into the triglycerides, the two phase reaction mixture will composed of several components which are triglycerides, diglycerides, monoglycerides, FAME, free fatty acid, glycerol, methanol and potassium hydroxide. During the reaction, methanol and triglycerides will diffuse towards the reaction zone which is at the inter-phase of the two phase immiscible systems and the products which are FAME will diffuse away from the reaction zone. The acid-catalyzed esterification and transesterification reactions have two-step mechanisms that involve contact between the protonated FFA, DG, or TG molecules and MeOH.

The first step in the reaction mechanism involves protonation of the carbonyl group of the ester by the acid catalyst, forming a resonance stabilized complex, thereby converting it into a strong electrophile. The second step involves the reaction of the protonated species with the weak nucleophile, MeOH (14). It is the protonated FFA, DG, or TG molecules that need to interact with MeOH for a reaction to occur (14,15). The transesterification reaction between the protonated TG molecules and MeOH occurs at the MeOH-TG interface. (14,15) The FFA-H3O+ micelles and the TG molecules of the nonpolar-TG phase collide frequently during agitation, (15) and a proton species may contact and associate with a TG molecule at the FFA-H3O+ Mitchell-TG interface, forming a protonated TG molecule (15, 16)

ii. *Catalyst concentration*

The effect of catalyst concentration by weight percentage on the transesterification of crude palm oil was investigated with its amount varying from 0.6 to 1.8 wt%. The operating conditions during the whole reaction process were fixed at: reaction temperature of 60 °C, reaction time of 1 hour and molar ratio of methanol to oil at 8:1.

As shown in Fig. 4, the FAME yield and FAME content are proportional each other. From 0.6 to 1.0 wt% of catalyst, the FAME yield and FAME content is relatively small. This is due to insufficient amount of KOH resulted in incomplete conversion of triglycerides into FAME. As the catalyst was increased from 1.2 wt%, the reaction rate starts to accelerate and achieve 96% FAME content. The FAME content reached an optimal value when the KOH concentration reaches a certain level, and remains relatively constant with a further increase in the catalyst concentration [17].
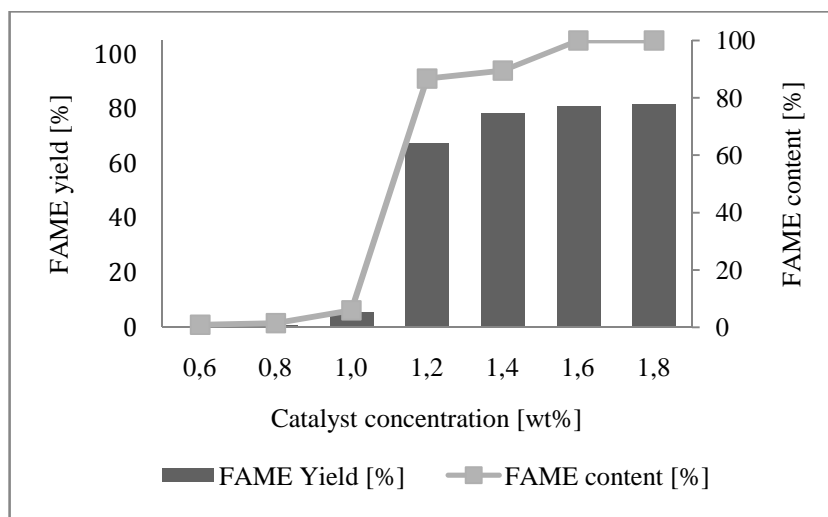
Fig. 4. Effect of catalyst concentration

Solid precipitate was observed in the biodiesel [for catalyst concentration 0.6, 0.8, 1.0 wt%] stored at room temperature. Solid precipitate is the unconverted triglycerides that still remain in the oil which have high melting point. The solid precipitate had lowered down the FAME yield.
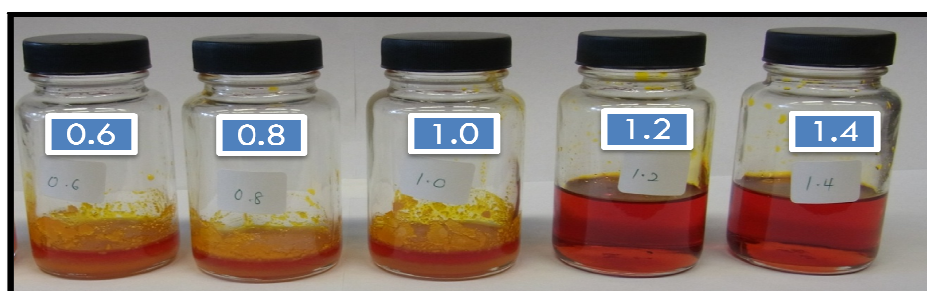

Fig. 5. Physical observation

4.3. Rubber seed oil blend with crude palm oil

The second part of this paper is to study the effect of RSO blend in the CPO on the FAME yield obtained. The experiment was conducted in two step esterification-transesterification experiment. The reaction parameters are fixed for both blends. For esterification 3 wt% of sulfuric acid as catalyst and 15:1 methanol to oil molar ratio with 1 hour reaction time and 60oC reaction temperature. The fixed parameter for transesterification was 7:1 methanol to oil molar ratio and 1.4 wt% potassium hydroxide as catalyst. The reaction time is 60 min at 60°C reaction temperature.

As we can observe from Fig. 6, adding RSO in the CPO is generally lowered down the FAME yield. The highest yield achieved was 81% FAME yield for 10% RSO blend, and 90% FAME yield for 30% RSO blend. This is due to soap formation from high free fatty acid in RSO.
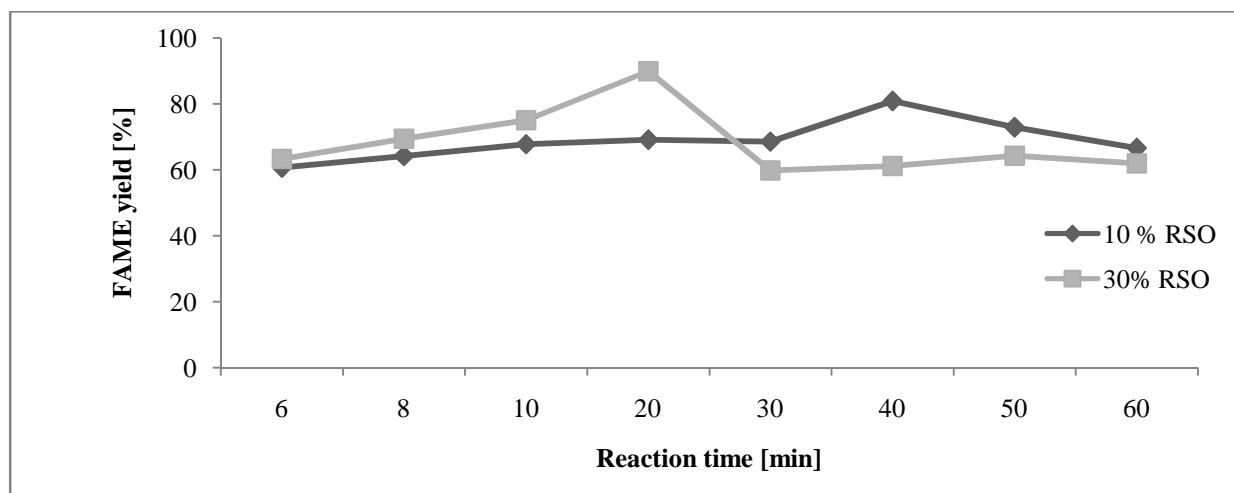
Fig. 6. FAME yield for 10% and 30% RSO blend in CPO

Several studies (18–20) have shown that the transmethylation reaction decelerates prematurely. Most of them concluded that this was due to the destruction of catalyst through soap formation. Feuge and Gros (21) said that for the transesterification of peanut oil using ethanol, more than 50% of the catalyst was destroyed in the first 15–20 min at 50°C. Boocock et al. (22) also found out that for base-catalyzed methanolysis of soybean oil (SBO) at 23°C, 67–83% of the catalyst was depleted.

Zhou and Boocock studied the phase behavior of two-phase base-catalyzed transesterification of TG (23). The results showed that the depletion of catalyst was largely due to its removal by the glycerol-rich phase, which has been separated at the separating stage.

5. Conclusion

The present studydeveloped transesterification process for crude palm oil to produce FAME. The process managed to achieve optimum 99% FAME yield at 60 min reaction time with 7:1 methanol to oil molar ratio and 1.4 wt% catalyst concentration. Crude palm oil with 4.0 % of free fatty acid is possible to undergo one step transesterification without pretreatment acid-esterification step. The blend of 10% and 30% rubber seed oil was found to decrease the FAME yield. More research should be done to improve the cold flow properties of the crude palm oil while maintaining the high biodiesel yield.

Acknowledgements

References

1. Lang X, Dalai AK, Bakhshi NN, Reany MJ, Hertz PB. Preparation and characterization of bio-diesels from various bio-oils.Bioresource Technology 2001;80:53–62
2. StrunkJr W, White EB. *The elements of style*.3rd Ed. New York: Macmillan; 1979.
3. J.H.Hashim. Palm oil as biofuel, the case of Malaysia.Presented at the IOM's Roundtable on Environmental Health Sciences, Research and Medicine: The Nexus of Biofuel Energy, Climate Change and Health, Washington DC. (2013)
4. Meher LC, VidyaSagar D, Naik SN. Technical aspects of biodiesel production by transesterification a review. Renewable and Sustainable Energy Reviews 2006; 10 (3): 248-6
5. Canakci, M. and J.VanGerpen. Biodiesel production via catalysis. Trans. ASAE Paper 42(1999):1203-1210
6. M.M. Gui, K.T. Lee, S. Bhatia. Feasibility of edible oil vs. non-edible oil vs. waste edible oil as biodiesel feedstock Energy 33 (2008), 1646– 1653
7. Pedro Felizardo, João Machado, Daniel Vergueiro, M. Joana N. Correia, João Pereira Gomes, JoãoMouraBordado, Study on the glycerolysis reaction of high free fatty acid oils for use as biodiesel feedstock. Fuel Processing Technology 92. 2011. 1225–1229

8. Md. EnamulHoque, Amrit Singh, Yong LengChuan, Biodiesel from low cost feedstocks: The effects of process parameters on the biodiesel yield, Biomasss and bioenergy 2011- 1582- 1587

9. Bradshaw, G.B., and W.C. Meuly, (1944) US Patent 2,360,844

10. Bradshaw, G.B., Soap Sanit. (1942).Chem. 18:23

11. Feuge, R.O., and T. Gros, (1949). JAOCS 26:97

12. Gauglitz, E.J., and L.W. Lehman, Ibid. (1963). 40:I97

13. Lehman, L.W., and E.J. Gauglitz, Ibid. *(1966).*43:383

14. McMurry, J. *Organic Chemistry,* 1996. *4th ed.; Brooks/Cole Pub. Co.:* New York,

15. Ataya, F.; Dubé, M. A.; Ternan, M. Acid-Catalyzed Transesterification of Canola Oil to Biodiesel fuel under Single and Two-Phase Reaction Conditions. *Energy Fuels **2007, 21, 2450.***

16. Fadi A, Marc.A.D, Marten. T. Variables affecting the induction period during acid catalyzed transesterification of canola oil to FAME. Energy & Fuel 2008, 22, 679-685.

17. D.Y.C. Leung, Y. Guo Transesterification of neat and used frying oil: Optimization for biodiesel production. Fuel Processing Technology (2006) 87: 883–89

18. Freedman, B., F. Pryde, and T.J. Mounts, Variables Affecting the Yields of Fatty Esters from Transesterified Vegetable Oils, J. Am. Oil Chem. Soc. (1984). 61 1638–1643

19. Freedman, B., R.O. Butterfield and E.H. Pryde, Transesterification Kinetics of Soybean Oil, Ibid. (1986) 63:1375–1380

20. Darnoko, D., and M. Cheryan, Kinetics of Palm Oil Transesterification in a Batch Reactor, Ibid. (2000) 77:1263–1267

21. Feuge, A.J., and A.T. Gros, Modification of Vegetable Oils. VII, Alkali Catalyzed Interesterification of Peanut Oil with Ethanol, Ibid. (1949).26:97–102

22. Boocock, D.G.B., S.K. Konar, V. Mao, C, Lee and S. Buligan, Fast Formation of High Purity Methyl Esters from Vegetable Oils, Ibid. (1998). 75:1167–1172

23. Zhou, W., and D.B.G. Boocock, Phase Behavior of the Base- Catalyzed Transesterification of Soybean Oil, Ibid. (2006). 83:xxx–xxx

24. Juan A. Melero∗, L. Fernando Bautista, Gabriel Morales, Jose Iglesias, Rebeca Sánchez-Vázquez, Biodiesel production from crude palm oil using sulfonic acid-modified mesostructured catalysts, (2010), Chemical Engineering Journal 161:323–331

International Conference and Workshop on Chemical Engineering UNPAR 2013

Biodiesel production from palm frying oil using sulphated zirconia catalyst in a bubble column reactor

Is Sulistyati Purwaningsih[a*], Joelianingsih[a], Wahyudin[a]

[a]*Chemical Engineering Department, Institut Technology of Indonesia, Jl. Raya Puspiptek Serpong, Tangerang Selatan 15320, Indonesia*

Abstract

Homogeneous catalysts are promising for the transesterification reaction of vegetable oil to produce biodiesel since this catalyst offer certain advantages such as high activity, easily reached reaction condition and less expensive; however homogeneous catalyst has some drawbacks such as high energy consumption, costly separation of catalyst from the reaction mixture and the purification of the product. The use of bubble column reactor (BCR) in producing biodiesel fuel without catalyst has been developed. In the BCR, the role of catalyst was replaced by high operating temperature, while the role of agitation was taken over by the formed vapor bubbles. The experimental result concluded that the higher the operating temperature, the higher the product conversion as well as the reaction yield, although it lowers the biodiesel's purity. Nowadays, heterogeneous catalysts have been more widely favoured over the homogeneous one since they are easily separated from reaction mixture and reused for many times. In this study, transesterification reaction of refined palm oil (palm frying oil) was conducted in a bubble column reactor using sulphated zirconia (SO_4/ZrO_2)as the solid heterogeneous catalyst. The experiment was carried out at 250 ^{o} C. At first, the influence of methanol flow rate towards vapor bubble formation was investigated, the experiments were then run catalytic and non-catalytically by varying the catalyst to reactant mass ratio. The experimental result showed at 5 mL/min of methanol flow rate, the amount of methanol vapor bubbles were continuously produced and uniformly distributed in the oil phase. This condition was then selected for the remaining study. It was noted that the highest yield of biodiesel product was achieved at 0.5 % (m/m) of catalyst concentration, meanwhile yield of product that run without catalyst was the lowest among all experimental results. However, at 1% (w/w) of catalyst to reactant mass ratio, the product phase was changed to solid.

Keywords: biodiesel; refined palm oil (palm frying oil); SO4/ZrO2 catalyst; bubble column reactor

_____

1. Introduction

The catalytic alcoholysis of vegetable oil use to produce biodiesel, is an important industrial process. Biodiesel is a promising fuel for substitution or blending with petroleum based diesel fuel, while these two kinds of fuel share similar physical and chemical properties[1]. Some of the first industrial processes to produce biodiesel used either strong base or strong acid homogeneous catalyst for transesterification reaction, such as potassium and sodium hydroxides, sulfuric, hydrochloric or sulphonic acids. The homogeneous catalyst offer certain advantages such as high activity, easily reached reaction condition (25-130°C at atmospheric pressure) and less expensive, but face variety of technical difficulties[1]. Homogeneous catalysts are normally carried out in batch-mode processing. Furthermore, a drawback of homogeneous base-catalyzed transesterification is that the oil that contain significant amounts of free fatty acids could not be convert into biodiesel completely and remained as soap in high quantity[2]. Separation of the product from the soap and spent waste catalyst appears to be technically challenging and brings additional cost to the product. It was reported that generally acid catalyzed reactions are performed at high alcohol to oil molar ratios, low to moderate temperatures and pressures, and high acid catalyst concentrations. Unfortunately, ester yields do not equally increase with molar ratio of reactans. Despite its insensitiveness to free fatty acids, acid-catalyzed trans-esterificataion is relatively slow reaction rate[3]. However, Saka and Kusdiana[4] revealed that producing biodiesel fuel from rapeseed oil which was prepared in super-critical methanol (at 350 ^{0}C and 200 Bar) had highly reduced reaction time. Unfortunately, such kind of reactor is not only high risk but also high capital and operating cost.

Yamazaki et al.[5] and Joelianingsih et al.[6,7]have studied the production of non catalytic biodiesel oil employed by Bubble ColumnReactor (BCR) at atmospheric condition. In the semi-batch system, Joelianingsih[7] had varied the temperature reaction in the range between 250 and 290 ^{0}C with flow rate of methanol vapor set at 4 g/min. Transesterification reaction of triglycerides (TG) to form methyl

* Corresponding author. Tel.: +628125714335; fax: +62217560542.
E-mail address: ispurwaningsih@iti.ac.id

139

ester (ME) in the BCR showed that this reactor acts as reactive distillation (RD); the reactor is not only as a reaction place, but also as a product separator as well. The RD concept works appropriately on equilibrium reaction such as in vegetable oil transesterification reaction, because straight and continuous separation of reaction product will drive the equilibrium to the product side and raise the conversion. According to Yamazaki et al.[5] and Joelianingsih et al.[6], in the BCR, the role of catalyst was replaced by high operating temperature, while the role of agitation was taken over by the formed vapor bubbles. Their experimental result concluded that the higher the operating temperature, the higher the product conversion as well as the reaction yields although it lowers the biodiesel's purity. It was also revealed that BCR that runs with high temperature condition will cause more monoglyceride (MG)formed as impurity in the product. According tothe Indonesian National Standard[8], the ME content in biodiesel should be less than 96.5% (m/m). Many studies have been reported that utilization solid or heterogeneous catalyst can be done to improve quality and conversion of biodiesel product[1].

Producing biodiesel oil incorporated heterogeneous catalyst has the potential to offer some relief to the biodiesel producers by improving their ability to process other cheaper feedstocks and to use a shortened and less expensive manufacturing process[1]. In addition, compared to the homogeneous one, this catalyst can be easily separated from reaction mixture and reused for many times. Moreover, using heterogeneous catalyst, biodiesel processing can be run continuously. Several solid acid catalysts have been reported to have the potential to replace strong liquid acid. These catalysts are zeolites, heteropoly acids, functionalized zirconia & silica, and some metals oxide[3]. Zeolites normally can be synthesized with extensive variation of acidic properties. However due to their uniform pore structure, the hydrophobicity of the catalyst is still in the stage of trial and error[3,9]. Previous study[10], reported that sulphated zirconia (SO_4-ZrO_2) has been utilized as a catalyst for transesterification vegetable oil to produce biodiesel. Study by Kiss[1] revealed that this catalyst was the most active catalyst for esterification. Petchmala et al.[11] reported that transesterification of palm oil with SO_4-ZrO_2 catalyst in super-critical methanol at 250^0C and within 10 minutes reaction, its conversion reached to 90 %.

Based on the above information, in this study, experiment was carried atmospherically in a set of BCR apparatus incorporated with SO_4-ZrO_2as a catalyst. Previous study [5] revealed that transesterification reaction carried out in the BCR, run non catalytically at atmospheric pressure and at 250 ^{o}C temperature , produced biodiesel oil with high purity (almost reach the standrad value), but its conversion was very low (55%). However , the superiority of BCR over other type of reactors is based on the capability act as RD proces. Even though the rate of the reaction is very slow, the product is directly separated from the reactans and produces higher purity of ME. In addition, reaction can be proceed continuously although with low capacity. It is expected by combining the BCR technology with the advantage of sulphated zirconia as the catalyst in transesterification of vegetable oil[11], will increase quality and productivity of the biodiesel.

2. Experimental methods

2.1 Materials

Palm Frying Oil (PFO, Bimoli brand) was purchased at Alfa-Mart grocery store. The fatty acids composition of palm frying oil was determined by gas chromatography (GC) equipped with a flame ionization detector and a cyanopropylmethyl silicone column (60 m × 0.25 mm internal diameter and film thickness of 0.25 μm). Thecarrier gas was helium at 1 mL.min-1. The oven temperature was initially held at 160 ^{o} C for 5 minutes then increased to 220 ^{o}C. This analysis was conducted at the Integrated Laboratory of Bogor Agricultural University. Methanol (MeOH) with 99.8 % purity (analytical grade) was produced by PT. Smart-Lab. Indonesia. Sulphated zirconia (SO_4-ZrO_2) catalyst.

2.2 Preparation of catalyst

Sulphated zirconia (SO_4-ZrO_2) catalyst was prepared by Center of Physics Research - The Indonesian Institute of Sciences, Puspiptek Serpong South Tangerang. As for catalyst preparation, 100 gram of $ZrOCl_2$ $8H_2O$ was disolved into 1000 mL of aquadest water. Ammonium hydroxide solution was added dropwise into well-stirred solution of $ZrOCl_2$ until pH reach to 9 at room temperature till ZrO_2 solid formed. The resulting precipitate was removed by filtration and then washed by aquadest

until free of chlor. The solid was then dried in the oven at 120°C, for 16 hours. The sulphated zirconia was then prepared by impregnation of H_2SO_4 overZr(OH)$_4$ by immersing in 1.0 N solution of H_2SO_4 (1 gram sample in 15 mL H_2SO_4) for 30 min.The solid was then filtered and dried at 120°C. Next, solid sample was calcined (650°C, 3.5 hr). Differential Thermal Analyzer (DTA) was applied to determine calcination temperature of catalyst. The sulphated zirconia catalyst was characterizied using the Fourier Transform Infra Red (FTIR) analyzer, the XRD and the Brunauer-Emmett-Teller (BET) value. The FTIR analysis was conducted prior impregnation the ZrO_2 with sulphate solution and after calcined at the ITI Chemical Engineering laboratory. The crystal structure was determined using X Ray Diffractometer at the Center of Integrated laboratory of University of Islam Negeri Syarif Hidayatullah Jakarta, while the BET analysis was carried out at the BATAN laboratory ,Puspiptek Serpong.

2.3 Apparatus
A photograph and a schematic diagram of a BCR apparatus are presented in Fig. 1 .The apparatus was equipped with a methanol tank, vaporizer, reactor, heater, and condenser columns.

2.3. Experimental procedures
Initially, the reactor was filled with PFO until reach the minimum mark level. Then another 250 ml of palm oil was filled into reactor, put the reactor lid and bring it into tight. Secondly, the vaporizer was filled with MeOH till the maximum mark level followed by filling up the MeOH tank. Next, switched the reactor heater on and held until reached the setting temperature. Afterwards, the super-heater was turned on until temperature reached to 250 ^{0}C, followed by running the water cooler. Then, switched the MeOH vaporizer on and adjusted its vapor flow rate, followed by turning MeOH pump on and adjusted its pumping rate according to the vapor rate. Reaction time was counted after the vapor bubble uniformly formed and evenly distributed in the reactor. Finally, samples were taken within 20 minutes interval time, and were analyzed using GC.

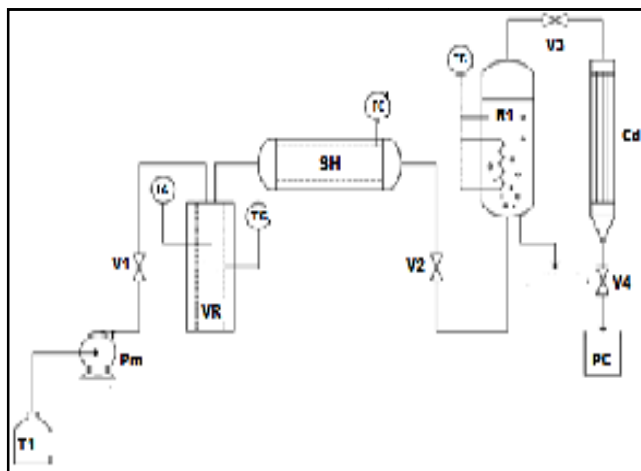**Fig 1(a).** The photograph of biodiesel apparatus set up

Fig 1(b). The schematic diagram of biodiesel experiment apparatus.
T1: MeOH tank, Pm: MeOH, pump, V1-V4: valves, VR: vaporizer, LC: level controller, TC: temperature controller, SH; superheater, R1: reactor, Cd: condenser, PC: product collector.

2.4. Product analysis
The biodiesel products analysis was carried out using a gas chromathograph, Shimadzu 2010 model with a flame ionization detector (FID), using helium as a carrier gas. The GC featured a capillary column (RTX-1 restex nonpolar phase; Cross bond® dimethyl polysiloxane, 30 M, 0.32 mm ID, 0.5μM). Method of analysis follows the modified EN 14105[12].

3. Results and discussion

3.1. Fatty Acid composition of palm frying oil material

The major fatty acid composition of PFO was tabulated in Table 1 and its result was compared to fatty acid composition of several palm oils analyzed by Petchmala et al. [11] and Kataren [13].

Table 1. Comparison of Fatty Acid Composition

Fatty Acids	Fatty Acids Composition (% w/m)		
	Sample (avg)	Reference [11]	Reference [13]
Miristic Acid	1.2	1.0	1.1 – 2.5
Palmitic Acid	43.9	45.6	40 – 46
Stearic Acid	3.9	3.8	3.6 – 4.7
Oleic Acid	41.7	33.3	39 – 45
Linoleic Acid	9.3	7.7	7 – 11

It can be observed that the fatty acid composition of PFO sample in this experiment is in accordance with the results of previous studies [11,13].

3.2. Catalyst characterization

Sulphated zirconia (SO_4-ZrO_2) catalyst that was prepared from the impregnation of H_2SO_4 over $Zr(OH)_4$ resulted in 48 % (w/w) yield. The FTIR analysis prior H_2SO_4 impregnation and after H_2SO_4 impregnation followed by catalyst cacination were presented in figures 2 and 3.
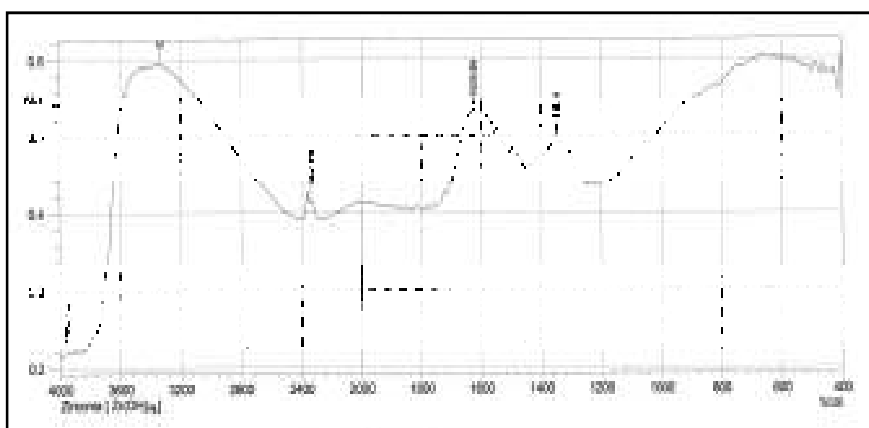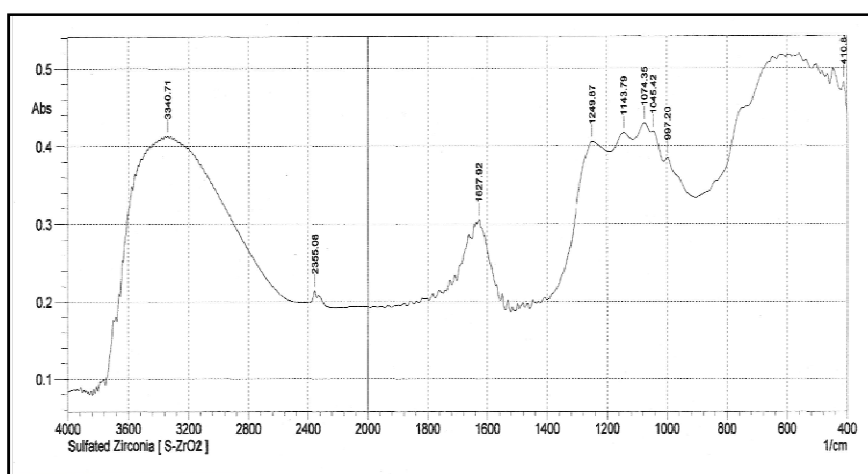

Fig 2. FTIR Spectrum of Zr (OH)$_4$

Fig 3. FTIR spectrum of SO_4-ZrO_2

Fig.2 indicates the spectrum of FTIR analysis of $Zr(OH)_4$ prior to H_2SO_4 impregnation and Fig. 3 shows the spectrum of FTIR analysis of SO_4-ZrO_2. It was noted that there is a difference absorbance profile between these two figures at the range of 1000 – 1280 cm^{-1} wave lengths. According to Stuart [14] the SO_2 and SO groups of sulphur compounds produce strong infra red band at wave length of 1000–1400 cm^{-1}. It can be concluded that H_2SO_4 impregnation over the $Zr(OH)_4$ occurred, since sulphates group were identified at 997,20; 1045,42; 1074,35; 1143,79 and 1249,87 cm^{-1} wave lengths.

The specific surface area of catalyst was determined by the BET method and found to be 53.26 m^2/g. This result is represented in fig 4.
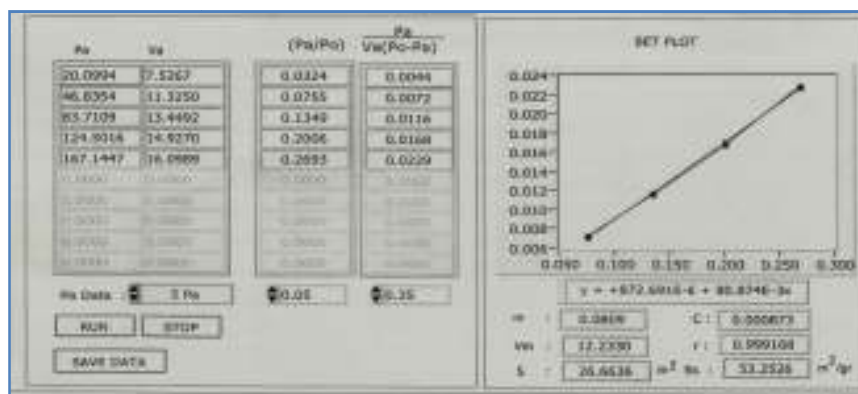

Fig 4. Analysis of surface area of SO_4-ZrO_2 catalyst
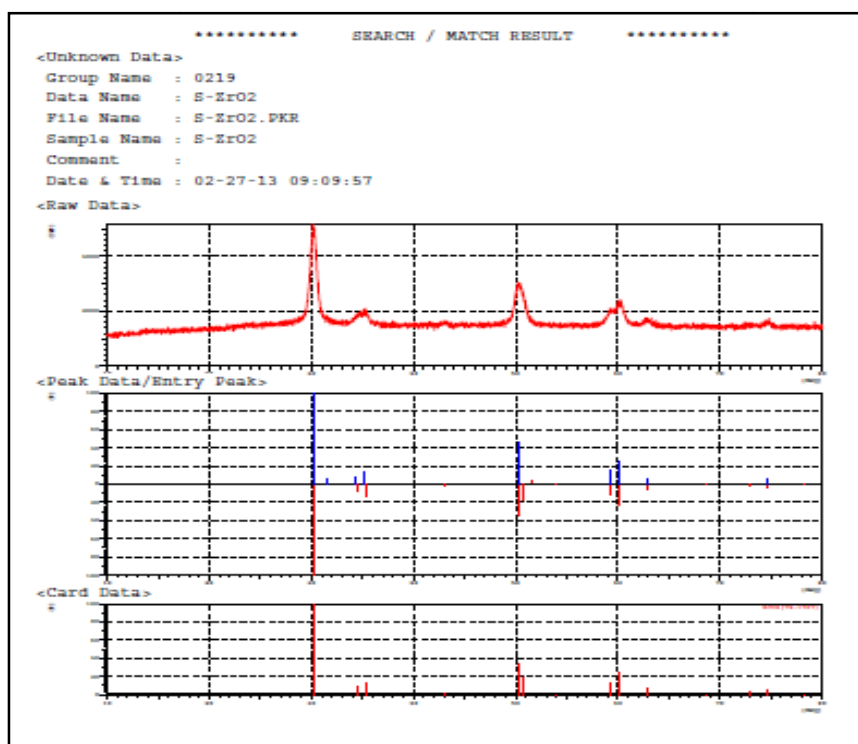

Fig 5. XRD analysis of Sulphated zirconia catalyst

While XRD measurement showed that only one single phase available as depicted on Figure 5. This result confirms that only ZrO_2 was detected, considering that during calcinations process all the $Zr(OH)_4$ was changed into ZrO_2.

3.3. The effect of methanol flow rates in bubble formation

The effect of methanol flow rates in bubble formation are shown in Figure 6. These figures show the flow rate differences in bubble formation. The bubble sact as substitutes for stirring the biodiesel

manufacturing process in which the reaction occurs at the contact interface of the bubbles. The methanol flow rates affect the amount and uniformity of the formed bubbles.
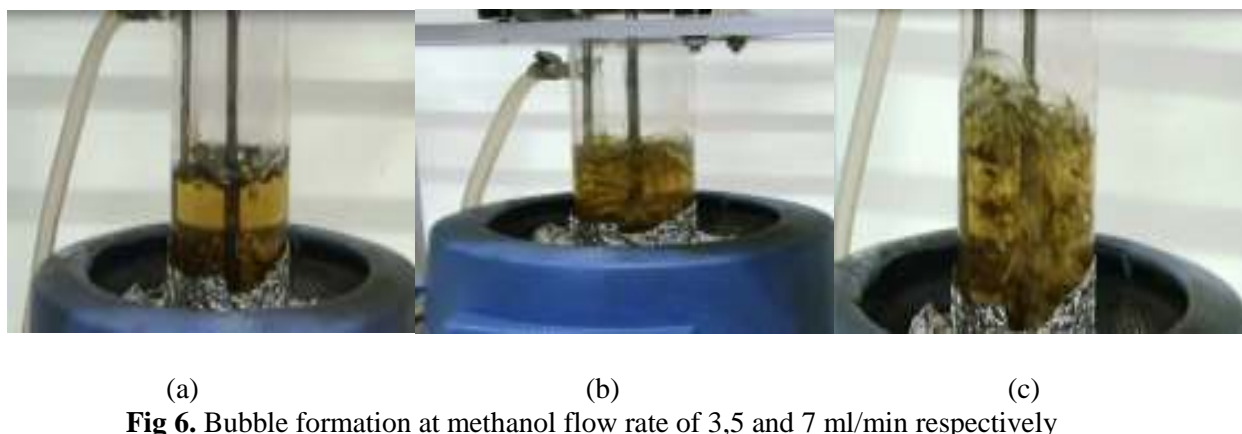

(a)   (b)   (c)

Fig 6. Bubble formation at methanol flow rate of 3,5 and 7 ml/min respectively

Fig. 6 (a) shows bubble formation at 3 ml/min of MeOH flow rate. The number of bubbles produced was slight and uneven. Resulting in interfacial contact between MeOH and oil is not optimal due to the lack of MeOH vapor flows into the reactor column. Consequently, the reactants which supposed to be changed into the product become even and less likely to be a product. Fig. 6 (b) indicates bubble formation at 5ml/min of MeOH flow rate. It is shown that the number ofbubbles formed are muchmore uniform and even. Therefore, there were more frequent contact interface between the reactants which more reactants changed to the product. Fig. 6 (c) depicts a large amount of bubbles produced with in homogeneous and uneven form. This condition occured as MeOH flow rate run at 7 ml/min. Resulting in interfacial contact between reactants becomes excessively fast and the product formation was not at optimal state. Utilizing this flow rate would be risky because of the numerous bubbles outburst happened and difficulty to be controlled.

It is observed that the MeOH vapor flow rate becomes unstable when the process of filling the liquid methanol as fresh feed is not done continuously. Filling with liquid MeOH is conducted whenthe liquid level has below the lineof fluid indicator specified in the vaporizer. The formation of bubbles in the reactor is affected by the height of liquid MeOH in the vaporizer. If sudden refilling of liquid MeOH into the vaporizer occured because of temperature of the vaporizer has reached the temperature stability of the MeOH evaporation, the cold physical characteristics of the liquid methanol will interfere with high temperature distribution process.The MeOH with temperature below evaporation point would require more time to reach its evaporation temperature causing the methanol's flow heading towards the reactor tends to wane or even none (based on the number of bubbles formed).Therefore, refilling the liquid MeOH into the vaporizer must be done continuouslyby generatingsuch system that refillingand evaporating the MeOH to occur simultaneously, in order to maintain the amount ofliquidmethanolat a stable predetermined threshold. Additional flow meter is required before feeding liquid MeOH into the vaporizer to maintain the continuous flow of liquid MeOH

According to Kantarci et al.[15], the fluid dynamic characterization of bubble column reactors has a significant effect on the operation and performance of bubble columns. They noted that the performance of bubble columns strictly depend on the regime prevailing in the column that can be classified and maintained according to the superficial gas velocity employed in the column. The methanol vapor superficial velocity obtained in this study was presented in Table 2.

Table 2. Superficial velocity of methanol vapor

Flow rate ($^{ml}/_{mint}$)	Vapor Velocity ($^{cm}/_{s}$)
3	1,370
5	2,300
7	3,219

Kantarci et al.[15] reported that the bubbly flow regime, also called the homogeneous flow regime is obtained at low superficial gas velocities, approximately less than 5 cm/s. This flow regime is characterized by bubbles of relatively uniform small sizes. In addition, a uniform bubble distribution and relatively gentle mixing is observed over the entire cross-sectional area of the column. Based on the above table, it was showed that the superficial velocities of methanol vapor employed in this study were in agreement with Kantarci et al.[15]. Based on the vizualisation of above figures obtained, and supported by literature data, the flow rate of 5ml/min of methanol was then selected for further studies.

3.4. The effect of catalyst to reactant mass ratio in biodiesel yield

Experimental study was conducted with and without catalyst. Amount of catalyst were varied in the range of 0.1 – 1.0 % (w/w) catalyst to reactant ratio when sulphated zirconia catalyst was employed. Experimental result is presented inTable3.

It was shown that average yield of product accumulation of biodesel run catalitycally is higher than that of non catalitycally (4.41% after 100 min run). Previous study conducted by Joelianingsih et al[7] at thesame temperature (250°C), non catalytically, revealed that product yield was 1.25% and 10.96 %(w/w) after 60 and 180 min run respectively. There is a significance difference if these data are compared to this non-catalytically experiment result. The yield obtained in previous study[7] was total yield of product in the vapor and liquid phases. Their experiment was conducted in a four-necked flask equipped with a condenser and a pipe for MeOH vapor feed, and the TLC/FID was used to analyze content of product. In this experiment, the yield obtained was yield in the vapor phase only. The BCR form is different to the reactor used in the previous study[7]. In addition, the GC was used to analyze the product in this experiment. Some differences mentioned above that might cause product yield run non-catalytically in this experiment lower than the previous study.

It can be observed also that the biodiesel product yield obtained run with catalyst were significantly low compared to the previous studies[6,7,11]. Petchmala et al.[11] indicated that the specific surface area and calcination temperature of sulphated zirconia catalyst play an important role in transesterification reaction of vegetable oil. The BET surface area of sulfated circonia employed in this study was only 52.26 m^2/g, with calcination temperature at 650 °C, while Petchmala et al.[11] concluded that the most active catalyst of their synthesized sulphated zirconia catalyst has the BET value of 234,9 m^2/g and calcination temperature at 500 °C. The specific surface area of sulphated zirconia considerably decreases as calcination temperature is increased from 500 to 700 °C, since the amount of active sites of catalyst was reduced. In addition, the low yield obtained in this study might be due to the short contact time between oil and methanol vapor, resulting the reactions to be incomplete. The mechanism reactions of transesterification of PFO can be presented as follows:

Table 3. Experiment results of biodiesel production (methanol flow rate at 5 ml/min, reactor temperature at 250°C, time 100 min)

Catalyst to reactant ratio, % (w/w)	Product yield, %	Product picture
0.00	4.41	
0.10	6.09	
0.50	7.91	
1.00	5.53	

$$TG + MeOH \leftrightarrow DG + FAME \qquad (1)$$
$$DG + MeOH \leftrightarrow MG + FAME \qquad (2)$$
$$MG + MeOH \leftrightarrow GL + FAME \qquad (3)$$

The third reaction, in which MG with methanol turns to Fatty Acid Methyl Esters (FAME)/biodiesel and glycerol (GL), is considered the slowest reaction among all above reactions, because MG, as an intermediate compound, is the most stable compound compared to triglyceride and diglyceride[16], and resulted that the amount of MG formed was excessive.

It is shown from Table3 that the reaction run with 0.5 % (w/w) catalyst produces the highest yield than the run using 0.1 % and 1.0% (w/w) catalyst. Catalytic experiment run with 0.1% (w/w) sulphated zirconia resulted in 6.9 % of product yield, while with 0.5 % (w/w) catalyst, yield obtained was 7.91 %. Several literatures[3,9,11] revealed that the highest yield of biodiesel products was achieved at catalyst to reactants mass ratios between 0.1 and 0.5 %. These findings support our experimental results.

Since method of product analysis in this experiment follows the modified EN 14105[12], in which in the list of EN 14105 parameters standard noticed to calculate the impurities of biodiesel product, such as free GL, MG, DG, TG, and total GL, instead of purity of biodiesel product, so that in this study, purity of the product did not directly analyzed . However, it could be calculated using equation (1) to (3) with several assumptions.

Utilization of 1% catalyst to reactant mass ratio in this study causes biodieselproduct to change intosolid phase with the acquisition ofa lowyield. The low yield of product indicated that more MG

present in the biodiesel. According to literature [17], melting and solidification points of MGs are higher than room temperature. This condition might be caused by the biodiesel product phase that changed into solid at room temperature. The result study confirms employee of 1% (w/w) catalysts to reactant ratio is unappropriate in transesterification of vegetable oil for biodiesel production as revealed by literatures[3,11].

Conclusion

Biodiesel production by transesterification of palm frying oil carried out in bubble column reactor in the presence of SO_4/ZrO_2 catalyst, unfortunately, beyond the expectation, because all experimental results showed lower biodiesel yield than previous studies. The highest yield was 7.91% run with 0.5 % (w/w) catalyst to reactant mass ratio.

Acknowledgements

References

1. Yan S, DiMaggioC., Mohan S.KimM., Stalley S.O., and Simon Ng, K.Y., Advancements in Heterogeneous Catalyst for Biodiesel Synthesis, *Top Catal* 2010: **53**,721-736.
2. Furuta S., Matsuhashi H., and Arata K. ,Biodiesel Fuel Production with Solid Superacid Catalysis in Fixed Bed Reactor under Atmospheric Presure. *Catal.Commun*.2004:**5**,721-723.
3. HelwaniZ., M.R.Othman, N.Aziz, J. Kim and W.J.N. Fernando., Solid Heterogeneous Catalyst for Transesterification of Triglycerides with Methanol: A Review. *Applied Catalyst A:General*, 2009:**363**, 1-10.
4. Saka ,S. and D. Kusdiana., Biodiesel Fuel from Rapeseed Oil as Prepared in Supercritical Methanol. *Fuel*, 2001: **80,** 225-231
5. Yamazaki R, Iwamoto S, Nabetani H, Osakada K, Miyawaki O, Sagara Y.,. Non catalytic alcoholysis of oils for biodiesel fuel production by semi-bach process. *Jpn J.Food Eng*. 2007; **8**,11-19.
6. Joelianingsih, H. Nabetani, S. Hagiwara, Y. Sagara Y, T.H. Soerawidjaya, A.H. Tambunanan, K. Abdullah. , Performance of a Bubble Colum Reactor for the Non-catalytic Methyl Esterification of Free Fatty Acids at Atmospheric Pressure. *J. Chem. Eng. Japan*. 2007: **40** (9),780-785.
7. Joelianingsih, H. Maeda, H. Nabetani, Y. Sagara Y, T.H. Soerawidjaya, A.H. Tambunanan, K. Abdullah. Biodiesel Fuels from Palm Oil via the Non-Catalytic Transesterification in a Bubble Column Reactor at Atmospheric Pressure: a kinetic study. *Renewable Energy* 2008.: **33** (7). pp 1629-1636.
8. Dirjen Energi baru, Terbarukan dan Konservasi Energi, Indonesia ministry of energy and mineral resources, Standar dan mutu bahan bakar nabati jenis biodiesel, 2013 ,SK No.. 723 K/10/DJE/2013
9. Chopade ,S.G., K.S. Kulkarni, A.D. Kulkarni, and N.S. Topare.. Solid Heterogeneous Catalyst for Production of Biodiesel From Trans-esterification of Triglycerides with Methanol: A Review. *Acta Chim.Pharm.Indica*.2012: **2**(1), 8-14
10. Omota f., Dimian A.C., and Bliek A. Fatty acid Esterification by Reactive Distillation Part2-Kinetica-baced design for Sulphated Zirconia Catalyst. *Chem.Eng.Sci*. 2003: **58**(14).3175-3185
11. Petchmala, A., Laosiripojana, N., Jongsomjit, B., Goto, M., Panpranot, J., Mekasuwan-dumrong, O., and Shotipruk, A. Transesterification of Palm Oil and Esterication of Palm Fatty Acid in Near- and Super-Critical Methanol with SO4–ZrO2 Catalysts, Fuel 2010:**89**, 2387–2392.
12. Joelianingsih, Indra, I., and Purwaningsih, I.S. Modification Method of EN14105 for Determination of Free Glycerol and Mono-Di-TriglyceridesContents in Biodiesel, International Seminar on Biorenewable Resources Utilization for Energy and Chemicals 2013 Bandung, 10-11 October.
13. Ketaren S., *Pengantar teknologi minyak dan lemak pangan*, 1st ed.,Jakarta,UI-Press, 1986
14. Stuart, B. *InfraredSpectroscopy : Fundamentals and Applications*, John Wiley & Son, 2004
15. Kantarci N., Borak F., Ulgen K.O. Bubble Column Reactor-Review, *J. Process Biochemistry* 2007: **40**, 2263-2283.
16. Warabi, Y., Kusdiana, D., and Saka, S., Reactivity of Triglycerides and Fatty Acids of Rapeseed Oil in Supercritical Alcohols, *Bioresource Technology*2004 :**91**, 283-287.
17. Gunstone, F.D., Harwood, J.L., and Padley, F.B. *The Lipid Handbook*, 2nd ed. Cambrigde , Chapman & Hall, University Press,1994.

International Conference and Workshop on Chemical Engineering UNPAR 2013

The Mass Transfer Coefficient of Red Food Coloring Extraction from Rosella

Ariestya Arlene A.[a*], Anastasia Prima K.[a], Tisadona Mulyanto[a], Cynthia Suriya[a *]

[a]*Jurusan Teknik Kimia, Fakultas Teknologi Industri, Universitas Katolik Parahyangan*
Jl. Ciumbuleuit No. 94 Bandung-40141

Abstract

Rosella is one of the plant in Indonesia that can be used as natural dyes. The red color in the rosella sourced from the anthocyanin in the petal of the flower. The anthocyanin in the rosella consists of cyanidin-3-sambubioside, delphinidin-3-glucose, and delphinidin-3-sambubioside. Anthocyanin can be used as a safer natural coloring foodstuff to replace synthetic dyes. The purpose of this research is to find out the mass transfer coefficient (k_Ca) of the dyes extraction. The mass transfer coefficient is the value showed the distribution of mass transfer, occurred in the extraction processes. Isolation of these dyes is conducted by batch extraction method. Batch extraction is accomplished by using RO (Reverse Osmose) water and ethanol 70% as solvent with stirring, with F/S (Feed/Solvent) ratio = 1:5, 1:10, 1:15, and extraction temperature 30^0C, 50^0C, and 70^0C. The higher temperature of extraction will increase the value of k_Ca. The extraction which uses etanol 70% as the solvent has a greater value of k_Ca than the extraction which use RO water as the solvent. F/S ratio does not influence the value of k_Ca.

Keywords: coefficient, coloring, extraction, food, red, Rosella.

1. Introduction

A colored food is interesting. They can induce people's appetite. However, nowadays, people would prefer to use synthetic food dyes rather than natural dyes because they are cheaper. However, synthetic food coloring which is misused by adding textile dye or non-food grade food coloring. It is proved by research that some of synthetic food coloring such as phloxine, erythrosine, and rose bengal are harmful for the human body [1]**.** The anthocyanin is one of the natural food coloring which is safer than that of synthetic one. However the safety depends on the method of extraction and the source of the feed[2]. In this experiment, the source of anthocyanin is rosella petal commonly used as beverage and the solvents are food grade. One of the alternative sources for natural coloring is rosella. This coloring can replace the synthetic food coloring and minimize the misuse. The part of plant that can be used for natural coloring is its petals. Rosella petals contain vitamin C, vitamins A, amino acids, protein, calcium and anthocyanin pigments that form flavanoids which act as an antioxidant [2]. Rosella or *Hisbiscus sabdariffa L.*, is one of the flower species which comes from Africa. Rosella grows from sowing dry seeds. Rosella can reach heights up to 3-5 meters and it blooms almost all through the year. Rosella have a bright color with dark red petals (Mukaromah, 2010). The benefits of rosella petals reduce the viscosity of bloods, help digestion, prevent inflammation of the urinary tract and kidneys, filters toxins in the body, preventing vitamin C deficiency, blood circulation, smooth bowel movements, decrease the levels of alcohol absorption, retention spasms, and many more. The diseases which can be treated by rosella are high blood pressure (hypertension), kidney stones, cough, impotence, lethargy, fever, bleeding gums, skin diseases, insect bites, sores, and anemia [3]. Flower parts which can be used as a food coloring are the petals. Rosella petals contain vitamin C, vitamin A, and amino acids. Eighteen of essential amino acids for our body contained in the Rosella petals include arginine and lignin that play a role in the process of body cells renewing. Rosella petals also contain protein, calcium and anthocyanin pigments which form flavonoids (eg: gossypetin, hibiscetin, etc.) that act as anti-oxidant. Anthocyanin in rosella petals are delphinidin-3-glucoside, sambubioside, and cyanidin-3-sambubioside [4]. Anthocyanin has the highest

---

* Corresponding author. Tel.: +62-22-203-2700; fax: +62-22-203-2700.
E-mail address: ariestya.arlene@unpar.ac.id.

antioxidant activity among the other antioxidants (delphinidin, cyanindin, pelargonidin, malvidin, peonidin). The anthocyanin is a potential antioxidant agent aside from its role as natural colorant [5].

The extraction of red dye depends on certain factors, which are temperature, ratio of feed to solvent, type of solvent, the speed of stiring, and the extractor used for the extraction process. The speed of stiring and the extractor are the same for all the variations. The lack of information about temperature, type of solvent, and ratio of feed to solvent become the background of the selected variation of this experiment.

2. Material And Methods

2.1 Pretreatment of The Extraction Feed

The Rosella petals obtained from Pasar Baru (traditional market) in Bandung, Indonesia, was dried until the water content lower than 8%. The size was reduced using electric dry blender until the size is -20+60 mesh.

2.2 Soxhlet Extraction

The Soxhlet extraction was done using RO water and ethanol 70%. Ten grams of dried rosella petals (-20+60 mesh) was extracted at the boiling temperature of each solvent. The extract was separated from the solvent using vacuum evaporator then the extract was dried in the vacuum oven until the mass remains constant. The extract from this Soxhlet extraction was used in the determination of maximum wavelength.

2.3 Determination of Maximum Wave Length

The extract from Soxhlet extraction was diluted in each solvent then the absorbance was measured at different value of wavelength. The maximum wave length was at the highest value of the measured absorbance.

2.4 Main Experiment

The determined amount of solvent was placed in the batch extraction equipment with stirring speed 180 rpm. The temperature was varied and controlled from the water bath which was placed surround the extraction equipment. The setting of the equipment can be seen at Figure 1. The sample of extraction process was taken every 5 minutes and the absorbance was measured using UV spectrophotometer. The extraction process was carried out until absorbance showed the constant value. The variation was the type of solvent (Reverse Osmoses (RO) water and ethanol), F/S ratio (1:5, 1:10, 1:15), and extraction temperature (30^0C, 50^0C, and 70^0C). The absorbance of the solution of extract was measured every 5 minutes until reaching the constant value. The value of k_Ca was calculated using these absorbance data.
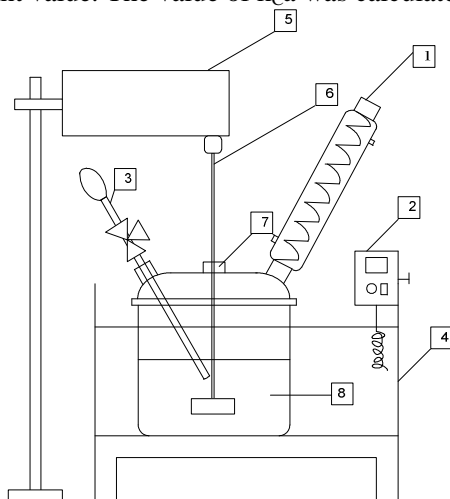
Note: (1) Condenser; (2) Thermostat; (3) Sampling device; (4) Waterbath; (5) Stirring motor; (6) Impeller; (7) Stuffing box; (8) Batch Extractor

Fig 1. Batch Extraction Equipment

3. Result And Discussion

The mass transfer coefficients were determined by the first order kinetic model. According to Samun [6], the speed of leaching depends on the two main steps, which are, the mass transfer of the extract from the inside of solid phase to the solid surface and the mass transfer from the solid surface to the solvent. If there is no difference between the two steps, the speed of extraction is determined by the both step. However, if there is a significant difference of the two steps, the speed of extraction is determined by the slower step. In dye extraction of rosella, the size of the solid phase is made to small pieces (-20+60 mesh) in order to get the faster diffusion process of the dye so that the diffusion coefficient can be neglected. The determining process is the mass transfer process from the surface of the solid phase to the liquid phase of the solvent. The velocity of mass transfer of the dye from the surface of the solid phase to the liquid phase of the solvent follows the first equation:

$$N = k_C \left(C^* - C \right) \qquad (1)$$

The value of C is extract concentration (the red dye) in the solution and the C* is the extract concentration in the solution in the equilibrium with the extract concentration on the solid surface. The mass transfer coefficient is calculated using mathematical method approximation with several assumptions, these are, the size of the solid is uniform and the volume of the sistem is constant in the whole extraction process, the density of feed (solid phase) and solvent (liquid phase) are constant, and the process is isothermal. The extract mass balance in the batch extractor is:

$$R_{in} - R_{out} + R_{solute} = R_{total} \qquad (2)$$

$$0 - 0 + k_C \left(C^* - C \right) V = V \frac{dC}{dt} \qquad (3)$$

Because of the constant volume of the system, the equation becomes:

$$k_c \left(C^* - C \right) = \frac{dC}{dt} \qquad (4)$$

$$\frac{dC}{dt} + k_C . C = k_C . C^* \qquad (5)$$

The first order differential equation is solved using the integrating factor method, and then the equation will become:

$$C = e^{\int -k_c dt} \left[\int e^{\int k_c dt} k_C . C^* + K \right] \qquad (6)$$

$$C = C^* + K e^{-k_c t} \qquad (7)$$

At $t = 0$, the $C = 0$, and the equation will become:

$$C = C^* + K e^{-k_c . 0} \qquad (8)$$

$$K = -C^* \qquad (9)$$

$$C = C^* \left(1 - e^{-k_c t} \right) \qquad (10)$$

$$C = C^* - C^* e^{-k_c t} \qquad (11)$$

The next step is doing the linier regression on the equation (11) so the equation will become:

$$\ln \left(C^* - C \right) = \ln C^* - k_C . t \qquad (12)$$

Furthermore, the making of the curve is doing by plotting the data of "$\ln \left(C^* - C \right)$" as the ordinat and "$t$" as the absis. The line equation of the linier regression is:

$$y = ax + b \qquad\qquad (13)$$

with $y = \ln\left(C^* - C\right)$, $x = t$, $a = -k_C$, and $b = \ln C^*$

The maximum wave length of anthocyanin is in the range of 515 – 545 nm and the maximum wave length of red color is 500 – 550 nm. The maximum wave length of the extract is 540 nm, this shows that the value lies on the range of anthocyanin and red color wave length. The absorbance of the extraction process increases from time to time until it reaches a constant value. Therefore, it can be concluded that the red dye of rosella is stable at RO water and ethanol 70% at different temperatures which are varied in the experiments.

The value of k_C of RO water and ethanol 70% as solvent can be seen in the Table 1 and the graph can be seen in Fig. 2. The value of k_C in the ethanol 70% as solvent is bigger than RO water as solvent. This phenomenon shows that the solubility of the dye is better in ethanol 70% than RO water. It can be seen that at the RO water as solvent, at the F/S = 1:5, the value of k_C is increasing as the temperature increases. The higher the temperature is, the faster the mass transfer (of the dye), and the bigger the mass transfer coefficient will be. The temperature increases the solubility of the solute in the solvent, so the leaching rate also increases [7]. However, the tendency of the F:S ratios is different from that of the temperature. At F:S = 1:10, there are almost no differences of the k_C value and at F:S = 1:15, the k_C value decreases as the temperature increases. This phenomenon also occurs in ethanol 70% as solvent. The increase of k_C value occurs at F:S = 1:5. The constant k_C value is at F:S = 1:15 and the decrease of k_C value occurs at F:S = 1:10. Ethanol 70% gives higher value of the mass transfer coefficient at all variations. Then it can be concluded that the solubility of the dye is better at the ethanol 70%.
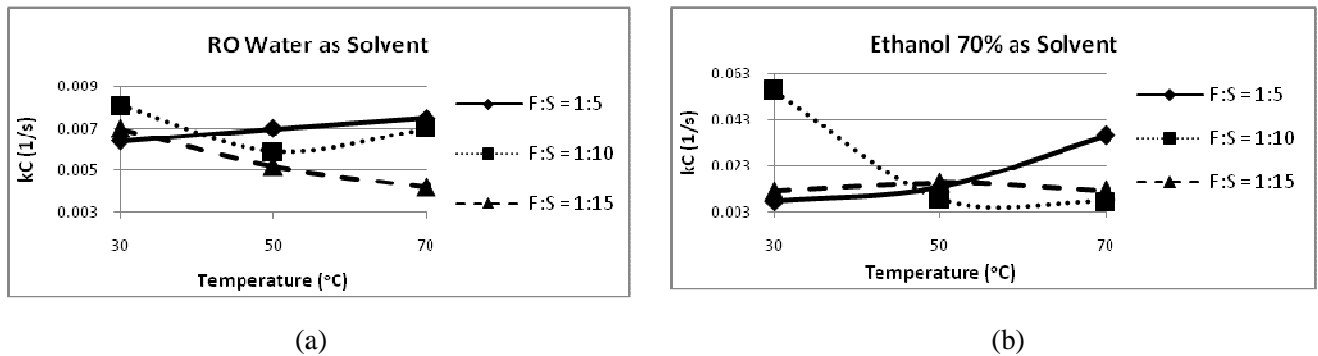

(a)   (b)

Fig 2. The Chart of k_C at All Variation

Table 1. The value of k_C for all variations

Temperature (^{0}C)	F:S (gr/gr)	k_C (1000/s)	
		RO water	Ethanol 70%
30	1:5	6,4	7,7
	1:10	8,1	55,5
	1:15	7	11,9
50	1:5	7	13,6
	1:10	5,9	8,7
	1:15	5,2	15,6
70	1:5	7,5	36,1
	1:10	7	7,6
	1:15	4,2	12,4

The experimental design is used to find out the significance of the variation. From the table of ANOVA (table 2) it can be concluded that all the factors that influences the mass transfer in the dye extraction. There are interactions of two combinations from the factor of temperature, type of solvent, and F:S, and also the three combination of them.

Table 2. ANOVA of Mass Transfer Coefficient

Variation	Fo calculation	Fo from table
Temperature (A)	122,04207	3,55
Solvent (B)	6,17947	4,41
F:S (C)	558,28152	3,55
Interaction of AB	38,57216	3,55
Interaction of AC	27,40981	2,93
Interaction of BC	8,25788	3,55
Interaction of ABC	49,92769	2,93

Conclusion
1. The highest value of transfer mass coefficient of RO water and ethanol 70% is obtained at F:S = 1:10 and temperature 30°C.
2. Ethanol 70% gives the higher value of mass transfer coefficient.
3. Type of solvent, temperature, and F:S influence the value of mass transfer coefficient.
4. There are interaction of two combination from the factor of temperature, type of solvent, and F:S, and also the three combination of them.

References
[1] Mitzutani, Takaharu, 2009. Toxicity of Xanthene Food Dyes by Inhibition of Human Drug-Metabolizing Enzymes in a Noncompetitive Manner, Journal of Environmental and Public Health, Volume 2009 (2009), p. 1-9.
[2] European Food Safety Authority, 2013. Scientific Opinion on the re-evaluation of anthocyanins (E 163) as a food additive, EFSA Journal, 11(4): 3145.
[3] Mardiah, Sawarni, H., R. W. Ashadi., A. Rahayu, 2009. *Budi Daya dan Pengolahan Rosela si Merah Segudang Manfaat*, Cetakan 1, Agromedia Pustaka, Jakarta
[4] Mukaromah, Umu, 2010. Kadar Vitamin C, Mutu Fisik, pH, dan Mutu Organoleptik Sirup Rosela Berdasarkan Cara Ekstraksi, *Skripsi*, Universitas Muhamadiyah Semarang .
[5] Wang, Hong; Cao, Guohua; and Prior, Ronald L., 1997. Oxygen Radical Absorbing Capacity of Anthocyanins, Journal of Agricultural and Food Chemistry, Volume 45 (2), pp. 304-309.
[6] Samun, 2008. Koefisien Transfer Massa Volumetris Ekstraksi Zat Warna Alami dari Rimpang Kunyit (*Kurkuminoid*) di Dalam Tangki Berpengaduk, *Ekuilibrium Vol. 7*, p.18.
[7] Asbi, B.A., 1994. Mass Transfer on A Closed-cycle Solid-Liquid Extraction Unit, Pertanika Journal of Science and Technology, Vol.2, No.2, p. 237-241.

International Conference and Workshop on Chemical Engineering UNPAR 2013

CO$_2$ Absorption through Nonporous Membrane Contactor

Sutrasno Kartohardjono[a*], Maulana Abdul Rasyid[a] and Setijo Bismo[a]

[a]Chemical Engineering Department,Universitas Indonesia, Depok 16424, Indonesia

Abstract
This research utilized nonporous membrane as a contactor to absorb CO$_2$ using water and 5% diethanolamine (DEA) solution as absorbents. Recently, membrane contactors based on hydrophobic micro porous materials show remarkable performance for gas-liquid contacts especially for CO$_2$ absorption. However, membrane mass transfer performance drastically drops if wetting occurs on the membrane during the process. One way to prevent membrane wetting is to apply higher gas pressure in the gas-liquid membrane contactor. Therefore, a highly permeable membrane material is required to maintain and to accommodate the fast chemical reaction which takes place in the liquid phase. In addition, membrane material must withstand long term contact with a chemically reactive solvent such as DEA. The membrane material used in the experiment is dense polyamide membrane, which has surface area of 0.5 m^2. Experimental results show that the CO$_2$ absorption flux as well as mass transfer coefficient for 5% DEA solution increased with increasing the solvent flow rateAt the regime of low solvent flow rates (Q_L< 6.7e-6 m^3/s or 400 CC/min) in the membrane contactor, and relatively constant at solvent flow rate, Q_L> 6.7e-6 m^3/s. Meanwhile, for water absorbent the CO$_2$ absorption flux and the mass transfer coefficient slightly decreased with increasing solvent flow rate in the contactor due to the membrane wetting.

Keywords: DEA, mass transfer coeficient, membrane contactor, polyamide, wetting

1. Introduction

Natural gas containing CH$_4$ as the main component and is considered as an important source of a fuel. However, natural gas also contains impurities such as, CO$_2$, H$_2$S and H$_2$O, and must be removed before the natural gas can be used as a fuel or a feedstock. CO$_2$ is a greenhouse gas that decreases the efficiencies in production, transportation and storage of natural gas Meanwhile, H$_2$S has a pungent odor, corrosion to piping and equipment, and the most important is because of its toxicity [1]. These impurities are usually removed through conventional absorption processes in the absorption tower and packed or plate columns. The conventional columns are subjected to flooding, unloading and foaming. In addition, conventionalprocesses are high in capital and operating costs [2].

An alternative technology to overcome these disadvantages is a membrane process, which also offers more interfacial area than conventional tower or column. Hollow fiber membrane contactor has attracted many researchers to be used as a gas-liquid contacting device in the last decade [3], as its provides a very high specific interfacial area for gas-liquid contact [4]. The driving force for gas transfer in the membrane contactor is a concentration gradient rather than a pressure gradient as in conventional membrane processes such as microfiltration, ultra filtration and reverse osmosis [5]. Therefore, only a very small pressure drop is required to ensure that the gas/liquid interface remains in the membrane pores [6-8]. Type of Absorbent and membrane material is very important to maximize the efficiency of the absorption process through the membrane contactor. Most of absorbents with a higher CO$_2$ loading capacity are usually highly corrosive. The chemical attack of the absorbents to the membrane material may result in poor performance of the system [9]. Hydrophobic micro porous membrane contactor, recently, has shown remarkable performance for gas-liquid contacts especially for CO$_2$ absorption. However, membrane wetting can drastically reduce mass transfer performance of the contactor. To prevent the membrane wetting occurred; the feed gas must be at higher pressure so that the membrane pores always filled with gas. Therefore, high membrane permeability is necessary to maintain and to accommodate the fast chemical reaction which takes place in the liquid phase. The membrane material must also resist to the

long term contact with a chemically reactive solvent such as DEA [10]. In this work we utilize dense membrane of polyamide as contactor to absorb CO_2 gas using water and 5% diethanolamine solution as absorbents.

2. Materials and Methods

Commercial spiral wound membrane CSM® Model RE1812-50 provided by Shenzhen Tao Shi was used as a membrane contactor. The membrane has effective contact area of 0.32 m². The amine used as solvent was diethanolamine (DEA reagent grade > 98%) and was purchased from MERCK-Schuchardt.   Meanwhile, CO_2 gas used in the experiment was provided by Samator Indonesia with purity > 99%. An experimental set-up, as shown in Figure 1, was employed to conduct mass transfer and hydrodynamic experiments. The setup mainly consists of membrane contactor, gas flow meter, liquid flow meter, pH meter, water pump, feed tanks for CO_2 and 5% DEA solution. To begin with, CO_2 feed gas was sent to the membrane contactor, whilst absorbent solution from the feed tank at a given flow rate was pumped to the membrane contactor counter-currently with CO_2 gas stream. The Gas and liquid flow rates were adjusted by the control valves. In addition, pH of absorbent solution as well as its pressure drop entering and leaving the membrane contactor was also measured for each experiment. In the experiment solvent flow rates were varied in the range of 100 to 1400 CC/min, whilst gas flow rates were kept constant at around 700 CC/min.

The overall mass transfer coefficient from the experiment was calculated by Eq. 1,

$$K_L = (Q_L/Am) \ln ((C^* - C_0)/(C^* - C_1)) \tag{1}$$

Where K_L, Q_L and A_m are overall mass transfer coefficient, liquid flow rate and membrane area, whilst C^*, C_0 and C_1 are CO_2 concentrations in the equilibrium, absorbent inlet and outlet to and from the contactor, respectively. Meanwhile, CO_2 flux from the membrane contactor, J, was calculated by Eq. 2,

$$J = (Q_L/Am) \Delta C \tag{2}$$

Where J and ΔC are CO_2 absorption flux and CO_2 concentration difference at outlet and inlet of the membrane contactor, respectively.
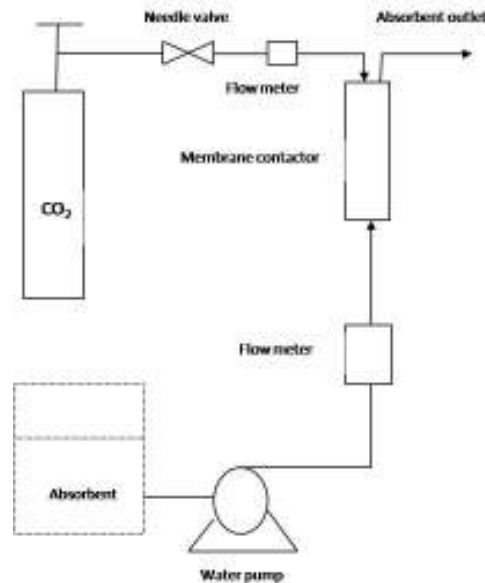

Fig 1. Schematic diagram of experimental set-up.

.

3. Results and Discussions

The effect of solvent flow rates on the absorption performance of membrane contactor is shown in Fig. 2 and Fig. 3. CO_2 absorption flux for 5% DEA solution increased by increasing the solvent flow rate, as shown in Fig. 2, due to the decrease of boundary layer thickness by increasing solvent flow rate, which reduced solvent saturation in the liquid side and enhanced CO_2 flux [11]. A similar trend was also occurred for the overall mass transfer coefficients as shown in Fig. 3. It can also be seen that the influence of the 5% DEA solution flow rates on the CO_2 absorption may present slightly different depending on the DEA solution flow rate. At the regime of low liquid flow rates (Q_L< 6.7e-6 m^3/s or 400 CC/min), the CO_2 absorption flux and mass transfer coefficients increased with the increase of the liquid flow rate. This can be attributed to the depletion of active amines in the solution was significant at low liquid flow rate. The increase of liquid flow rate could accelerate the active amines and reduce the depletion effectively. Therefore, the CO_2 absorption flux and mass transfer coefficient increased with the increase of the liquid flow rate. At the regime of high liquid flow rates (Q_L> 6.7e-6 m^3/s), the concentration of active amine in the liquid phase could be maintain at a constant value. As a result, the CO_2 absorption rate was not affected significantly by the change of the liquid flow rate [9]. In contrast, the CO_2 absorption flux as well as the overall mass transfer coefficients is slightly decreased with the increase of liquid flow rate for water absorbent, especially at higher solvent flow rates, as shown in Fig. 2 and Fig. 3. It is likely that the membrane was partially wetted during CO_2 absorption process, leading to performance deterioration in the membrane contactor [9, 12].In the wetting membrane, the mass transfer reseistance by the liquid in the membrane pores to the overall mass transfer become more significant. As a result, the influence of membrane wetting at a higher liquid flow rate was more readily obtainable than that at a relatively lower liquid flow rate. Therefore, the prevention of membrane wetting was very important in keeping the high performance of CO_2 absorption in the membrane contactor [9].

The CO_2 concentration at the absorbent outlet membrane contactor as a function of absorbent flow rate is shown in Fig. 4. Absorption is provided by chemical reaction in the presence of DEA solution as absorbent. As expected, CO_2 concentration decreased with the increase of absorbent flow rate in the membrane contactor. In addition, 5% DEA solution, which has higher reaction rates with CO_2, gave higher CO_2 concentration than water. A similar phenomenon was also demonstrated by Kim et al., [13]. They used monoethanolamine (MEA) 12wt% to absorb CO_2 gas through polytetrafluoroethylene (PTFE) membrane contactor, and also found that CO_2 concentration decreased with the increase of absorbent flow rate in the membrane contactor.
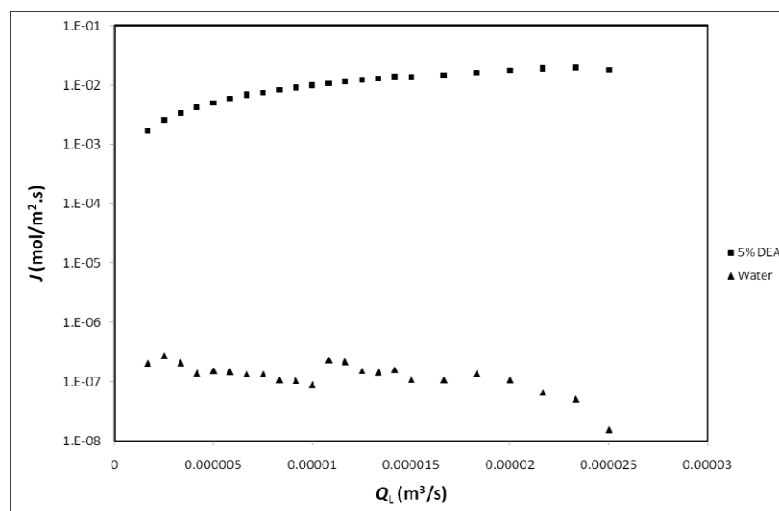

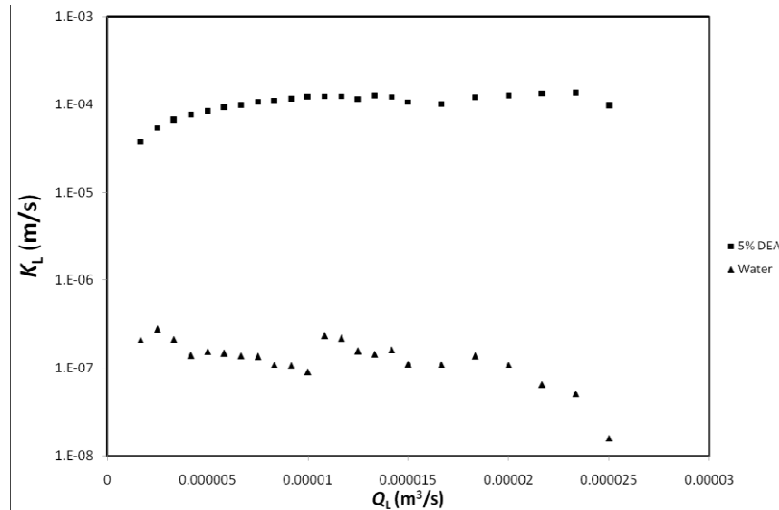**Fig 2.** Effect of absorbent flow rate, Q_L, on the CO_2 absorption flux, J.

Fig 3. Effect of absorbent flow rate, Q_L, on the CO_2 mass transfer coefficient, K_L.
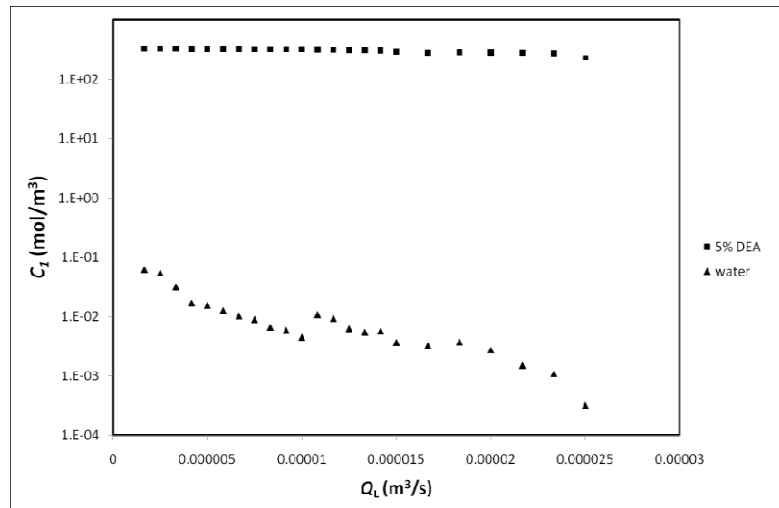

Fig 4. Effect of absorbent flow rate, Q_L, on the CO_2 concentration on the absorbent outlet the membrane contactor, C_1

4. Conclusions

Experiments have been conducted to evaluate the performance of nonporous membrane contactor to absorb CO_2 using 5% DEA solution and water as absorbents. The results show that CO_2 absorption flux as well as mass transfer coefficient for 5% DEA solution increased with the increase of the absorbent flow rate. Meanwhile, for water as absorbent, CO_2 absorption flux as well as mass transfer coefficient slightly decreased with the increase of the absorbent flow rate. The CO_2 concentration at the absorbent outlet membrane contactor, as expected, decreased with the increase of absorbent flow rate.

Acknowledgements

References

[1] R. Faiz and M. Al-Marzouqi, 2010, CO2 removal from natural gas at high pressure using membrane contactors: Model validation and membrane parametric studies, Journal of Membrane Science, vol. 365, pp. 232-241.
[2] A. Gabelman and S.-T. Hwang, 1999, Hollow fiber membrane contactors, Journal of Membrane Science, vol. 159, pp. 61-106.

[3]   J.-L. Li and B.-H. Chen, 2005, Review of CO2 absorption using chemical solvents in hollow fiber membrane contactors, Separation and Purification Technology, vol. 41, pp. 109-122.

[4]   F. Lipnizki and R. W. Field, 2001, Mass transfer performance for hollow fibre modules with shell-side axial feed flow: using an engineering approach to develop a framework, Journal of Membrane Science, vol. 193, pp. 195-208.

[5]   V. Y. Dindore and G. F. Versteeg, 2005, Gas–liquid mass transfer in a cross-flow hollow fiber module: Analytical model and experimental validation, International Journal of Heat and Mass Transfer, vol. 48, pp. 3352-3362.

[6]   T. Ahmed, M. J. Semmens, and M. A. Voss, 2000, Energy loss characteristics of parallel flow bubbleless hollow fiber membrane aerators, Journal of Membrane Science, vol. 171, pp. 87-96.

[7]   V. Y. Dindore, D. W. F. Brilman, and G. F. Versteeg, 2005, Hollow fiber membrane contactor as a gas–liquid model contactor, Chemical Engineering Science, vol. 60, pp. 467-479.

[8]   S. P. Lim, X. Tan, and K. Li, 2000, Gas/vapour separation using membranes: Effect of pressure drop in lumen of hollow fibres, Chemical Engineering Science, vol. 55, pp. 2641-2652.

[9]   R. Wang, H. Y. Zhang, P. H. M. Feron, and D. T. Liang, 2005, Influence of membrane wetting on CO2 capture in microporous hollow fiber membrane contactors, Separation and Purification Technology, vol. 46, pp. 33-40.

[10] P. T. Nguyen, E. Lasseuguette, Y. Medina-Gonzalez, J. C. Remigy, D. Roizard, and E. Favre, 2011, A dense membrane contactor for intensified CO2 gas/liquid absorption in post-combustion capture, Journal of Membrane Science, vol. 377, pp. 261-272.

[11] A. Mansourizadeh, 2012, Experimental study of CO2 absorption/stripping via PVDF hollow fiber membrane contactor, Chemical Engineering Research and Design, vol. 90, pp. 555-562.

[12] A. Mansourizadeh and A. F. Ismail, 2011, A developed asymmetric PVDF hollow fiber membrane structure for CO2 absorption, International Journal of Greenhouse Gas Control, vol. 5, pp. 374-380.

[13] Y.-S. Kim and S.-M. Yang, 2000, Absorption of carbon dioxide through hollow fiber membranes using various aqueous absorbents, Separation and Purification Technology, vol. 21, pp. 101-109.

Organized by :
Department of Chemical Engineering
Faculty of Industrial Technology
Parahyangan Catholic University
in Collaboration With :
Indonesian Institute of Science Research Center for Chemistry
Indonesian Center for Estate Corps Research and Development

Sponsored by :
PT. Lautan Luas Tbk.

PT. Lautan Luas Tbk.
Distributor and Manufacturer - Basic and Specialty Chemicals

LIPI

9 772339 209003